



# University of Granada

Doctoral School of Science, Technologies, and Engineering  
Chemical Doctoral Program

Department of Chemical Engineering  
Waste Valorization Technologies and Catalytic Process Research Group

## Doctoral Thesis

---

**Thermochemical and catalytic recycling of plastic waste from the rejected fraction of urban solid waste treatment plants to obtain commercial chemical products**

---

By:

**D. Marco Favio Paucar Sánchez**

Directed by:

**D.<sup>a</sup> María Ángeles Martín Lara  
D. Mario Jesús Muñoz Batista**

Granada, march 2024

Editor: Universidad de Granada. Tesis Doctorales  
Autor: Marco Favio Paucar Sánchez  
ISBN: 978-84-1195-343-6  
URI: <https://hdl.handle.net/10481/92575>

*Para quienes mi camino sea una inspiración*





---

# Acknowledgments

Thank the life circumstances for bringing me to this beautiful moment of tireless effort and an incredible crossing.

Eternal thanks to my directors of the thesis, Prof. María Ángeles Martín Lara and Prof. Mario Jesús Muñoz Batista, to the professors' staff of the Waste Valorization Technologies and Catalytic Process Research Group, as well as administrative and support personnel from the Department of Chemical Engineering of the University of Granada.

To my understanding and lovely companion of life, Carolina, for her constant and unwearyingly support, my loved sons Mayra (†), Diana, and Richard, and my family, in a particular manner, to my sister for cheering me up to travel and continue my studies at this excellent University.



---

## Summary

In the last decades, energy recovery by incineration and deposits in landfills have been the main options for contaminated mixed plastic waste management unrecovered by mechanical means due to technical and economic reasons. Nevertheless, the legislation has changed, and a vast inversion is ongoing in plastic waste mechanical and chemical recycling new technologies. Thus, chemical recycling by pyrolysis appears as a featured technology, and although it is still little industrially implemented, many companies have announced pyrolysis plant constructions for different plastic waste types; it is expected an increase plants numbers along with the production capacity in the following years.

Recycling plastic waste by pyrolysis allows processing for different waste flows. It is precisely for complex waste streams, which can be formed by a very heterogeneous mixture of polymers and present high contamination levels or waste with substances that need to be extracted from recycled plastics, where pyrolysis surge as an attractive alternative to mechanical recycling for valuable product generation.

The investigation work, which results are presented in the present Doctoral Thesis, was developed in the “Waste Valorization Technologies and Catalytic Process” research group from the Department of Chemical Engineering of Granada University within the project “Converting the nonrecyclable mix plastic from municipal solid waste in chemical products and high-value carbonaceous materials” (reference PID2019-108826RB-I00) from Science and Innovation Ministry and “Valorization of the plastic waste coming from the rejected fraction of the urban solid waste treatment plants by pyrolysis” (reference B-RNM-78-UGR20) from University Counseling, Investigation and Innovation of Andalucía Board.

In that context, this Doctoral Thesis pretends to develop a flex pyrolysis technology integrated to treat dirty plastic waste and mixed non-recyclable from urban solid litter, whose usual destination is the landfill or incineration, for fuel production through controlled pyrolysis conditions and the use of new catalysts.

This Doctoral Thesis is presented for its evaluation as a paper grouping published organized in eight chapters. The first chapter is an introductory character, followed by a dedicated to the thesis objectives (chapter 2), later to continue with four additional chapters corresponding to published papers in impact journals indexed in the Journal Citation Reports. Appear, in addition, a conclusion chapter (chapter 7) and the last one with future works (chapter 8).

A bit summary of the content of each one of the chapters corresponding to the published articles is shown as follows.

Firstly, the results obtained in the study of the **characterization of the liquid fraction obtained from the thermal pyrolysis of the mixture of non-recyclable post-consumer plastic waste from urban solid waste** are presented. This study used a real mixture of plastic waste from the rejection fraction of an urban solid waste treatment plant belonging to the province of Granada (Spain). This waste mixture comprises polypropylene, expanded polystyrene, high-impact polystyrene, and film-type plastic (mainly low-density polyethylene). Different pyrolysis tests were carried out in a horizontal tubular reactor with a nitrogen flow of 100 L/h in the temperature range of 450 to 550 °C. The different products (solid, liquid, and gas) were collected, and the liquid fraction obtained was analyzed in detail (density, specific weight, refractive index, elemental analysis, simulated distillation curve, etc.). Subsequently, some mathematical correlations used in the refining industry were applied to estimate specific characteristic parameters of crude oil and analyze its suitability for pyrolysis oils. The results of this study are shown in Article I: "Characterization of liquid fraction obtained from pyrolysis of post-consumer mixed plastic waste: A comparing between measured and calculated parameters," published in the journal *Process Safety and Environmental Protection* from the Elsevier Publishing House. with impact factor 7.8 (2022) and Q1 relative position in JCR.

Secondly, the results of the **study of the ex-situ thermal and catalytic pyrolysis of the mixture of non-recyclable post-consumer plastic waste from municipal solid waste on different catalysts (CaO, MgO, HY, HZSM-5)** are presented. In this study, pyrolysis was carried out at 500 °C in a horizontal tubular reactor with the individual plastics and the mixture. The catalysts were characterized, and a detailed analysis of the composition of the liquid fraction with emphasis on the determination of the hydrocarbon groups present in the gasoline product. The results of this study are shown in Article II: "Thermal and catalytic pyrolysis of a real mixture of post-consumer plastic waste: An analysis of the gasoline-range product," published in the journal *Process Safety and Environmental Protection* of the publisher Elsevier with impact factor 7.8 (2022) and Q1 relative position in JCR.

Thirdly, as an alternative to the commercial catalysts analyzed in the previous study, the results of the **study of the in-situ catalytic pyrolysis of the mixture of non-recyclable post-consumer plastic waste from urban solid waste on clays, which are especially abundant in Spain like sepiolite and montmorillonites K10 and K30**, are shown. In this study, pyrolysis is repeated at 500 °C in the same horizontal tubular reactor with the mixture of plastic adding catalyst (in-situ); characterization of the catalysts used, and a detailed analysis of the composition of the gaseous and liquid fractions obtained was made. About the liquid fraction, the composition of the

---

different products is determined in detail and compared by analogy with the fuels obtained from crude oil: gasoline and naphtha, kerosene, gas oils, and residual fuel oils. The results of this study are shown in Article III: "Towards fuels production by a catalytic pyrolysis of a real mixture of post-consumer plastic waste," published in the magazine Fuel from Elsevier publishing house with impact factor 7.4 (2022) and Q1 relative position in JCR.

In the fourth and final stage, the **study of the ex-situ catalytic pyrolysis of the mixture of non-recyclable post-consumer plastic waste of urban solid waste on commercial zeolites impregnated with metals (nickel and cobalt)** is performed. In this study, pyrolysis is carried out at 500 °C in a horizontal tubular reactor with a mixture of plastics, a characterization of the catalysts used, and a detailed analysis of the composition of the liquid fraction obtained is realized with emphasis on the determination of the groups of hydrocarbons present in the gasoline product. The metal-impregnated catalysts were prepared using the incipient humidity by precipitation on the zeolite (precursor) from a metal salt solution, evaporating the solvent to dryness. The results of this study are shown in Article IV: "Impact of metal impregnation of commercial zeolites on the catalytic pyrolysis of a real mixture of post-consumer plastic waste," sent for publication to the journal Catalysts of the MDPI publishing house with impact factor 3.9 (2022) and relative position Q2 in JCR.



---

# Resumen

En las últimas décadas la incineración con recuperación de la energía y el depósito en vertedero han sido las opciones de gestión principales para los residuos plásticos mezclados que están contaminados, y que no son aptos de ser reciclados mecánicamente por motivos técnicos y/o económicos. No obstante, la legislación ha cambiado y se están realizando enormes inversiones en nuevas tecnologías que se utilizan para reciclar de forma mecánica y química los residuos plásticos. Así, el reciclado químico por pirólisis aparece como una tecnología destacada y, aunque aún está poco implantada a nivel industrial, un gran número de empresas han anunciado la construcción de plantas de pirólisis para diferentes tipos de residuos plásticos por lo que se prevé un aumento del número de plantas y de la capacidad de producción en los próximos años.

El reciclado de los residuos plásticos por pirólisis permite procesar diferentes flujos de residuos. Es precisamente para los flujos de residuos complejos, que pueden estar formados por una mezcla muy heterogénea de polímeros y presentar altos niveles de contaminación o residuos con sustancias que necesitan ser extraídas de los plásticos reciclados, donde la pirólisis surge como una alternativa atractiva al reciclado mecánico para generar productos valiosos.

El trabajo de investigación cuyos resultados se presentan en la presente Tesis Doctoral se ha desarrollado en el grupo de investigación “Tecnologías de Valorización de Residuos y Procesos Catalíticos” del Departamento de Ingeniería Química de la Universidad de Granada en el marco de los proyectos “Convirtiendo el plástico mezcla no reciclable de residuos sólidos municipales en productos químicos y materiales carbonosos de alto valor” (referencia PID2019-108826RB-I00) del Ministerio de Ciencia e Innovación y “Valorización de residuos plásticos procedentes de la fracción rechazo de las plantas de tratamiento de residuos sólidos urbanos mediante pirólisis” (referencia B-RNM-78-UGR20) de la Consejería de Universidad, Investigación e Innovación de la Junta de Andalucía.

En este contexto, con esta Tesis Doctoral se pretende desarrollar una tecnología de pirólisis flexible e integrada que trate residuos plásticos sucios y mezclados no reciclables de los desechos sólidos urbanos; cuyo destino habitual es el depósito en vertedero o la incineración, para producir combustibles a través del control de las condiciones del proceso de pirólisis y el uso de nuevos catalizadores.

Esta Tesis Doctoral se presenta para su evaluación como un conjunto de trabajos publicados organizada en ocho capítulos. El primer capítulo es de carácter introductorio seguido por otro donde se incluyen los objetivos de la tesis (capítulo 2) para, posteriormente, continuar con cuatro capítulos adicionales correspondientes a los artículos publicados en revistas de impacto

indexadas en el Journal Citation Reports. Aparecen, además, un capítulo de conclusiones (capítulo 7) y otro de trabajos futuros (capítulo 8).

Se describe brevemente a continuación un resumen sucinto del contenido de cada uno de los capítulos correspondientes a los artículos publicados.

En primer lugar, se presentan los resultados obtenidos en el estudio de la **caracterización de la fracción líquida obtenida de la pirólisis térmica de la mezcla de residuos plásticos post-consumo no reciclables de residuos sólidos urbanos**. En dicho estudio se empleó una mezcla real de residuos plásticos procedentes de la fracción rechazo de una planta de tratamiento de residuos sólidos urbanos perteneciente a la provincia de Granada (España). Esta mezcla de residuos está formada principalmente por polipropileno, poliestireno expandido, poliestireno del alto impacto y plástico tipo film (principalmente polietileno de baja densidad). Se realizaron diferentes ensayos de pirólisis con un flujo de nitrógeno de 100 L/h en el rango de temperaturas de 450 a 550 °C en un reactor tubular horizontal. Se recogieron los diferentes productos (sólido, líquido y gas) y se analizó detalladamente la fracción líquida obtenida (densidad, peso específico, índice de refracción, análisis elemental, curva de destilación simulada, etc.). Posteriormente se emplearon algunas correlaciones matemáticas usadas en la industria de la refinación para estimar ciertos parámetros característicos del petróleo crudo, para analizar su idoneidad en la aplicación a los aceites de pirólisis. Los resultados de este estudio se muestran en el artículo I: *“Characterization of liquid fraction obtained from pyrolysis of post-consumer mixed plastic waste: A comparing between measured and calculated parameters”*, publicado en la revista *Process Safety and Environmental Protection* de la editorial Elsevier con factor de impacto 7.8 (2022) y posición relativa Q1 en JCR.

En segundo lugar, se presentan los resultados del **estudio de la pirólisis térmica y catalítica ex-situ de la mezcla de residuos plásticos post-consumo no reciclables de residuos sólidos urbanos sobre diferentes catalizadores (CaO, MgO, HY, HZSM-5)**. En dicho estudio se realizó la pirólisis a 500 °C en un reactor horizontal tubular con los plásticos individuales y luego con la mezcla, se realiza la caracterización de los catalizadores empleados junto a un análisis detallado de la composición de la fracción líquida haciendo énfasis en la determinación de los grupos de hidrocarburos presentes en el producto gasolina. Los resultados de este estudio se muestran en el artículo II: *“Thermal and catalytic pyrolysis of a real mixture of post-consumer plastic waste: An analysis of the gasoline-range product”*, publicado en la revista *Process Safety and Environmental Protection* de la editorial Elsevier con factor de impacto 7.8 (2022) y posición relativa Q1 en JCR.

En tercer lugar, como alternativa a los catalizadores comerciales analizados en el estudio anterior, se presentan los resultados del **estudio de la pirólisis catalítica in-situ de la mezcla de residuos**



---

**plásticos post-consumo no reciclables de residuos sólidos urbanos sobre arcillas que son especialmente abundantes en España, la sepiolita y las montmorillonitas K10 y K30.** En dicho estudio se realiza la pirólisis nuevamente a 500 °C en el mismo reactor horizontal tubular con la mezcla de residuos plásticos adicionando junto a estos el catalizador (in-situ), se realiza una caracterización de los catalizadores empleados y un análisis detallado de la composición de las fracciones gaseosa y líquida obtenidas. En relación con la fracción líquida, se determina detalladamente la composición de los diferentes productos y se compara por analogía con los combustibles que se obtienen del crudo del petróleo: gasolinas y naftas, queroseno, gasóleos, fuelóleos residuales. Los resultados de este estudio se muestran en el artículo III: *“Towards fuels production by a catalytic pyrolysis of a real mixture of post-consumer plastic waste”*, publicado en la revista *Fuel* de la editorial Elsevier con factor de impacto 7.4 (2022) y posición relativa Q1 en JCR.

En una cuarta y última etapa, se efectúa el **estudio de la pirólisis catalítica ex-situ de la mezcla de residuos plásticos post-consumo no reciclables de residuos sólidos urbanos sobre zeolitas comerciales impregnadas con metales (nickel y cobalto).** En dicho estudio se realiza la pirólisis a 500 °C en un reactor horizontal tubular con la mezcla de plásticos y se realiza una caracterización de los catalizadores empleados y un análisis detallado de la composición de la fracción líquida obtenida con énfasis en la determinación de los grupos de hidrocarburos presentes en el producto gasolina. Los catalizadores impregnados de metal fueron preparados empleando el método de la humedad incipiente por precipitación sobre la zeolita (precursor), a partir de una disolución de la sal metálica, evaporando a sequedad el disolvente. Los resultados de este estudio se muestran en el artículo IV: *“Impact of metal impregnation of commercial zeolites on the catalytic pyrolysis of a real mixture of post-consumer plastic waste”*, enviado para su publicación a la revista *Catalysts* de la editorial MDPI con factor de impacto 3.9 (2022) y posición relativa Q2 en JCR.



# Organization of the Thesis

According to article 18.4 of the Regulatory Standards of Official Doctoral Education and the Doctorate Degree by Granada University, this doctoral thesis has been structured around a series of published papers, each of which contributes to a specific aspect of the overall research. The references of included articles according to the redaction of this thesis are as follows:

- **Paucar-Sánchez, M. F.**, Calero, M., Blázquez, G., Muñoz-Batista, M. J., & Martín-Lara, M. A. (2022). Characterization of liquid fraction obtained from pyrolysis of post-consumer mixed plastic waste: A comparing between measured and calculated parameters. *Process Safety and Environmental Protection*, 159, 1053-1063. <https://doi.org/10.1016/j.psep.2022.01.081>
- **Paucar-Sánchez, M. F.**, Calero, M., Blázquez, G., Solís, R. R., Muñoz-Batista, M. J., & Martín-Lara, M. A. (2022). Thermal and catalytic pyrolysis of a real mixture of post-consumer plastic waste: An analysis of the gasoline-range product. *Process Safety and Environmental Protection*, 168, 1201-1211. <https://doi.org/10.1016/j.psep.2022.11.009>
- **Paucar-Sánchez, M. F.**, Martín-Lara, M. A., Calero, M., Blázquez, G., Rodríguez Solís, R., & Muñoz-Batista, M. J. Towards fuels production by a catalytic pyrolysis of a real mixture of post-Consumer Plastic Waste. *Fuel*, 352, 129145. <https://doi.org/10.1016/j.fuel.2023.129145>
- **Paucar-Sánchez, M. F.**, Calero, M., Blázquez, G., Solís, R. R., Muñoz-Batista, M. J., & Martín-Lara, M. A. Impact of metal impregnation of commercial zeolites on the pyrolysis of a real mixture of post-consumer plastic waste. *Catalysts*, 14(3), 168. <https://doi.org/10.3390/catal14030168>.

In addition, although this work is not directly related, a co-authored paper was developed and published during the doctoral period (found in the Annex).

- Lucía Quesada, Mónica Calero, María Ángeles Martín-Lara, Antonio Pérez, **Marco F. Paucar-Sánchez** and Gabriel Blázquez (2022). Characterization of the different oils obtained through the catalytic in situ pyrolysis of polyethylene film from municipal solid waste. *Applied Sciences*, 12(8), 4043. <https://doi.org/10.3390/app12084043>

First, the Thesis provides a comprehensive introduction (Chapter 1) that includes a summary of previous research on the topic; then, the Thesis objectives are presented in Chapter 2. The research findings are presented, analyzed, interpreted, and discussed in published papers (Chapters 3, 4, 5, and 6). Additionally, the main conclusions are given in Chapter 7, and finally, the Thesis is finished with a chapter with suggestions and recommendations for future research (Chapter 8).



# Content

ACKNOWLEDGMENTS.....	V
SUMMARY .....	VII
RESUMEN .....	XI
ORGANIZATION OF THE THESIS .....	XV
<b>I INTRODUCTION.....</b>	<b>1</b>
CHAPTER 1 .....	3
1. Introduction .....	3
1.1. <i>Plastics Production and Importance</i> .....	3
1.2. <i>Environmental Impacts of Post-Consumer Plastic Waste</i> .....	4
1.3. <i>Post-Consumer Plastics Waste Management</i> .....	6
1.3.1. Mechanical Recycling.....	6
1.3.2. Chemical Recycling.....	7
1.3.2.1. Solvent Purification .....	7
1.3.2.2. Chemical Depolymerization .....	7
1.3.2.3. Thermal Depolymerization .....	8
1.3.2.4. Gasification.....	8
1.3.2.5. Pyrolysis.....	8
1.3.2.6. Catalytic Pyrolysis.....	9
1.4. <i>Chemicals from Plastic Waste</i> .....	10
1.4.1. Backgrounds .....	10
1.4.2. Research works on the production of chemicals from plastic waste pyrolysis .....	11
1.4.3. Naphtha and aromatics industrial production .....	12
References .....	20
<b>II OBJECTIVES .....</b>	<b>29</b>
CHAPTER 2 .....	31
2. <i>Objectives</i> .....	31
<b>III RESULTS .....</b>	<b>33</b>
CHAPTER 3 .....	35
CHARACTERIZATION OF LIQUID FRACTION OBTAINED FROM PYROLYSIS OF POST-CONSUMER MIXED PLASTIC WASTE: A COMPARING BETWEEN MEASURED AND CALCULATED PARAMETERS .....	35
<i>Abstract</i> .....	37
3.1. <i>Introduction</i> .....	37
3.2. <i>Materials and methods</i> .....	39
3.2.1. Materials.....	39
3.2.2. Methods.....	39
3.2.2.1. Pyrolysis tests.....	39
Thermolysis experimental tests were carried out in a horizontal fixed-bed reactor (Nabertherm R 50/250/12 Model) integrated with a flow meter to regulate the inert entrainment fluid and a condensation container immersed in a cold bath to separate the liquid and the gas phases. ....	40
3.2.2.2. Density and specific gravity (SG) .....	40
3.2.3. Refractive index ( $n_{D20}$ ) and refractive index parameter (I).....	40
3.2.3.1. Elemental analysis .....	41
3.2.3.2. Compositional analysis by gas chromatography.....	41
3.2.3.3. Simulated distillation (SD) .....	41
3.2.3.4. ASTM D86 distillation .....	42
3.2.4. True boiling point curve (TBP).....	42
3.2.5. Mean average boiling point (MeABP) .....	43

3.2.5.1. Mathematical correlation for hydrocarbons .....	44
3.3. <i>Results and discussion</i> .....	45
3.3.1. Effect of operating temperature on liquid fraction .....	45
3.3.2. Experimental data on basic properties of pyrolytic oil samples .....	47
3.3.3. Conversion of measured properties into parameters for hydrocarbon characterization .....	50
3.3.4. Application of mathematical correlations for hydrocarbons .....	52
3.3.5. Performance estimation of products .....	54
3.4. <i>Conclusions</i> .....	56
<i>References</i> .....	57
CHAPTER 4 .....	61
THERMAL AND CATALYTIC PYROLYSIS OF A REAL MIXTURE OF POST-CONSUMER PLASTIC WASTE: AN ANALYSIS OF THE GASOLINE-RANGE PRODUCT .....	61
<i>Abstract</i> .....	63
4.1. <i>Introduction</i> .....	63
4.2. <i>Materials and methods</i> .....	67
4.2.1. Raw material .....	67
4.2.2. Preparation and characterization of the catalysts .....	67
4.2.3. Pyrolysis reactor and pyrolysis conditions .....	68
4.2.4. Liquid product analysis .....	69
4.2.4.1. Analytical procedure .....	69
4.2.4.2. Simulated distillation (SD) .....	69
4.2.4.3. Hydrocarbon types in the gasoline-range product .....	70
4.2.5. Coke deposition on the catalysts .....	70
4.3. <i>Results and discussion</i> .....	71
4.3.1. Characterization of the catalysts .....	71
4.3.2. Effect of type of polymer on thermal pyrolysis performance .....	71
4.3.2.1. Effect of type of polymer on product yields .....	71
4.3.2.2. Effect of type of polymer on simulated distillation boiling points.....	73
4.3.2.3. Effect of the type of polymer on hydrocarbon types in the gasoline-range product.....	76
4.3.3. Effect of type of catalyst on catalytic pyrolysis performance.....	78
4.3.3.1. Effect of type of catalyst on product yields .....	78
4.3.3.2. Effect of type of catalyst on simulated distillation boiling points .....	79
4.3.3.3. Effect of type of catalyst on hydrocarbon types in the gasoline-range product .....	81
4.4. <i>Conclusions</i> .....	83
<i>References</i> .....	83
4.5. <i>Supplementary materials</i> .....	91
CHAPTER 5 .....	93
TOWARDS FUELS PRODUCTION BY A CATALYTIC PYROLYSIS OF A REAL MIXTURE OF POST-CONSUMER PLASTIC WASTE .....	93
<i>Abstract</i> .....	95
5.1. <i>Introduction</i> .....	95
5.2. <i>Materials and methods</i> .....	97
5.2.1. Raw material .....	97
5.2.2. Preparation and characterization of the catalysts .....	97
5.2.3. Pyrolysis reactor and operation conditions .....	97
5.2.4. Gases analysis .....	99
5.2.5. Liquid analysis.....	99
5.2.5.1. Elemental analysis .....	99
5.2.5.2. Chemical constitution.....	99
5.2.5.3. Simulated distillation (SD) .....	99
5.2.5.4. ASTM D86 distillation from the fuels.....	100
5.2.5.5. Hydrocarbon types analysis.....	100
5.3. <i>Results and discussion</i> .....	101
5.3.1. Characterization of the catalysts.....	101
5.3.2. Fraction yields and chemical composition .....	102

5.3.3.	Simulated distillation and product yield .....	107
5.3.4.	Chemical composition of the products .....	108
5.3.4.1.	Gasoline.....	108
5.3.4.2.	Kerosine.....	110
5.3.4.3.	Diesel.....	111
5.3.4.4.	Bottoms .....	111
5.4.	<i>Conclusions</i> .....	113
	<i>References</i> .....	114
5.S.	Supplementary materials.....	119
CHAPTER 6	.....	123
IMPACT OF METAL IMPREGNATION OF COMMERCIAL ZEOLITES ON THE PYROLYSIS OF A REAL MIXTURE OF POST-CONSUMER PLASTIC WASTE .....		
	<i>Abstract</i> .....	125
6.1.	<i>Introduction</i> .....	125
6.2.	<i>Results and discussion</i> .....	126
6.2.1.	Characterization of the catalytic materials .....	126
6.2.2.	Catalytic performance of the metal-impregnated zeolites .....	131
6.2.2.1.	Effect on product yields and the functional groups of the liquid product.....	131
6.2.2.2.	Effect on simulated distillation boiling points of the liquid product.....	134
6.3.	Materials and methods.....	139
6.3.1.	Raw material.....	139
6.3.2.	Preparation and characterization of the catalysts .....	139
6.3.3.	Pyrolysis reactor and pyrolysis conditions .....	140
6.3.4.	Liquid product analysis .....	142
6.4.	<i>Conclusions</i> .....	143
	<i>References</i> .....	145
<b>IV</b>	<b>CONCLUSIONS</b> .....	<b>151</b>
CHAPTER 7	.....	153
	<i>Conclusions</i> .....	153
	<i>Conclusiones</i> .....	155
<b>V</b>	<b>FUTURE WORK</b> .....	<b>157</b>
CHAPTER 8	.....	159
	<i>Future works</i> .....	159
	<i>Trabajos Futuros</i> .....	161
<b>VI</b>	<b>ANNEX</b> .....	<b>163</b>
CHARACTERIZATION OF THE DIFFERENT OILS OBTAINED THROUGH THE CATALYTIC IN-SITU PYROLYSIS OF POLYETHYLENE FILM FROM MUNICIPAL SOLID WASTE.....		
	<i>Abstract</i> .....	167
1.	<i>Introduction</i> .....	167
2.	<i>Materials and Methods</i> .....	169
2.1.	Materials.....	169
2.2.	Characterization of the catalysts.....	170
2.2.1.	Textural parameters .....	170
2.3.	Catalytic pyrolysis tests .....	171
2.4.	Physical characterization of the pyrolytic oils .....	171
2.5.	Chemical characterization of the pyrolytic oils .....	172
2.5.1.	Elemental analysis and calorific value .....	172
2.5.2.	Thermogravimetry analysis (TGA).....	172
2.5.3.	Fourier-transform infrared spectroscopy (FTIR) analysis .....	172
2.5.4.	Gas chromatography–mass spectrometry (GC-MS).....	172

---

3.	<i>Results and discussions</i> .....	173
3.1.	Characterization of the catalysts.....	173
3.2.	Physical characterization of pyrolytic oil.....	174
3.3.	Chemical characterization of pyrolytic oil.....	175
3.3.1.	TGA analysis.....	175
3.3.2.	FTIR analysis of the pyrolytic oil.....	177
4.	<i>Conclusions</i> .....	181
	<i>References</i> .....	183
S.	Supplementary materials.....	187
	<i>References</i> .....	191



# I INTRODUCTION



# Chapter 1

## 1. Introduction

### 1.1. Plastics Production and Importance













The advantages of plastics are unquestionable: they are easily moldable, resistant, slight, hygienic, and budget-friendly, qualities that drove a boom in their production during the last century, with a trend to increase by the following ten years [1]. Comparing 2019, its use projected growth to about two points, seven times by 2060 worldwide and two times in Europe [2]. Unlike metals, most are photodegraded and decompose slowly in small fragments known as microplastic [3]. They intervene are and will be an essential part of everyday life [1][4][5]. Due to its myriad composition, types, and shapes, the list of plastic applications is limitless, in pieces or assemblies within an endless domestic (across each interior and exterior category to food utensils), commercial, or industrial environment, from mechanical to electrical to chemical to structures [6][7], as well as sophisticated biomedical products such as orthopedic implants (prosthetic hip and knee joints [7]), valves heart, artificial organs, vascular grafting materials, dialyzing sets, syringes, blood transfusion sets, various kinds of catheters, etc., [8]; many of which are conceived and designed to be reused or for long-lasting [9].

Single-use or disposable plastics are typically designed to be used just once or for a short period [9], manufactured from two plastic categories (thermoplastics and thermosets) [10][11] and comprise the most significant segment in plastics production [12]; in 2021, 44% was destined for this purpose worldwide, while in Europe it was 39% in 2022 [13][14]. They are mostly made based on thermoplastics like polyethylene (PE), low–high-density polyethylene (LDPE and HDPE), polyethylene terephthalate (PET), polystyrene (PS), expanded polystyrene (EPS), and polypropylene (PP) of reversible characteristics [1][4]; which, they are seldom used in pure form since, to procure their desired properties like color, flexibility, and other characteristics of plastics [8], organic and inorganic additives are added during their manufacturing [5] to protect them from oxygen, sun, and heat [15]. The main plastic product components are 58% plasticizers, 12% colorants, 9% blowing agents, 8% flame retardants, 3% heat stabilizers, and 7% others [8]; Table 1.1 shows the everyday single-use products, manufacturing materials, identification recycling codes, and the products obtained by recycling.

Since the fifties, their production has depended on fossil hydrocarbons exclusively [10][11] because they are the least expensive and can be transformed into their raw materials or intermediate chemicals easily for later being converted into olefin derivatives and aromatics (primary petrochemicals such as ethylene, propylene, butadiene, benzene, toluene, and xylenes);

and then, by polymerization, plastics [5][16][17]. In 2022 global, 90.5% was fossil-based, of which 20.9% was PP, 15.6% was PE (low and low-low densities), 14% was PVC, 13.5% was PE (high and middle densities), 6.9% was PET, and 5.7% was PS and EPS; in the same year in Europe, the plastics of fossil-origin were 80.4%, of which 19.2% corresponded to the PP, 16.7% to the PE (low and low-low densities – LDPE and LLDPE), 11.3% to the PVC, 10.8% to PE (high and middle densities – HDPE and MDPE), 6.2% to the PET, and 6.7% were PS plus EPS [14].

**Table 1.1.** Recycling codes and common plastic products [18][19].

					
PET	HDPE	PVC	LDPE	PP	PS
					
<b>Common products</b>					
Soda & water bottles, cups, jars, trays, clamshells	Milk jugs, detergent & shampoo bottles, flower pots, grocery bags	Cleaning supply, jugs, pool liners, twine, sheeting, automotive products, bottles, sheeting	Bread bags, paper towels & tissue, overwrap, squeeze bottles, trash bags, six-pack rings	Yogurt tubes, cups, juice bottles, straws, hangers, sand & shipping bags	To-go containers & flatware, hot cups, razors, CD case, shipping cushion, cartons, trays
<b>Recycled products</b>					
Clothing, carpet, clamshells, soda & water bottles	Detergent bottles, flower pots, crates, pipe, decking	Pipe, wall siding, binders, carpet, backing, flooring	Trash bags, plastic lumber, furniture, shipping envelopes, compost bins	Paint cans, speed bumps, auto parts, food containers, hangers, plant pots, razor handles	Picture frame, crown molding, rulers, flower pots, hangers, toys, tape dispensers

## 1.2. Environmental Impacts of Post-Consumer Plastic Waste

Most single-use plastics are discarded in the same year they are produced. In 2015, single-use plastics accounted for about 47% of the waste plastics at the global level. According to recent estimates, 79% of the waste plastics are discarded in landfills or the environment, 12% are incinerated, and 9% are only recycled; if this trend continues, there will be 12 billion tons of plastic waste by 2050 [10][20]. Despite improvements in litter collection and waste management infrastructure, the projection of landfilling or incineration by 2060 would double that registered in 2019 [2].

By December 2017, the European Council, the Parliament, and the European Commission had reached a preliminary political agreement establishing a specific objective to recycle 50% of plastic waste by 2025, with a projection of 55% by 2030 [1]. In 2020, Europe recorded 34.6% of the recycling of plastic waste generated post-consumer; 42% was used as an energy resource, and 23.4% was sent to landfills [21]. Spain reported that 43% of post-consumer plastic waste was recycled, with 21% used for energy recovery and 36% shipped to landfills [13]. These data show that Europe still has a long way to go to meet its recycling targets for plastic waste. While some progress has been made, with Spain reporting a recycling rate of 43%, a significant amount of plastic waste is still being sent to landfills. More efforts are needed to increase recycling rates and reduce the amount of plastic waste being disposed of in an unsustainable manner.

Although many efforts have been put into recycling waste, all processes generate significant amounts of mixed, dirty, or contaminated plastic, and their sorting is not economically viable. As a result, the primary alternative for their treatment has been incineration instead of landfill deposition, but its high calorific value is a significant problem [11], in addition to the concerns about hazardous substances such as polychlorinated dibenzo-p-dioxins, dibenzofuran, and organo-halogens released into the atmosphere during the combustion, which are present even though the energy was recovered [22]. In Spain, from 2018 to 2020, energy recovery decreased by 5.9% and recycling increased by 6%; nevertheless, landfill disposal increased by 4.5% [13].

Single-use plastics will continue accumulating in the environment and landfills. Under ambient solar radiation, the most commonly used plastics (PE and PP) release methane and ethylene over time and hydrocarbon gases when aged in water or air [23]. These gases contribute to the greenhouse effect and climate change. On the other hand, even though the landfill technique was designed to avoid the decomposition of materials that leads to the release of carbon dioxide [15], plastics, especially PP and PE, degrade despite low oxygen levels until they can no longer hold weight without breaking (as long as it is not buried too deeply); fragments that will remain or be present in the soil for a long time [24][25][26], in addition to the long-term risk of contamination of soil and the aquatic environment by plasticizers like bisphenol A through discharge of the leachates [27] and, together with these, microplastics generated by the breaking down of plastic debris on land by physical, biological, and chemical processes, as well as UV radiation exposure and abrasive actions [28]; whose relative abundance is predominated by the PE and PP [3]. These microplastics can persist in the environment for years, posing a significant threat to ecosystems and wildlife. The accumulation of these plastic particles in soil and water can disrupt nutrient cycling and harm organisms at various trophic levels. Additionally, the ingestion of microplastics by animals can lead to internal injuries, blockages in the digestive system, and even death [29][30][31].

One possible strategy is to promote the use of biodegradable alternatives to plastics, such as plant-based materials or compostable packaging [32][33]. Another approach is implementing stricter plastic production and disposal regulations, encouraging companies to adopt more sustainable practices [34]. Additionally, educating the public about the dangers of plastic pollution and the importance of recycling can help raise awareness and promote behavior change [35]. By taking these measures, work should be done to minimize the impact of plastic waste on the environment and safeguard the health of the ecosystems.

Although landfills could solve plastic waste management, the space for these fillings is becoming scarce [36]. Furthermore, landfills are not a sustainable solution as they contribute to soil and water pollution, releasing harmful chemicals into the environment. This highlights the urgent need for alternative waste management strategies, such as recycling, to help reduce plastic waste in landfills. Additionally, implementing stricter regulations and policies on plastic production and usage can incentivize companies to find more environmentally friendly alternatives, reducing reliance on landfills for plastic waste disposal.

### **1.3. Post-Consumer Plastics Waste Management**

Plastic pollution has been a topic of concern for years, and the need to reduce its impact has gained importance over time since when these reach the end of their use life, their quantity is too high [37]. To mitigate some damage caused by these, non-durable and single-use plastics must be recycled appropriately through separation techniques employing different mechanical and chemical recycling technologies [38] [39].

#### **1.3.1. Mechanical Recycling**

It is a standard route where mechanical means of treatment are used to recycle plastic waste into secondary raw materials; it is usually the preferred path from an environmental perspective [39][40]. However, this process has constraints since it requires sorting and cleaning as pretreatment; in addition, many of these technologies also degrade plastic properties and face difficulties such as heterogeneity when high mechanical purity recycling is needed due to quality requirements. Although its potential can be improved through innovation and design, a stream of heterogeneous mixes of dirty and contaminated, or not, plastic waste will remain unrecovered [39][40][41]; therefore, there is a need to adopt a distinct approach that promotes new complementary processes like chemical recycling [42]. Typically, it involves separating and sorting according to color, composition, or physic properties, packing unsorted plastics, decontaminating plastics by washing, flake crushing, and extrusion into granulates [39][40].

## 1.3.2. Chemical Recycling

Chemical recycling of plastic waste refers to breaking down plastic materials into their original chemical components, which can be used to create new plastic products [43]. Unlike mechanical recycling, which involves melting and reshaping plastic waste, chemical recycling utilizes various chemical processes to convert plastic waste into its basic building blocks, such as monomers or polymers [44][45]. The advantages of chemical recycling over mechanical recycling include processing a wider range of plastic types, including those that are difficult to recycle mechanically [46][47]. Chemical recycling also allows for the recycling of contaminated plastic waste or mixed with other materials, which would typically be rejected in mechanical recycling processes [48]. Additionally, chemical recycling can produce higher-quality recycled plastics, as it allows for the removal of impurities and additives that may be present in the original plastic waste [49].

### 1.3.2.1. Solvent Purification

Solvent separation involves a high polymer solubility compared to additives and other contaminants and a series of purifications to get the polymer precipitate near-virgin quality [50]. Although there is a need for more clarity over most technologies regarding impurity treatment and hazardous toxicity, they could be used to process multi-materials as long as sufficient stages exist [51][52]. Nevertheless, it is very energy-intensive due to the required complexity and environmental costs and leads, in addition, to chain degradation [53][54]. Excluding VinyLoop plants (closed) and those approaching the pilot plant level, this technique has yet to reach the commercial scale [53]. Generally, most operate using contaminated mono-material feedstock that is usually not mechanically recycled [55].

### 1.3.2.2. Chemical Depolymerization

Chemical plastics depolymerization is realized through agent chemicals under controlled conditions to produce their pure monomers, dimers, or oligomers [55][56]; these are recovered and separated from the contaminants to then be processed alone or with pure monomers[53][50]. According to the agent of scission, depolymerization can be glycolysis, methanolysis, aminolysis, hydrolysis, or hydrolysis catalyzed by enzymes [40][55]. However, this technique is limited to monostreams that are relatively clean due to economic reasons [41]. Still, this technology is being tested at the pilot plant level and used for depolymerizing PET and PUR (polyurethane) at the industrial pilot stage [41][53].

### 1.3.2.3. Thermal Depolymerization

Thermal depolymerization, or pyrolysis, is an uncontrolled breakdown pathway that uses heat in the absence of oxygen (or a limited amount in the gasification case) to obtain various hydrocarbon products that need additional energy-intensive purification to get an adequate feedstock for polymer production [53][55].

At the industrial level, there was a particular interest in the 1960s for plastics mass production advances. Various processes were developed from the 1970s to the late 1990s, and multiple reactors were designed for the thermal processing of plastic waste. Until the early 2000s, thermal cracking was used to convert plastic waste into liquid fuels and monomers and reduce agents in furnaces or substitutes for coal in coke plants. The most relevant European initiatives in thermochemical cracking, despite being suspended because few polymers can be recycled under economically favorable conditions, were realized by Hamburg University, BASF, BP, and Veba Oil [11][57]. Similarly, between 1993 and 2000, academic groups and industrial researchers, under the auspices of the United States Department of Energy (Office of Fossil Energy), explored fuel production through pyrolysis followed by thermal hydro-processing or catalysis [11].

### 1.3.2.4. Gasification

It is a thermal cracking over 800 °C with a limited oxygen quantity for partially oxidizing the waste [58]. One of the main advantages is its ability to process all polymers and almost all organic materials. Nevertheless, although it could treat mixed and soiled plastics, it requires stable composition freedom of metals, fermentable composites, and moisture; pre-treatment steps are required as final gas purification steps [55][59]. Although this technology is less impactful than incineration and pyrolysis and is more emissive than mechanical recycling, it is well-developed for waste-to-fuel production, while waste-to-plastics is still under prototype. Its energy consumption is higher than that of other processes for recycling [55][60].

### 1.3.2.5. Pyrolysis

The main objective of this technique is to obtain liquid fractions in the 350 - 650 °C temperature range in oxygen absence. Nevertheless, although a varied mixture of waste can be handled, the yields highly depend on the feedstocks, of which some resins (PVC, PET, or PU, as non-plastic additives) should be removed previously. Some developers of this technology have processed mixed plastic-rich, post-consumer, and post-industrial waste with polyolefins (PE, LDPE, HDPE, PP), polystyrene, and other polymers [55].



The drawbacks of chemical recycling lie in the high costs that its implementation can entail and the requirement of large amounts of plastic waste to make it commercially viable. As a result of the economic cost and complexity involved in the process, its research and development are quite incipient, so there are few examples of chemical recycling technology being used in industrial-scale production. On the other hand, its future in downstream processes is promising. At the pilot plant level, some of them have had successful implementations to obtain raw materials for virgin polymer production, new plastics, or other petrochemical products or to deliver them like synthetic crude to refiners [61].

Several petrochemical companies have considered introducing them as feed to existing refining processes to avoid additional investment in new process construction based on the similarity between the composition of plastics and hydrocarbon fractions. Nevertheless, the main associated problem is the presence of unwanted elements and compounds, so this feed must be treated and conditioned before its addition to load currents [57]. The co-processing of molten plastic waste with oil cuts such as vacuum gas oil, light crude oil residues, light cyclic oils, lubricating oils, or benzene has also been extensively investigated; however, the result indicated that the underlying objective is to reduce its high viscosity. Another option for improving the properties and composition of pyrolysis oils has been co-pyrolysis, which involves two or more different materials as feedstock [11], along with or without catalytic materials [62].

#### 1.3.2.6. Catalytic Pyrolysis

Catalytic pyrolysis allows the processing of waste rejected by centers of treatment of waste recycling and mixtures from the production and manufacturing of plastics, as well as those generated by post-consumer or post-industrial. Depending on the technology developed, some deal with homogeneous feedstocks and others with mixed plastic waste (PP, PE, or PS mixed waste). Yet, due to the significant reaction yield reduction caused by catalyst deactivation, most only admit some plastics (PVC and PET are frequently avoided) and no high levels of contaminants such as paper, metals, or non-plastic additives [55].

The catalytic material's presence solves certain limitations concerning temperature dependence by reducing it compared to the traditional thermal process and increasing the product's performance by including specific catalytic characteristics such as surface area, pore size distribution, and acidity [55][63][64][65], as well certain benefits from the presence of active sites (impregnated metals) [66][67]. Catalysts used have been mainly zeolites as well as metal oxides (CaO and MgO) or available low-cost materials such as natural clays (bentonite and montmorillonites) [68][62], which ones have good thermal stability, selectivity, high surface, easy separation, are environment friendly, and external configuration tunnels expose over the surface,

in addition to channels in their framework [69][70][71]. Natural clays would be the first cracking catalysts used in fixed and fluid bed processes that would later be replaced by silica-aluminas [67]; industrially, they are part or base in the catalyst matrixes and improve the mechanical properties as the heat transfer in the cracking catalytic of hydrocarbon [67][72].

## **1.4. Chemicals from Plastic Waste**

### **1.4.1. Backgrounds**

The issue of plastic waste has gained significant attention in recent years due to its adverse impact on ecosystems, human health, and the overall sustainability of our planet. Addressing this is crucial as it requires the development of innovative solutions that can effectively manage and repurpose plastic waste, and one potential solution lies in the utilization of chemicals derived from this waste. These chemicals could revolutionize various industries and applications by providing sustainable alternatives to traditional materials and reducing the reliance on fossil fuels.

Different chemicals can be derived from plastic waste, including monomers, polymers, and additives [45][73]. Monomers are the building blocks of plastics and can be used to create new plastics or other materials. Polymers, on the other hand, are long chains of monomers and can be processed into various products, such as fibers or films. Additives, like plasticizers or flame retardants, can also be extracted from plastic waste and repurposed for different applications. Understanding the different types of chemicals that can be derived from plastic waste is crucial for developing effective recycling processes and maximizing the potential of these resources.

One method of converting plastic waste into chemicals is through pyrolysis. This involves heating the waste without oxygen, causing it to break down into smaller molecules. These molecules can then be further refined and used as building blocks for various chemicals and materials. Another approach is depolymerization, which breaks down the long polymer chains into their monomers. These monomers can then create new plastics or other chemical compounds. Both processes offer great potential for reducing waste and creating a circular economy for plastics.

The importance of using advanced technologies to extract chemicals from plastic waste efficiently cannot be overstated. By employing these technologies, we can maximize the recovery of valuable materials from plastic waste and minimize the amount of waste in landfills that pollutes our environment. Additionally, advanced extraction methods can help reduce the energy and resources required to produce new plastics, leading to a more sustainable and environmentally friendly approach. We must invest in and adopt these advanced technologies effectively to tackle the global plastic waste crisis.

### 1.4.2. Research works on the production of chemicals from plastic waste pyrolysis

Most studies have explored monomer production by thermal and catalytic cracking under different operational conditions with varied configurations and sizes, from the laboratory level to the pilot plant extent, testing thermoplastics of individuals or in a mixture manner with small and large sample quantities. The majority of small samples focus on determining total liquid yield with a few details of the distribution of products and almost null data on their chemical composition. Some of these have investigated the conversion of polyethylene of high density (HDPE) onto aromatics using Y-zeolite impregnated with transitional metals (Ni, Fe, Mo, Ga, Ru, and Co) [74] or by co-pyrolysis with wood sawdust over HZSM-5 [75] as different featuring of HZS-5 with LDPE [76]; the synergy effect between wood and polypropylene (PP) through metal oxides (ZnO, CaO, Fe<sub>2</sub>O<sub>3</sub>, and MgO) identified aromatics in the presence of Fe<sub>2</sub>O<sub>3</sub> [77]. In addition, comparisons have been made of total content aromatics and non-aromatics among commercial fuels and cracked liquid fractions from PE, PP, and PS by bentonite pellets [62]. Polyolefins (HDPE, LDPE, and PP) at different operating conditions have also been cracked over HZSM-5 to obtain olefins [78] as their liquefaction on MgO and CaO in CO<sub>2</sub> and N<sub>2</sub> atmospheres [79]. The processability of LDPE, PP, PVC/LDPE, and PVC/PP along with heavy vacuum gas oil(HVGO) has been investigated employing HZSM-5, Co-Ac (cobalt-active carbon), and commercial silica-alumina under hydrogen atmosphere [80]. Polycarbonate (PC) and polystyrene (PS) catalytic co-pyrolysis over HZSM-5 facilitated significantly more aromatic hydrocarbons forming than HY zeolite, which was highest when PC was blended with polyolefins 1:3 relation [81]. PE, PP, PS, and PET synergy using HZSM-5 in H<sub>2</sub> and He atmospheres were analyzed in situ and ex-situ for the hydrocarbon liquid increase [82]. Without matter the individual target, all of them have produced pyrolytic oil with a potential yield of fuel production.

Nevertheless, although plastic-to-fuel conversion reduces plastic waste from urban solid waste, it does not solve the demand for virgin plastics because these would still be made from fossil fuels, but naphtha recovered from plastic waste would allow obtaining a new feedstock for their production [83], especially aromatics. Hence, to add value to circularity and plastic waste recycling, technologies should be developed to convert plastic waste into naphtha [42]. This would avoid introducing them as feed to the separation processes of existing refining and elude the additional investment by new plant construction for its treatment and condition [57].

In general, pyrolysis is not a highly selective process because the products of plastic wastes are somewhat unpredictable by their quantity, behavior, and nature during the thermal cracking as a result of the eventual influence of the products and by-products in the reaction mechanisms,

principally when the origin of plastic wastes is unknown or coming from their blend (to which must be added plastic-based stabilizers, antioxidants, plasticizers, internal lubricants, pigments, multi-layer, or polymeric components, including toxic compounds as flame retardant additives [4][84]). However, their schemes are relatively flexible since, depending on the operation conditions, polymer, or mixture, the composition of gaseous and liquid products can vary broadly [2][85][86], and, although, in some instances, the outcomes obtained from the mixture have opposite effects to those observed when its polymers degrade, where the real and theoretical yields proposed that the primary products formed by each polymer can react with other by-products of the other plastics of the mixture, modifying its framework significantly [57], the catalytic material would help to solve certain limitations of the traditional thermal process, like reducing temperature dependence and increasing product yields by including specific catalytic characteristics such as the surface area, pore size distribution, and acidity [63][64][65], as of certain benefits by the presence of particular metals [66] deposited or impregnated as active components [67].

This doctoral research contributes to reducing landfills by converting plastic waste into raw material (naphtha) to produce primary petrochemicals through thermal and catalytic cracking by testing different low-cost solid promoters and, at the same time, providing added value to their processing by increasing the aromatics content as proposing analysis techniques for small samples, without implying a prior physical separation or distillation, to determine the chemical composition of their cuts or fractions.

### 1.4.3. Naphtha and aromatics industrial production

The petroleum industry development and demand growth for aromatics have caused fossil hydrocarbon to become their primary production source, historically dominated by coal tar liquor, a by-product of the coking industry [87]; nevertheless, although the chemical intermediates from petroleum contain various hydrocarbon derivative types, not all are used in petrochemical production. Low-boiling hydrocarbon or gases and higher-boiling hydrocarbon mixtures such as naphtha (the main feedstock to produce primary petrochemicals), kerosene, and gas oil are generally used; these last are held to cracking pretreatment for building various petrochemical products. Different feedstocks' coking and fluid catalytic cracking produce olefin derivatives and aromatics. However, steam cracking or thermal cracking processes reduce the need for fractionating but do not produce a high yield of the desired product [5][16][17][88]. Currently, pyrolysis gasoline and naphtha catalytic reforming are the primary and significant aromatic sources [87]. A general refinery configuration with primary petrochemical product streams such as ethylene, propylene, butadiene, benzene, toluene, and xylenes from raw materials (naphtha) is shown in Figure 1.1.

Naphtha is one of the more important products from a refinery. It is a light, volatile hydrocarbon mixture commonly used as a feedstock in the petrochemical industry for producing plastics, resins, and synthetic fibers. Particularly, it is composed of light (LN boiling point between 25 and 90 °C [89]) and heavy (HN boiling point ranges from 85 to 190 °C [89]) fractions, which are usually separated to form part feedstocks to obtain primary chemicals, mostly olefins from LN by steam cracking and aromatics from HN by catalytic reforming [90][91]. Its composition depends on the crude oil type, the boiling range, and the precedence, i.e., the atmospheric distillation or the catalytic or thermal cracking of heavy fractions, as shown in Table 1.2 [92][5]

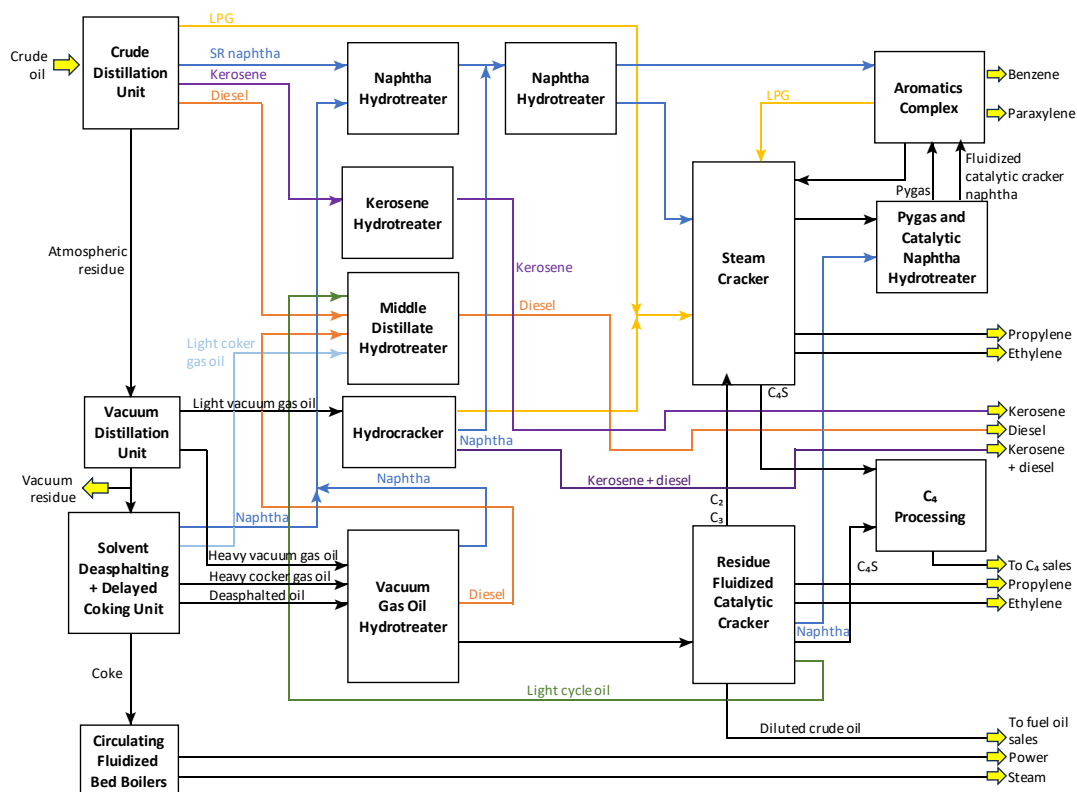


Figure 1.1. Refinery configuration for chemicals and fuels [90].

Table 1.2. Naphthas composition from crude oil fractionation, catalytic and thermal cracking [92].

Naphtha	Paraffins (wt. %)	Olefins (wt. %)	Naphthenes (wt. %)	Aromatics (wt. %)
Light SR	55	-	40	5
Medium SR	31	-	50	19
Heavy SR	30	-	44	26
Treated FCC	34	23	11	32
Light VB	64	10	25	1
Heavy VB	46	30	16	8

SR, straight-run; FCC, fluid catalytic cracker; VB, visbreaker (thermal cracking)

In addition, naphtha may be prepared by solvent extraction, cracked distillate hydrogenation, unsaturated olefins polymerization, alkylation, or by the mixture of more than one of these streams [5]. Table 1.3 shows the composition of some of those streams.

**Table 1.3.** Typical naphtha composition from other sources [91].

Processes	Paraffins (wt. %)	Olefins (wt. %)	Naphthenes (wt. %)	Aromatics (wt. %)
WTI SR	49	-	36	15
Coker	34	45	14	7
Hydrocracker	45	-	43	12
Solvent Refined Coal	38	62	36	13

WTI SR, West Texas Intermediate straight-run

On the other hand, due to its varied composition in paraffins, naphthenes, and aromatics, naphtha is divided into aliphatic and aromatic naphthas; the first is obtained directly by distillation and is subdivided into paraffinic and naphthenic naphthas, while the second is rarely obtained from petroleum as a straight-run [5][91]. Aliphatic naphthas are typically feedstock for the catalytic reforming process, and their composition varies within the ranges evidenced in Table 1.4.

**Table 1.4.** Typical aliphatic naphthas composition range [91].

Naphtha	Paraffins (v %)	Naphthenes (v %)	Aromatics (v %)
Paraffinic	50 - 70	20 - 30	5 - 15
Naphthenic	40 - 55	30 - 40	10 - 20

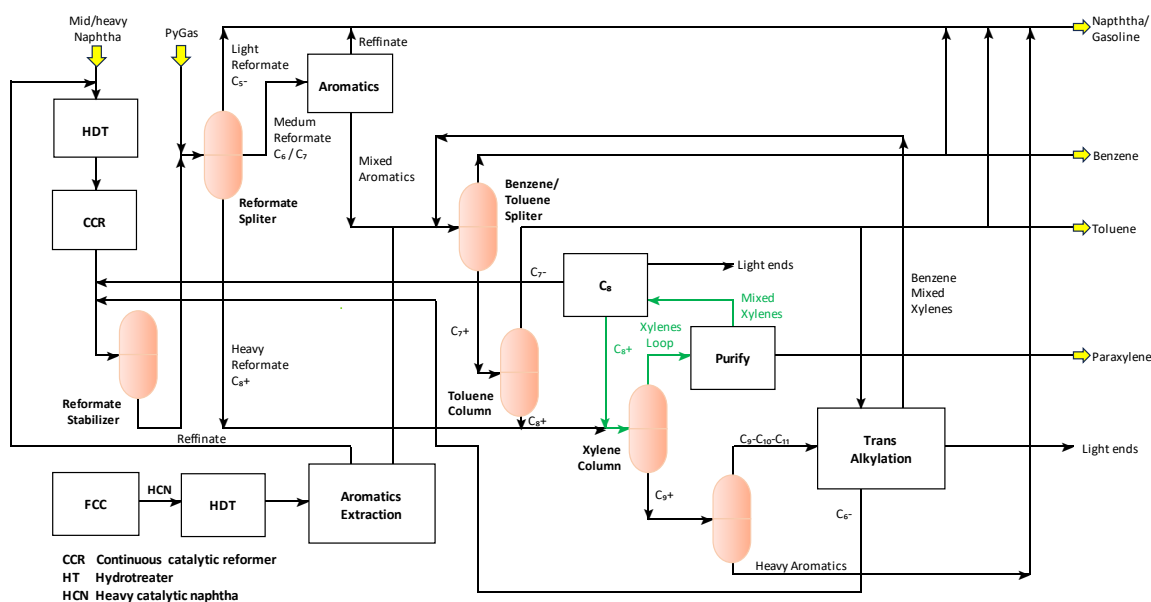
Catalytic reforming is the primary means for producing valuable aromatics (benzene, toluene, and xylenes – BTX) from fossil-based naphtha by bifunctional catalysts (metal active site and acid function) [93] whose performance depends on charge quality as is shown in Table 1.5 [91]. A typical plant configuration is shown in Figure 1.2.

Aromatics are a class of organic compounds with a specific ring structure, known as an aromatic ring, “formed by dehydrogenation of naphthenes; isomerization of alkylnaphthenes followed by dehydrogenation; dehydrocyclization of paraffins followed by dehydrogenation” in petroleum refining [87]. Due to their unique chemical properties, they are widely used in various industries, such as pharmaceuticals, dyes, and polymers. For this reason, plastic waste pyrolysis is a promising method to convert plastic waste into valuable products, including aromatics. Understanding the composition and properties of aromatics derived from plastic waste pyrolysis is crucial for developing efficient and sustainable strategies for plastic waste management and resource recovery. Therefore, studying aromatics from plastic waste pyrolysis is significant in addressing the global plastic waste crisis and promoting a circular economy.

**Table 1.5.** Effect of naphtha composition on catalytic reforming output [91].

Naphtha	Paraffinic	Naphthenic
<b>Feed, v %</b>		
Paraffins	68.6	32.6
Naphthenes	23.4	55.5
Aromatics	8.0	11.9
<b>Performance</b>		
Hydrogen, SCF/B	1200	1400
C <sub>1</sub> – C <sub>3</sub> (SCF/B)	335	160
C <sub>5</sub> + yield, v %	73.5	84.7
Aromatics, v %	67.9	69.9

SCF/B, standard cubic foot per barrel

**Figure 1.2.** Aromatics configuration plant [94].

Most studies to obtain chemicals from plastic waste have been performed with single thermoplastics polymers and with specific combinations of them, and only a few ones with real dirty and contaminated plastic waste coming from mechanical biological treatment (MBT) systems, without focusing on the conversion to aromatics or obtaining raw materials (naphtha) to produce them. During plastic waste pyrolysis, aromatics are formed partially through the breakdown of complex polymers present in the plastic waste. Factors such as temperature, pressure, reaction time, and the type of pyrolyzed plastic can influence the yield and composition. The potential uses for aromatics derived from plastic waste pyrolysis include the production of fuels, solvents, and even new plastics. However, there are challenges and opportunities in maximizing aromatics production, such as developing efficient catalysts to enhance the pyrolysis

process that increases aromatics yield through the synergy between converting heavy fractions to naphtha and their subsequent reforming.

Additionally, the purification and separation of aromatics from other by-products is crucial to ensure high-quality and marketable end products. Developing cost-effective and sustainable pyrolysis technologies is also essential to make the production of aromatics from plastic waste economically viable. Despite these challenges, the increasing global concern for plastic waste management provides an opportunity for research and innovation in plastic waste pyrolysis, paving the way for a more sustainable and circular economy.

Using aromatics from plastic waste pyrolysis in various industries can have significant environmental implications. By replacing virgin fossil-based aromatics with those derived from plastic waste, industries can reduce their carbon footprint and dependence on non-renewable resources. However, further research is needed to assess the potential environmental risks associated with the production and use of these recycled aromatics, such as emissions of harmful pollutants and the generation of hazardous waste streams.

The development of refinery configurations involving advanced technologies such as pyrolysis and catalytic cracking or integrating chemicals and fuels, like those petroleum derivatives, from plastic waste in the existing refineries will create a more efficient and sustainable refining system where the traditional oil refinery products include fuels such as gasoline, diesel fuel, jet fuel, heating oil, and other products as various types of lubricants; all of these are derived through separation processes that involve distillation, thermal cracking, steam cracking, hydrocracking, fractionating of the stream of catalytic cracking, and other chemical processes.

Pyrolytic oil is a complex mixture of compounds, just like hydrocarbons [11], and a complete interpretation of its properties and characteristics are essential to the optimum design and proper operation of any system built for its processing [106]. Despite the pilot plants allowing an understanding of the processes in general, including potential waste streams, due to operating with more feed and their technological readiness level being higher than the bench types, these, with continuous feeding of small samples during a prolonged period, provide reasonable results [95]; indeed, as of a laboratory configuration operating in batch, valuable data could be acquired through adequate and detailed analysis focused on repeatability and optimal operation conditions. Table 1.6 shows a representative collection of research carried out under different configurations and conditions to obtain chemicals and fuels from plastic waste that have reported the composition of gases and gasoline, especially olefins (on the gases) and aromatics (on gasoline).



**Table 1.6.** Thermal and catalytic cracking of thermoplastics.

Catalyst	Feedstock	Reactor	Condition	Liquid wt. %	Products Distribution	Composition	Ref.		
None	PE (30-40 g)	Parr Mini Bench Stirred	500 °C, 19.2MPa H <sub>2</sub> Atm	93	None	None	[96]		
	PP 30-40 g)			95					
	PS 30-40 g)			71					
	PET 30-40 g)			15					
None	PE	Fixed Bed Laboratory Bench	760 °C	42	None	None	[97]		
	PP			740 °C				49	
	PS			581 °C				25	
	Mix			750 °C				47	
None	HDPE (9.0 kg/h)	Pilot Scale Continuous Reactor	520 °C	96	Gsln: 18.5%	P: 52.6%, A: 0%	[98]		
ZSM-5 (5%)	HDPE (9.0 kg/h)				89	LCO: 16.1%		P: 52.5%, A: 0%	
				None		pp (9.0 kg/h)		96	HCO: 61.4%
ZSM-5 (5%)	PP (9.0 kg/h)				86				Gsln: 33.9%
				None		HDPE (9.0 kg/h)		74	LCO: 23.4%
ZSM-5 (5%)	PP (9.0 kg/h)				86				HCO: 26.6%
				None		HDPE (500 g)		Batch Reactor 2 Liters	440 °C
None	LDPE (60 g/h)				Fluidized Sand Bed Bench Scale				
		None	HDPE (900 g)	Conical Spouted Bed Reactor		500 °C	None	HCO: 43.5%	Not Specified
None	LDPE (60 g/h)				Fluidized Sand Bed Bench Scale			515 °C	90
		None	HDPE (900 g)	Conical Spouted Bed Reactor		500 °C	None		
None	LDPE (60 g/h)				Fluidized Sand Bed Bench Scale			515 °C	90
		None	HDPE (500 g)	Batch Reactor 2 Liters		440 °C	74		
None	LDPE (60 g/h)				Fluidized Sand Bed Bench Scale			515 °C	90
		None	HDPE (900 g)	Conical Spouted Bed Reactor		500 °C	None		
None	LDPE (60 g/h)				Fluidized Sand Bed Bench Scale			515 °C	90
		None	HDPE (900 g)	Conical Spouted Bed Reactor		500 °C	None		
None	LDPE (60 g/h)				Fluidized Sand Bed Bench Scale			515 °C	90
		None	HDPE (900 g)	Conical Spouted Bed Reactor		500 °C	None		
None	LDPE (60 g/h)				Fluidized Sand Bed Bench Scale			515 °C	90
		None	HDPE (900 g)	Conical Spouted Bed Reactor		500 °C	None		
None	LDPE (60 g/h)				Fluidized Sand Bed Bench Scale			515 °C	90
		None	HDPE (900 g)	Conical Spouted Bed Reactor		500 °C	None		
None	LDPE (60 g/h)				Fluidized Sand Bed Bench Scale			515 °C	90
		None	HDPE (900 g)	Conical Spouted Bed Reactor		500 °C	None		
None	LDPE (60 g/h)				Fluidized Sand Bed Bench Scale			515 °C	90
		None	HDPE (900 g)	Conical Spouted Bed Reactor		500 °C	None		
None	LDPE (60 g/h)				Fluidized Sand Bed Bench Scale			515 °C	90
		None	HDPE (900 g)	Conical Spouted Bed Reactor		500 °C	None		
None	LDPE (60 g/h)				Fluidized Sand Bed Bench Scale			515 °C	90

Products: Gsln, gasoline; LCO, light cycle oil; HCO, heavy cycle oil  
Composition: P, paraffins; N, naphthenes; A, Aromatics

Continuation...

Catalyst	Feedstock	Reactor	Condition	Liquid wt. %	Products Distribution	Composition	Ref.					
None	LDPE (60 g/h)	Fluidized Sand Bed Bench Scale	654 °C N <sub>2</sub> Atm 30 min	72	Not Specified	Not Specified	[100]					
			730 °C N <sub>2</sub> Atm 30 min	31								
			532 °C N <sub>2</sub> Atm 30 min	89								
	615 °C N <sub>2</sub> Atm 30 min		83									
	708 °C N <sub>2</sub> Atm 30 min		83									
	PS (60 g/h)											
None				-								
Al <sub>2</sub> O <sub>2</sub> (10 %)				-								
SiO <sub>2</sub> (10 %)			400 °C	-								
ZHY (10 %)			0.1-0.2 Torr	91								
ZREY (10 %)				93								
SA (10 %)	PE (2 g)	Pyrex Vessel Inside an Oven		92	Not Specified	Not Specified	[101]					
None			29									
Al <sub>2</sub> O <sub>2</sub> (10 %)			76									
SiO <sub>2</sub> (10 %)			75									
ZHY (10 %)			87									
ZREY (10 %)			87									
Si-Al (10 %)			91									
Si-Al (0.2-0.3g)			LDPE (0.5-0.25g)	Fixed Bed Reactor				375 °C 0.15 MPa	58	Gsln: 59% Wax: 1.5%	A: 26.1% Not Specified	[102]

Products: Gsln, gasoline; LCO, light cycle oil; HCO, heavy cycle oil

Composition: P, paraffins; N, naphthenes; A, Aromatics

Continuation...

Catalyst	Feedstock	Reactor	Condition	Liquid wt. %	Products Distribution	Composition	Rf.
Si-Al (0.2-0.3g)	LDPE (0.5-0.25g)	Fixed Bed Reactor	400 °C 0.15 MPa	52	Not Specified	Not Specified	[102]
			425 °C 0.15MPa	41	Not Specified	Not Specified	
			375 °C 0.15 MPa	47	Gsln: 46.5% Wax: 0.5%	A: 58% Not Specified	
HZSM-5 (0.2-0.3g)			400 °C 0.15 MPa	35	Not Specified	Not Specified	
			425 °C 0.15MPa	35	Not Specified	Not Specified	
HZSM-5 (8 g)	HDPE (5 g/min)	Conical Spouted Bed Reactor	500 °C N <sub>2</sub> Atm 5 h	Not Spf.	Gas: 1.5%	P: 23.3%, O: 76.7%	[103]
					Gsln: 5.86%	P: 5.7%, IP: 42.6% O: 43.6%, N: 3.2%	
					Dsl: 25.64%	A: 4.9%	
					Wax: 67.0%	P: 36 % DO: 12%, O: 53%	
NiCaAl (0.1 g)				65			
NiAl (0.1 g)				63			
Ni/Al <sub>2</sub> O <sub>3</sub> (0.1 g)				62			
Ni/CeO <sub>2</sub> (0.1 g)				61			
Ni/Y <sub>2</sub> O <sub>3</sub> (0.1 g)	LDPE (2 g)	Fixed Bed Two Stage Reactor	S1: 500 °C	64	Not Specified	Not Specified	[104]
Ni/SiO <sub>2</sub> (0.1 g)			S2: 800 °C N <sub>2</sub> Atm	69			
Ni/MgO (0.1 g)				68			
Ni/ZSM-5 (0.1 g)				71			
Ni/TiO <sub>2</sub> (0.1 g)				68			
Al <sub>2</sub> O <sub>3</sub> (0.1 g)				76			
None	LDPE: 31.5 HDPE: 21.5 PP: 35, PS: 12	Batch Reactor 23 Liters	520 °C 1 Atm	65	Gsln: 74.5%	P: 15%, O: 50.6%, IP: 4.8%, A: 18.7% N: 9.7%	[105]

Products: Gsln, gasoline; LCO, light cycle oil; HCO, heavy cycle oil

Composition: P, paraffins; O, olefins; IP, isoparaffins; N, naphthenes; A, Aromatics

## References

- [1] A. R. Calhoun and J. Golmanavich, *Fundamental Skills and Polymer Science*. Denton-Texas: Society of Plastics Engineers, 2004.
- [2] Organisation for Economic Co-operation and Development, "Global Plastics Outlook: Policy Scenarios to 2060," *Glob. Plast. Outlook*, p. 10, 2022, [Online]. Available: <https://www.oecd.org/environment/plastics/>.
- [3] A. Vianello *et al.*, "Microplastic particles in sediments of Lagoon of Venice, Italy: First observations on occurrence, spatial patterns and identification," *Estuar. Coast. Shelf Sci.*, vol. 130, pp. 54–61, 2013, doi: 10.1016/j.ecss.2013.03.022.
- [4] G. J. and M. S. Molgas Michael, Hubball Jack, "Overview of Polymer, Additives, and Processing," in *Handbook for the chemical analysis of plastic and polymer additives*, T. & F. Group, Ed. Boca Raton - Florida: CRC Press, 2008, pp. 1–9.
- [5] J. G. Speight, *Handbook of Petrochemical Processes*. Boca Raton: CRC Press, 2019.
- [6] C. A. Harper, "Preface," in *Handbook of Plastic Processes*, C. A. Harper, Ed. Hoboken, New Jersey: John Wiley & Sons, Inc., 2006, p. ix.
- [7] C. A. Harper, "Thermoplastics," in *Modern Plastics Handbook*, C. A. Harper, Ed. Lutherville, Maryland: McGraw-Hill, 2000, p. 1.1.
- [8] M. Hassanpour and S. A. Unnisa, "Plastics; Applications, Materials, Processing and Techniques," *Plast. Surg. Mod. Tech.*, vol. 2, no. 1, 2017, doi: 10.29011/2577-1701.100009.
- [9] European Council, "Directive (Eu) 2019/904 of the European Parliament and of the Council of 5 June 2019 on the reduction of the impact of certain plastic products on the environment," *Www.Plasticseurope.De*, vol. 2019, no. March, pp. 1–19, 2019, [Online]. Available: <https://www.plasticseurope.org/en/resources/publications/1689-working-together-towards-more-sustainable-plastics%0Ahttps://www.plasticseurope.org/en/resources/publications%0Ahttps://eur-lex.europa.eu/legal-content/EN/TXT/PDF/?uri=CELEX:32019L0904&from=EN>.
- [10] United Nation Environment Programme, *SINGLE-USE PLASTICS: A Roadmap for Sustainability*, Tara Canno. United Nations Environment Programme, 2018.
- [11] J. and K. W. Scheirs, *Feedstock Recycling and Pyrolysis of Waste Plastics*. West Sussex: John Wiley & Sons, Ltd, 2006.
- [12] Y. Chen, A. K. Awasthi, F. Wei, Q. Tan, and J. Li, "Single-use plastics: Production, usage, disposal, and adverse impacts," *Sci. Total Environ.*, vol. 752, p. 141772, 2021, doi: 10.1016/j.scitotenv.2020.141772.
- [13] Plastics Europe, "Plastics – the Facts 2022," *Plastics Europe*, no. October. Plastics Europe, Brussels, Belgium, p. 79, 2022.
- [14] Plastics Europe, "Plastics – the fast Facts 2023," Brussels, Belgium, 2023.
- [15] D. Lane and T. Park, *The Plastics Paradox: Facts for a Brighter Future*. 2020.

- 
- [16] W. Vermeiren and J. P. Gilson, "Impact of zeolites on the petroleum and petrochemical industry," *Top. Catal.*, vol. 52, no. 9, pp. 1131–1161, 2009, doi: 10.1007/s11244-009-9271-8.
- [17] J. Burn, "Global refining capacity," *The Oil Drum*, 2011. <http://theoildrum.com/node/7641> (accessed Oct. 17, 2023).
- [18] C. Batista, "Understanding The 7 Types Of Plastic," *The Eco Hub*, 2022. <https://theecohub.com/types-of-plastic/> (accessed Oct. 24, 2023).
- [19] "Plastic Food Packing Symbols and What They Mean," *THONG GUAN INDUSTRIES BERHAD*, 2019. <https://www.thongguan.com/plastic-food-packaging-symbols-and-what-they-mean/> (accessed Oct. 24, 2023).
- [20] R. Geyer, J. R. Jambeck, and K. L. Law, "Production, use, and fate of all plastics ever made," *Sci. Adv.*, vol. 3, no. 7, pp. 25–29, 2017, doi: 10.1126/sciadv.1700782.
- [21] Plastics Europe, *Plastics - the Facts 2021*. Brussels, Belgium: Plastics Europe, 2021.
- [22] J. Gilpin, R., Wagel, D., Solch, "Production, distribution, and fate of polychlorinated dibenzo-p-dioxins, dibenzofur-ans, and related organohalogens in the environment," in *Dioxins and health*, 2nd ed., A. S. and T. A. Gasiewicz, Ed. Hoboken, New Jersey.: John Wiley & Sons, Inc., 2003, pp. 55–88.
- [23] S. J. Royer, S. Ferrón, S. T. Wilson, and D. M. Karl, "Production of methane and ethylene from plastic in the environment," *PLoS One*, vol. 13, no. 8, pp. 1–13, 2018, doi: 10.1371/journal.pone.0200574.
- [24] I. E. Napper and R. C. Thompson, "Environmental Deterioration of Biodegradable, Oxo-biodegradable, Compostable, and Conventional Plastic Carrier Bags in the Sea, Soil, and Open-Air over a 3-Year Period," *Environ. Sci. Technol.*, vol. 53, no. 9, pp. 4775–4783, 2019, doi: 10.1021/acs.est.8b06984.
- [25] K. E. Micales, J.A. & Skog, "The Decomposition of Forest Products in Landfills Compiled by :," vol. 39, no. 2, pp. 145–158, 2005.
- [26] C. Longo, M. Savaris, M. Zeni, R. N. Brandalise, and A. M. C. Grisa, "Degradation study of polypropylene (PP) and Bioriented polypropylene (BOPP) in the environment," *Mater. Res.*, vol. 14, no. 4, pp. 442–448, 2011, doi: 10.1590/S1516-14392011005000080.
- [27] J. Oehlmann *et al.*, "A critical analysis of the biological impacts of plasticizers on wildlife," *Philos. Trans. R. Soc. B Biol. Sci.*, vol. 364, no. 1526, pp. 2047–2062, 2009, doi: 10.1098/rstb.2008.0242.
- [28] W. M. Wu, J. Yang, and C. S. Criddle, "Microplastics pollution and reduction strategies," *Front. Environ. Sci. Eng.*, vol. 11, no. 1, pp. 1–4, 2017, doi: 10.1007/s11783-017-0897-7.
- [29] S. Karbalaei, P. Hanachi, T. R. Walker, and M. Cole, "Occurrence, sources, human health impacts and mitigation of microplastic pollution," *Environ. Sci. Pollut. Res.*, vol. 25, no. 36, pp. 36046–36063, 2018, doi: 10.1007/s11356-018-3508-7.
- [30] A. K. Priya *et al.*, "Microplastics in the environment: Recent developments in characteristic,

- occurrence, identification and ecological risk,” *Chemosphere*, vol. 298, no. February, p. 134161, 2022, doi: 10.1016/j.chemosphere.2022.134161.
- [31] J. Li, H. Liu, and J. Paul Chen, “Microplastics in freshwater systems: A review on occurrence, environmental effects, and methods for microplastics detection,” *Water Res.*, vol. 137, pp. 362–374, 2018, doi: 10.1016/j.watres.2017.12.056.
- [32] T. D. Moshood, G. Nawanir, F. Mahmud, F. Mohamad, M. H. Ahmad, and A. AbdulGhani, “Biodegradable plastic applications towards sustainability: A recent innovations in the green product,” *Clean. Eng. Technol.*, vol. 6, p. 100404, 2022, doi: 10.1016/j.clet.2022.100404.
- [33] “Biodegradable Vs Compostable: Breaking Down The Differences,” *KEEO*, 2023. <https://www.keeo.com.au/blogs/news/biodegradable-vs-compostable-breaking-down-the-differences#:~:text=Both compostable and biodegradable packaging,providing nutrients to the plants.> (accessed Oct. 25, 2023).
- [34] D. Knoblauch and L. Mederake, “Government policies combatting plastic pollution,” *Curr. Opin. Toxicol.*, vol. 28, pp. 87–96, 2021, doi: 10.1016/j.cotox.2021.10.003.
- [35] E. M. Bennett and P. Alexandridis, “Informing the public and educating students on plastic recycling,” *Recycling*, vol. 6, no. 4, 2021, doi: 10.3390/recycling6040069.
- [36] J. Hopewell, R. Dvorak, and E. Kosior, “Plastics recycling: Challenges and opportunities,” *Philos. Trans. R. Soc. B Biol. Sci.*, vol. 364, no. 1526, pp. 2115–2126, 2009, doi: 10.1098/rstb.2008.0311.
- [37] V. Heath, “The perils of plastic,” *Nat. Rev. Endocrinol.*, vol. 6, no. 5, p. 237, 2010, doi: 10.1038/nrendo.2010.48.
- [38] EMF, “The New Plastics Economy: Rethinking the Future of Plastics & Catalysing Action,” *Ellen MacArthur Found.*, 2017, [Online]. Available: <https://www.ellenmacarthurfoundation.org/publications/the-new-plastics-economy-rethinking-the-future-of-plastics-catalysing-action>.
- [39] S. M. Al-Salem, P. Lettieri, and J. Baeyens, “The valorization of plastic solid waste (PSW) by primary to quaternary routes: From re-use to energy and chemicals,” *Prog. Energy Combust. Sci.*, vol. 36, no. 1, pp. 103–129, 2010, doi: 10.1016/j.pecs.2009.09.001.
- [40] K. Ragaert, L. Delva, and K. Van Geem, “Mechanical and chemical recycling of solid plastic waste,” *Waste Manag.*, vol. 69, pp. 24–58, 2017, doi: 10.1016/j.wasman.2017.07.044.
- [41] V. Rizos, P. Urban, E. Righetti, and A. Kassab, “Chemical Recycling of Plastics: Technologies, trends and policy implications,” *Ceps in-Depth Anal.*, p. 54, 2023.
- [42] L. Dai *et al.*, “Pyrolysis technology for plastic waste recycling: A state-of-the-art review,” *Prog. Energy Combust. Sci.*, vol. 93, no. June, p. 101021, 2022, doi: 10.1016/j.pecs.2022.101021.
- [43] T. C. G. Forum, “Chemical Recycling in a Circular Economy for Plastics,” *Consum. Goods Forum*, no. April, p. 33, 2022, [Online]. Available:

- <https://www.theconsumergoodsforum.com/wp-content/uploads/2022/04/Chemical-Recycling-in-a-Circular-Economy-A-Vision-and-Principles-Paper.pdf>.
- [44] J. P. Lange, "Managing Plastic Waste-Sorting, Recycling, Disposal, and Product Redesign," *ACS Sustain. Chem. Eng.*, vol. 9, no. 47, pp. 15722–15738, 2021, doi: 10.1021/acssuschemeng.1c05013.
- [45] I. A. Ignatyev, W. Thielemans, and B. Vander Beke, "Recycling of polymers: A review," *ChemSusChem*, vol. 7, no. 6, pp. 1579–1593, 2014, doi: 10.1002/cssc.201300898.
- [46] S. Huysveld *et al.*, "Technical and market substitutability of recycled materials: Calculating the environmental benefits of mechanical and chemical recycling of plastic packaging waste," *Waste Manag.*, vol. 152, no. April, pp. 69–79, 2022, doi: 10.1016/j.wasman.2022.08.006.
- [47] M. Gear, J. Sadhukhan, R. Thorpe, R. Clift, J. Seville, and M. Keast, "A life cycle assessment data analysis toolkit for the design of novel processes – A case study for a thermal cracking process for mixed plastic waste," *J. Clean. Prod.*, vol. 180, pp. 735–747, 2018, doi: 10.1016/j.jclepro.2018.01.015.
- [48] O. Dogu *et al.*, "The chemistry of chemical recycling of solid plastic waste via pyrolysis and gasification: State-of-the-art, challenges, and future directions," *Prog. Energy Combust. Sci.*, vol. 84, p. 100901, 2021, doi: 10.1016/j.pecs.2020.100901.
- [49] M. Kusenberg *et al.*, "Towards high-quality petrochemical feedstocks from mixed plastic packaging waste via advanced recycling: The past, present and future," *Fuel Process. Technol.*, vol. 238, no. June, p. 107474, 2022, doi: 10.1016/j.fuproc.2022.107474.
- [50] M. et. al. Crippa, *A circular economy for plastics – Insights from research and innovation to inform policy and funding decisions*. Brussels: European Union, 2019.
- [51] J. M. Simon and Matin Sarah, "Zero Waste Europe 'El Dorado of Chemical Recycling - State of play and policy challenges,'" Brussels, Belgium, 2019.
- [52] J. Sherwood, "Closed-Loop Recycling of Polymers Using Solvents : Remaking plastics for a circular economy," *Johnson Matthey Technol. Rev.*, vol. 64, no. 1, pp. 4–15, 2019, doi: 10.1595/205651319x15574756736831.
- [53] S. Hann and T. Connock, "Chemical Recycling: State of Play," Bristol, UK, 2020.
- [54] Y. B. Zhao, X. D. Lv, and H. G. Ni, "Solvent-based separation and recycling of waste plastics: A review," *Chemosphere*, vol. 209, pp. 707–720, 2018, doi: 10.1016/j.chemosphere.2018.06.095.
- [55] E. Harscoet, S. Chouvinc, A.-C. Faugeras, and F. Ammenti -Deloitte, "Chemical and Physico-Chemical Recycling of Plastic Waste Final Report," Villeurbanne, France, 2022. [Online]. Available: [www.record-net.org](http://www.record-net.org).
- [56] M. Hong and E. Y. X. Chen, "Chemically recyclable polymers: A circular economy approach to sustainability," *Green Chem.*, vol. 19, no. 16, pp. 3692–3706, 2017, doi: 10.1039/c7gc01496a.

- [57] J. Aguado and D. Serrano, *Feedstock Recycling of Plastic Wastes*, The Royal. Cambridge, 1999.
- [58] C. Delavelle and B. De Caemel, "Recyclage chimique des déchets plastiques : Situation et perspectives. Etat de l'art et avis d'experts," Villeurbanne, France, 2015. [Online]. Available: [www.record-net.org](http://www.record-net.org).
- [59] SYSTEMIQ, "ReShaping Plastics: Pathways to a Circular, Climate Neutral Plastics System in Europe," Amsterdam, 2022. [Online]. Available: <https://plasticseurope.org/knowledge-hub/systemiq-reshaping-plastics/%0A>.
- [60] R. P. Lee, M. Tschoepe, and R. Voss, "Perception of chemical recycling and its role in the transition towards a circular carbon economy: A case study in Germany," *Waste Manag.*, vol. 125, pp. 280–292, 2021, doi: 10.1016/j.wasman.2021.02.041.
- [61] Sarah Casey (World Refining Association), "Waste recycling : an opportunity," *Digit. Refin.*, no. January, pp. 1–4, 2020, [Online]. Available: <https://cdn.digitalrefining.com/data/articles/file/1002493-wra-waste-recycGBPe.pdf>.
- [62] S. Budsareechai, A. J. Hunt, and Y. Ngernyen, "Catalytic pyrolysis of plastic waste for the production of liquid fuels for engines," *RSC Adv.*, vol. 9, no. 10, pp. 5844–5857, 2019, doi: 10.1039/c8ra10058f.
- [63] S. D. Anuar Sharuddin, F. Abnisa, W. M. A. Wan Daud, and M. K. Aroua, "A review on pyrolysis of plastic wastes," *Energy Convers. Manag.*, vol. 115, pp. 308–326, 2016, doi: 10.1016/j.enconman.2016.02.037.
- [64] R. Miandad, M. A. Barakat, A. S. Aburizaiza, M. Rehan, and A. S. Nizami, "Catalytic pyrolysis of plastic waste: A review," *Process Saf. Environ. Prot.*, vol. 102, pp. 822–838, 2016, doi: 10.1016/j.psep.2016.06.022.
- [65] Y. Peng *et al.*, "A review on catalytic pyrolysis of plastic wastes to high-value products," *Energy Convers. Manag.*, vol. 254, no. December 2021, p. 115243, 2022, doi: 10.1016/j.enconman.2022.115243.
- [66] R. H. Nielsen and P. K. Doolin, "Metals passivation," *Stud. Surf. Sci. Catal.*, vol. 76, no. C, pp. 339–384, 1993, doi: 10.1016/S0167-2991(08)63833-1.
- [67] J. T. Richardson, *Principles of Catalyst Development*, Second Pri. New York: Springer Science+Business Media, LLC, 1992.
- [68] G. Fadillah, I. Fatimah, I. Sahroni, M. M. Musawwa, T. M. I. Mahlia, and O. Muraza, "Recent progress in low-cost catalysts for pyrolysis of plastic waste to fuels," *Catalysts*, vol. 11, no. 7, 2021, doi: 10.3390/catal11070837.
- [69] F. W. Harun, E. A. Almadani, and S. M. Radzi, "Metal cation exchanged montmorillonite K10 (MMT K10): Surface properties and catalytic activity," *J. Sci. Res. Dev.*, vol. 3, no. 3, pp. 90–96, 2016, [Online]. Available: [www.jsrad.org](http://www.jsrad.org).
- [70] J. Pérez Pariente, V. Fornés, A. Corma, and A. Mifsud, "The surface acidity and hydrothermal stability of sepiolite derivatives," *Appl. Clay Sci.*, vol. 3, no. 4, pp. 299–306,



- 1988, doi: 10.1016/0169-1317(88)90021-X.
- [71] C. H. Zhou *et al.*, "Roles of texture and acidity of acid-activated sepiolite catalysts in gas-phase catalytic dehydration of glycerol to acrolein," *Mol. Catal.*, vol. 434, pp. 219–231, 2017, doi: 10.1016/j.mcat.2016.12.022.
- [72] Bartholomew C.H. and Farrauto R.J., *Fundamentals of Industrial Catalytic Processes*, Second. Hoboken: John Wiley & Sons, Ltd, 2006.
- [73] S. Ügdüler, K. M. Van Geem, M. Roosen, E. I. P. Delbeke, and S. De Meester, "Challenges and opportunities of solvent-based additive extraction methods for plastic recycling," *Waste Manag.*, vol. 104, pp. 148–182, 2020, doi: 10.1016/j.wasman.2020.01.003.
- [74] K. Akubo, M. A. Nahil, and P. T. Williams, "Aromatic fuel oils produced from the pyrolysis-catalysis of polyethylene plastic with metal-impregnated zeolite catalysts," *J. Energy Inst.*, vol. 92, no. 1, pp. 195–202, 2019, doi: 10.1016/j.joei.2017.10.009.
- [75] X. Lin, L. Kong, X. Ren, D. Zhang, H. Cai, and H. Lei, "Catalytic co-pyrolysis of torrefied poplar wood and high-density polyethylene over hierarchical HZSM-5 for mono-aromatics production," *Renew. Energy*, vol. 164, pp. 87–95, 2021, doi: 10.1016/j.renene.2020.09.071.
- [76] A. Inayat, A. Inayat, W. Schwieger, B. Sokolova, and P. Lestinsky, "Enhancing aromatics and olefins yields in thermo-catalytic pyrolysis of LDPE over zeolites: Role of staged catalysis and acid site density of HZSM-5," *Fuel*, vol. 314, no. January, p. 123071, 2022, doi: 10.1016/j.fuel.2021.123071.
- [77] X. Lin, Z. Zhang, Z. Zhang, J. Sun, Q. Wang, and C. U. Pittman, "Catalytic fast pyrolysis of a wood-plastic composite with metal oxides as catalysts," *Waste Manag.*, vol. 79, pp. 38–47, 2018, doi: 10.1016/j.wasman.2018.07.021.
- [78] G. Elordi, M. Olazar, G. Lopez, M. Artetxe, and J. Bilbao, "Continuous polyolefin cracking on an HZSM-5 zeolite catalyst in a conical spouted bed reactor," *Ind. Eng. Chem. Res.*, vol. 50, no. 10, pp. 6061–6070, 2011, doi: 10.1021/ie2002999.
- [79] J. F. tczak and H. de P. C. José Miguel Hidalgo Herrador \*, Martyna Murat, Zdeneĭk Tišler, "Direct Polypropylene and Polyethylene Liquefaction in CO<sub>2</sub> and N<sub>2</sub> Atmospheres Using MgO Light and CaO as Catalysts," *MDPI*, vol. 15, no. 3, p. 844, 2022.
- [80] S. Uçar, S. Karagöz, T. Karayildirim, and J. Yanik, "Conversion of polymers to fuels in a refinery stream," *Polym. Degrad. Stab.*, vol. 75, no. 1, pp. 161–171, 2002, doi: 10.1016/S0141-3910(01)00215-4.
- [81] J. Wang *et al.*, "Converting polycarbonate and polystyrene plastic wastes into aromatic hydrocarbons via catalytic fast co-pyrolysis," *J. Hazard. Mater.*, vol. 386, no. 16, p. 121970, 2020, doi: 10.1016/j.jhazmat.2019.121970.
- [82] Y. Xue, P. Johnston, and X. Bai, "Effect of catalyst contact mode and gas atmosphere during catalytic pyrolysis of waste plastics," *Energy Convers. Manag.*, vol. 142, pp. 441–451, 2017, doi: 10.1016/j.enconman.2017.03.071.

- [83] L. Dai *et al.*, "Catalytic fast pyrolysis of low density polyethylene into naphtha with high selectivity by dual-catalyst tandem catalysis," *Sci. Total Environ.*, vol. 771, p. 144995, 2021, doi: 10.1016/j.scitotenv.2021.144995.
- [84] M. S. Qureshi *et al.*, "Pyrolysis of plastic waste: Opportunities and challenges," *J. Anal. Appl. Pyrolysis*, vol. 152, no. February, 2020, doi: 10.1016/j.jaap.2020.104804.
- [85] S. H. Gebre, M. G. Sendeku, and M. Bahri, "Recent Trends in the Pyrolysis of Non-Degradable Waste Plastics," *ChemistryOpen*, vol. 10, no. 12, pp. 1202–1226, 2021, doi: 10.1002/open.202100184.
- [86] S. M. Al-Salem, A. Antelava, A. Constantinou, G. Manos, and A. Dutta, "A review on thermal and catalytic pyrolysis of plastic solid waste (PSW)," *J. Environ. Manage.*, vol. 197, no. 1408, pp. 177–198, 2017, doi: 10.1016/j.jenvman.2017.03.084.
- [87] G. M. Wells, *Handbook of Petrochemicals and Processes*. New York, USA: Routledge Revivals, 2018.
- [88] R. Larraz, "A brief history of oil refining," *Substantia*, vol. 5, no. 2, pp. 129–152, 2021, doi: 10.36253/Substantia-1191.
- [89] G. Totten, S. Westbrook, and R. Shah, *Fuels and Lubricants Handbook: Technology, Properties, Performance, and Testing*, ASTM. Glen Burnie: ASTM International, 2003.
- [90] B. Stamateris and D. Gillis, "Towards a zero gasoline production refinery: Part 2 'Refinery configurations can suit various processing objectives, such as variations to the propylene-to-ethylene ratio and production of middle distillates and aromatics,'" *Pet. Technol. Q.*, vol. 18, no. 5, pp. 17–27, 2013.
- [91] S. Oyekan, "Basic Principles of Catalytic Reforming Processes," in *Catalytic Naphtha Reforming Process*, Boca Raton - Florida: CRC Press, 2019, pp. 111–152.
- [92] G. Antos and A. Aitani, "Compositional Analysis of Naphtha and Reformate," in *Catalytic Naphtha Reforming*, 2nd ed., G. Antos and A. Aitani, Eds. New York, USA: Marcel Dekker, Inc., 2004, pp. 1–23.
- [93] M. R. Rahimpour, M. Jafari, and D. Iranshahi, "Progress in catalytic naphtha reforming process: A review," *Appl. Energy*, vol. 109, pp. 79–93, 2013, doi: 10.1016/j.apenergy.2013.03.080.
- [94] B. Stamateris, "Towards a zero gasoline production refinery: Part 1 'Integrating products from the steam cracker, aromatics complex, and FCC unit to produce petrochemicals without gasoline may offer more attractive margins,'" *Pet. Technol. Q.*, vol. 18, no. 3, 2013.
- [95] F. Wood-Balck, "Considerations for Scale-Up – Moving from the Bench to the Pilot Plant to Full Production," in *Academia and Industrial Pilot Plant Operations and Safety*, vol. 1163, M. More and E. Ledesma, Eds. Houston, Texas: ACS Symposium Series, 2014, pp. 36–45.
- [96] P. T. Williams and E. Slaney, "Analysis of products from the pyrolysis and liquefaction of single plastics and waste plastic mixtures," *Resour. Conserv. Recycl.*, vol. 51, no. 4, pp. 754–769, 2007, doi: 10.1016/j.resconrec.2006.12.002.

- 
- [97] A. G. Buekens and H. Huang, "Catalytic plastics cracking for recovery of gasoline-range hydrocarbons from municipal plastic wastes," *Resour. Conserv. Recycl.*, vol. 23, no. 3, pp. 163–181, 1998, doi: 10.1016/S0921-3449(98)00025-1.
- [98] N. Miskolczi, A. Angyal, L. Bartha, and I. Valkai, "Fuels by pyrolysis of waste plastics from agricultural and packaging sectors in a pilot scale reactor," *Fuel Process. Technol.*, vol. 90, no. 7–8, pp. 1032–1040, 2009, doi: 10.1016/j.fuproc.2009.04.019.
- [99] B. K. Sharma, B. R. Moser, K. E. Vermillion, K. M. Doll, and N. Rajagopalan, "Production, characterization and fuel properties of alternative diesel fuel from pyrolysis of waste plastic grocery bags," *Fuel Process. Technol.*, vol. 122, pp. 79–90, 2014, doi: 10.1016/j.fuproc.2014.01.019.
- [100] D. S. Scott, S. R. Czernik, J. Piskorz, and D. S. A. G. Radlein, "Fast Pyrolysis of Plastic Wastes," *Energy and Fuels*, vol. 4, no. 4, pp. 407–411, 1990, doi: 10.1021/ef00022a013.
- [101] P. L. Beltrame, P. Carniti, G. Audisio, and F. Bertini, "Catalytic degradation of polymers: Part II-Degradation of polyethylene," *Polym. Degrad. Stab.*, vol. 26, no. 3, pp. 209–220, 1989, doi: 10.1016/0141-3910(89)90074-8.
- [102] Y. Uemichi, J. Nakamura, T. Itoh, M. Sugioka, A. A. Garforth, and J. Dwyer, "Conversion of polyethylene into gasoline-range fuels by two-stage catalytic degradation using silica-alumina and HZSM-5 zeolite," *Ind. Eng. Chem. Res.*, vol. 38, no. 2, pp. 385–390, 1999, doi: 10.1021/ie980341+.
- [103] M. Artetxe, G. Lopez, M. Amutio, G. Elordi, J. Bilbao, and M. Olazar, "Cracking of high density polyethylene pyrolysis waxes on HZSM-5 catalysts of different acidity," *Ind. Eng. Chem. Res.*, vol. 52, no. 31, pp. 10637–10645, 2013, doi: 10.1021/ie4014869.
- [104] J. Huang, A. Veksha, W. P. Chan, and G. Lisak, "Support effects on thermocatalytic pyrolysis-reforming of polyethylene over impregnated Ni catalysts," *Appl. Catal. A Gen.*, vol. 622, no. May, p. 118222, 2021, doi: 10.1016/j.apcata.2021.118222.
- [105] Z. Dobó, G. Kecsmár, G. Nagy, T. Koós, G. Muránszky, and M. Ayari, "Characterization of Gasoline-like Transportation Fuels Obtained by Distillation of Pyrolysis Oils from Plastic Waste Mixtures," *Energy & Fuels*, vol. 35, no. 3, pp. 2347–2356, 2021, doi: 10.1021/acs.energyfuels.0c04022.
- [106] M. R. Riazi, *Characterization and Properties of Petroleum Fractions*, 1st ed., vol. 1, no. 1. Philadelphia: ASTM, 2005.



## **II OBJECTIVES**



## Chapter 2

### 2. Objectives

This doctoral thesis aims to solve the drawbacks of chemical recycling for their implementation by intensifying thermal and catalytic processes that allow their liquid products to be co-processed in the hydrocarbon refining industry for transfer to the productive sector and contribute to reducing landfills. Therefore, the main objective of the thesis is to provide innovative technological solutions based on pyrolysis to support the transition towards a circular economy of plastics. The thesis is primarily focused on mixed post-consumer plastic waste comprised of various plastic types intermingled with contaminants that cannot be mechanically recycled.

Following, the specific, measurable goals that the study aims to achieve grouped by articles are presented:

- 2.1. The main objective of the first published paper is to identify the optimal conditions to obtain high yields of the liquid fraction as of a real mixture of post-consumer plastic waste and evaluate specific mathematical models used in hydrocarbon characterization to calculate the physical and chemical properties of the liquid product.

Specific objectives:

- 2.1.1. To identify the optimal conditions to obtain maximum yields of the liquid fraction.
- 2.1.2. To experimentally measure the basic characteristic parameters of pyrolytic oils.
- 2.1.3. To use correlations or equations used in the hydrocarbon industry to estimate the measured properties, making a comparison between the measured and calculated properties by predictive mathematical expressions.
- 2.1.5 To develop new correlations for estimating pyrolytic oil properties.

- 2.2. The primary goal of the second article is to examine the thermal and catalytic pyrolysis of different types of plastic waste and a dirty mixture of post-consumer plastic waste that comes from municipal solid waste over commercial acid zeolites (HY and HZSM-5) and low-cost, basic materials (CaO and MgO) to produce gasoline-range products.

Specific objectives:

- 2.2.1. To determine the structural, chemical, and morphological properties of the catalysts.
- 2.2.2. To analyze the product yields of liquid oil of thermal and catalytic pyrolysis of individual plastics and the real mixture of plastics.
- 2.2.3. To analyze the hydrocarbon types in the gasoline-range product in both thermal and catalytic pyrolysis to investigate the influence of the polymer and catalyst on the gasoline-range product characteristics.

- 2.3. To produce traditional fuels (such as gasoline, kerosine, and diesel), the primary goal of the third published paper is to develop a pyrolysis process for non-recyclable plastics using an in-situ catalytic scheme employing sepiolite and two montmorillonites (MK10 and MK30) as catalysts.

Specific objectives:

- 2.3.1. To determine the structural, chemical, and morphological properties of the catalysts.  
2.3.2. To determine the yields of different fuel fractions, including a detailed study of the composition of gases, gasoline, kerosine, diesel, and bottom products.

- 2.4. The main objective of the fourth paper is to investigate the effects of commercial zeolite catalysts HY and HZSM-5 and their metal-loaded catalysts (Ni or Co) in catalytic pyrolysis of post-consumer plastic waste collected in municipal solid waste.

Specific objectives:

- 2.4.1. To determine the structural, chemical, and morphological properties of the catalysts.  
2.4.2. To determine the yields of different fuel fractions, including a detailed study of the composition of gasoline, light cycle oil, and heavy cycle oil products.



## **III RESULTS**



## Chapter 3

# Characterization of liquid fraction obtained from pyrolysis of post-consumer mixed plastic waste: A comparing between measured and calculated parameters

M.F. Paucar-Sánchez, M. Calero, G. Blázquez, M.J. Muñoz-Batista, M.A. Martín-Lara

*Department of Chemical Engineering University of Granada, 18071 Granada, Spain*

Process Safety and Environmental Protection, ISSN: 0957-5820, eISSN: 1744-3598. Published by Elsevier Ltd on behalf of Institution of Chemical Engineers.

*Volume:* 159

*Pages:* 1053-1063

*Country:* United Kingdom

*DOI:* <https://doi.org/10.1016/j.psep.2022.01.081>

- *Category:* Engineering, Environmental. *Journal Impact Factor, JIF (2022):* 7.8. *Category Ranking:* 11/55 (Q1).
- *Category:* Engineering, Chemical. *Journal Impact Factor, JIF (2022):* 7.8. *Category Ranking:* 15/140 (Q1).

*Article history:*

Received 10 December 2021

Received in revised form 11 January 2022

Accepted 30 January 2022

Available online 2 February 2022



## Abstract

In this study, thermal pyrolysis of a real mixture of plastic wastes collected from municipal solid waste of Granada (Spain) was performed to obtain a liquid oil. The goals of the present study were: 1) identify the optimal conditions to obtain maximum yields of the liquid fraction, 2) experimentally measure basic characteristic parameters of pyrolytic oils, 3) use correlations or equations used in the hydrocarbon industry to estimate the measured properties, 4) make a comparison between the measured and calculated properties by predictive mathematical expressions, 5) develop new correlations for estimating pyrolytic oil properties. As the main result, the optimal temperature to obtain the maximum yield of liquid fraction was 500 °C. The physical and chemical properties of pyrolytic oils changed as temperature increased due to hydrogenation and dehydrogenation reactions. Also, the approximation of the chromatography data allowed us to determine, by simulated distillation, the potential fuel yields that will be obtained if processed as synthetic crude in an atmospheric tower and a vacuum tower. Finally, two novel modified equations were proposed to estimate the specific gravity and refractive index parameters for pyrolytic oils.

**Keywords:** Thermal cracking, waste plastics, pyrolysis, hydrocarbons characterization

### 3.1. Introduction

The pyrolysis or thermal cracking products of plastic wastes are somewhat unpredictable due to their nature, quantity, and behavior during thermolysis, as well as the eventual influence of reaction products and mechanisms, especially when it comes to plastic wastes of unknown origin or their blend. Depending on the polymer or their mixes and operating conditions, the gaseous and liquid products' yield and composition can vary widely (Scheirs, 2006). About this, few studies have been conducted to determine interactions and synergistic effects during degradation of the polymer mix and real pool of plastic wastes. In certain cases, the results and conclusions are contradictory due to different results observed when a blend degrades compared to the conversion of their individual polymers. On the other hand, the real and theoretical yields suggested that the primary products formed by the degradation of each polymer can react with those of the decomposition of other plastics present in the mixture, modifying its structure significantly (Aguado and Serrano, 1999). As a result, pyrolytic oil is a complex mixture of compounds, so individual identification of them is impossible (Scheirs, 2006); however, a complete interpretation of its properties and characteristics is important to the optimum design and right operation of any system built for its processing (Riazi, 2005). An assay allows one to determine the products that can be produced with a given technology, difficulties, and

downstream processing to optimize yields and specification products, but the overriding issue when performing a comprehensive test is the cost of getting the whole information (Rand, 2010).

The hydrocarbon industry has developed a technique semiempirical that allows the calculation of basic parameters to know the quality and properties of crude oils and fuels, from easily measurable laboratory data, applying standard methods, correlation of corresponding states, equations of state, and others from acceptable precision. Establishing the average boiling temperature from distillation data, transforming various distillation curves from one type to another, and estimating molecular weight and chemical composition are the initial steps to its characterization (Riazi, 2005).

The basic laboratory data useful in the characterization methods, based on their significance and simplicity, are the boiling temperature ( $T_b$ ), specific gravity ( $SG$ ), chemical composition, molecular weight ( $M$ ), refractive index ( $n$ ), elemental analysis and kinematic viscosity ( $\nu$ ), of these at least two must be known for this purpose where the easiest and convenient to measure are  $n$  and  $SG$ , nevertheless, for light fractions the most suitable pair is the boiling temperature and specific weight, but for the heavy fractions three items are required as  $SG$  and  $\nu$  at 37.8 and 98.9 °C (Riazi, 2005).

Thus, to obtain the  $T_b$ , simulated distillation by gas chromatography is used. This is a separation method developed to reproduce the physical distillation of a mixture of hydrocarbons based on their volatilities due to the fact that these elute through a nonpolar absorbent column according to its boiling point and with a unique retention time, yet compounds with the same volatility and different molecular structure cannot be identified (Wauquier, 2004; Riazi, 2005; Montemayor, 2008); the simulated distillation does not provide information to assess its quality, but it does give details of the products to be obtained (Rand, 2010). The  $n$  is another characterization parameter that allows estimating the composition and quality of hydrocarbons, especially molecular composition when determining the aromaticity and unsaturation by calculating the rate of paraffins and naphthenes (Riazi, 2005; Rand, 2010); unlike others, this analysis is the most accurate because it allows the detection of small differences in the quality of hydrocarbons (Wauquier, 2004). On the other hand, elemental analysis provides information on the quality of petroleum products by determining the content of sulfur, nitrogen, oxygen, carbon, and hydrogen (Riazi, 2005).

Various studies have been developed searching waste plastics utility alternatives, such as recycling or using it as energetic sources, like fuels or chemical precursors; however, all of them focused on yields and chemical composition using specialized instruments along with measurement of basic physic properties without determining correlations that allow their

calculation based on laboratory data when experimental data are not available, due to the absence of special types of equipment. Although some of them have employed hydrocarbon correlations to calculate certain properties, mainly from the higher heating value (HHV) (Dobó et al., 2019; Quesada et al., 2020) and other like cetane index (Quesada et al., 2019), Isoparaffin Index and RON (Das and Tiwari, 2018a and 2018b), no one has established their deviation respect from real measurement.

Since a form of evaluation and comparison of hydrocarbon correlations to estimate a certain property from the same input parameters is through a data set used to obtain them, the objectives of this study, in addition to identifying the optimal conditions to obtain maximum yields of the liquid fraction when thermal cracking severity increases to different temperatures from 450 °C to 550 °C from a real mix of plastic wastes with a similar composition of the municipal waste plastics collected in Granada–Spain, were to evaluate a number of existing models for the characterization of hydrocarbons using pyrolytic oil and make a comparison between the results obtained by instrumental analytic measurements carried out on the liquid fraction of distillation, density, refractive index, and elemental analysis with those predicted by these mathematical correlations.

## **3.2. Materials and methods**

### **3.2.1. Materials**

Waste plastic materials were taken from the rejected fraction, unrecovered and fines from mechanical treatment of Ecocentral Plant (37° 03' 03.5'' N, 3° 42' 17.8'' W), compacted in bales for their end disposal at landfills; which ones were selected samples made of polypropylene (PP), polystyrene (PS), mainly high impact polystyrene with paper from tags (HIPS + P) and expanded polystyrene (EPS) and film (PE). The average composition of bales was 55.71% of polypropylene, 25.71% of the film, 10% of expanded polystyrene, and 8.57% of high-impact polystyrene.

To facilitate the homogeneity of the samples for the different pyrolysis tests, the different polymers were separated, washed, dried, and manually crushed to an approximate size of 1–3 mm. Subsequently, in the different pyrolysis experimental tests, a mixture was prepared with the same proportion of polymers as that in the bales obtained in the Ecocentral plant.

### **3.2.2. Methods**

#### **3.2.2.1. Pyrolysis tests**

Thermolysis experimental tests were carried out in a horizontal fixed-bed reactor (Nabertherm R 50/250/12 Model) integrated with a flow meter to regulate the inert entrainment fluid and a condensation container immersed in a cold bath to separate the liquid and the gas phases.

Approximately 25 g of sample was loaded inside the reactor; then it was heated to a rate of 10 °C/min from room temperature to reach different operating temperatures between 450 and 550 °C, which were kept for 90 min with a constant flow rate of nitrogen of 100 L/h. After the experiments, the reactor was cooled to room temperature under a constant nitrogen purge, and then the solid residues were collected. Solid residue and oil were directly measured, and the yields were calculated according to the following equations (gas fraction by difference to 100%):

$$\eta_l = \frac{m_l}{m_m} \cdot 100 \quad (3.1)$$

$$\eta_s = \frac{m_s}{m_m} \cdot 100 \quad (3.2)$$

$$\eta_g = 100 - (\eta_l + \eta_s) \quad (3.3)$$

Where  $\eta_l$ ,  $\eta_s$ ,  $\eta_g$  and  $m_l$ ,  $m_s$ , and  $m_g$  are the yields and weights of liquid, solids, and gases, respectively.

The experiments were repeated three times for each pyrolysis temperature, and an average value was presented in figures and tables.

### 3.2.2.2. Density and specific gravity (SG)

The density measurements were done in a handheld density meter Desnyto2Go from Mettler Toledo on 2 mL of sample according to the ASTM D7777 designation (ASTM, 2013).

In order to obtain the specific gravity, the observed density was corrected to the density at 15 °C using Table 53 A (Generalized for Crude Oil) from the Manual of Petroleum Measurement Standards and then using the relationship defined by the SI system of the following way:

$$SG = 1.001 d_4^{15} \quad (3.4)$$

Where  $d_4^{15}$  is the ratio of hydrocarbon density at 15 °C to that of water at 4 °C (API, 2003).

### 3.2.3. Refractive index ( $n_{D20}$ ) and refractive index parameter (I)



Refractive index or refractivity is a fundamental physical property that can be used with other properties to characterize pyrolysis oils. These were evaluated on a Mettler Toledo refractometer RM40 model from 1.32 to 1.70. The measurement was carried out with 0.5 mL of oil free of impurities at 20 °C according to the ASTM D1218 and D1747 designations (ASTM, 1999 and ASTM, 2000); a calibration curve was plotted using the primary referential materials from both methods to correct the observed measurements.

The Refractive Index Parameter ( $I$ ) was calculated according to Eq. 5, Huang characterization parameter (Huang, 1977; Riazi, 1980).

$$I = \frac{n_{D\ 20}^2 - 1}{n_{D\ 20}^2 + 2} \quad (3.5)$$

### 3.2.3.1. Elemental analysis

The main elements present in pyrolysis oil (carbon, hydrogen, nitrogen, oxygen and sulfur) were measured using a Termo Scientific Flash 2000 CHNS/O Analyzer by rapid combustion with pure oxygen where the flue gases pass through a chromatographic separation column and a thermal conductivity detector in accordance to ASTM D5291 designation (ASTM, 2008a).

### 3.2.3.2. Compositional analysis by gas chromatography

Oils samples were analyzed through of Gas Chromatography by Spectrometry Masses (GC-MS) using the Agilent 8860 Gas Chromatograph System endowed with a Phenomenex GC column and nonpolar phase ZB-1HT (30 *m* long, 0.25 *mm* internal diameter and 0.25  $\mu$ *m* of fill thickness) coupled to a triple-quadrupole Mass Spectrometer 5977 GC/MSD model from Agilent with analysis scan speed  $\leq 20000$  *Da/s* and ionization energy by electronic impact of 70 *eV*.

Samples were weighted and diluted in 1 *mL* of chloroform, then were injected in split mode (10:1) to 250 °C together with 1.8 *mL/min* carry gas Helium at constant flow. The heated rate was 10 °C/*min* from 35 up to 350 °C. The transfer line and detector stayed at 250 °C.

### 3.2.3.3. Simulated distillation (SD)

To determine the boiling range distribution of pyrolytic oil products, such as petroleum fractions with an equivalence to a 100 theoretical-plate physical distillation performed at atmospheric pressure, simulated distillation curves were constructed according to the ASTM D2887 (ASTM, 2008b) designation using the individual chromatograms of each sample analyzed. For this, the

retention time of their compounds was taken to determine the boiling points by linear interpolation as follows:

$$BP_x = \left( \frac{BP_2 - BP_1}{RT_2 - RT_1} \right) \cdot (RT_x - RT_1) + BP_1 \quad (3.6)$$

Where  $BP_1$ ,  $BP_2$  and  $RT_1$ ,  $RT_2$  are the boiling points and retention times of referential normal paraffins, and  $BP_x$  and  $RT_x$  are the boiling points and retention times of the compounds in the sample.

The referential retention times of normal paraffins were identified from the polyethylene pyrolytic oil spectrometer using the mass spectroscopy library of the National Institute of Standards and Technology (NIST) (ASTM, 2008b).

### 3.2.3.4. ASTM D86 distillation

In order to reduce the conversion error between the  $SD$  to the True Boiling Point ( $TBP$ ) curve by direct conversion, the  $SD$  was first transformed into ASTM distillation according with Standard Test Practice ASTM STP 577 as report in Table 3.1 (Riazi, 2005, ASTM, 2015).

**Table 3.1.** Correlation equations of ASTM STP 577 (ASTM, 2015)

D86 – IBP = 46.566 + 0.58289 (D2887 10 %) + 0.34795 (D2887 IBP)
D86 – 10% = 33.308 + 0.61562 (D2887 10 %) + 0.35110 (D2887 20 %)
D86 – 20% = 22.411 + 0.48903 (D2887 30 %) + 0.27528 (D2887 20 %) + 0.21713 (D2887 10 %)
D86 – 30% = 14.431 + 0.47035 (D2887 30 %) + 0.28369 (D2887 20 %) + 0.22784 (D2887 50 %)
D86 – 50% = 4.876 + 0.97597 (D2887 50 %)
D86 – 70% = 0.911 + 0.51975 (D2887 80 %) + 0.33260 (D2887 70 %) + 0.10159 (D2887 30 %)
D86 – 80% = 0.279 + 0.75936 (D2887 80 %) + 0.28333 (D2887 95 %) – 0.09975 (D2887 FBP)
D86 – 90% = – 1.973 + 0.61459 (D2887 90 %) + 0.31909 (D2887 95 %)
D86 – FBP = 34.179 + 1.14826 (D2887 95 %) – 0.59208 (D2887 90 %) + 0.31542 (D2887 FBP)

where D86 and D2887 are ASTM methods, IBP is initial boiling point, FBP is final boiling point and temperatures are in Fahrenheit.

### 3.2.4. True boiling point curve (TBP)

The distillation data available in the form of ASTM D86 can be converted to TBP according to American Petroleum Institute (API) Procedure 3A1.1 with the following equations (ASTM, 1999).

$$TBP (50\%) = 0.8718 (ASTM 50\%)^{1.0258} \quad (3.7)$$

where  $TBP (50\%)$  is the true boiling point temperature at 50vol percent distilled, °F, and the  $ASTM (50\%)$  is the ASTM D86 temperature at 50 vol percent distilled, °F.

$$Y_i = A \cdot X_i^B \quad (3.8)$$

where  $Y_i$  is the true boiling point temperature difference between tow cuts points, °F,  $X_i$  is the ASTM D86 temperature difference between tow cuts points, °F, and  $A$  and  $B$  are constants varying for each cut point and are given in Table 3.2.

Finally, to determine the true boiling point temperature at any percent distilled, the equations reported in Table 3.3 are applied.

**Table 3.2.** Constants and Restrictions of Eq. 7 (ASTM, 1999)

i	Cut Point Range	A	B	Approximate Maximum Allowable $X_i$ (°F)
1	100% – 90%	0.11798	1.6606	-
2	90% – 70%	3.0419	0.75497	100
3	70% – 50%	2.5282	0.82002	150
4	50% – 30%	3.0305	0.80076	250
5	30% – 10%	4.9004	0.71644	250
6	10% – 0%	7.4012	0.60244	100

**Table 3.3.** Correlations equations of API procedure 3A1.1 (ASTM, 1999)

$TBP (0\%) = TBP (50\%) - Y_4 - Y_5 - Y_6$
$TBP (10\%) = TBP (50\%) - Y_4 - Y_5$
$TBP (30\%) = TBP (50\%) - Y_4$
$TBP (70\%) = TBP (50\%) + Y_3$
$TBP (90\%) = TBP (50\%) + Y_3 + Y_2$
$TBP (100\%) = TBP (50\%) + Y_3 + Y_2 + Y_1$

### 3.2.5. Mean average boiling point (MeABP)

Generally, an average boiling point is defined to determine the single characterization boiling ( $T_b$ ). One of these average boiling temperatures is  $MeABP$  (Mean average boiling point) that can be determined by ASTM D86 curve according the following equations (API, 1999; Wauquier, 2004):

$$V_{ABP} = \frac{T_{10\%} + T_{30\%} + T_{50\%} + T_{70\%} + T_{90\%}}{5} \quad (3.9)$$

$$SL = \frac{T_{90\%} - T_{10\%}}{80} \quad (3.10)$$

$$\ln(\Delta T_{Me}) = -1.53181 - 0.0128 * V_{ABP}^{0.6667} + 3.646064 * SL^{0.333} \quad (3.11)$$

$$Me_{ABP} = V_{ABP} - \Delta T_{Me} \quad (3.12)$$

where  $T_i\%$  are temperatures at “ $i$ ” vol% distilled and are in K.

### 3.2.5.1. Mathematical correlation for hydrocarbons

Following, several correlations for the estimation of specific gravity, refractive index parameter and carbon-hydrogen weight ratio are reported. These correlations were obtained by Raizi and Daubert (1980) and Riazi and Daubert (1987) from data on approximately 140 pure hydrocarbons in the molecular weight range of 70–300 and boiling point range between 300 and 620 K. These authors proposed correlations that can be expressed in terms of two parameters as follows:

$$\theta = a \cdot \theta_1^b \cdot \theta_2^c \quad (3.13)$$

$$\theta = a \cdot \exp(b \cdot \theta_1 + c \cdot \theta_2 + d \cdot \theta_1 \cdot \theta_2) \cdot \theta_1^e \cdot \theta_2^f \quad (3.14)$$

Values of constants in Eqs. 3.13 and 3.14 for SG, I and CH ratio and pairs of  $\theta_1$  and  $\theta_2$  listed above are given in Tables 3.4, 3.5, 3.6 and 3.7. All temperatures are in K.

**Table 3.4.** Information about equations used to predict SG

Equation number	Equation Type	Needed parameters	Constants
15	$SG = a \cdot \theta_1^b \cdot \theta_2^c$	$T_{10\%}$ and $T_{50\%}$	Table 5 for choosing “a”, “b” and “c” parameters.
16	$SG = a \cdot \exp(b \cdot \theta_1 + c \cdot \theta_2 + d \cdot \theta_1 \cdot \theta_2) \cdot \theta_1^e \cdot \theta_2^f$	$T_b$ and I	$a=2.4381 \cdot 10^7$ $b=-4.194 \cdot 10^{-4}$ $c=-23.5535$ $d=3.98736 \cdot 10^{-3}$ $e=-0.3418$ $f=6.9195$
17	$SG = a \cdot \exp(b \cdot \theta_1 + c \cdot \theta_2 + d \cdot \theta_1 \cdot \theta_2) \cdot \theta_1^e \cdot \theta_2^f$	$T_b$ and CH ratio	$a=2.86706 \cdot 10^{-3}$ $b=-1.83321 \cdot 10^{-3}$ $c=-0.081635$ $d=6.49168 \cdot 10^{-5}$ $e=0.890041$ $f=0.73238$

**Table 3.5.** Restrictions and Constants for Eq. 15

Distillation type	T <sub>10%</sub> range, °C	T <sub>50%</sub> range, °C	SG Range	A	b	c
ASTM D86	35 – 295	60 – 365	0.70 – 1.00	0.08342	0.10731	0.26288
TBP	10 – 295	55 – 320	0.67 – 0.97	0.10431	0.12550	0.20862

**Table 3.6.** Information about equations used to predict I

Equation number	Equation Type	Needed parameters	Constants
18	$I = a \cdot \theta_1^b \cdot \theta_2^c$	T <sub>b</sub> and SG	a=0.3773 b=-0.02269 c=0.9182
19	$I = a \cdot \exp(b \cdot \theta_1 + c \cdot \theta_2 + d \cdot \theta_1 \cdot \theta_2) \cdot \theta_1^e \cdot \theta_2^f$	T <sub>b</sub> and SG	a=0.02343 b=7.0294·10 <sup>-4</sup> c=2.46832 d=-1.0268·10 <sup>-3</sup> e=0.05721 f=-0.71990
20	$I = a \cdot \exp(b \cdot \theta_1 + c \cdot \theta_2 + d \cdot \theta_1 \cdot \theta_2) \cdot \theta_1^e \cdot \theta_2^f$	T <sub>b</sub> and SG	a=3.2709·10 <sup>-3</sup> b=8.4377·10 <sup>-4</sup> c=4.59487 d=-1.0617·10 <sup>-3</sup> e=0.03201 f=-2.34887 Used for heavy hydrocarbons
21	$I = a \cdot \exp(b \cdot \theta_1 + c \cdot \theta_2 + d \cdot \theta_1 \cdot \theta_2) \cdot \theta_1^e \cdot \theta_2^f$	T <sub>b</sub> and CH ratio	a=5.60121·10 <sup>-3</sup> b=-1.7774·10 <sup>-4</sup> c=-6.0737·10 <sup>-2</sup> d=-7.9452·10 <sup>-5</sup> e=0.447 f=0.9896

### 3.3. Results and discussion

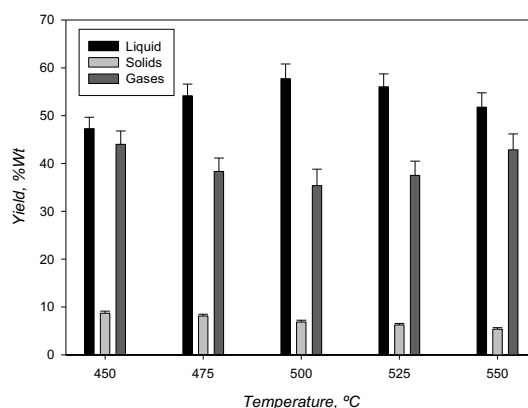
#### 3.3.1. Effect of operating temperature on liquid fraction

Fig. 3.1 shows the yields to products when the mix of plastic waste from municipal solid waste was pyrolyzed at temperatures between 450 and 550 °C with a heating rate of 10 °C/min. Results showed that the pyrolytic oil yield was high, performing pyrolysis at 500°C and reaching a liquid

product yield of 57.7%. An increased operating temperature to 550 °C decreased the pyrolytic oil yield to 51.8%. It can be attributed to the formation of more non-condensable gases due to the secondary cracking or reforming reactions of the heavy-heavy-molecular-weight compounds in the pyrolysis vapors (Shadangi and Mohanty, 2014). Also, a decrease of the pyrolysis temperature to 450 °C decreased the pyrolytic oil yield to 47.3%. The lower liquid product yield at this low temperature can be because the temperature was not high enough for complete pyrolysis (Islam et al., 1999).

**Table 3.7.** Information about equations used to predict the CH ratio

Equation number	Equation Type	Needed parameters	Constants
22	$CH = a \cdot \exp(b \cdot \theta_1 + c \cdot \theta_2 + d \cdot \theta_1 \cdot \theta_2) \cdot \theta_1^e \cdot \theta_2^f$	$T_b$ and SG	$a=3.47028$ $b=1.4850 \cdot 10^{-2}$ $c=16.94020$ $d=-0.012491$ $e=-2.72522$ $f=-6.79769$
23	$CH = a \cdot \exp(b \cdot \theta_1 + c \cdot \theta_2 + d \cdot \theta_1 \cdot \theta_2) \cdot \theta_1^e \cdot \theta_2^f$	$T_b$ and SG	$a=8.7743 \cdot 10^{-10}$ $b=7.176 \cdot 10^{-3}$ $c=30.06242$ $d=-7.35 \cdot 10^{-3}$ $e=-0.98445$ $f=-18.2753$ This equation was developed based on data in the range of $C_{20}$ - $C_{50}$ . However, it can also be used for hydrocarbons from $C_6$ to $C_{50}$ .
24	$CH = a \cdot \exp(b \cdot \theta_1 + c \cdot \theta_2 + d \cdot \theta_1 \cdot \theta_2) \cdot \theta_1^e \cdot \theta_2^f$	$T_b$ and I	$a=8.39640 \cdot 10^{-13}$ $b=7.7171 \cdot 10^{-3}$ $c=71.6531$ $d=-0.02088$ $e=-1.3773$ $f=-13.6139$



**Figure 3.1.** Individual yields from pyrolysis of the waste plastic mix.

Other researchers also observed these results. For example, Quesada et al. (2020) studied the pyrolysis of a plastic waste mixture with a composition of 50% of PE, 25% of PP, and 25% of PS at 500 °C for 120 min with a heating ratio of 10 °C /min and they obtained 64% of pyrolytic oil. Also, Miandad et al. (2017) worked at 450 °C for 75 min with the same heating rate and a mixture of plastic materials (PS 50%, PE 25%, and PP 25%), and they got 49% of the liquid fraction. Dobó et al. (2021) prepared three blends using high-density polyethylene HDPE (15%), low-density polyethylene LDPE (22%), PP (49%), and PS (14%) to be pyrolyzed up to 520 °C in a batch reactor obtaining 72.85% of liquid product. Auxilio et al. (2017) collected 82% oil from 27.5% LDPE, 27.5% HDPE, 17% PS and 28% PP at 425 °C in a continuous stirred tank reactor CSTR for 250min. Ibrahim et al. (2018) made thermal degradation of mixed HDPE (25%), LDPE (30%), PP (30%), and PS (15%) at 400 °C, and they achieved about 95% liquid oil. Costa et al. (2021) performed pyrolysis experiments with self-generated pressure, for 30 min at 440 °C and 5.5 °C/min of heating, of the mixture of LDPE (60 y 80%), PP (20 y 10%) and PS (20% and 10%) of which they drew 87% and 92.5% of liquid. A thermal decomposition up to 430 °C for 20 min under 3.5 MPa of pressure was carried out by Pinto et al. (1999a), and they extracted 90% of the liquid from 68% PP, 16% PE, and 16% PS. An increase of 3.5% was gained when the composition changed to 68% PE, 16% PP, and 16% PS.

The differences in the results indicate that the operating conditions, the system configuration used, the nature of the plastic waste, and its composition are determining factors in obtaining better yields from the liquid fraction.

### 3.3.2. Experimental data on basic properties of pyrolytic oil samples

As an example, some of the numerical values of liquid fractions measured experimentally are shown in Table 3.8. Also, the behavior of basic properties of pyrolytic oil samples with increasing

operating temperatures is presented in Fig. 3.2. The observed density of pyrolytic oils is in the range of 0.8266–0.8333  $g/cm^3$ . The refractive index was found in the range of 1.4682–1.4738, values that are between those characteristics of naphthenes and aromatics (Riazi, 2005). Regarding the change of the carbon-hydrogen weight ratio from 6.19 to 7.31, quality measurement shows that as temperature increases, the pyrolytic oil is heavier (Riazi, 2005).

Regarding the effect of pyrolysis temperature, Fig. 3.2a shows that the observed density of the oils increased when the pyrolysis temperature increased, mainly between 500 and 550 °C. Fig. 3.2b exhibits a slight decrease in refractive index from 450 to 500 °C and an appreciable growth when the pyrolysis temperature changed from 500 to 550°C due to hydrogenation and dehydrogenation reactions shown by increasing and decreasing the hydrogen weight ratio. Finally, Fig. 3.2c shows that as the pyrolysis temperature increases, the carbon-hydrogen ratio increases as result of presence of more unsaturated compounds due to decreasing hydrogen content and increase of carbon.

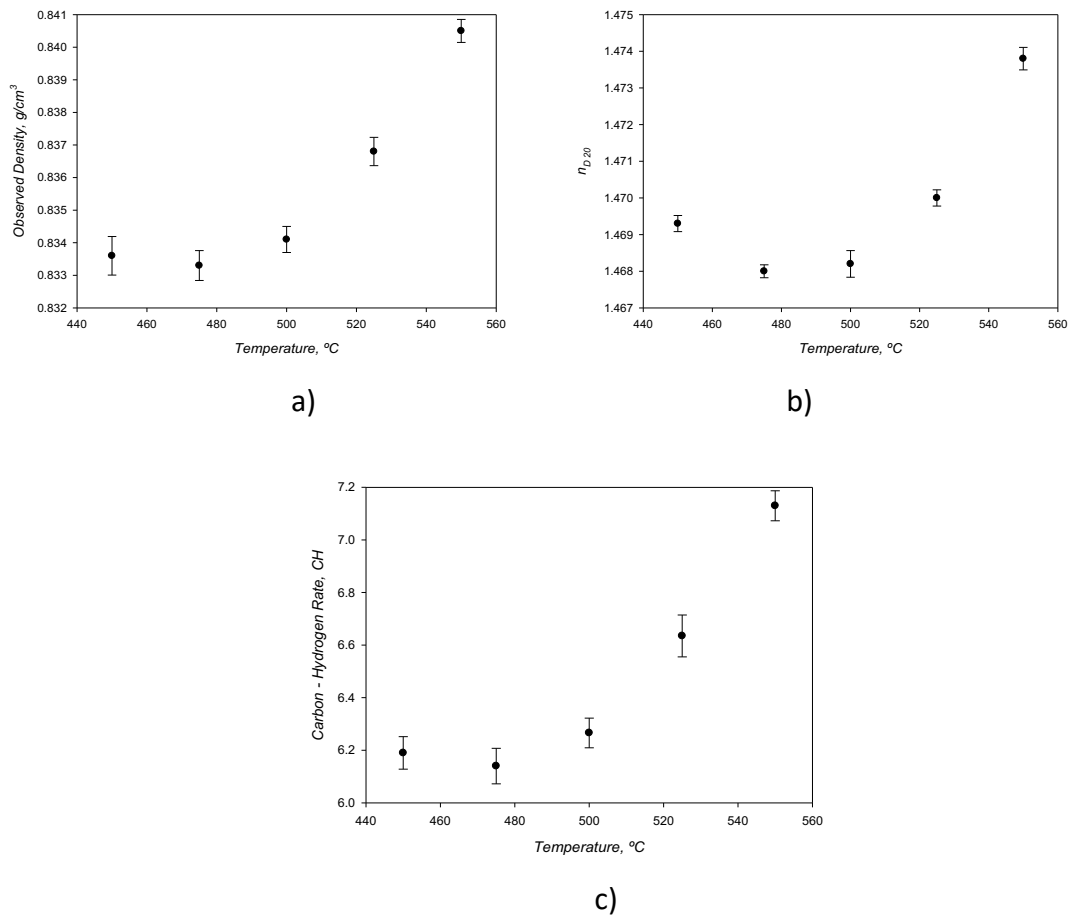


**Figure 3.2.** The behavior of a) the specific gravity, b) the refractive index, and c) the carbon-hydrogen ratio of the pyrolytic oils.



**Table 3.8.** Deviation from Measured and Calculated Data

Estimated Parameter	Pyrolysis temperature, °C	Experimental value	Estimated value	Deviation, %
SG	450	0.8344	0.8249 – Eq. 15	-1.14
			0.8416 – Eq. 16	0.86
			0.8208 – Eq. 17	-1.62
	500	0.8349	0.8833 – Eq. 15	5.79
			0.8453 – Eq. 16	1.24
			0.8312 – Eq. 17	-0.45
	550	0.8413	0.8870 – Eq. 15	5.43
			0.8561 – Eq. 16	1.76
			0.8928 – Eq. 17	6.12
I	450	0.2786	0.2770 – Eq. 18	-0.59
			0.2761 – Eq. 19	-0.92
			0.2767 – Eq. 20	-0.69
			0.2710 – Eq. 21	-2.74
	500	0.2781	0.2764 – Eq. 18	-0.60
			0.2752 – Eq. 19	-1.03
			0.2771 – Eq. 20	-0.34
			0.2738 – Eq. 21	-1.53
	550	0.2846	0.2782 – Eq. 18	-0.97
			0.2767 – Eq. 19	-1.52
			0.2792 – Eq. 20	-0.62
			0.2846 – Eq. 21	1.32
CH ratio	450	6.05	6.38 – Eq. 22	3.10
			6.73 – Eq. 23	8.73
			6.79 – Eq. 24	9.61
	500	6.25	6.25 – Eq. 22	0.01
			6.45 – Eq. 23	3.11
			6.53 – Eq. 24	4.36
	550	7.31	6.30 – Eq. 22	-13.93
			6.54 – Eq. 23	-10.55
			6.68 – Eq. 24	-8.69

Fig. 3.3 shows the CG-MS results. PE chromatogram with the retention times of the normal paraffins to cover the boiling range from  $n$  C5 to  $n$  C44, according to the carbon numbers

suggested by ASTM D2887 designation, to construct the simulated distillation curves of the pyrolytic oils by gas chromatography was included. Throughout the experimental chromatograms, it is evident to observe the reduction of the peak areas of some light hydrocarbons due to over-cracking and the increase of the peak areas of the heavy hydrocarbons due to the more significant presence of these as the pyrolysis temperatures increase.

In pyrolysis, the temperature effect is reflected in the observed or measured oil properties due to the presence of hydrogenation and dehydrogenation reactions, the first by the over-cracking of the light vapors at low experimental temperature to produce hydrogen and the latter by the cracking of heavy compounds at high experimental temperature.

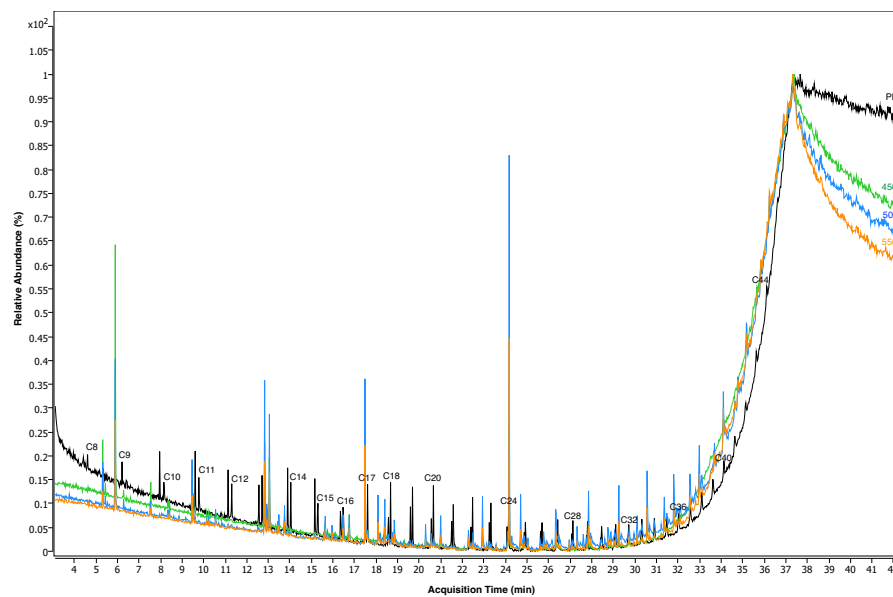


**Figure 3.3.** Chromatograms of the pyrolytic oils obtained from the mixture of plastic waste at 450, 500, and 550 and calibration mixture.

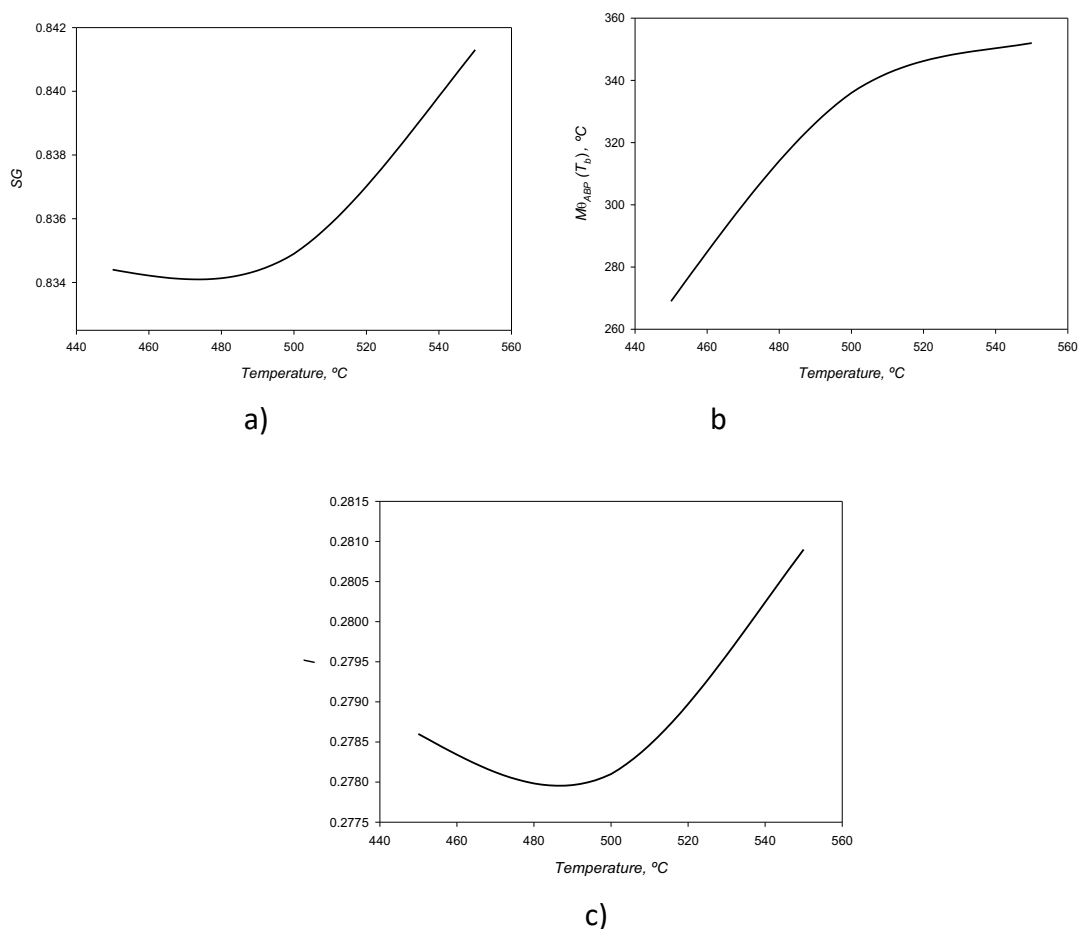
### 3.3.3. Conversion of measured properties into parameters for hydrocarbon characterization

Figure 3.4 shows the calculated  $CSG$ ,  $Me_{ABP}$  and  $I$ . Specific gravity showed an appreciable rise when it reached 550 °C, changed from 0.8344 at 450 °C to 0.8413 at 550 °C. The mean average boiling point increase when was increased from 450 to 550 °C, maintain mainly constant between 500 and 550 °C. Regarding refractive index parameter, it showed a substantial increase at 550 °C when the severity in pyrolysis rise, this due to minor hydrogenation reactions and intense dehydrogenation reactions. The values of refractive index indicated that the three samples are

predominantly naphthenic (0.278–0.308) (Riazi, 2005) with increasing order for the pyrolytic oils of 500, 450 and 550 °C.

Figure 3.5 shows simulated distillation (*SD*), ASTM D86 distillation and True Boiling Point (*TBP*) curves. They represent characteristic curves like those of hydrocarbons but with a lower proportion of light and heavy hydrocarbons compounds than those of crude oils. Of these, the pyrolytic oils got at 500 and 550 °C are heavier than 450 °C oil and 550 °C oil more than 500 °C oil. On the other hand, as shown the TBP curves of Escravos and Brent (Treese, 2015), typical crude oils with specific gravities near to pyrolytic oils, have marked differences in trends and composition, but those crude oils with a close tendency that the pyrolytic oils, as Pennington and Brent (Treese, 2015), have different specific gravities.

The specific gravity and the refractive index parameter reflect the changes of the chemical structure of the pyrolytic oil as experimental temperature increase. The simulated distillation curves show a lower proportion of light and heavy compounds than those of hydrocarbons.



**Figure 3.4.** Trend of a) the specific gravity, b) the boiling temperature and c) the refractive index parameter of the pyrolytic oils obtained from the mixture of plastic waste at 450, 500 and 550 °C.

### 3.3.4. Application of mathematical correlations for hydrocarbons

In this section, a comparison between experimental and estimated parameters (Specific Gravity, Refractive Index Parameter and Carbon-Hydrogen ratio) of pyrolytic oils is presented. Fig. 3.6 shows the main obtained results (as an example, some of the numerical values are shown in Table 3.8).

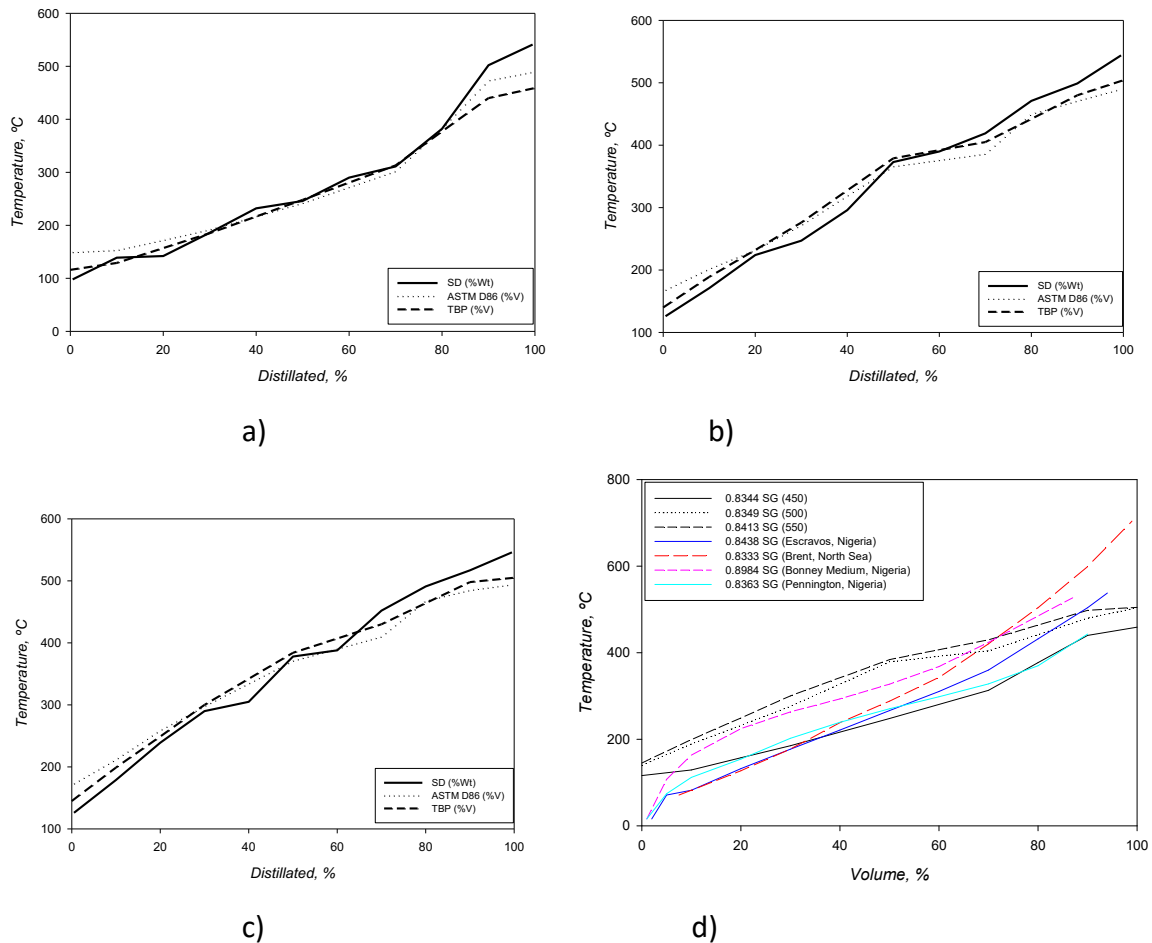


**Figure 3.5.** Simulated distillation, ASTM D86 curve and true boiling point at a) 450 °C, b) 500 °C, c) 550 °C and d) the three TBP curves of the pyrolytic oils obtained from the mixture of plastic waste and selected crude oils.

Since the trends by Eqs. 14 and 16 are approximately similar to those of the experimental data, these equations have been used as a base to fitting the exponential values and obtain the following new correlations, which give  $R^2$  of 0.9963 and 0.9862 for equations 3.25 and 3.26 with average deviations of 0.14% and 0.12%, respectively.

$$SG = 2.4381 \cdot 10^7 \cdot \exp(-4.79 \cdot 10^{-4} \cdot Me_{ABP} - 23.4593 \cdot I + 3.988 \cdot 10^{-3} Me_{ABP} \cdot I) \cdot Me_{ABP}^{-0.3419} \cdot I^{6.921} \quad (3.25)$$

$$I = 0.3773 \cdot T_b^{-0.0217} \cdot SG^{0.92} \quad (3.26)$$

where  $T_b$  has been changed for  $Me_{ABP}$  in K, SG is the specific gravity at 15.5 °C and I is the refractive index parameter at 20 °C and 1 atm.

The specific gravity and the refractive index parameter calculated by Ec. 3.25 and Ec. 3.26 has a deviation of less than 0.15% from the experimentally measured data and its tendency as the temperature increases is identical from 450 to 500 °C to that formed by the experimental data.

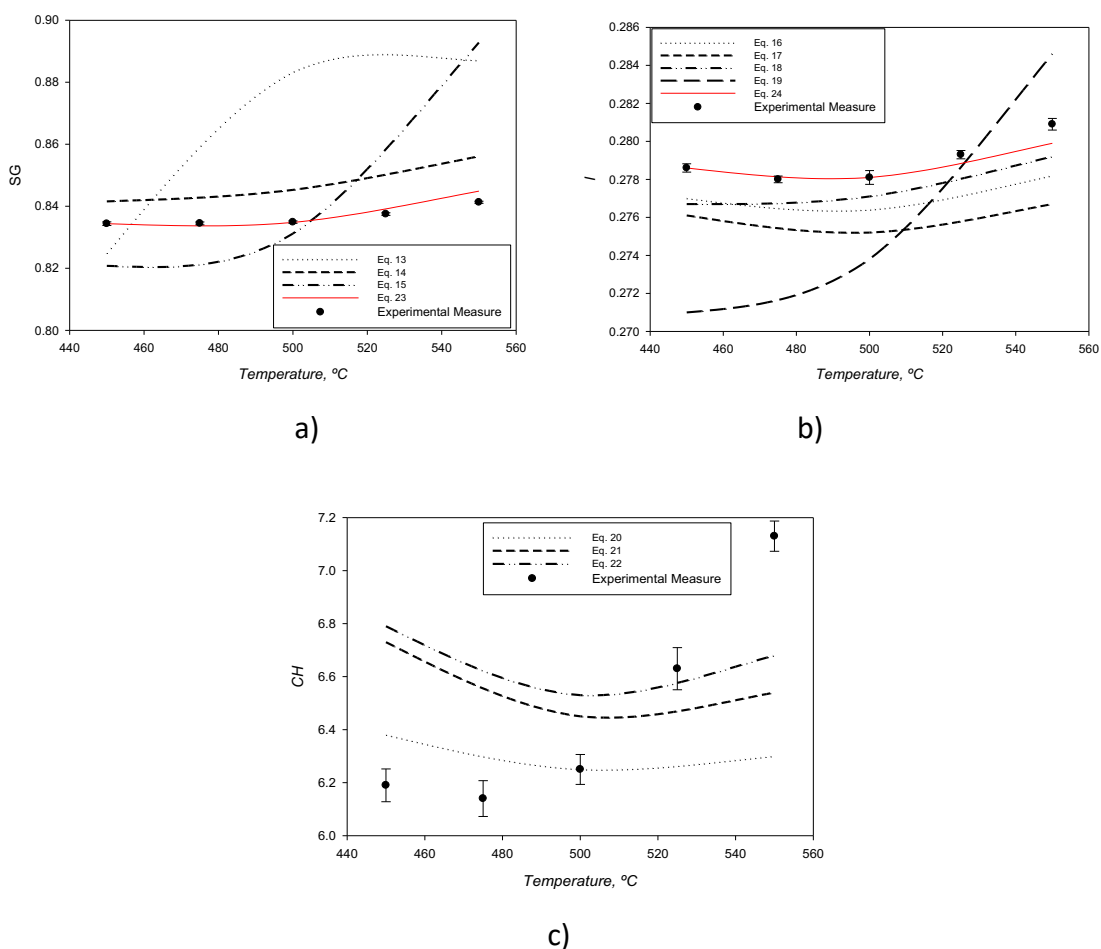


**Figure 3.6.** Deviations of the calculated and measured properties of the pyrolytic oils obtained from the mixture of plastic waste at 450, 500, and 550 °C: a) the specific gravity, b) the refractive index parameter, and c) the carbon-hydrogen ratio.

The mathematical correlations of hydrocarbons, which are based on the properties of their pure compounds, indicate that they are not suitable for the pyrolytic oil characterization obtained from plastic waste mixtures of the investigated composition, but modified equations 3.25 and 3.26 give a better fit with less deviation for the calculation of specific gravity and refractive index parameter and seem to be appropriate to obtain these parameters when experimental data, including the boiling temperature, are not available and the molecular weights are in range of 70–300 or boiling point between 300–660 K.

To develop models for predicting the pyrolytic oil properties, taking into account variables easily measured, provide an economically attractive alternative to direct analysis. However, at this time, the equations proposed are limited to conditions used in our work.

### 3.3.5. Performance estimation of products

The yield of the possible products to be obtained by simulated distillation at atmospheric pressure, such as petroleum cuts (Montemayor, 2008) (heavy naphtha 121–191 °C, kerosene 191–277 °C, diesel 277–343 °C, light vacuum gas oil 343–455 °C, and heavy vacuum gas oil 455–566 °C), of the pyrolytic oils from plastic waste at operating temperatures of 450, 500 and 550 °C were calculated and results are summarized in Fig. 3.7. In them, it can be deduced that, in pyrolytic oil obtained at 450 °C, the naphtha cut predominates with 31.8% followed in a decreasing way by kerosene (27.2%), diesel (15.7%), light (17.5%) and heavy vacuum gas oils (7.7%). Increasing the heat of pyrolysis to 500 °C, the amount of naphtha (10.6%), kerosene (19.6%), and diesel (12.9%) was decreased, but percentages of light (40.3%) and heavy (16.6) vacuum gas oils were increased. An additional increase in pyrolysis temperature, up to 550 °C, changed the distribution of the products, favoring the diesel recuperation yield (14.8%) and increasing the recovery of heavy vacuum gas oil (19.1%).

Other authors also reported the composition of pyrolysis oils as petroleum cuts. For example, Dobó et al. (2021) investigated the thermal pyrolysis of HDPE, LDPE, PP, and PS plastic waste mixtures with mass ratios representing the plastic demands in Hungary, the European Union and the world obtained yields between 70.3% and 74.9% of gasoline (cut from 20 to 200 °C) and between 18.8% and 21.7% of diesel (cut from 200 to 350 °C). Other authors (Sarker and Rashid, 2013) pyrolyzed a mixture of PP (50%) and PS (50%) from 200 to 420 °C for 4.5h in a reactor with a fractionation column and obtained 17% of kerosene, a value similar to that obtained in our work at 550 °C with different composition of the raw material (less proportion of PS and addition of other polymers). Also, the thermal decomposition of a mixture with mass ratios representing the three main plastics present in municipal solid waste in Portugal was investigated in the works of Pinto et al. (1999a) and (1999b). The plastic mixture was formed by 68% PP, 16% PE, and 16% PS, and pyrolysis tests were performed at a temperature of 430 °C during a reaction time of 20

min and a mean pressure of 3.5 MPa, producing between 49% and 55% of gasoline (cut from 36 to 199 °C), values higher than those obtained here (34% at 450 °C). Also, Ibrahim et al. (2018) analyzed the thermal pyrolysis at 400 °C of a mixture of PP, LDPE, PS, and HDPE at percentages of 30%, 30%, 25%, and 15%, respectively, at 400 °C. The authors reported a hydrocarbon composition in pyrolysis oil of 25% naphtha (cut from 45 to 170 °C), 52% diesel 1 (cut from 170 to 265 °C), and 21.5% diesel 2 (cut from 265 to 370 °C). Comparing our results at the same cut-off temperatures, the value of naphtha is almost similar to that obtained in our investigation (24.6%) at 450 °C. However, the amount of diesel 1 (30.7%) was lower, and the amount of diesel 2 (23.7%) was higher. Finally, Singh et al. (2020) analyzed the pyrolysis oil obtained at 450, 500, and 550 °C from a mixture of PE, PP, PS, and PET and determined hydrocarbon fractions in pyrolysis oil based on carbon number. Percentages of 71.60%, 70.32%, and 68.75% of cut from 36 to 216 °C (C5-C12); 16.17%, 19.64%, and 24.10% of cut from 235 to 330 °C (C13-C19) and 12.16%, 10.04% and 7.15% of cut greater than 330 °C (>C19) were obtained. Values differ from those obtained in our paper to identical carbon numbers.

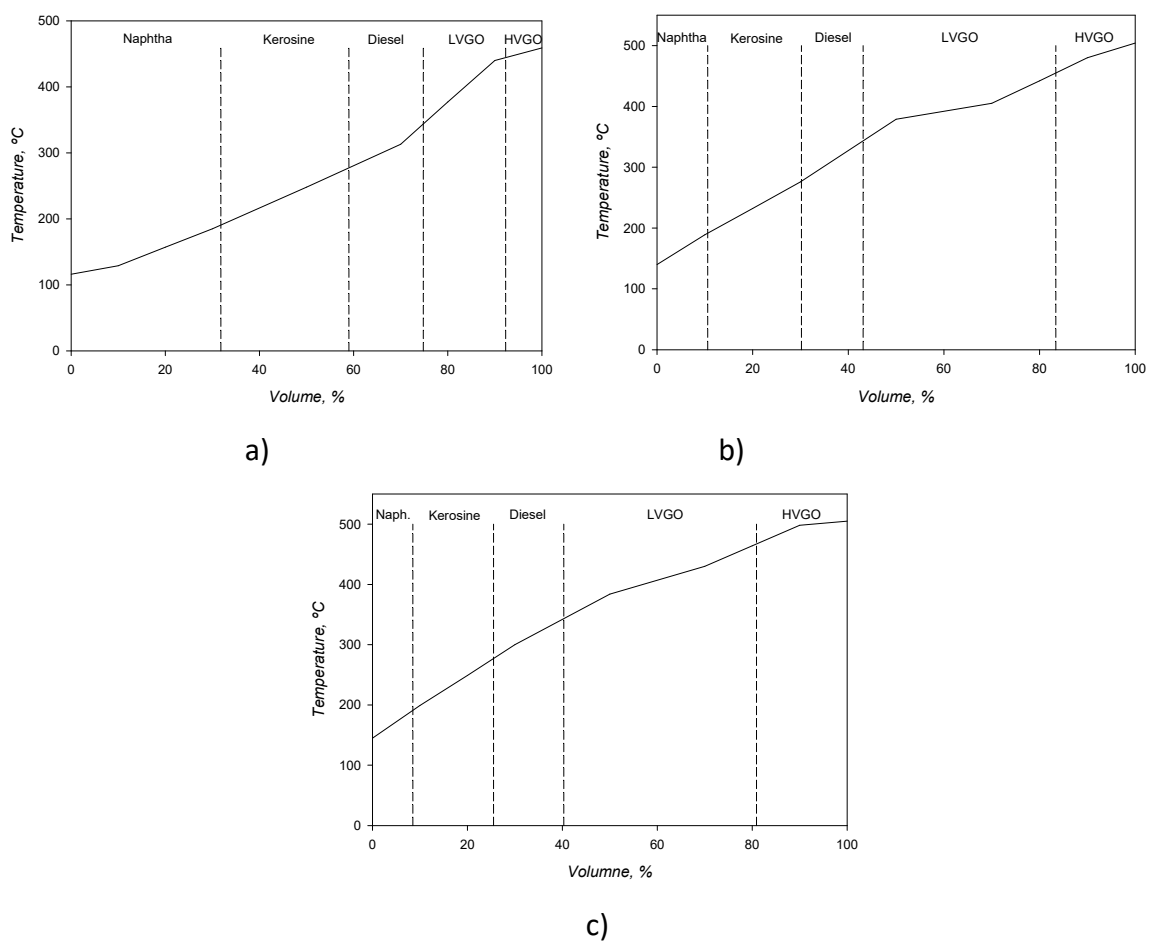


**Figure 3.7.** Product yields of pyrolytic oils obtained from the mixture of plastic waste at a) 450 °C, b) 500 °C and c) 550 °C.

According to the results, the differences show that raw material, process temperature, heating rates, volatile residence time, pressure, and type of reactor are significant parameters influencing the reactions that are carried out during the conversion of waste plastic by pyrolysis and, consequently, the composition and characteristics of the oil samples. In this sense, Dobó et al. (2021), using a laboratory-scale batch reactor with a pyrolysis temperature of 520 °C, conclude that product yield and composition are highly influenced by the type of initial plastic waste. Pinto et al. (1999a) also found this influence of the type of plastic in the yield to product and the composition, using a purged with nitrogen and pressurized autoclave as a pyrolysis reactor. These authors conclude that it would be possible to obtain the desired final product by controlling the mixture of plastic waste, although it is not always technically and economically possible to obtain this mixture. In addition, Sing et al. (2020), as indicated above, pyrolyze three individual plastic wastes (HDPE, PP, and PS), a sample of mixed plastic waste containing PE, PP, PS, and PET and a simulated mixture of these polymers using a semi-batch reactor electrically heated. The authors find that the yield of products and the properties of the oil obtained depend on the type of plastic and the operating conditions, such as the heating rate or temperature. These authors find, for example, a higher concentration of heavy hydrocarbons in the pyrolysis oil when the operating temperature increases.

### **3.4. Conclusions**

The nature of the plastic waste and its composition, along with the operating conditions and the system configuration to process it, are determined to obtain better yields of pyrolytic oil with a profitable distribution of valuable products. In the investigated plastic waste, from a real mix of plastic wastes with similar composition to the municipal waste plastics collected in Granada–Spain, the optimal temperature to obtain maximum yield of the liquid fraction under atmospheric pressure was 500 °C, in which a 10.6% of the naphtha cut would be achieved, 19.6% of kerosene, 12.9% of diesel, 40.3% of light vacuum gas oil and 16.6% of heavy vacuum gas oil if it is processed as synthetic crude.

The effect of the pyrolysis temperature is reflected in the oil properties due to chemical changes induced by the presence of hydrogenation reactions, by over-cracking light vapors that produce hydrogen at low experimental temperatures, and dehydrogenation reactions, by cracking of heavy compounds at high experimental temperatures.

To be within the accuracy of each of the predictive mathematical correlations of hydrocarbon, which are based on the properties of pure hydrocarbons, does not necessarily indicate that these are adequate methods for pyrolytic oils characterization of the investigated composition; in some cases, due to restrictions, the source of data or its quantity.



However, Ec. 3.25 and Ec. 3.26 (Ec. 3.14 and Ec. 3.16 modified) seem suitable for calculating the specific gravity and refractive index parameter of pyrolytic oils obtained from the plastic waste mixture of the same investigated composition when experimental data are unavailable.

#### **ACKNOWLEDGEMENTS**

This work has received funds from the project PID2019-108826RB-I00/SRA (State Research Agency)/10.13039/501100011033.

## **References**

Aguado, J., Serrano, D. Feedstock Recycling of Plastic Wastes, The Royal Society of Chemistry Publishing, Cambridge, 1999.

American Petroleum Institute, Technical Data Book - Petroleum Refining, 6th Edition, American Petroleum Institute (API), 1999.

American Petroleum Institute, Generalized Crude Oils - Correction of Observed Density to Density at 15 °C, in Manual of Petroleum Measurement Standards, Volume VII, American Petroleum Institute, Washington, 2003.

American Society for Testing and Materials, Standard Test Method for Refractive Index of Viscous Materials, vol. 4. ASTM International, 1999.

American Society for Testing and Materials, Standard Test Method for Refractive Index and Refractive Dispersion of Hydrocarbon Liquids, ASTM International. 2000.

American Society for Testing and Materials, Standard Test Methods for Instrumental Determination of Carbon, Hydrogen, and Nitrogen in Petroleum Products and Lubricants, Man. Hydrocarb. Anal. 6th Ed., 852-855, 2008a, <https://doi.org/10.1520/mnl10969m>.

American Society for Testing and Materials, Standard Test Method for Boiling Range Distribution of Petroleum Fractions by Gas Chromatography, ASTM International. 2008b.

American Society for Testing and Materials, Standard Test Method for Density , Relative Density , and API Gravity of Liquids by Digital Density Meter, ASTM International, Reapproved 2018, 2013.

American Society for Testing and Materials, Calculation of Physical Properties of Petroleum Products From Gas Chromatographic Analyses. 2015.

Auxilio, A.R., Choo, W.L., Kohli, I., Chakravartula Srivatsa, S., Bhattacharya, S. An experimental study on thermo-catalytic pyrolysis of plastic waste using a continuous pyrolyser, Waste Manag. 67 (2017) 143–154. <https://doi.org/10.1016/j.wasman.2017.05.011>.

Costa, P., Pinto, F., Mata, R., Marques, P., Paradela, F., Costa, L. Validation of the application of the

- pyrolysis process for the treatment and transformation of municipal plastic wastes, *Chem. Eng. Trans.* 86 (2021) 859–864. <https://doi.org/10.3303/CET2186144>.
- Das, P., Tiwari, P. Valorization of packaging plastic waste by slow pyrolysis, *Resour. Conserv. Recycl.* 128 (2018a) 69–77. <https://doi.org/10.1016/j.resconrec.2017.09.025>.
- Das, P., Tiwari, P. The effect of slow pyrolysis on the conversion of packaging waste plastics (PE and PP) into fuel, *Waste Manag.* 79 (2018b) 615–624. <https://doi.org/10.1016/j.wasman.2018.08.021>.
- Dobó, Z., Jakab, Z., Nagy, G. Koós, T., Szemmelveisz, K., Muránszky, G. Transportation fuel from plastic wastes: Production, purification and SI engine tests, *Energy* 189 (2019) 116353. <https://doi.org/10.1016/j.energy.2019.116353>.
- Dobó, Z., Kecsmár, G., Nagy, G., Koós, T., Muránszky, G., Ayari, M. Characterization of Gasoline-like Transportation Fuels Obtained by Distillation of Pyrolysis Oils from Plastic Waste Mixtures, *Energy & Fuels* 35 (2021) 2347–2356. <https://doi.org/10.1021/acs.energyfuels.0c04022>.
- Huang, P.K. Characterization and Thermodynamic Correlations for Undefined Hydrocarbon Mixtures, Ph. D. Dissertation, Pennsylvania State University, 1977.
- Ibrahim, H., Abdelbagi, H., Ahmed, M., Ahmed, S.M. Thermal Degradation of mixed Plastic Solid Waste HDPE, LDPE, PP and PS, no. July, 2018, <https://doi.org/10.13140/RG.2.2.32160.89601>.
- Islam, M.N., Zailani, R., Ani, F.N. Pyrolytic oil from fluidised bed pyrolysis of oil palm shell and its characterisation, *Renew. Energy* 17 (1999) 73–84. [https://doi.org/10.1016/S0960-1481\(98\)00112-8](https://doi.org/10.1016/S0960-1481(98)00112-8).
- Miandad, R., Barakat, M.A., Aburizaiza, A.S., Rehan, M., Ismail, I.M.I., Nizami, A.S. Effect of plastic waste types on pyrolysis liquid oil, *Int. Biodeterior. Biodegrad.* 119 (2017) 239–252. <https://doi.org/10.1016/j.ibiod.2016.09.017>.
- Montemayor, R.G. Distillation and Vapor Pressure Measurement in Petroleum Products, ASTM International, West Conshohocken, 2008.
- Pinto, F., Costa, P., Gulyurtlu, I., Cabrita, I. Pyrolysis of plastic wastes. 1. Effect of plastic waste composition on product yield, *J. Anal. Appl. Pyrolysis* 51 (1999a) 39–55. [https://doi.org/10.1016/S0165-2370\(99\)00007-8](https://doi.org/10.1016/S0165-2370(99)00007-8).
- Pinto, F., Costa, P., Gulyurtlu, I., Cabrita, I. Pyrolysis of plastic wastes. 2. Effect of catalyst on product yield, *J. Anal. Appl. Pyrolysis*, 51 (1999b) 57–71. [https://doi.org/10.1016/S0165-2370\(99\)00008-X](https://doi.org/10.1016/S0165-2370(99)00008-X).
- Quesada, L., Calero, M., Martín-Lara, M.A., Pérez, A., Blázquez, G. Production of an Alternative

- Fuel by Pyrolysis of Plastic Wastes Mixtures, *Energy Fuels* 34 (2020) 1781–1790. <https://doi.org/10.1021/acs.energyfuels.9b03350>.
- Quesada, L., Calero, M., Martín-Lara, M.A., Pérez, A., Blázquez, G. Characterization of fuel produced by pyrolysis of plastic film obtained of municipal solid waste, *Energy* 186 (2019) 115874. <https://doi.org/10.1016/j.energy.2019.115874>.
- Rand, S.J. *Significance of Tests for Petroleum Products*, 8th ed, ASTM, Newburyport, 2010.
- Riazi, M.R., Daubert, T.E. Simplify Properties Predictions, *Hydrocarb. Process.* 59 (1980) 115–116.
- Riazi, M.R., Daubert, T.E. Characterization Parameters for petroleum fractions, *Ind. Eng. Chem. Res.* 26 (1987) 755–759. <https://doi.org/10.1021/ie00064a>.
- Riazi, M.R. *Characterization and Properties of Petroleum Fractions*, 1st ed., vol. 1, ASTM, Philadelphia, 2005.
- Sarker, M., Rashid, M.M. Production of Aromatic Hydrocarbons Related Kerosene Fuel from Polystyrene and Polypropylene Waste Plastics Mixture by Fractional Distillation Process, *Int. J. Appl. Chem. Sci. Res.* 1 (2013) 10–23.
- Scheirs, J. *Feedstock Recycling and Pyrolysis of Waste Plastics*, John Wiley & Sons, Ltd, West Sussex, 2006.
- Shadangi, K.P., Mohanty, K. Production and characterization of pyrolytic oil by catalytic pyrolysis of Niger seed, *Fuel* 126 (2014) 109–115. <https://doi.org/10.1016/j.fuel.2014.02.035>.
- Singh, R.K., Ruj, B., Sadhukhan, A.K., Gupta, P. Thermal degradation of waste plastics under non-sweeping atmosphere: Part 2: Effect of process temperature on product characteristics and their future applications, *J. Environ. Manage.* 261 (2020) 110112. <https://doi.org/10.1016/j.jenvman.2020.110112>.
- Treese, S.A., Pujadó, P.R., Jones, D.S.J. *Handbook of petroleum processing*, Second., vol. 1, Springer, Switzerland, 2015.
- Wauquier, J.P. *El Refino Del Petróleo*, Díaz de Santos - ISE, Madrid, 2004.



## Chapter 4

# Thermal and Catalytic Pyrolysis of a Real Mixture of post-consumer Plastic Waste: An Analysis of the gasoline-range Product

Paucar-Sánchez, M.F.; Calero, M.; Blázquez, G.; Solís, R.R.; Muñoz-Batista, M.J.; Martín-Lara, M.A.

*Department of Chemical Engineering University of Granada, 18071 Granada, Spain*

Process Safety and Environmental Protection, ISSN: 0957-5820, eISSN: 1744-3598. Published by Elsevier Ltd on behalf of the Institution of Chemical Engineers.

*Volume:* 168

*Pages:* 1201-1211

*Country:* United Kingdom

*DOI:* <https://doi.org/10.1016/j.psep.2022.11.009>

- *Category:* Engineering, Environmental. *Journal Impact Factor, JIF (2022):* 7.8. *Category Ranking:* 11/55 (Q1).
- *Category:* Engineering, Chemical. *Journal Impact Factor, JIF (2022):* 7.8. *Category Ranking:* 15/140 (Q1).

*Article history:*

Received 21 July 2022

Received in revised form 16 October 2022

Accepted 4 November 2022

Available online 7 November 2022



## Abstract

In this work, the thermal and catalytic pyrolysis of different types of plastic waste and a real mixture were investigated in a fixed-bed reactor over different catalysts (CaO, MgO, HY, HZSM-5). Important differences in gas, liquid, and solid yields were found as a function of polymer type. The highest gas yield was obtained with expanded polystyrene (52.3%) and the maximum oil production with high-impact polystyrene (55.5%), while polypropylene film led to the highest char release (17.5%). Regarding the composition of the liquid oil, high-impact polystyrene showed the highest yield of gasoline-range products (426 g per kg of pyrolyzed plastic), mainly composed of aromatics compounds (90%). The addition of catalysts increased the gas yield to the detriment of the oil produced. The effect was more evident for zeolite-type catalysts, i.e., the gas yield raised from 43.3 (non-catalytic) to 51.5% (HZSM-5). Low influence on the oil composition, i.e., gasoline-range product, was detected. This can be explained by the fast deactivation of catalysts because of coke deposition. Only an increase in the fraction of gasoline in liquid oil was observed when low-cost catalysts (CaO and MgO) were used, without significant changes in the composition of this product.

**Keywords:** Plastic waste; Pyrolysis; Catalysts; Gasoline-range product; Hydrocarbon types.

## 4.1. Introduction

Today, the benefits of plastics are unquestionable: low cost, lightweight, aseptic, durable, resistant, and easy to mold. Unlike metals, they do not rust or corrode; most photodegrade and slowly break down into small fragments known as microplastics. Since the 1950s, their production, which relies heavily on fossil hydrocarbons, has overtaken the manufacture of any material due to the global shift from making durable plastics to single-use ones, which are discarded by the same year of manufacture (United Nations Environment Programme, 2018). According to recent estimations in Europe, only one-third of the collected post-consumer plastic waste (10.2 Mt) was sent to recycling facilities, but over 23% (6.9 Mt) was still sent to landfill (Plastics Europe, 2021). Depositing plastic waste in a landfill does not mean eliminating the problem; rather, it can generate another one in the future. In this sense, plastic buried deep in landfills can leach harmful chemicals that spread into the soil and water. Also, some recent works have shown that microplastics that are generated in a landfill without sufficient protection can be transferred to the environment and could have a very negative effect on ecosystems (Sun et al., 2021; Su et al., 2019; Wan et al., 2022). The European Strategy for Plastics in a Circular Economy (Commission, 2020) proposes a series of key measures to improve the economy and quality of plastic recycling and reduce waste and littering, among which are favor the use of recycled plastics and reuse and recycling against the landfilling or incineration, eradicate illegal

and non-compliant landfills and use economic instruments to increase the cost of landfilling and incineration.

Although many sorting processes have been implemented, only plastic waste, especially rigid plastics composed of one type of polymer, can be recycled through mechanical procedures. However, many more contaminated or mixed dirty plastics and plastics made of multi-materials that cannot be mechanically recycled for technical or economic reasons are accumulated in landfills (Hopewell et al., 2009). Chemical recycling offers a solution for these unrecovered plastic wastes, incorporating them as secondary raw materials in different industrial ecosystems. Chemical recycling is, therefore, a complementary solution to mechanical recycling, as it can be used to process a broader scope of plastic waste that is currently unsuitable for mechanical recycling.

Pyrolysis is one of the most investigated chemical recycling technologies for plastic waste (Collias et al., 2021). In the last few years, many studies have been published about the pyrolysis of different plastic waste. Most pyrolysis studies have been carried out with individual plastics and mixtures. Particularly, thermal conversion by pyrolysis of polyethylene (PE), both high-density polyethylene (HDPE) and low-density polyethylene (LDPE), polypropylene (PP), polystyrene (PS), polyethylene terephthalate (PET) and polyvinyl chloride (PVC), individually and in mixtures have been deeply examined (Rodríguez Lamar et al., 2021; Williams and Williams, 1997; Costa et al., 2021; Singh et al., 2019; Singh et al., 2020; Parku et al., 2020; Rodríguez-Luna et al., 2021; Miandad et al., 2017; López et al., 2010). For example, Rodríguez Lamar et al. (Rodríguez Lamar et al., 2021) investigated the kinetic thermal pyrolysis of PP, HDPE, and LDPE. Also, the liquid fractions obtained from the pyrolysis were characterized according to ASTM standards and gas chromatography. Williams and Williams (Williams and Williams, 1997) analyzed the thermal pyrolysis of mixed plastics to simulate the plastic composition of municipal solid waste (MSW) found in Europe, and the interaction between polymers was investigated. Costa et al. (Costa et al., 2021) also examined the thermal pyrolysis of a plastic mixture derived from MSW containing PE, PP, PS, and small amounts of PET and PVC. The liquid fractions were analyzed using the gas chromatography-mass spectrometry technique, and the effect of the presence of the different types of polymers on the hydrocarbons produced was discussed. Also, Singh et al. (Singh et al., 2019; Singh et al., 2020) analyzed the effect of heating rates, the residence time of volatiles in the reactor, and pyrolysis temperature on product yield and its composition on the pyrolysis of a post-consumer plastic waste mixture also composed of PE, PP, PS, PET, and PVC. Other authors analyzed the pyrolysis of PP under atmospheric and vacuum pressure at different temperatures and heating rates and reported volatile composition as a function of pyrolysis conditions (Parku et al., 2020). Recently, Rodríguez-Luna et al. (Rodríguez-Luna et al., 2021) investigated the pyrolysis of HDPE in a two-step process to increase pyrolysis oil yield. The sequential process used



in this study consisted of two pyrolysis steps, one focused on wax production and the other on oil yield operating parameters optimized based on statistical analysis. Other studies examined the effect of different types of plastic waste (PE, PP, PS, and PET) and their mixtures on the yield and quality of produced liquid oil from the pyrolysis process (Miandad et al., 2017), even working with real streams of plastic waste rejected from the industrial plant (López et al., 2010).

In most cases, crude pyrolysis oils cannot be used directly, and many studies emphasized the need to upgrade the pyrolysis oils (Qureshi et al., 2020). In this sense, fractional distillation, commonly used to separate petroleum oils, can be used to upgrade oil properties/composition. Some authors, such as Wiriyaumpaiwong and Jamradloedluk (Wiriyaumpaiwong and Jamradloedluk, 2017), studied the distillation of two pyrolytic oil samples derived from the pyrolysis of PE and mixed plastic wastes. Also, extensive research on producing determined valuable compounds from plastic waste pyrolysis has been widely conducted. For example, Jung et al. (Jung et al., 2010) and Sarker and Rashid (Sarker and Rashid, 2013) pyrolyzed PE and PP under various reaction conditions and analyzed the content of benzene, toluene, and xylenes (BTX aromatics), which are very important petrochemical materials, in the oil product. For both PE and PP materials, it was found that the BTX aromatics content increased with the reaction temperature. Other authors examined the potential of liquid oil samples derived from the pyrolysis of plastic film waste as automotive diesel fuel. Distilled pyrolysis liquids in the diesel range and the liquid fractions were characterized according to automotive diesel standards (Gala et al., 2020). Also, Baena-González et al. (2020) reported compounds and materials that can be recovered from the distillation of pyrolysis oil obtained from PS. Other researchers completed a study to optimize liquid products obtained through refinery distillation bubble cap plate column (Thahir et al., 2019). These authors found important differences in product yield and characterization on each tray depending on the pyrolysis temperature. In addition, Demirbas (2004) and Dobo' et al. (2021) pyrolyzed three plastic wastes (PE, PP, and PS) and their mixtures to obtain valuable gasoline-range hydrocarbons from the pyrolytic oil. Other researchers studied the hydrogen production from PE, PP, PS, and PET and their mixture (Barbarias et al., 2018).

Other options for improving the properties and composition of pyrolysis oils are co-pyrolysis and the use of catalytic materials in the process. Regarding co-pyrolysis, it is thermal pyrolysis involving two or more different materials as feedstock; in this option, the mixing ratio of the materials is one of the most important influencing factors. Regarding catalytic pyrolysis, many catalysts, mainly zeolites (predominantly HZSM-5 and HY) with remarkable acidic character, high surface area, and high pore volume, have been investigated. Also, available low-cost materials such as bentonite or metal oxides (CaO and MgO) have been extensively applied in both in-situ and ex-situ catalytic pyrolysis patterns (Fadillah et al., 2021; Budsareechai et al., 2019). The lower cost of these materials compared to synthetic zeolites makes them competitive for real

applications at a large scale. For example, some authors have enhanced the formation of benzene, toluene, and ethylbenzene (BTE) aromatics by using the ammonium-type ZSM-5 zeolite as a catalyst in the pyrolysis of expanded polystyrene (EPS) (Verma et al., 2021). Elordi et al. (2011) also used HZSM-5 supported on bentonite and alumina to pyrolyze HDPE, LDPE, and PP. Also, PE, PP, PS, and PET were catalytically pyrolyzed by Xue et al. (Xue et al., 2017). The authors found differences in product distribution and composition at in-situ and ex-situ configurations and reported positive synergies between PE and PS or PE and PET. A simulated mixture of plastics representing the plastic mixture found in municipal solid waste was pyrolyzed using spent zeolite from a fluid catalytic cracker (FCC), and HY and HZSM-5 acidic zeolites (Onwudili et al., 2019), and authors reported that aromatic contents of oils increased with the presence of catalysts as well as increased the bed temperature. Especially, HY acidic zeolite promoted the formation of low molecular weight aromatic hydrocarbons. Also, co-pyrolysis of polycarbonate (PC) with PS was conducted to produce aromatic hydrocarbons using HZSM-5 as a catalyst (Wang et al., 2020). A reaction temperature of 700 °C reached a maximum aromatic hydrocarbon content, and PC co-pyrolysis with PS produced more monocyclic aromatic hydrocarbons. Other researchers studied the catalytic pyrolysis of individual PE, PP, PS, and PET and its mixture in the presence of CaO under a steam atmosphere. Authors reported that CaO enhanced the gas and liquid production from mixtures, and the wax content derived from PE and PP was reduced (Kumagai et al., 2015). MgO and CaO were also used as catalysts for the pyrolytic conversion of PE and PP. These low-cost catalysts improved the conversion to liquid products, decreasing the gas and char yields and producing liquid results in the gasoline, diesel, and kerosene ranges (Hidalgo Herrador et al., 2022).

Although thermal and catalytic pyrolysis of plastics is being studied individually and in blends, including by co-pyrolysis, few studies have determined the possible interactions and synergic effects of the combination of polymers, especially coming from real post-consumer waste plastic that at present are being sent to landfills. In this work, the thermal and catalytic pyrolysis of a real mixture of post-consumer plastic waste comes from the rejected plastic fraction of non-selective collection of MSW was investigated over low-cost, basic materials (CaO and MgO), and commercial acid zeolites (HZSM-5 and HY). The product yields of liquid oil of thermal and catalytic pyrolysis of individual plastics and the real mixture of plastics were analyzed. Analysis of hydrocarbon types in the gasoline-range product was specially examined in both thermal and catalytic pyrolysis. Specifically, the comparison performed between the results of the evaluation of gasoline-range products derived from plastic pyrolysis of individual plastics and the real mixture is especially innovative. To the best of our knowledge, the present study is among the first to profoundly investigate the influence of the polymer and catalyst, which can certainly affect the pyrolysis products on the gasoline-range product.

## 4.2. Materials and methods

### 4.2.1. Raw material

The mixture of plastic waste used in this study came from the rejected plastic fraction of a mechanical biological treatment (MBT) plant in Granada (Spain). The mixture was composed of rigid polypropylene (PP), expanded polystyrene (EPS), high impact polystyrene (HIPS), polypropylene film (PP film), and polyethylene film (PE film). Before thermal and catalytic pyrolysis experiments, these polymeric fractions were identified by Near Infrared Spectroscopy (NIR) using a portable Panatec Thermo Scientific microPhazir AG analyzer with a wavelength range of 2400–1600 nm, separated, and subjected to a size reduction process (1–3 mm). Particularly, the received raw material showed an average composition (wt%) of 56.10% of PP, 12.65% of PP film, 12.65% of PE film, 10.05% of EPS, and 8.55% of HIPS. Information about characteristics such as proximate and elemental analysis can be found in previous works (Martín-Lara et al., 2021; Quesada Lozano, 2021), and a summary is provided in Table 4.1.

**Table 4.1.** Characteristics of raw materials. Data from [37,38].

	<b>Analysis</b>	<b>PP</b>	<b>PP film</b>	<b>PE film</b>	<b>EPS</b>	<b>HIPS</b>
Proximate	Moisture, %	0.00	0.20	1.00	0.00	1.80
	Volatile matter, %	99.3	99.0	95.5	99.8	88.9
	Ash content, %	0.70	0.70	1.00	0.10	7.60
	Fixed carbon, %	0.00	0.10	2.40	0.10	1.70
Elemental	C, %	82.92	83.54	77.61	91.69	66.47
	H, %	14.47	13.95	11.91	8.28	7.63
	N, %	0.16	0.12	0.10	0.11	0.14
	S, %	0.00	0.00	0.00	0.00	0.00
	O, %	1.75	1.69	10.38	0.00	17.84

### 4.2.2. Preparation and characterization of the catalysts

Available low-cost catalysts, CaO and MgO materials, were supplied by Scharlab S.L. and PanReac, respectively. The commercial acidic zeolites used were HZSM-5 zeolite (zeolyst ZSM-5, SiO<sub>2</sub>/Al<sub>2</sub>O<sub>3</sub> mole ratio = 30) and Y-zeolite (zeolyst Y, hydrogen, SiO<sub>2</sub>/Al<sub>2</sub>O<sub>3</sub> mole ratio = 5.2) both supplied by Alfa Aesar.

The catalysts were calcined under an air atmosphere at 550 °C for 3.5 h in a muffle furnace (Nabertherm, L 3/11/B180 Model) before using to stabilize their chemical, structural and morphological properties. Although commercial catalysts used in this contribution are well-characterized by manufacturers, the morphological modifications of the samples after calcination were analyzed, i.e., surface area and pore volume by N<sub>2</sub> adsorption-desorption isotherms conducted at – 196 °C in an ASAP2429 device from Micromeritics. The total surface area was determined by the BET method, the total pore volume by the N<sub>2</sub> uptake at P/P<sub>0</sub>~0.99, the microporous surface and pore volume from the t-plot method, and the average pore size from the DFT method.

### 4.2.3. Pyrolysis reactor and pyrolysis conditions

The pyrolysis experiments were performed on a horizontal laboratory-scale fixed-bed tubular reactor (internal diameter 4 cm and length 34.25 cm) R50/250/12 model of Nabertherm made of stainless steel 316 and integrated with a flowmeter to regulate the inert nitrogen flow, see Fig. 4.1. The experiments were carried out with approximately 20 g of plastic waste placed in a closed 316 stainless steel tube (internal diameter of 27.25 cm and 30.6 cm of length) with a chimney hole at a heating rate of 10 °C·min<sup>-1</sup> from room temperature to 500 °C determined as optimum temperature for maximize liquid yield in a previous work (Paucar-Sánchez et al., 2022) and with a constant flow rate of 0.8 L·min<sup>-1</sup> of N<sub>2</sub>. Reached pyrolysis temperature, kept the reactor at this temperature for 60 min. Then, the pyrolysis test was finished; the reactor was cooled under a low nitrogen flow of 0.2 L·min<sup>-1</sup> until room temperature was achieved. When used, the catalyst (1 g) was placed in a basket at the outlet line of the reactor but within the radiant zone.

Regarding the sampling of the products, the liquid fraction was collected using an ore-weighted glass receiver submerged in a liquid bath at – 7 °C, and the solid product was taken from the steel tube when the reactor was cooled.

The solid residue and the liquid products were directly weighted, and their yields were determined according to the following equations (gas yield by difference to 100%):

$$\eta_l = \frac{m_l}{m_m} \cdot 100 \quad (4.1)$$

$$\eta_s = \frac{m_s}{m_m} \cdot 100 \quad (4.2)$$

$$\eta_g = 100 - (\eta_l + \eta_s) \quad (4.3)$$

where  $m_m$ ,  $m_l$  and  $m_s$  are the weights of the plastic sample, liquid, and solid products, respectively, and  $\eta_l$ ,  $\eta_s$  and  $\eta_g$  are the yields of liquid, solid, and gases, respectively. Experiments were conducted in triplicate, and the average value obtained led to a relative standard deviation inferior to 5%.

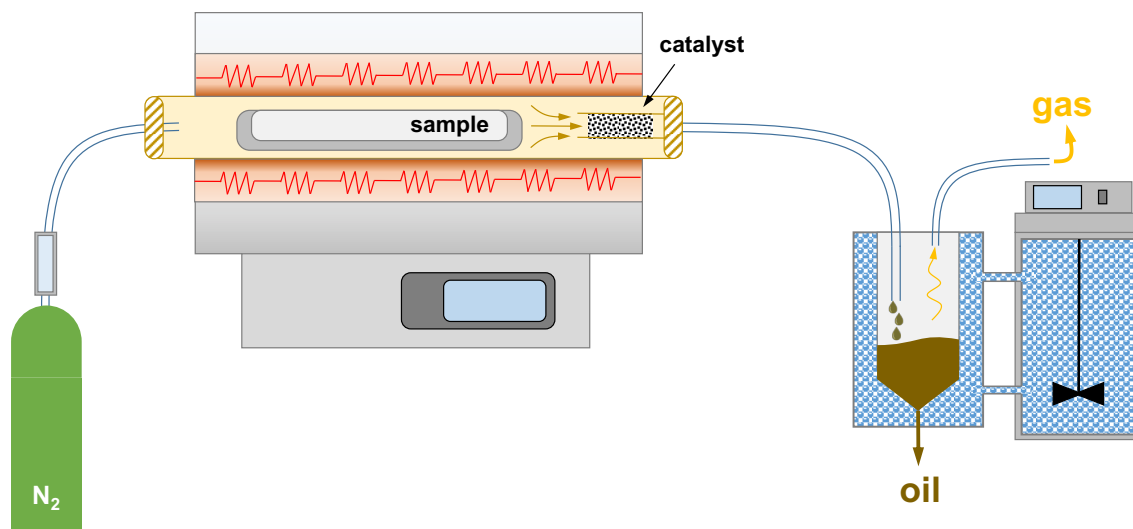


**Figure 4.1.** Representation of the installation used for the pyrolysis experiments.

#### 4.2.4. Liquid product analysis

##### 4.2.4.1. Analytical procedure

The identification of the components of the liquid fraction was carried out by gas chromatography (Agilent 8860 model) coupled to a triple-quadrupole mass spectrometer detector (Agilent 5977 model) with analysis scan speed  $\leq 20,000 \text{ Da}\cdot\text{s}^{-1}$  and ionization energy by the electronic impact of 70 eV. The column was a Phenomenex with a nonpolar phase ZB-5 ms (30 m, 0.25 mm internal diameter, and 0.25  $\mu\text{m}$  of fill thickness). The oven temperature was programmed in two modes with initial temperatures of 40 and 42 °C for 5 and 4 min, injector temperature of 240 °C in both ways and final temperatures of 240 and 320 °C for 6 and 4 min with 15 and 6 °C $\cdot\text{min}^{-1}$  gradients, respectively. The samples were weighed and diluted in 1 mL of chloroform and injected in split mode (10:1 for gasoline-range product and 5:1 for pyrolytic oil) at a constant flow of Helium of 1 mL $\cdot\text{min}^{-1}$ .

##### 4.2.4.2. Simulated distillation (SD)

The determination of the distribution of the boiling range of the compounds identified in the chromatograms of the gasoline fraction and pyrolytic oils was performed using D7096–19 and

D2887–19a standard test methods of ASTM, respectively (American Society for Testing and Materials, 2021; American Society for Testing and Materials, 2021). Synthetic mixtures of pure liquid hydrocarbons encompassing the boiling range of both analytical techniques were used to determine reference retention times. The referential compounds were also confirmed using the National Institute of Standards and Technology (NIST) mass spectrum library database (NIST 08).

To calculate the boiling point based on the retention time of the compounds in the samples, the referential times and boiling points of the referential compounds were used according to the following equation:

$$BP_x = \left( \frac{BP_2 - BP_1}{RT_2 - RT_1} \right) \cdot (RT_x - RT_1) + BP_1 \quad (4.4)$$

where  $BP_1$ ,  $BP_2$  and  $RT_1$ ,  $RT_2$  are the boiling point and retention times of referential compounds, and  $BP_x$  and  $RT_x$  are the boiling points and retention times of the compounds in the sample.

The boiling range distribution was reported as a function of weight percent distilled and the following products were analyzed according to ASTM designation D5154/D5154M-18 (American Society for Testing and Materials, 2022): gasoline product, C5 compounds through compounds boiling up to 216 °C, the light cycle oil (LCO) product defined to have a boiling point range of 216–343 °C and the heavy cycle oil product (HCO) determined to have a minimum boiling point of 343 °C.

#### 4.2.4.3. Hydrocarbon types in the gasoline-range product

The total concentration of total paraffins, monocycloparaffins, dicycloparaffins, alkylbenzenes, indans, tetralins and naphthalenes in the gasoline-range product was determined by the standard test method ASTM D2789–95 by mass spectrometry, based on the summation of characteristic mass fragments (American Society for Testing and Materials, 2021).

#### 4.2.5. Coke deposition on the catalysts

Coke originates from undesirable side reactions and covers surface sites, ultimately blocking pores. It is a mixture of solid and non-volatile carbonaceous compounds which may include alkanes, alkenes or cyclic and aromatic molecules from feed or generated as an intermediate. To determine the coke yield on the catalysts, continued stripping and subsequent combustion of catalysts were carried out in a PerkinElmer TGA thermobalance STA6000 model. Approximately 20 mg of the spent catalyst was introduced in the thermobalance with a constant flow of 20 mL·min<sup>-1</sup> of nitrogen from room temperature to 500 °C at a heating rate of 15 °C·min<sup>-1</sup>. Then, the

desired temperature was maintained for 30 min, followed by flash combustion up to 550 °C. The weight percentages of volatile products were calculated and added to their respective cuts in the liquid product. In contrast, the total mass of the non-volatile fraction of coke was calculated according to Eq. 5:

$$\eta_c = \frac{m_i - m_f}{m_f} \cdot 100 \quad (4.5)$$

where  $\eta_c$  is the coke yield, and  $m_i$  and  $m_f$  are the mass of the sample at the beginning and end of the combustion stage, respectively.

### 4.3. Results and discussion

#### 4.3.1. Characterization of the catalysts

Table 4.2 shows the textural characterization of the different catalysts analyzed by N<sub>2</sub>adsorption-desorption isotherms after thermal treatment at 550 °C. According to the IUPAC classification of physisorption isotherms, depicted in Fig. 4S1, all the materials studied can be classified as type IV whose capillary condensation is accompanied by hysteresis loops of type H3, for basic low-cost catalysts, i.e., CaO and MgO and type H4, for acid zeolite-type catalysts (Thommes et al., 2015). The surface area and pore volume of CaO displayed the typical low values reported in the literature, in which the temperature does not considerably affect the textural properties (Micic et al., 2015). The surface area of MgO was higher than CaO, with a remarkable mesoporous character as deduced from the porous size distribution, see Fig. 4S2. Although MgO can be prepared with a more developed surface area, the value obtained in this case for the commercial formula treated thermally is in accordance with the reported for some MgO prepared after precipitation of hydroxide precursor formulas (Bartley et al., 2012). The acid zeolite-type catalysts, HY and HZSM-5, gave the highest micropore volume and surface area values. Particularly, the hieratically HY zeolite led to an extraordinarily high surface area and well-developed microporosity, i.e., over 90%, as reported from some ordered zeolite structures (Chen et al., 2020). In this case, the HY samples presented a high contribution of micropores of ca. 19 Å. The HZSM-5 displayed lower values within the range expected for this zeolite (Xu et al., 1994; Zhang et al., 2012).

#### 4.3.2. Effect of type of polymer on thermal pyrolysis performance

##### 4.3.2.1. Effect of type of polymer on product yields

Fig. 4.2 shows the gas, liquid, and solid yields resulting from the pyrolysis of individual studied plastic waste. EPS was the polymer that produced the highest yield of gas (52.3%), followed by

PP film (48.7%), PP (45.1%), PE film (38.1%), and HIPS (31.2%). Regarding the solid (char) yield, PP film, HIPS, and PE film were the plastic waste that generated more solids (17.5%, 13.4%, and 10.1%, respectively). About the liquid product, PP film generated a reduced amount of liquid (33.9%), while HIPS showed the highest liquid yield (55.5%). In addition, although some of the studied polymers (PP and PP film and EPS and HIPS) have the same thermoplastic base, significant differences in product yields were observed, perhaps due to different manufacturing processes; for example, EPS is prepared by impregnation with a blowing agent, such as isopentane, while HIPS is synthesized by emulsion polymerization in styrene-butadiene latex (Aguado and Serrano, 1999). Also, the HIPS plastic sample used in this work mainly came from yogurt packaging, and it was pyrolyzed with all the other materials from yogurt labels, i.e., painted paper.

**Table 4.2.** Textural properties characteristics of the different catalysts.

catalyst	$S_{\text{BET}}$ ( $\text{m}^2\cdot\text{g}^{-1}$ )	$S_{\text{MP}}$ ( $\text{m}^2\cdot\text{g}^{-1}$ )	$S_{\text{ext}}$ ( $\text{m}^2\cdot\text{g}^{-1}$ )	$V_{\text{T}}$ ( $\text{cm}^3\cdot\text{g}^{-1}$ )	$V_{\text{MP}}$ ( $\text{cm}^3\cdot\text{g}^{-1}$ )	Average pore size (Å)
MgO	58	2	56	0.131	< 0.001	90
CaO	5	0.1	5	0.011	< 0.001	90
HY	1384	1274	110	0.639	0.432	50
HZSM-5	488	440	48	0.204	0.147	31

$S_{\text{BET}}$ : specific BET surface area;  $S_{\text{MP}}$ , micropores specific surface area by t-plot method;  $S_{\text{EXT}}$ : external specific surface area as the difference of  $S_{\text{BET}}$  and  $S_{\text{MP}}$ ;  $V_{\text{T}}$ : total pore volume from  $\text{N}_2$  uptake at  $P/P_0 \sim 0.99$ ;  $V_{\text{MP}}$ : volume of micropores by t-plot method; average pore size by DFT method

If the theoretical (calculated yield according to the quantities of polymers present in the mixture) and real (experimental result obtained) product yields are compared, gas and char yields decreased from 44.2% to 43.4% (about 1.9%) and 8.1–6.3% (around 22.8%), respectively. In contrast, the production of the liquid product increased from 47.7% to 50.4%, approximately an increase of 5.6%.

In addition to the type of polymer (feedstock composition), other variables such as temperature, heating rate, particle size, use of catalyst, type of reactor, and type of system for collecting the different products, can influence the product yields. Therefore, very different data can be found in the literature. Table 4S1 summarizes product yields found by other researchers on thermal and catalytic pyrolysis of plastic waste. For example, in the thermal pyrolysis of EPS waste, Verma et al. Field (Verma et al., 2021) reported a maximum liquid yield of 94.4% at 650 °C. Other authors, by pyrolyzing a mixture of HDPE, LDPE, PS, PP, PET, and PVC at 700 °C, reported a liquid yield of around 75%, about 9% of gas, and a char yield of approximately 2% (Williams and Williams, 1997).



Also, Inayat et al. (Inayat et al., 2020) pyrolyzed PS at 400 °C and 500 °C, obtaining around 64% and 76% of liquid product, respectively. Similarly, a study of thermal pyrolysis of LDPE, PP, and their mixtures was done by Anene et al. (Anene et al., 2018) in a batch pyrolysis reactor at 460 °C, obtaining a liquid yield of 86% for PP and a liquid yield of 96% for LDPE. Additionally, López et al. (López et al., 2010) studied the pyrolysis of a complex combination of HDPE, PP, PS, EPS, PET, PVC, PE film, PP film, and other packing materials (blister, tetra-brick, Al film, Al, iron, etc.) at 500 °C and obtained approximately the same yield data of liquid (53%), gas (41.5%), and solid (5.5%) than those reported here. Also, Williams and Williams (Williams and Williams, 1999) obtained a liquid yield of 45.3% at 500 °C in the pyrolysis of LDPE.

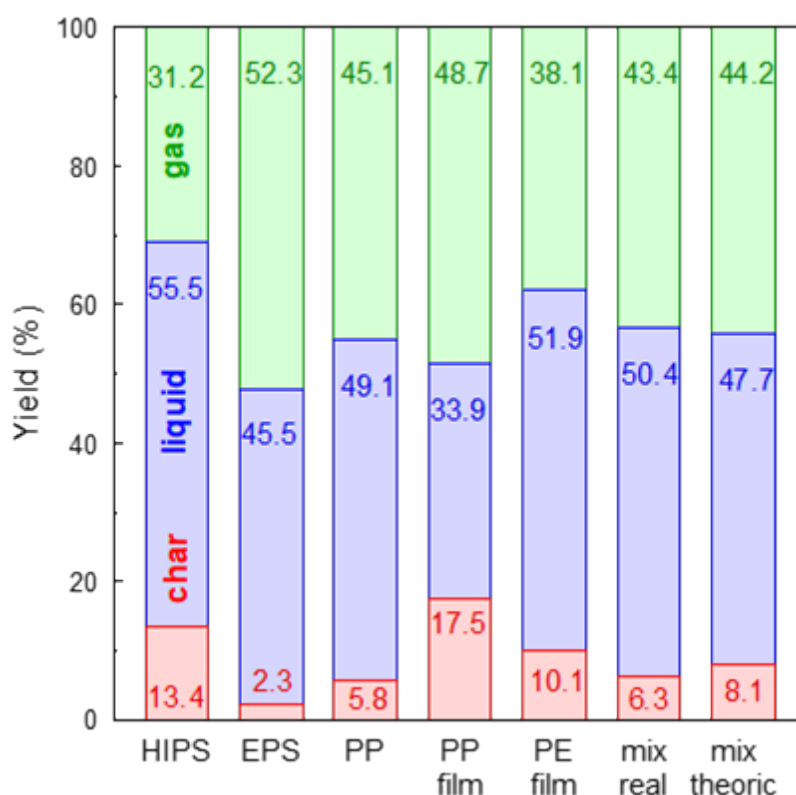


**Figure 4.2.** Gas, liquid, and solid yields as a function of polymer type.

#### 4.3.2.2. Effect of type of polymer on simulated distillation boiling points

The simulated distillation curves of the liquid product obtained from the pyrolysis of the individual plastic wastes and their mixture are shown in Fig. 4.3. Also, Table 4.3 reports the yields of gasoline, light cycle oil (LCO), and heavy cycle oil (HCO) products (as a mass percentage). The trend of the curves suggested that liquid product from pyrolysis of HIPS presented lower volatilization temperatures since, in general, higher distilled mass fractions were reached at different temperatures, mainly between 130 °C and 400 °C. In opposition, the simulated

distillation curve of PE film showed a low percentage of the gasoline-range product as higher boiling temperatures were needed to reach high distilled mass fractions; therefore, about 70% of the liquid was an HCO-range product. In addition, similar pattern curves were observed for PP, PP film, and the mixture of plastics with slight differences in yields of gasoline, LCO, and HCO-range products. Finally, EPS showed a different profile with similar product yields of gasoline and LCO-range and a lower yield of HCO-range.

Regarding the impact of the combination of the different plastic materials on gasoline, LCO, and HCO production, the mixture of plastic waste produced an average value of approximately 20% more gasoline-range product than that which would be obtained as a proportional balance of the gasoline got from the individual plastic waste pyrolysis. Also, making the same evaluation, an average reduction of LCO and HCO of around 12% and 14% was observed from the theoretical data from mixing LCO and HCO produced from the individual plastic pyrolysis, respectively.

Finally, Table 4.4 reports the yields of the different types of products obtained from each polymer and the mixture studied in this work. The major yield was observed for the gasoline-range product in oils from pyrolysis of HIPS, PP, and the mix of plastics with values ranging between 235.35 and 426.2 g·kg<sup>-1</sup> plastic. However, deficient gasoline production (40 g·kg<sup>-1</sup> plastic) was observed in liquid from PE film pyrolysis due to higher bottoms (HCO) output uncracked. In general, wax is the main product obtained in the thermal pyrolysis of polyolefins at moderate temperatures (Williams and Williams, 1999). Consequently, many authors have reported the greater production of waxes, depending on the thermal pyrolysis conditions, in the pyrolysis of PE (Predel and Kaminsky, 2000; Takuma et al., 2000).

Regarding LCO-range product yield, it was higher in the liquid of thermal pyrolysis of EPS (222.0 g·kg<sup>-1</sup> plastic) and lower in the case of HIPS pyrolysis (62.7 g·kg<sup>-1</sup> plastic). Finally, HCO-range product values ca. 66.0 (HIPS) and 385.7 (PE film) g·kg<sup>-1</sup> plastic was found. As indicated before, a high amount of heavy products was expected for PE film pyrolysis since the “liquid” obtained as the product was wax.

Dobó et al. (Dobó et al., 2021) also studied the gasoline production from pyrolytic oil of different mixtures containing HDPE, LDPE, PP, and PS, representing the plastic demand in Hungary, the EU, and the world. The gasoline-range product was obtained by atmospheric distillation with a yield of 473–512 g·kg<sup>-1</sup> solid waste. These authors attributed the enhanced gasoline yield to the installation design that recirculates high boiling point components into the reactor for further molecule scission. The researchers also reported an increase in gasoline-range product yield when the proportion of PS was raised. This result has been observed by the high gasoline yield obtained for HIPS material in this work.

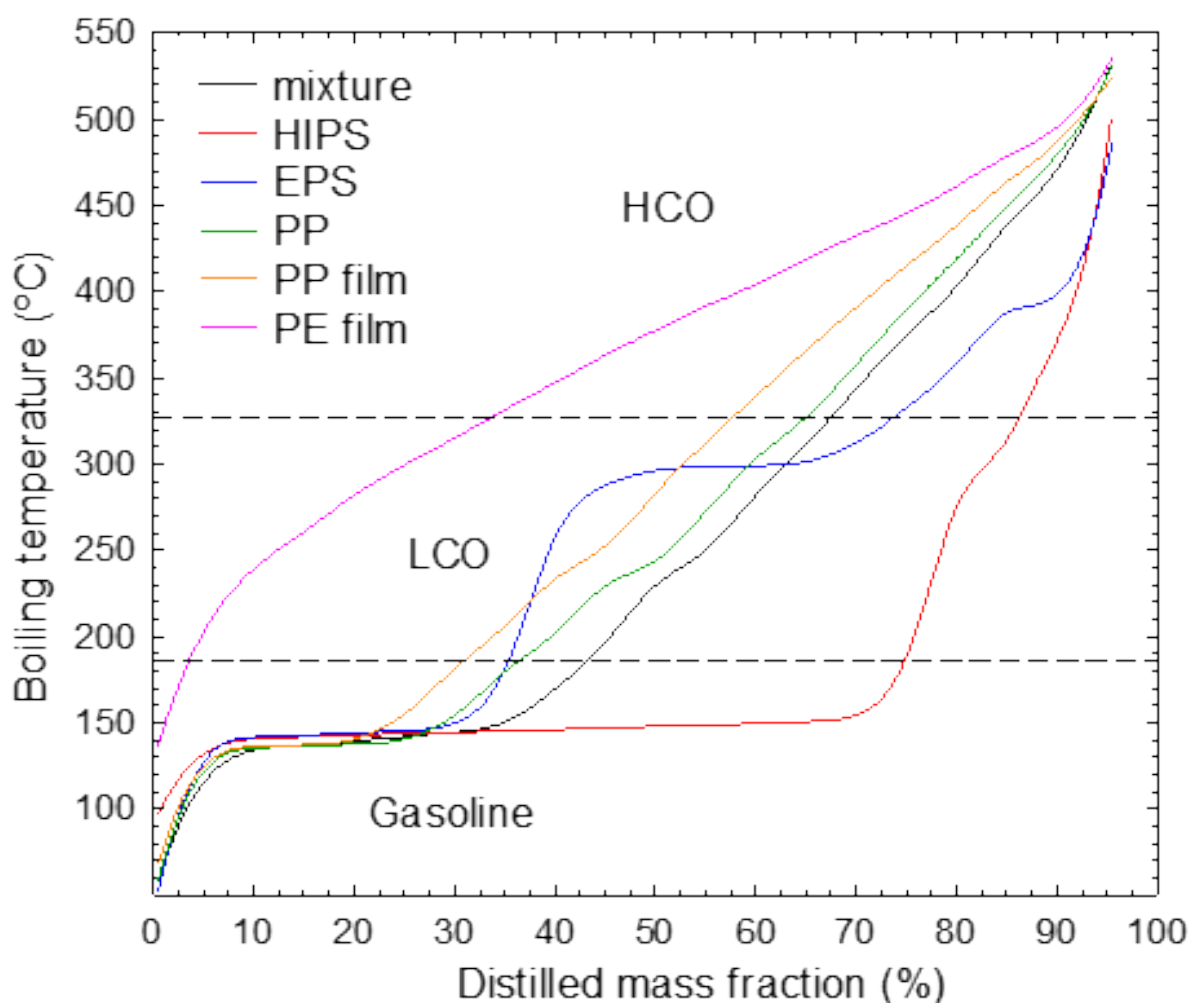


**Figure 4.3.** Boiling temperature as a function of distilled mass fraction (simulated distillation) of the liquid fraction from thermal pyrolysis of the mixed plastic waste and their residual polymers.

**Table 4. 3.** Gasoline, LCO, and HCO products yields (mass %) in thermal pyrolysis (non-catalytic) of post-consumer plastic waste

Plastic-type	Gasoline-range	LCO-range	HCO-range
Mixture (theoretical)	39.7	25.2	35.1
Mixture (experimental)	47.7	22.1	30.2
HIPS	76.8	11.3	11.9
EPS	37.3	40.0	22.7
PP	42.4	25.3	32.2
PP Film	36.8	24.0	39.2
PE Film	7.2	23.3	69.5

Average values with a relative standard deviation inferior to 5%.

#### 4.3.2.3. Effect of the type of polymer on hydrocarbon types in the gasoline-range product

The gasoline-range product has been analyzed in terms of the type of polymer pyrolyzed. The simulated distillation curves of this product are shown in Fig. 4.4A. For analogy with hydrocarbons present in crude petroleum, the gasoline-range product was first classified into three general types: paraffins, naphthenes, and aromatics (Fig. 4.4B), and then, a more detailed categorization was performed into naphthalenes, indans, or tetralins, alkylbenzenes, paraffins, monocycloparaffins, and dicycloparaffins (Fig. 4.4C).

**Table 4.4.** Gasoline, LCO, and HCO products yields (data in  $\text{g}\cdot\text{kg}^{-1}$  plastic) in thermal pyrolysis (non-catalytic) of post-consumer plastic waste.

Plastic-type	Gasoline-range	LCO-range	HCO-range
Mixture	240.4	111.4	152.2
HIPS	426.2	62.7	66.0
EPS	207.0	222.0	126.0
PP	235.3	140.4	178.7
PP Film	204.2	133.2	217.6
PE Film	40.0	129.3	385.7

Average values with a relative standard deviation inferior to 5%.

Some significant differences were observed in the composition of the gasoline-range product obtained by thermal pyrolysis of different types of polymers. The yields of aromatics, paraffins, and naphthenes significantly varied between HIPS and EPS plastics and polyolefins (PP, PP film, PE film) and the mixture of plastics. Especially, thermal pyrolysis of HIPS and EPS showed a high yield of aromatic compounds, reaching a value of 89.8% and 83.5% in gasoline derived from HIPS and EPS materials, respectively. Conversely, PP, PP film, PE film, and the mixture of plastics showed a high yield of naphthenes with values ranging between 50.3% and 58.9%.

In gasoline-range products obtained from pyrolysis of different mixtures of LDPE, HDPE, PP, and PS, Dobo' et al. (2021) reported that between 11.13% and 15.14% of paraffins, between 8.14% and 9.70% of naphthenes and between 18.74% and 21.94% of aromatics. Also, Miskolczi et al. (2004), from the determination of the composition of liquid products obtained from the thermal pyrolysis at 450 °C of a mixture of HDPE (90%) and PS (10%), reported that gasoline-range product contained 46.1% of paraffins and 11.9% of aromatics.

Finally, the feasibility of plastic pyrolysis processes may be improved if the derived products are dissolved and converted into suitable feedstock streams for refinery process units. The main advantage is the use of amortized units and the subsequent treatment of the products together

with ordinary refinery products (Lopez et al., 2017). In this sense, if the distribution of the gasoline-range derived products (total paraffins, naphthenes, and aromatics) is compared to the composition of commercial petroleum products, the gasoline of oil from pyrolysis of PP and PP film (paraffins: 27.8–31.4%, naphthenes: 50.8–58.9%, aromatics: 13.3–17.8%) showed a very close composition to the heavy fossil naphtha and could be sent to a hydrotreatment or catalytic reforming to convert low-octane hydrocarbons into more valuable high-octane components, producing more valuable aromatics such as benzene, toluene, and xylenes (BTX). However, the composition results of the oils derived from thermal pyrolysis of HIPS (paraffins: 2.2%, naphthenes: 8.0%, aromatics: 89.8%) and EPS (paraffins: 8.6%, naphthenes: 7.9%, aromatics: 83.5%) showed a more comparable composition of reformed naphtha which are directly available for the production of aromatic components (Rahimpour et al., 2013).

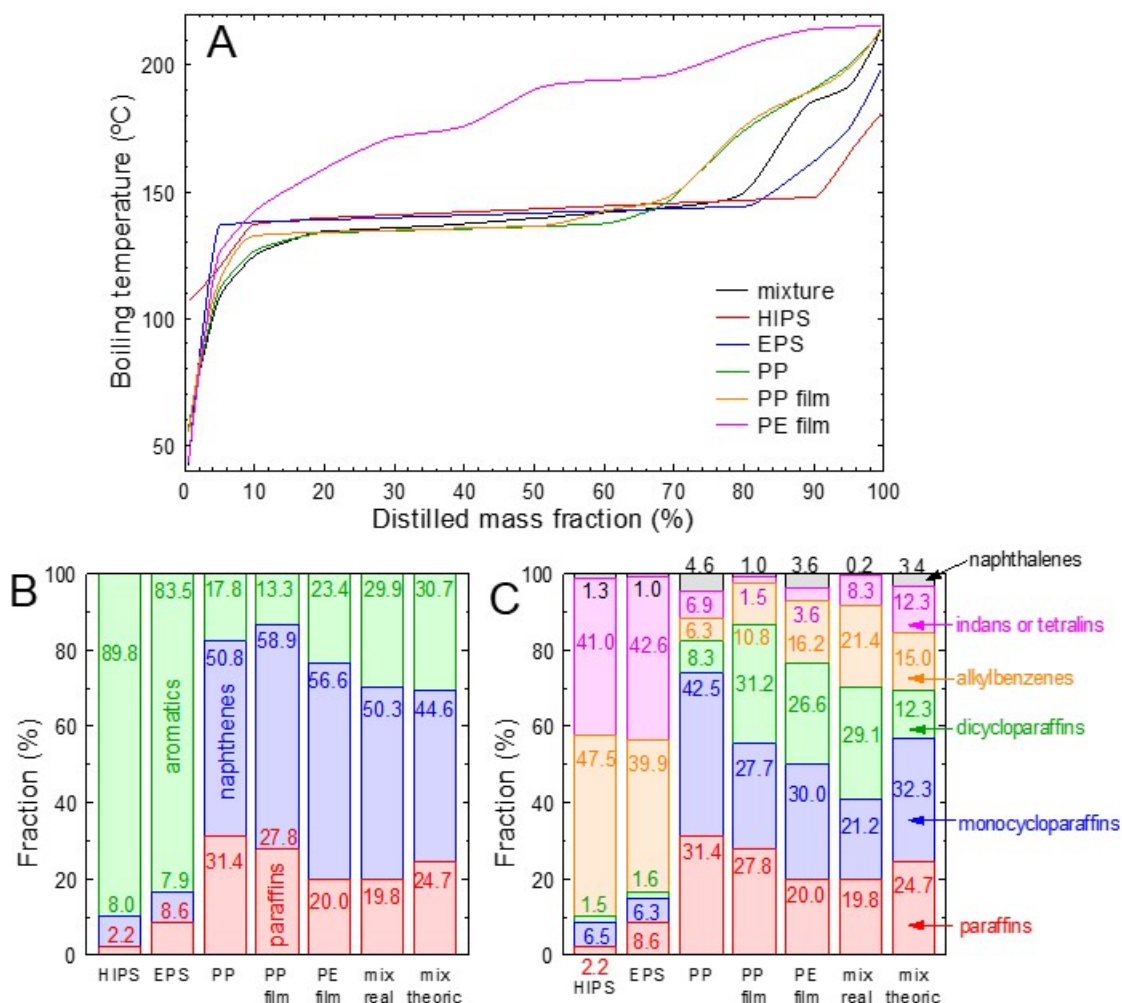


**Figure 4.4.** Simulated distillation (A), general hydrocarbon group distribution (B) detailed hydrocarbon groups (C) of the gasoline-range product obtained from the thermal pyrolysis of the mixed plastic waste and their individual components.

### 4.3.3. Effect of type of catalyst on catalytic pyrolysis performance

#### 4.3.3.1. Effect of type of catalyst on product yields

Fig. 4.5 shows the effect of the presence of a catalyst on the product yields, including the coke deposition, obtained from the catalytic pyrolysis of the studied mixture of plastic waste. In general, an increase in the gas yield and a decrease in liquid output were detected. The effect is especially more evident for zeolite-type catalysts (HY and HZSM-5). Regarding coke formation, similar coke deposition was observed for all tested catalysts (among 2.4–6.3%). Coke is the main drawback in the catalytic pyrolysis of plastics. It is an effect that should be minimized since it inhibits the catalytic activity and increases the costs for the regeneration of the catalyst (Daligaux et al., 2021). Xue et al. (2017) in the ex-situ catalytic pyrolysis at 600 °C of PE, PP, PET, and PS over HZSM-5 zeolite or Hidalgo et al. (Hidalgo Herrador et al., 2022) in the catalytic pyrolysis of PE and PP over CaO and MgO reported similar coke deposition data.

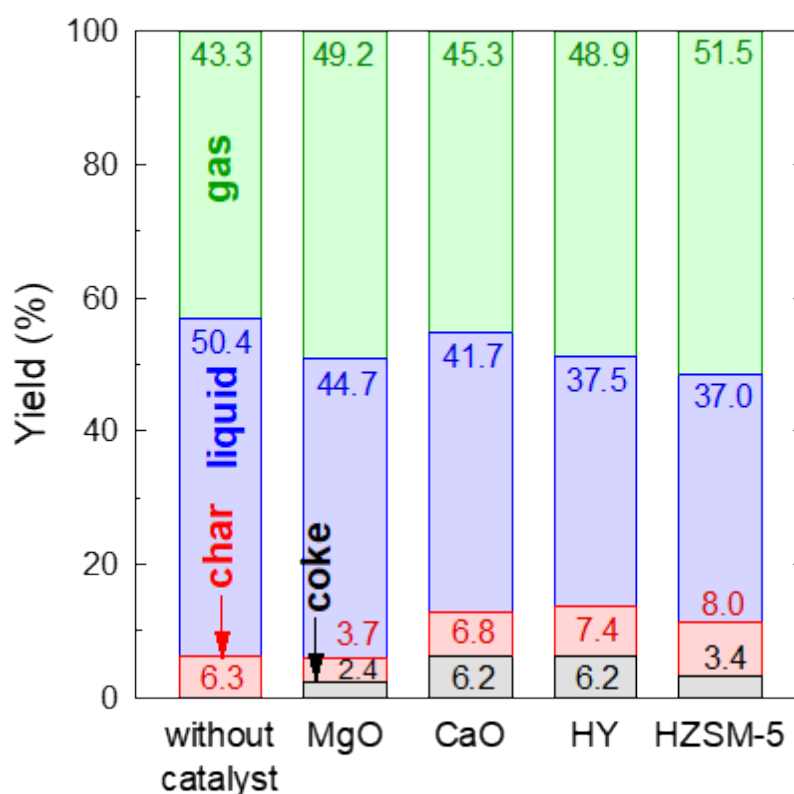


**Figure 4.5.** Gas, liquid, and solid yields as a function of catalyst.

Other authors also reported gases, liquid, and solid yields of catalytic pyrolysis of different plastics (see Table 4S1). For example, Verma et al. (2021) performed the catalytic pyrolysis of EPS waste at different feed/ZSM-5 ammonium catalyst ratios and, under the same experimental

conditions of this work, obtained approximately 1% of char, 26% of gas, and 76% of liquid products. Also, the catalytic pyrolysis of PS over MgO was performed at 500 °C by Inayat et al. (2020), leading to a liquid yield of approximately 90%. Other researchers, using MgO and CaO as catalysts, reported conversion to liquid products during the pyrolysis of PE and PP between 57.3% and 79.6% depending on the polymer and the catalyst used (PE-CaO: 57.3%; PE-MgO: 71.8%, PP-MgO: 78.6%, PP-CaO: 83.8%). Regarding the char yields, these authors reported yields of 10.3% (PP-MgO), 6.6% (PP-CaO), 21.5% (PE-MgO), and 15% (PE-CaO) (Hidalgo Herrador et al., 2022). Anene et al. (2018), in the catalytic pyrolysis of mixtures LDPE/PP at 460 °C using a patented zeolite, found that an increase in PP proportions decreased the liquid yields and increased the gas formation. Their values were similar to those obtained in our work. Also, Miskolczi et al. (2006) investigated the catalytic degradation of PE (90%) and PS (10%) in a batch reactor over FCC, ZSM-5, and clinoptilolite, between 410 and 450 °C with 2% of ZSM-5 at 430 °C, reported a yield of solids of approximately 9%, a liquid yield of 77% and gas yield of 14%. Other researchers, Onwudili et al. (2019), carried out catalytic pyrolysis of a mixture of plastics, including HDPE (19.0%), LDPE (43.0%), PP (8.0%), PS (15.0%) and PET (15.0%), in a fixed bed reactor at 500 °C over spent catalyst from FCC, HY, and HZSM-5 zeolites and obtained high liquid yields (FCC: 72%, HY: 73%, HZSM-5: 72%). Finally, López et al. (2010) studied catalytic pyrolysis over HZSM-5 with a complex mix of HDPE, PP, PS, EPS, PET, PVC, PE film, PP film, and other packing materials such as blister, tetra-brick, Al film, Al, iron, etc., at 440 °C. Particularly, in 92.3% of thermoplastics where, PE film (50.55%) was the highest proportion, followed by HDPE (13.44%), PP (9.63%), PS (6.6%), PP film (4.92%), PVC (4.28%) and PET (2.88%). These authors obtained approximately an equivalent value of solid yield (6.5%), a slightly low value of liquid yield (41.5%), and a slightly higher yield of gases (49.9%) than this work.

#### 4.3.3.2. Effect of type of catalyst on simulated distillation boiling points

The simulated distillations of liquid products derived from thermal and catalytic pyrolysis of the mixture of plastics are shown in Fig. 4.6. In all the liquids, the predominant product was gasoline, with yields between 57.7% (MgO) and 45.3% (HZSM-5 zeolite). Comparable gasoline yields were obtained by Hidalgo Herrador et al. (2022) using MgO and CaO. Also, Anene et al. (2018) obtained a similar gasoline yield in catalytic pyrolysis with zeolite at 460 °C (45.6%).

The results also suggest that the main differences between the liquids of pyrolysis were obtained in LCO and HCO-range products. In particular, low-cost MgO and CaO catalysts reduced the volatilization temperature of the components of these products compared to those of thermal pyrolysis. However, both studied zeolite-type catalysts (HZSM-5 and HY) showed a lower distilled mass fraction for a determined boiling temperature until approximately 350 °C and a very low

increase of distilled mass fraction at temperatures higher than 350 °C if compared to the curve of the liquid obtained from the thermal pyrolysis, i.e., the non-catalytic test. Other authors, like Miskolczi et al. (2006), did not find significant differences in the composition of the liquids obtained by catalytic pyrolysis of HDPE and PS over HZSM-5. The convenience of using LDPE, PP, PVC/LDPE, and PVC/PP in the hydrocracking unit of a refinery was investigated by Uçar et al. (2002) over different catalysts at 425–450 °C. For example, the blends of PE with vacuum gas oil (VGO) on HZSM-5 showed changes in distillation curves compared to the distillation curve of the liquid obtained in the thermal pyrolysis, reducing or increasing the boiling points depending on the analyzed temperature.

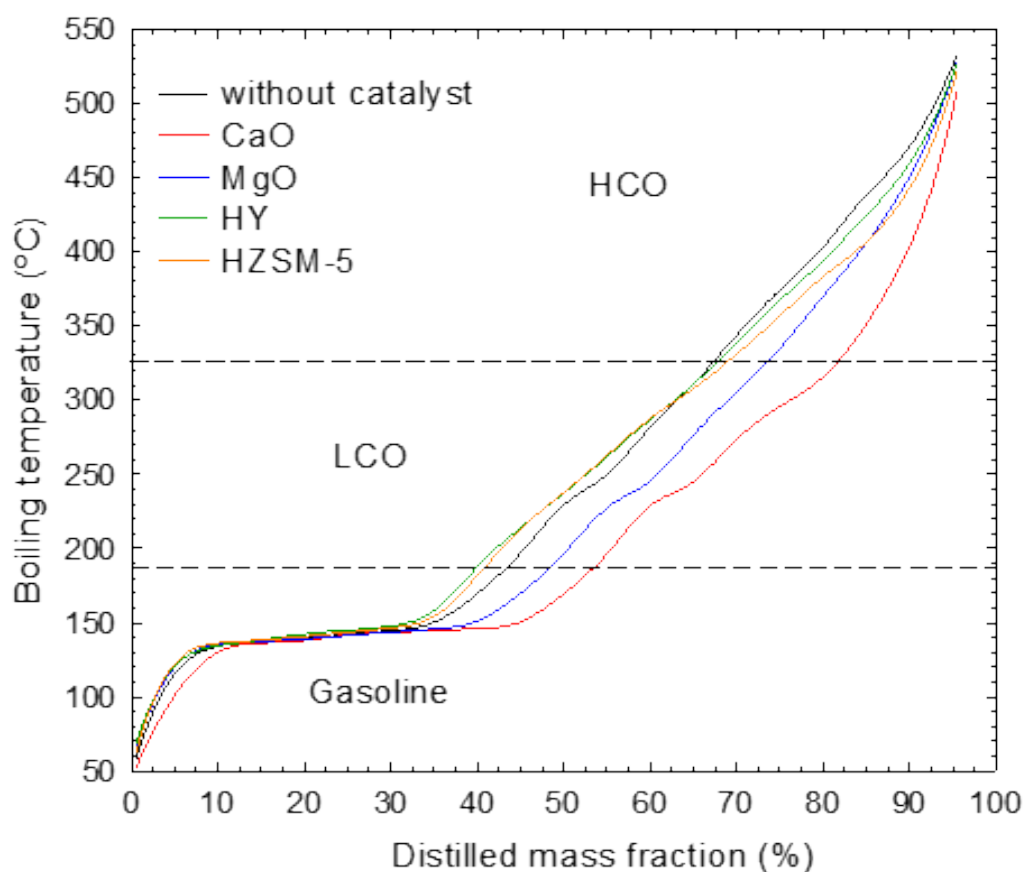


**Figure 4.6.** Boiling temperature as a function of the distilled mass fraction (simulated distillation) of the liquid fraction from catalytic pyrolysis of the mixed plastic waste.

If liquid yield was considered, the absolute data about product yields were calculated. Table 4.5 reports the different products obtained from the pyrolysis of the mixture studied in this work over each catalytic material.



Table 4.5 shows that basic low-cost catalysts (CaO and MgO) had better performance on gasoline-range product generation than acid zeolite-type catalysts. Especially, MgO showed a similar yield of this type of product compared to the composition of liquid of non-catalytic test. If a deep comparison between thermal and catalytic pyrolysis is performed, it can be observed that MgO and CaO transform heavier compounds (HCO-range product), increasing the fraction of lighter compounds in the liquid of pyrolysis. However, the great conversion of plastics to gas products in catalytic pyrolysis over acid zeolites reduces the yield of gasoline-range products, mainly attributed to micropores in the catalyst (Hertzog et al., 2018). In conclusion, the differences in product yields would result from geometric constraints due to the shape selectivity of each catalytic material (Bartholomew and Farrauto, 2010). According to pores size distribution (Fig. S3), starting at 50 Å radius, MgO and HY have additional pores volume than the other catalysts, which would allow higher bottoms (HCO) conversion, but HY has a significant reduction of volume between 100 and 300 Å radius that would not let it to break a larger number of bottoms like MgO (61.3%); however, additional pore volume in the range of 15–20 Å in radius would convert more LCO (19.8%) to gasoline, which in turn decomposes to gases through the micropores. This suggests that to crack LCO and HCO, the catalyst requires a bimodal pore size distribution (Mitchell et al., 1993). Finally, among CaO and HZSM-5, which have a similar trend of pores distribution, the last one has more additional pore volume, and as a result, fewer LCO and HCO yields than those obtained by CaO are detected.

**Table 4.5.** Gasoline, LCO, and HCO product yields obtained from the mixture (data in  $\text{g}\cdot\text{kg}^{-1}$  plastic) in thermal (non-catalytic) and catalytic pyrolysis

Catalyst	Gasoline-range	LCO-range	HCO-range
Without catalyst	240.5	111.2	152.3
MgO	241.0	113.5	62.9
CaO	236.2	104.6	106.1
HY	170.1	95.1	109.9
HZSM-5	167.3	101.5	101.0

Average values with a relative standard deviation inferior to 5%.

#### 4.3.3.3. Effect of type of catalyst on hydrocarbon types in the gasoline-range product

Regarding the simulated distillation of the gasoline-range product, see Fig. 4.7A, very low differences between thermal and catalytic pyrolysis were observed. Only a slight increase in the boiling point in the gasoline-range product generated by catalytic pyrolysis over CaO, if compared to the curve of the gasoline-range product obtained by thermal pyrolysis, was observed.

Concerning the hydrocarbon types, compared to the gasoline-range product obtained by thermal pyrolysis, no significant differences were observed in paraffins, naphthenes, and aromatics content, see Fig. 4.7B. More specifically, Fig. 4.7C shows that the catalysts marginally decreased the yield of monocycloparaffins and dicycloparaffins and increased the output of alkylbenzenes and naphthalenes. For example, alkylbenzenes yield increased from 21.4% for thermal pyrolysis to 26.3% for catalytic pyrolysis over HZSM-5 or 24.2% when MgO was used as the catalyst. However, no clear trend was found in indans or tetralins yields that changed between 7.8% for catalytic pyrolysis over HY and 12.1% over CaO. Also, changes in monocycloparaffins contents were very low, decreasing from 21.3% for thermal pyrolysis (the highest value determined) to 18.9% and 19.0% (the lowest values determined) for catalytic pyrolysis over MgO and CaO, respectively. These insignificant changes can be justified by the deactivation of the catalyst by coke deposition, which occurs preferably on the strong acid sites of zeolite-type catalysts (Elordi et al., 2011). The carbon deposition occurring in the micropores may block the access of the bio-oil compounds to acidic sites (Hertzog et al., 2018).

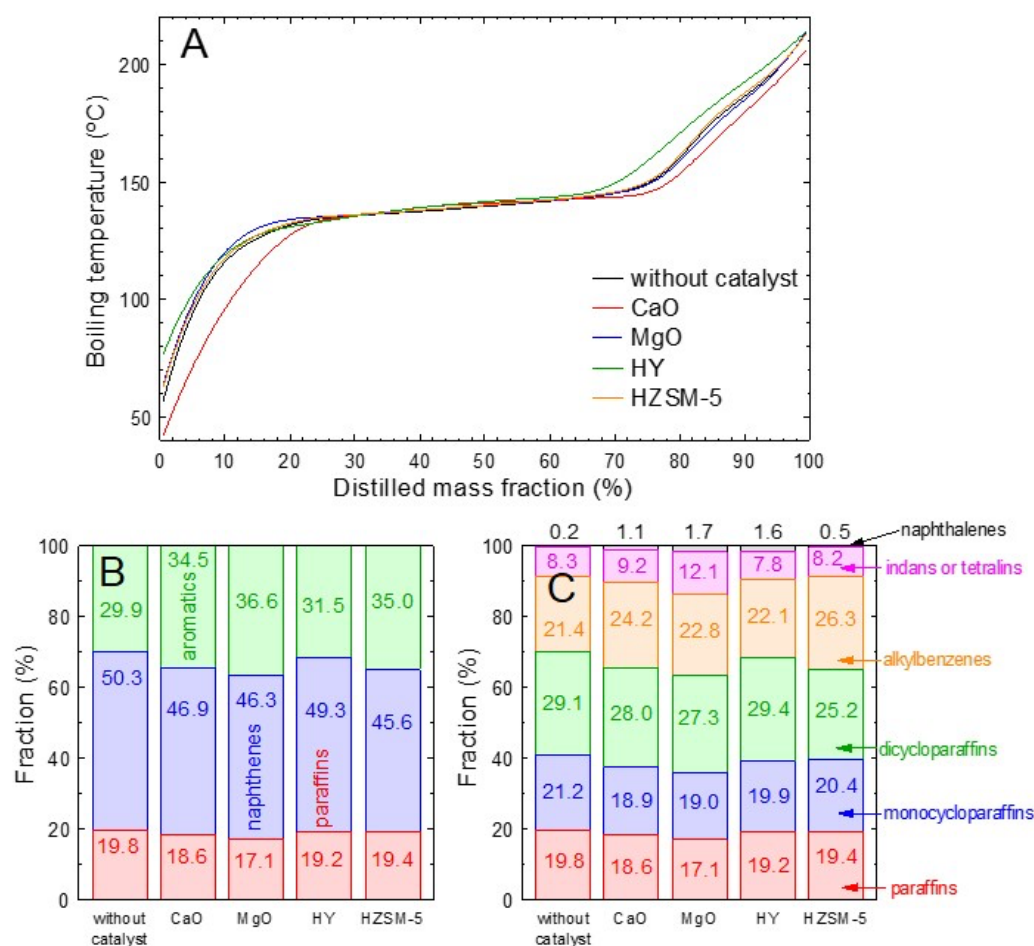


**Figure 4.7.** Simulated distillation (A), hydrocarbon group distribution (B), and hydrocarbon groups of the gasoline distribution (C) obtained from the catalytic pyrolysis of the mixed plastic.

## 4.2. Conclusions

The thermal and catalytic pyrolysis of a real mixture of post-consumer plastic waste representing the plastics present in the rejected fraction from municipal solid waste non-collected selectively was studied. Liquid oil from HIPS pyrolysis showed 76.8% of the gasoline-range product. However, liquid from pyrolysis of PE film showed a very low percentage of this product (7.2%). Significant variations were observed in the composition of the gasoline-range product obtained by thermal pyrolysis of different types of polymers. The yields of aromatics, paraffins, and naphthenes considerably varied between polystyrene plastics (HIPS and EPS), polyolefins (PP, PP film, PE film), and the mixture of plastics. High aromatics production was observed for HIPS and EPS (89.8% and 83.5%) and more paraffins (from 20.0% to 31.4%) and naphthenes (between 50.8% and 58.9%) for polyolefins.

Regarding the catalytic tests, low-cost MgO and CaO promoted gasoline fraction in the liquid product (241.0 and 236.2 g·kg<sup>-1</sup> plastic). However, very low differences between thermal and catalytic pyrolysis were observed in simulated distillation curves and the composition of the gasoline-range product. In future works, appropriate modifications of catalysts by thermal or hydrothermal procedures, with or without chemical treatment for changes of the framework, to increase their selectivity by cracking towards the gasoline-range product generation, effective ways to reduce coke deposition during catalytic pyrolysis and regeneration of the deactivated catalyst, could be studied.

### Acknowledgments

This work has received funds from the project PID2019-108826RB-I00/SRA (State Research Agency)/10.13039/501100011033, the project B-RNM-78-UGR20 (FEDER/Junta de Andalucía-Ministry of Economic Transformation, Industry, and Universities) and the project P20\_00167 (FEDER/Junta de Andalucía-Ministry of Economy, Transformation, Industry, and Universities). Funding for open access charge: Universidad de Granada / CBUA.

## References

- Aguado, J., Serrano, D., 1999. Feedstock recycling of plastic wastes. R., Camb. <https://doi.org/10.1039/9781847550804>.
- American Society for Testing and Materials, 2021. Standard test method for hydrocarbon types in middle distillates by mass spectrometry. ASTM Vol. 05. 01 Pet. Prod. Liq. Fuels, Lubr. C1234 – D4176, 1–15. <https://doi.org/10.1520/D2425-21>.
- American Society for Testing and Materials, 2021. Standard test method for determination of the boiling range distribution of gasoline by wide-bore capillary gas chromatography. ASTM

- Vol. 05. 03 Pet. Prod. Liq. Fuels, Lubr. D6469 – D7398, 1–15 <https://doi.org/0.1520/D7096-19.2>.
- American Society for Testing and Materials, 2021. Standard test method for boiling range distribution of petroleum fractions by gas chromatography. ASTM Vol. 05. 01 Pet. Prod. Liq. Fuels, Lubr. C1234 – D4176, 1–35. <https://doi.org/10.1520/D2887-19AE02>.
- American Society for Testing and Materials, 2022. Standard Test Method for Determining Activity and Selectivity of Fluid Catalytic Cracking (FCC) Catalysts by Microactivity Test 1. ASTM Vol. 05. 06 Gaseous Fuels; Coal Coke; Catal. Bioenergy Ind. Chem. Biomass-.-. 1–9. [https://doi.org/10.1520/D5154\\_D5154M-18](https://doi.org/10.1520/D5154_D5154M-18).
- Anene, A.F., Fredriksen, S.B., Sætre, K.A., Tokheim, L.A., 2018. Experimental study of thermal and catalytic pyrolysis of plastic waste components. *Sustainability* 10, 1–11. <https://doi.org/10.3390/su10113979>.
- Baena-González, J., Santamaria-Echart, A., Aguirre, J.L., González, S., 2020. Chemical recycling of plastic waste: Bitumen, solvents, and polystyrene from pyrolysis oil. *Waste Manag* 118, 139–149. <https://doi.org/10.1016/J.WASMAN.2020.08.035>.
- Barbarias, I., Lopez, G., Artetxe, M., Arregi, A., Bilbao, J., Olazar, M., 2018. Valorisation of different waste plastics by pyrolysis and in-line catalytic steam reforming for hydrogen production. *Energy Convers. Manag* 156, 575–584. <https://doi.org/10.1016/J.ENCONMAN.2017.11.048>.
- Bartholomew, C.H., Farrauto, R.J., 2010. *Fundamentals of Industrial Catalytic Processes*. John Wiley and Sons, <https://doi.org/10.1002/9780471730071>.
- Bartley, J.K., Xu, C., Lloyd, R., Enache, D.I., Knight, D.W., Hutchings, G.J., 2012. Simple method to synthesize high surface area magnesium oxide and its use as a heterogeneous base catalyst. *Appl. Catal. B Environ.* 128, 31–38. <https://doi.org/10.1016/J.APCATB.2012.03.036>.
- Budsareechai, S., Hunt, A.J., Ngernyen, Y., 2019. Catalytic pyrolysis of plastic waste for the production of liquid fuels for engines. *RSC Adv.* 9, 5844–5857. <https://doi.org/10.1039/C8RA10058F>.
- Chen, L.H., Sun, M.H., Wang, Z., Yang, W., Xie, Z., Su, B.L., 2020. Hierarchically structured zeolites: From design to application. *Chem. Rev.* 120, 11194–11294. <https://doi.org/10.1021/ACS.CHEMREV.0C00016>.
- Collias, D.I., James, M.I., Layman, J.M., 2021. *Circular Economy of Polymers: Topics in Recycling Technologies*. American Chemical Society, Washington, DC. <https://doi.org/10.1021/BK-2021-1391>.

- E. Commission, 2020, A European Strategy for Plastics in a Circular Economy, Comm. Commun. – Plast. Strateg. [〈https://environment.ec.europa.eu/strategy/plastics-strategy\\_en#documents〉](https://environment.ec.europa.eu/strategy/plastics-strategy_en#documents) (accessed September 1, 2022).
- Costa, P., Pinto, F., Mata, R., Marques, P., Paradela, F., Costa, L., 2021. Validation of the application of the pyrolysis process for the treatment and transformation of municipal plastic wastes. *Chem. Eng. Trans.* 86, 859–864. <https://doi.org/10.3303/CET2186144>.
- Daligaux, V., Richard, R., Manero, M.H., 2021. Deactivation and regeneration of zeolite catalysts used in pyrolysis of plastic wastes—a process and analytical review. *Catal Vol.* 11, 770. <https://doi.org/10.3390/CATAL11070770>.
- Demirbas, A., 2004. Pyrolysis of municipal plastic wastes for recovery of gasoline-range hydrocarbons. *J. Anal. Appl. Pyrolysis* 72, 97–102. <https://doi.org/10.1016/J.JAAP.2004.03.001>.
- Dobó, Z., Kecsmár, G., Nagy, G., Koo's, T., Muránszky, G., Ayari, M., 2021. Characterization of gasoline-like transportation fuels obtained by distillation of pyrolysis oils from plastic waste mixtures. *Energy Fuels* 35, 2347–2356. <https://doi.org/10.1021/ACS.ENERGYFUELS.0C04022>.
- Elordi, G., Olazar, M., Lopez, G., Artetxe, M., Bilbao, J., 2011. Continuous polyolefin cracking on an HZSM-5 zeolite catalyst in a conical spouted bed reactor. *Ind. Eng. Chem. Res.* 50, 6061–6070. <https://doi.org/10.1021/IE2002999>.
- Fadillah, G., Fatimah, I., Sahroni, I., Musawwa, M.M., Mahlia, T.M.I., Muraza, O., 2021. Recent progress in low-cost catalysts for pyrolysis of plastic waste to fuels. *Catalysts* 11, 837. <https://doi.org/10.3390/CATAL11070837>.
- Gala, A., Guerrero, M., Guirao, B., Domine, M.E., Serra, J.M., 2020. Characterization and Distillation of Pyrolysis Liquids Coming from Polyolefins Segregated of MSW for Their Use as Automotive Diesel Fuel. *Energy Fuels* 34, 5969–5982. <https://doi.org/10.1021/ACS.ENERGYFUELS.0C00403>.
- Hertzog, J., Carré, V., Jia, L., Mackay, C.L., Pinard, L., Dufour, A., Mašek, O., Aubriet, F., 2018. Catalytic fast pyrolysis of biomass over microporous and hierarchical zeolites: characterization of heavy products. *ACS Sustain. Chem. Eng.* 6, 4717–4728. <https://doi.org/10.1021/ACSSUSCHEMENG.7B03837>.
- Hidalgo Herrador, J.M., Murat, M., Tišler, Z., Frątczak, J., de Paz Carmona, H., 2022. Direct Polypropylene and Polyethylene Liquefaction in CO<sub>2</sub> and N<sub>2</sub> Atmospheres Using MgO Light and CaO as Catalysts. *Mater. (Basel)* 15, 844. <https://doi.org/10.3390/MA15030844>.

- Hopewell, J., Dvorak, R., Kosior, E., 2009. Plastics recycling: challenges and opportunities. *Philos. Trans. R. Soc. B Biol. Sci.* 364, 2115–2126. <https://doi.org/10.1098/RSTB.2008.0311>.
- Inayat, A., Klemencova, K., Grycova, B., Sokolova, B., Lestinsky, P., 2020. Thermo-catalytic pyrolysis of polystyrene in batch and semi-batch reactors: A comparative study. *Waste Manag. Res.* 39, 260–269. <https://doi.org/10.1177/0734242x20936746>.
- Jung, S.H., Cho, M.H., Kang, B.S., Kim, J.S., 2010. Pyrolysis of a fraction of waste polypropylene and polyethylene for the recovery of BTX aromatics using a fluidized bed reactor. *Fuel Process. Technol.* 91, 277–284. <https://doi.org/10.1016/J.FUPROC.2009.10.009>.
- Kumagai, S., Hasegawa, I., Grause, G., Kameda, T., Yoshioka, T., 2015. Thermal decomposition of individual and mixed plastics in the presence of CaO or Ca(OH)<sub>2</sub>. *J. Anal. Appl. Pyrolysis* 113, 584–590. <https://doi.org/10.1016/J.JAAP.2015.04.004>.
- Lopez, G., Artetxe, M., Amutio, M., Bilbao, J., Olazar, M., 2017. Thermochemical routes for the valorization of waste polyolefinic plastics to produce fuels and chemicals. A review. *Renew. Sustain. Energy Rev.* 73, 346–368. <https://doi.org/10.1016/J.RSER.2017.01.142>.
- López, A., de Marco, I., Caballero, B.M., Laresgoiti, M.F., Adrados, A., 2010. Pyrolysis of municipal plastic wastes: Influence of raw material composition. *Waste Manag* 30, 620–627. <https://doi.org/10.1016/j.wasman.2009.10.014>.
- Martín-Lara, M.A., Piñar, A., Ligeró, A., Bázquez, G., Calero, M., 2021. Characterization and use of char produced from pyrolysis of post-consumer mixed plastic waste. *Water* 13, 1188. <https://doi.org/10.3390/W13091188>.
- Miandad, R., Barakat, M.A., Aburiazaiza, A.S., Rehan, M., Ismail, I.M.I., Nizami, A.S., 2017. Effect of plastic waste types on pyrolysis liquid oil. *Int. Biodeterior. Biodegrad.* 119, 239–252. <https://doi.org/10.1016/J.IBIOD.2016.09.017>.
- Micic, R.D., Bosnjak Kiralj, M.S., Panic, S.N., Tomic, M.D., Jovic, B.D., Boskovic, G.C., 2015. Activation temperature imposed textural and surface synergism of CaO catalyst for sunflower oil transesterification. *Fuel* 159, 638–645. <https://doi.org/10.1016/J.FUEL.2015.07.025>.
- Miskolczi, N., Bartha, L., Deák, G., József, B., Kalló, D., 2004. Thermal and thermo-catalytic degradation of high-density polyethylene waste. *J. Anal. Appl. Pyrolysis* 72, 235–242. <https://doi.org/10.1016/J.JAAP.2004.07.002>.
- Miskolczi, N., Bartha, L., Deák, G., 2006. Thermal degradation of polyethylene and polystyrene from the packaging industry over different catalysts into fuel-like feed stocks. *Polym. Degrad. Stab.* 91, 517–526. <https://doi.org/10.1016/j.polyimdegradstab.2005.01.056>.

- 
- Mitchell, M.M., Hoffman, J.F., Moore, H.F., 1993. Chapter 9 residual feed cracking catalysts. *Stud. Surf. Sci. Catal.* 76, 293–338. [https://doi.org/10.1016/S0167-2991\(08\)63832-X](https://doi.org/10.1016/S0167-2991(08)63832-X).
- Onwudili, J.A., Muhammad, C., Williams, P.T., 2019. Influence of catalyst bed temperature and properties of zeolite catalysts on pyrolysis-catalysis of a simulated mixed plastics sample for the production of upgraded fuels and chemicals. *J. Energy Inst.* 92, 1337–1347. <https://doi.org/10.1016/j.joei.2018.10.001>.
- Parku, G.K., Collard, F.X., Görgens, J.F., 2020. Pyrolysis of waste polypropylene plastics for energy recovery: Influence of heating rate and vacuum conditions on composition of fuel product. *Fuel Process. Technol.* 209, 106522 <https://doi.org/10.1016/J.FUPROC.2020.106522>.
- Paucar-Sánchez, M.F., Calero, M., Blázquez, G., Muñoz-Batista, M.J., Martín-Lara, M.A., 2022. Characterization of liquid fraction obtained from pyrolysis of post-consumer mixed plastic waste: A comparing between measured and calculated parameters. *Process Saf. Environ. Prot.* 159, 1053–1063. <https://doi.org/10.1016/J.PSEP.2022.01.081>.
- Plastics Europe, 2021, *Plastics - the Facts 2021*. <https://plasticseurope.org/knowledge-hub/plastics-the-facts-2021/> (accessed April 11, 2022).
- Predel, M., Kaminsky, W., 2000. Pyrolysis of mixed polyolefins in a fluidised-bed reactor and on a pyro-GC/MS to yield aliphatic waxes. *Polym. Degrad. Stab.* 70, 373–385. [https://doi.org/10.1016/S0141-3910\(00\)00131-2](https://doi.org/10.1016/S0141-3910(00)00131-2).
- Quesada Lozano, L.M., 2021. Desarrollo de tratamientos térmicos sostenibles para la valorización del plástico procedente de la fracción de rechazo de las plantas de tratamiento de residuos sólidos urbanos. Doctoral Thesis. University of Granada.
- Qureshi, M.S., Oasmaa, A., Pihkola, H., Deviatkin, I., Tenhunen, A., Mannila, J., Minkkinen, H., Pohjakallio, M., Laine-Ylijoki, J., 2020. Pyrolysis of plastic waste: Opportunities and challenges. *J. Anal. Appl. Pyrolysis* 152, 104804. <https://doi.org/10.1016/J.JAAP.2020.104804>.
- Rahimpour, M.R., Jafari, M., Iranshahi, D., 2013. Progress in catalytic naphtha reforming process: A review. *Appl. Energy* 109, 79–93. <https://doi.org/10.1016/J.APENERGY.2013.03.080>.
- Rodríguez Lamar, Y., Noboa, J., Torres Miranda, A.S., Almeida Streitwieser, D., 2021. Conversion of PP, HDPE and LDPE Plastics into Liquid Fuels and Chemical Precursors by Thermal Cracking. *J. Polym. Environ.* 29, 3842–3853. <https://doi.org/10.1007/S10924-021-02150-1>.
- Rodríguez-Luna, L., Bustos-Martínez, D., Valenzuela, E., 2021. Two-step pyrolysis for waste HDPE valorization. *Process Saf. Environ. Prot.* 149, 526–536. <https://doi.org/10.1016/J.PSEP.2020.11.038>.

- Sarker, M., Rashid, M.M., 2013. Production of Aromatic Hydrocarbons Related Kerosene Fuel from Polystyrene and Polypropylene Waste Plastics Mixture by Fractional Distillation Process. *Int. J. Appl. Chem. Sci. Res* 1, 1–10.
- Singh, R.K., Ruj, B., Sadhukhan, A.K., Gupta, P., 2019. Impact of fast and slow pyrolysis on the degradation of mixed plastic waste: Product yield analysis and their characterization. *J. Energy Inst.* 92, 1647–1657. <https://doi.org/10.1016/J.JOEI.2019.01.009>.
- Singh, R.K., Ruj, B., Sadhukhan, A.K., Gupta, P., 2020. Thermal degradation of waste plastics under non-sweeping atmosphere: Part 2: Effect of process temperature on product characteristics and their future applications. *J. Environ. Manag.* 261, 110112 <https://doi.org/10.1016/J.JENVMAN.2020.110112>.
- Su, Y., Zhang, Z., Wu, D., Zhan, L., Shi, H., Xie, B., 2019. Occurrence of microplastics in landfill systems and their fate with landfill age. *Water Res* 164, 114968. <https://doi.org/10.1016/J.WATRES.2019.114968>.
- Sun, J., Zhu, Z.R., Li, W.H., Yan, X., Wang, L.K., Zhang, L., Jin, J., Dai, X., Ni, B.J., 2021. Revisiting Microplastics in Landfill Leachate: Unnoticed Tiny Microplastics and Their Fate in Treatment Works. *Water Res* 190, 116784. <https://doi.org/10.1016/J.WATRES.2020.116784>.
- Takuma, K., Uemichi, Y., Ayame, A., 2000. Product distribution from catalytic degradation of polyethylene over H-gallosilicate. *Appl. Catal. A Gen.* 192, 273–280. [https://doi.org/10.1016/S0926-860X\(99\)00399-3](https://doi.org/10.1016/S0926-860X(99)00399-3).
- Thahir, R., Altway, A., Juliastuti, S.R., 2019. Susianto, Production of liquid fuel from plastic waste using integrated pyrolysis method with refinery distillation bubble cap plate column. *Energy Rep.* 5, 70–77. <https://doi.org/10.1016/J.EGYR.2018.11.004>.
- Thommes, M., Kaneko, K., Neimark, A.V., Olivier, J.P., Rodríguez-Reinoso, F., Rouquerol, J., Sing, K.S.W.W., 2015. Physisorption of gases, with special reference to the evaluation of surface area and pore size distribution (IUPAC Technical Report). *Pure Appl. Chem.* 87, 1051–1069.
- Uçar, S., Karagoz, S., Karayildirim, T., Yanik, J., 2002. Conversion of polymers to fuels in a refinery stream. *Polym. Degrad. Stab.* 75, 161–171. [https://doi.org/10.1016/S0141-3910\(01\)00215-4](https://doi.org/10.1016/S0141-3910(01)00215-4).
- United Nation Environment Programme, 2018, SINGLE-USE PLASTICS: A Roadmap for Sustainability, Tara Canno, United Nations Environment Programme.
- Verma, A., Sharma, S., Pramanik, H., 2021. Pyrolysis of waste expanded polystyrene and reduction of styrene via in-situ multiphase pyrolysis of product oil for the production of



- 
- fuel range hydrocarbons. *Waste Manag* 120, 330–339. <https://doi.org/10.1016/J.WASMAN.2020.11.035>.
- Wan, Y., Chen, X., Liu, Q., Hu, H., Wu, C., Xue, Q., 2022. Informal landfill contributes to the pollution of microplastics in the surrounding environment. *Environ. Pollut.* 293, 118586 <https://doi.org/10.1016/J.ENVPOL.2021.118586>.
- Wang, J., Jiang, J., Wang, X., Wang, R., Wang, K., Pang, S., Zhong, Z., Sun, Y., Ruan, R., Ragauskas, A.J., 2020. Converting polycarbonate and polystyrene plastic wastes into aromatic hydrocarbons via catalytic fast co-pyrolysis. *J. Hazard. Mater.* 386, 121970 <https://doi.org/10.1016/J.JHAZMAT.2019.121970>.
- Williams, E.A., Williams, P.T., 1997. The pyrolysis of individual plastics and a plastic mixture in a fixed bed reactor. *J. Chem. Technol. Biotechnol.* 70, 9–20. [https://doi.org/10.1002/\(SICI\)1097-4660\(199709\)70:1<9::AID-JCTB700>3.0.CO;2-E](https://doi.org/10.1002/(SICI)1097-4660(199709)70:1<9::AID-JCTB700>3.0.CO;2-E).
- Williams, P.T., Williams, E.A., 1999. Fluidised bed pyrolysis of low density polyethylene to produce petrochemical feedstock. *J. Anal. Appl. Pyrolysis* 51, 107–126. [https://doi.org/10.1016/S0165-2370\(99\)00011-X](https://doi.org/10.1016/S0165-2370(99)00011-X).
- Wiriyaumpaiwong, S., Jamradloedluk, J., 2017. Distillation of pyrolytic oil obtained from fast pyrolysis of plastic wastes. *Energy Procedia* 138, 111–115. <https://doi.org/10.1016/J.EGYPRO.2017.10.071>.
- Xu, Y., Liu, S., Guo, X., Wang, L., Xie, M., 1994. Methane activation without using oxidants over Mo/HZSM-5 zeolite catalysts. *Catal. Lett.* 30, 135–149. <https://doi.org/10.1007/BF00813680>.
- Xue, Y., Johnston, P., Bai, X., 2017. Effect of catalyst contact mode and gas atmosphere during catalytic pyrolysis of waste plastics. *Energy Convers. Manag* 142, 441–451. <https://doi.org/10.1016/J.ENCONMAN.2017.03.071>.
- Zhang, W., Yu, D., Ji, X., Huang, H., 2012. Efficient dehydration of bio-based 2,3-butanediol to butanone over boric acid modified HZSM-5 zeolites. *Green. Chem.* 14, 3441–3450. <https://doi.org/10.1039/C2GC36324K>.



## 4.S. Supplementary materials

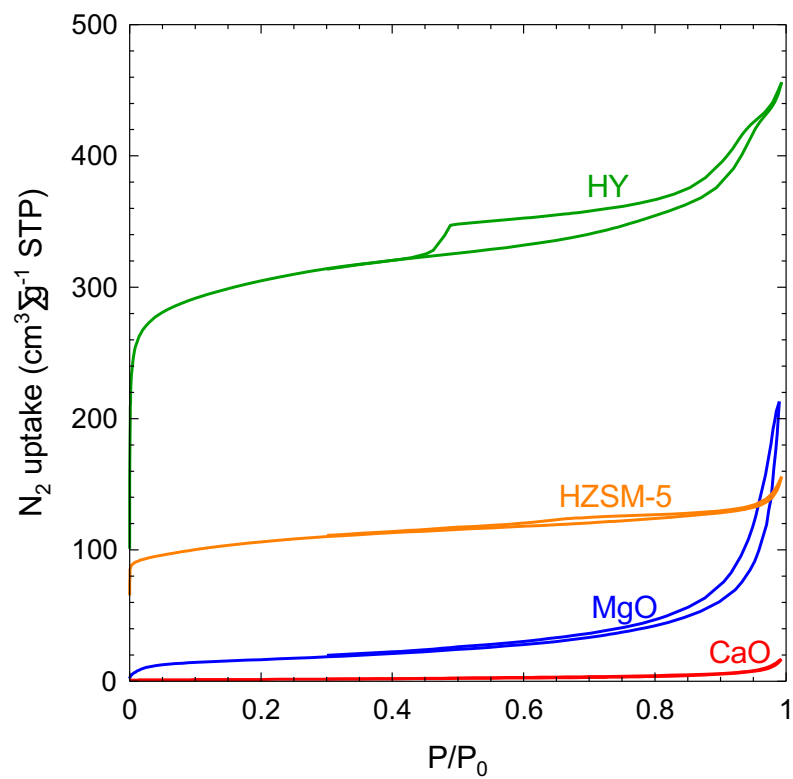


Figure 4.S1. N<sub>2</sub> adsorption-desorption isotherms of the commercial catalysts.

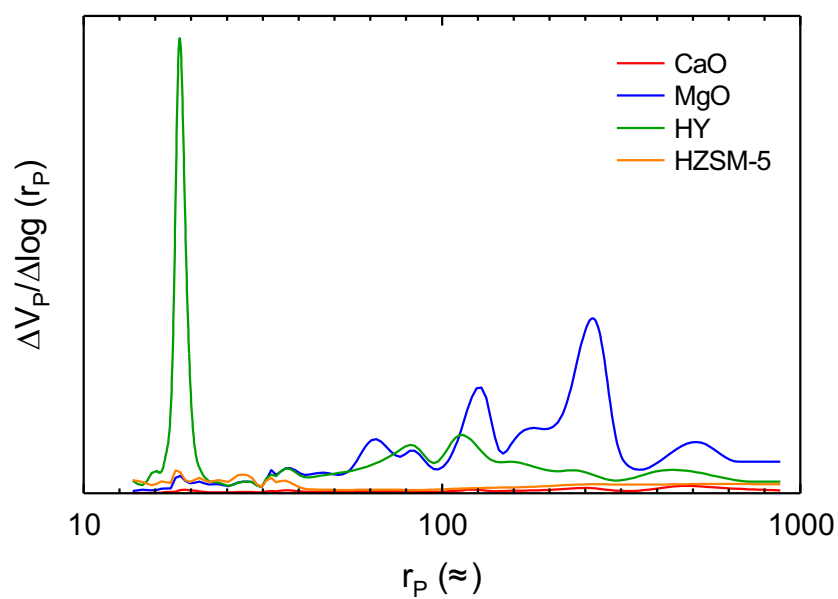


Figure 4.S2. Pore size distribution patterns of the different catalysts.



## Chapter 5

# Towards Fuels Production by a Catalytic Pyrolysis of a Real Mixture of Post-Consumer Plastic Waste

**Paucar-Sánchez, M.F.; Martín-Lara, M.A.; Calero, M.; Blázquez, G.; Solís, R.R.; Muñoz-Batista, M.J.**

*Department of Chemical Engineering University of Granada, 18071 Granada, Spain*

Fuel, ISSN: 0016-2361, eISSN: 1873-7153. Published by Elsevier Ltd.

Volume: 352

Number: 129145

Country: United Kingdom

DOI: <https://doi.org/10.1016/j.fuel.2023.129145>

- *Category: Energy & Fuel. Journal Impact Factor, JIF (2022): 7.4. Category Ranking: 32/115 (Q2).*
- *Category: Engineering, Chemical. Journal Impact Factor, JIF (2022): 7.4. Category Ranking: 19/140 (Q1).*

*Article history:*

Received 9 March 2023

Received in revised form 29 May 2023

Accepted 28 June 2023

Available online 4 July 2023



## Abstract

The contribution provides a valorization alternative for rejected plastic wastes from mechanical-biological treatment (non-recyclable material) *via* an in-situ catalytic pyrolysis process focused on the production of a liquid fraction with similar properties to traditional fuels (i.e., gasoline, kerosene, and diesel). According to the ASTM recommendations, on small samples without prior physical separation, fuel fraction identification was carried out by Simulated Distillation along with a hydrocarbon types analysis and complemented with CHNS-O analysis and Fourier Transform Infrared Spectroscopy. Two catalytic structures were employed, named Sepiolite and Montmorillonites, both K10 and K30, which, after simple heat treatment to stabilize the structure, were characterized to analyze the main properties affecting the catalytic activity and product yields (i.e., morphological and acidity properties). A whole screening of the products by analogy with hydrocarbon of the petroleum industry is presented. Such an approach allows a real evaluation of the studied technology in the current energy scenario.

**Keywords:** Plastic waste; Pyrolysis; Catalysts; Gasoline-range product; Hydrocarbon types.

## 5.1. Introduction

Plastics have played a crucial role in industrial development over the past 50 years, serving as a main component in a wide range of applications in various sectors. These applications encompass packaging, construction, healthcare, and electrical devices, among many others. [1–3]. The demand for plastic has been steadily enhanced, which has resulted in a tremendous increase in plastic waste generation. The reuse of plastic components should be the first alternative, but it is limited by deterioration after its useful lifetime. In addition, a very competitive cost adjustment for plastic production keeps down the proper development of this environmentally friendly scheme. On the other hand, several technical and economic bottlenecks limit the increased recycling of waste-related plastic [4]. It is even more complicated with some plastic-based components such as multi-element products (e.g., plastic-metallic or plastic-inorganic structures), multi-layer materials, or polymeric components including toxic compounds (e.g., additives like brominated flame retardants, phthalates) [2]. Besides, a lot of plastic waste is non-recyclable by traditional methods, such as, for example, that comes from rejected fractions of mechanical biological treatments. In this context, the development of valorization alternatives such as thermal and catalytic pyrolysis, gasification, and plasma are emerging as potential alternatives [1,2,3].

In particular, the pyrolysis process can convert the plastic waste into three fractions: liquid (which may have fuel properties) [5,6,7], solid (a char with a carbonaceous structure and potential

applications as adsorbents or catalytic supports) [8,9,10], and gases (with a high calorific value equivalent to natural gas  $\sim 44$  MJ/kg) at temperatures above  $300$  °C through thermal decomposition of the polymer structure [1,11,3]. Although, in general, pure pyrolysis is not a highly selective process, pyrolysis schemes are relatively flexible due to main operating conditions that can be manipulated to optimize product yields [3,12]. The catalytic alternative tries to solve some of the limitations of the traditional pyrolytic process. Several contributions under pure pyrolysis conditions of plastic-containing materials describe the presence of impurities in the liquid oil and low yields, which can be adjusted using a well-designed catalytic pyrolysis scheme [1,3]. Catalytic schemes also intend to reduce the inherent temperature dependence of the process by working at considerably low temperatures and including other catalytic-related parameters in the scheme that define the efficiency of the whole process. Surface area, pore distribution size, and acidity (total and strength type) are some critical features of the catalysts employed [13,14]. Thus, many catalytic materials have been applied to produce the gases, liquids, and chars with appropriate characteristics and high purity. It is well-described that, in general, catalytic schemes promote an enhancement of the gas yield and reduce the amount of the liquid fraction, which results in lighter hydrocarbon distributions. However, this liquid reduction can be compensated by a clear quality improvement, producing mixtures with greater commercial interest like gasoline, diesel, or jet fuel products. Zeolite catalysts have been extensively studied. For plastic-to-fuel applications, a few examples can be highlighted. HZSM-5, HY, HMOR, and HUSY with a dominated micropores structure, MCM-41, and SBA-15 as mesoporous catalysts are well-analyzed [14]. Traditional catalytic samples such as metal oxides, alkali carbonates, and metal complexes have been mainly used to improve monomer recovery [14]. Several clays have emerged as competitive alternatives by reducing process costs. Montmorillonites and their analogies (i.e., saponite, hectorite, beidellite), although usually less active than zeolites below  $600$  °K, have proven in many cases to be more efficient in processes at high working temperatures [14,15]. The catalytic response is also strongly related to the configuration of experimental scheme setups. Two schemes have usually been reported, taking into account the interaction of the catalyst with the starting raw material or generated pyrolytic vapors, as in-situ or ex-situ catalytic pyrolysis. In-situ catalytic pyrolysis is developed using a well-defined one-step in which the catalyst is mixed with the raw material to be pyrolyzed. Instead, ex-situ catalytic pyrolysis occurs when raw materials are pyrolyzed to generate vapors that will be transferred to a catalytic reactor (two steps) [16].

This contribution presents the development of a pyrolysis process for non-recyclable plastics, utilizing an in-situ catalytic scheme employing Sepiolite and two Montmorillonites (MK10 and MK30) as catalysts, with the objective of producing fuels. Through a rigorous analysis of Simulated Distillation and product characterization based on hydrocarbon types, conducted on small samples without prior physical separation or distillation, our aim is to provide a



comprehensive understanding of the proposed technology while establishing a parallel with conventional fuels generated by the petroleum industry. Our approach enables a critical evaluation of the resulting products for immediate applicability within the current fuel sector.

## **5.2. Materials and methods**

### **5.2.1. Raw material**

The plastic waste materials come from the rejected plastic fractions of Granada's mechanical biological treatment (MBT) plant (Spain) and follow a well-defined scheme including random selection and basic characterization as described in the Supplementary material document. The mixture was composed of rigid polypropylene (PP), expanded polystyrene (EPS), high impact polystyrene (HIPS), polypropylene film (PP film), and polyethylene film (PE film). These were previously separated, washed, dried, and subjected to a size reduction process (1–3 mm) to facilitate homogeneity in the pyrolysis test. The average composition of the raw material received showed 56.10% of PP, 12.65% of PP film, 12.65% of PE film, 10.05% of EPS, and 8.55% of HIPS.

### **5.2.2. Preparation and characterization of the catalysts**

Sepiolite (SE) and Montmorillonites K10 (MK10) and K30 (MK30) were supplied by Sigma Alrich. The chemical, structural, and morphological properties were stabilized by calcination at 550 °C under atmospheric pressure with air for 3.5 h in a Nabertherm, L 3/11/B180 Model furnace muffle and conserved in a desiccator. The morphological modifications were analyzed in a Micromeritics ASAP2429 Porosity Analyzer according to ASTM D3663 and ASTM D4365 designations [17,18]. At the same time, the pore size distributions were calculated by ASTM D4641 standard [19]. The strength of active sites measurement on the surface of catalytic materials was carried out by temperature-programmed ammonia desorption under helium flow (50 mL/min) from room to 500 °C with 30 °C/min heating gradient over approximately 0.085 g of sample on a chemisorption analyzer AutoChem II 2920 model from Micromeritics Instrument Corporation provided with a Thermal Conductivity Detector. Before the chemisorption, the samples were pretreated at 450 °C under He flows for one hour and then cooled to room temperature. Chemisorption was performed using a mixture of ammonia and helium at 10% (v/v) for 20 min.

### **5.2.3. Pyrolysis reactor and operation conditions**

The plastic waste pyrolysis experiments were carried out on a fixed horizontal laboratory-scales reactor made of stainless steel 316 (internal diameter: 4 cm and length: 34.25 cm) inserted in a

Nebertherm R 50/ 250/12 Model furnace. A flowmeter and a chiller were integrated to regulate the inert drag gas flow and cracked gas cooling (see Fig. 5.1).

20 g of sample with 1 and 2 g of catalytic material, uniformly spread over the plastics blend, were collocated in a closed 316 stainless steel tubular vessel (internal diameter: 27.25 mm and length: 30.6 cm) with a chimney hole and heated to a rate of 10 °C/min from room temperature to 500 °C, which was kept by 60 min more with a constant flow rate of 0.8 L/min of nitrogen. Then, the reactor was cooled to room temperature under a permanent nitrogen purge. A cooling bath separated liquid and gas products at – 7 °C. The liquids were collected in an ore-weighted glass vessel, while the gases were in a TEDLAR gas sampling bag every fifteen minutes. The sampling TEDLAR bags were filled for 2.5 min (2 L).

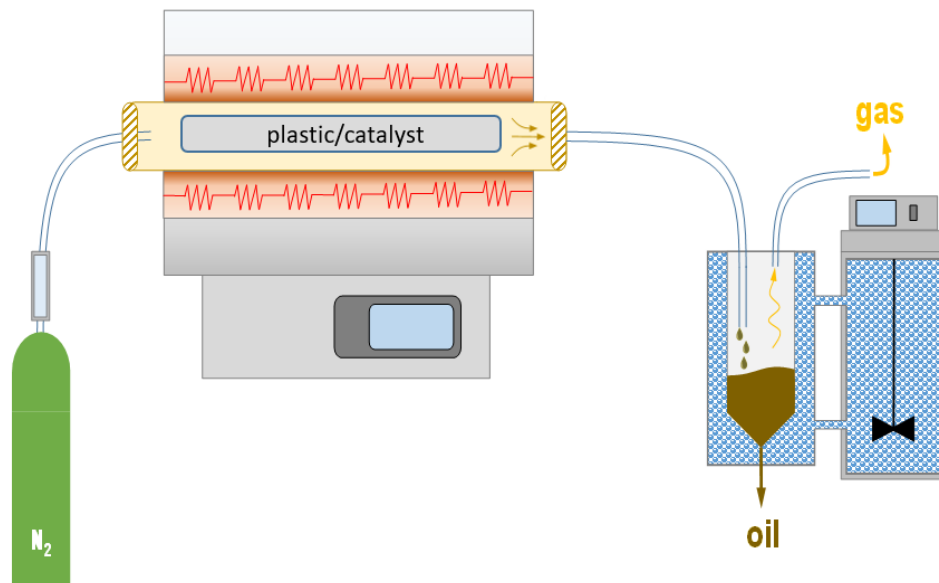


**Fig. 5.1.** Schematic representation of the pyrolysis setup.

Solid residue and oil product were directly measured and then the yields were calculated according to the following equations (gas yield by difference):

$$\eta_l = \frac{m_l}{m_m} \cdot 100 \quad (5.1)$$

$$\eta_s = \frac{m_s}{m_m} \cdot 100 \quad (5.2)$$

$$\eta_g = 100 - (\eta_l + \eta_s) \quad (5.3)$$

where  $m_m$ ,  $m_l$ , and  $m_s$  are the weights of the plastic sample, liquid, and solid products, respectively, and  $\eta_l$ ,  $\eta_s$ , and  $\eta_g$  are the yields of liquid, solid, and gases, respectively. The solids included char and coke.

#### 5.2.4. Gases analysis

Non-condensed hydrocarbons and gases were identified on a Micro GC Agilent 990 Bio-Gas analyzer with two channels and thermal conductivity detectors (TCD). Two Agilent J&W Molesieve (5 Å zeolite molecular sieve with 20 m length and inner diameter of 0.25 mm and a film unit of 30 μm) and PoraPLOT Q (Polystyrene-divinylbenzene with 10 m length and inner diameter of 0.25 mm and 8 μm of film thickness) capillary columns were used. The operating conditions included backflushes, an injector temperature of 110 °C, and the oven at an isothermal temperature of 80 °C with pressures of 200 and 150 kPa, respectively, at constant helium flow. The samples were injected directly from TEDLAR bags.

#### 5.2.5. Liquid analysis

##### 5.2.5.1. Elemental analysis

Elemental analysis of the pyrolytic and catalyzed oils was carried out in a Thermo Scientific Flash 2000 CHNS-O Analyzer by rapid combustion with pure oxygen. The gases pass across a chromatographic separation column and a thermal conductivity detector to the ASTM D5291 designation [20].

##### 5.2.5.2. Chemical constitution

A PerkinElmer Spectrum 65 of Infrared absorption spectroscopy by Fourier-Transform analysis was used to qualitatively identify organic and inorganic compounds by functional groups in non-catalyzed and catalyzed oils. The spectrums were recorded between the 4000 and 550  $\text{cm}^{-1}$  frequency range with a resolution of 1  $\text{cm}^{-1}$ .

##### 5.2.5.3. Simulated distillation (SD)

The boiling range of the pyrolytic and catalyzed oils, such as the petroleum derivatives, was determined on a PerkinElmer Clarus 590 Gas Chromatograph with a flame ionization detector (FID) according to the designation ASTM D2887 [21]. An ELITE 2887 capillary column with a cross bond of dimethylpolysiloxane of 10 m in length and 0.53 of inner diameter and 2.65 μm of the film was used. The liquid samples were injected directly, and no liquids reduced the viscosity with

carbon disulfide. The assessment of potential products that could be recovered from oils was evaluated according to **Table 5S1** of fractions criteria [22].

#### 5.2.5.4. ASTM D86 distillation from the fuels

Atmospheric distillation of liquid fuel products quantitatively determines the boiling range characteristics of light and middle distillates by performing a simple batch distillation. The volatility characteristics provide information about safety and performance, composition, properties, and behavior during the storage and use of the fuels. To evaluate the stream performance and fuel distillation specification requirements similar to what might be achieved in an atmospheric distillation unit, the streams' simulated distillation curves were calculated from the SD curve according to the boiling range [23] shown in **Table 5S2**, then converted to ASTM D86 distillation curves by 3A3.2 API procedure (**Tables 5S3** and **Table 5S4**) [24]. The overlapping areas between cuts were normalized to determine the decreasing cumulative fraction, then multiplied by their corresponding areas to add them to the uppercut and the difference to the lower stream.

#### 5.3.5.5. Hydrocarbon types analysis

Hydrocarbon types were determined by mass spectroscopy based on the summation of characteristic mass fragments scanning specified in the methods ASTM D2789, ASTM D2425, ASTM D2786, and ASTM D3239 [25–27] for hydrocarbons boiling within the range C5 to 205 °C (light fraction) and 205 to 540 °C (middle distillate plus bottoms). For this, a gas chromatograph Agilent 8860 model coupled to a triple-quadrupole Agilent 5977 model mass spectrometer detector with analysis scan speed  $\leq 20000$  Da/s and ionization energy by the electronic impact of 70 eV and provided by nonpolar phase ZB-5 ms (30 m, 0.25 mm internal diameter and 0.25  $\mu\text{m}$  of fill thickness) Phenomenex capillary column was used. The oven was programmed with an initial temperature of 42 °C for 4 min, an injector temperature of 240 °C, and a final temperature of 320 °C for 4 min with a 6 °C/min gradient. The samples were weighed and diluted in 1 mL of chloroform and injected in split mode (5:1) at a constant flow of helium of 1 mL/min. A suitable synthetic mixture of pure hydrocarbons encompassing the boiling range specified by the ASTM D2887 method [5] was analyzed previously to identify the range of the retention times of streams for analysis. The referential retention times of each stream were calculated according to the following linear regression:

$$RT_x = \left( \frac{RT_2 - RT_1}{BP_2 - BP_1} \right) \cdot (BP_x - BP_1) + RT_1 \quad (5.4)$$

where the boiling point and retention times of referential paraffins are represented by  $BP_1$ ,  $BP_2$ ,  $RT_1$ , and  $RT_2$ , while the boiling points and retention times of the compounds in the sample are doing by  $BP_x$  and  $RT_x$ .

Obtained the referential retention times, the concentration analysis of the total paraffins, monocycloparaffins, di-cycloparaffins, alkylbenzenes, indans and tetralins, and naphthenes from naphtha were determined by the standard test method ASTM D2789 [25]. In contrast, the saturated hydrocarbon and aromatics types from kerosine and diesel were identified by the ASTM D2425 designation. At the same time, the bottoms were set out by the ASTM D2786 and ASTM D3239 standards [26,27,28]. The characteristic mass fragments were added to each stream according to its boiling range, considering the abovementioned overlapping criteria.

## 5.3. Results and discussion

### 5.3.1. Characterization of the catalysts

Fig. 5.2 (A, B) shows the  $N_2$  adsorption–desorption isotherms and pore size distribution, respectively. According to the IUPAC classification of physisorption isotherms, all materials can be classified as type IV, accompanied by capillary condensation hysteresis loops of type H3 for sepiolite and type H4 for montmorillonites [29]. Table 5.1 summarizes the morphologic characteristics of the catalytic materials analyzed by  $N_2$  adsorption–desorption isotherms after calcination. It is appreciable the absence of micropores in montmorillonite structures, a condition that is not changed from the raw state, as shown in Table 5.1 and Table 5S5; however, the calcinated ones have a decreased BET surface (7 to 9 percent), a total volume reduction of ca. 2.8%, and lessened average pore size of 7 to 12 percent, while, although calcinated sepiolite has a diminished BET (51.6%), micropore (93.7%), and external surfaces (9.8%), its total volume and average pore size increased by 30.8% and 5.1%, respectively. Despite the calcination, the surface area and pore volume of sepiolite displayed typical variations from the natural forms reported in the literature [30–31]. Conversely, montmorillonites exhibited close values [32–33]. As well known that acidic sites are the main active sites for the cracking effect over the surfaces of catalysts during catalytic pyrolysis processes [34], identified as weak (Brønsted acid) and strong (Lewis acid) sites on the studied samples; of these, both contributions both weak acid sites and moderate acid sites, were observed (Fig. 5.2C) [35–36]. However, a clear difference can be seen for catalytic samples with Sepiolite and Montmorillonite structures. MK10 and MK30 showed a well-defined peak centered at 170 °C, which can be associated with characteristics of weak acid sites, while the SE sample described a broadband caused by the contribution of weak acid sites, but with an important contribution from moderate acid sites according to the identification of the maximum intensity situated at 315 °C [35].  $NH_3$ -TPD also allows calculating the total acidity

at the surface of the catalysts. The acidity expressed as millimoles of NH<sub>3</sub> per gram reached a maximum for SE, followed by MK30 and MK10 (Table 5.1). As a result, stable acidic materials with a remarkable and defined mesoporous character, deduced from the porous size distribution, were obtained.

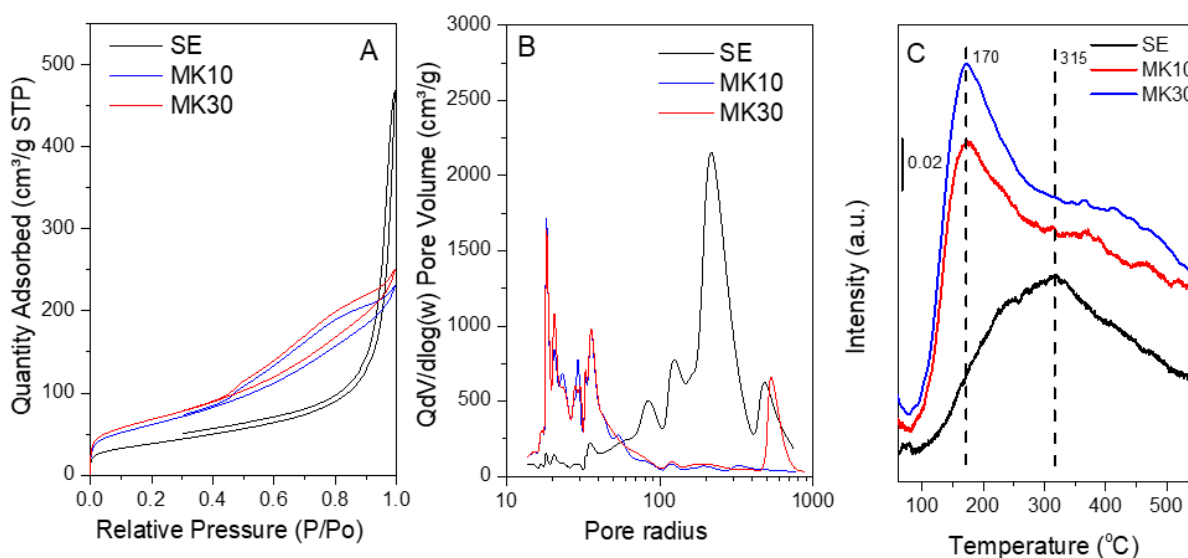


**Fig. 5.2.** Analysis of morphological and acidity properties of the samples (A) N<sub>2</sub> isotherms, (B) pore size distribution and (C) NH<sub>3</sub> temperature programmed desorption curves.

**Table 5.1.** Properties of the catalytic materials.

Catalyst	$S_{\text{BET}}$ ( $\text{m}^2 \cdot \text{g}^{-1}$ )	$S_{\text{MP}}$ ( $\text{m}^2 \cdot \text{g}^{-1}$ )	$S_{\text{EXT}}$ ( $\text{m}^2 \cdot \text{g}^{-1}$ )	$V_{\text{T}}$ ( $\text{cm}^3 \cdot \text{g}^{-1}$ )	$V_{\text{MP}}$ ( $\text{cm}^3 \cdot \text{g}^{-1}$ )	Average Pore Size (Å)	Acidity ( $\text{mmol} \cdot \text{g}^{-1}$ )
SE	138	9	129	0.726	0.004	82	0.290
MK10	224	-	224	0.357	-	55	0.233
MK30	245	-	245	0.389	-	54	0.276

### 5.3.2. Fraction yields and chemical composition

Table 5.2 shows the effect of sepiolite and montmorillonites on the average fraction yields obtained from the catalytic pyrolysis of the studied mixture of waste plastics in triplicate. As can be seen, an increase in gas fraction and a reduction in the amount of liquid were registered as a general trend. An enhancement of gases and a reduction of the liquid fraction when more catalytic material is added is also detected, while the solids showed wt. % between 6.6 and 8.1. The average values obtained led to a less than 5 % relative standard deviation.

As expected after treatments, MK10 and MK30 remain similar in morphological terms (Table 5.1 and 5S5); however, total acidity quantification provides some differences. As summarized in Table 5.1, the total acidity of the MK30 sample is relatively higher than the MK10 sample, approaching the values measured for the SE one, which, as aforementioned, has a higher contribution from moderate acid centers (above 300 °C). As morphologic and acidity remarkably influence on the selectivity, a ratio between total acidity/total superficial area is determined for each catalyst. This quantitative parameter allows a preliminary analysis of yield to the gas and liquid fraction. Such ratio, defined in Fig. 5.3A-D as Acidity/SBET (millimoles of NH<sub>3</sub> per m<sup>2</sup> of the catalytic surface), allows identifying two clearly defined areas. MK10 and MK30 to lower ratios produce fewer amounts of gas and a higher liquid fraction, while SE provides a higher gas fraction. The described trend is also independent of the used catalyst percentage (5 or 10% wt.). The correlation of Fig. 5.3 suggests that the selectivity profile is preferably associated with the type of acid centers rather than the total acidity of the sample. Obviously, and as discussed below, the pore distribution of the samples must also be considered a relevant factor.

**Table 5.2.** Gas, liquid, and solid yield (wt.%).

Catalyst percentage in the waste plastic feed	Gas	Liquid	Solid
0%	36.69	56.70	6.61
5% SE	42.14	50.44	7.43
10% SE	44.20	48.50	7.30
5% MK10	39.00	54.26	6.74
10% MK10	40.70	52.62	6.68
5% MK30	37.57	54.32	8.11
10% MK30	38.69	53.57	7.74

The increase of solids percentage concerning the pyrolysis without catalytic materials could also be attributed to coking formation due to acid sites of catalytic material [37], in addition to the porosity effects because of transport limitations, mainly when bulky molecules are involved [38]. Microporous in SE, and mesoporous volume extra of MK30 in the 500 and 600 Å range concerning MK10 (Fig. 5.2B), suggest that coke formation is due to heavy compounds adsorbed and trapped in these as well as catalyst/waste-plastic relation by the coke reduction when more catalyst is added than the individual acidic strength of each one. Nevertheless, although the acidity of SE is higher than MK30, coke reduced production could be due to the Lewis centers associated with a small number of exchangeable cations' [39]. The gas composition, Fig. 5.4, shows that probably condensable gases (propane and butane) and liquid light fractions (pentane) produced by catalytic cracking are under the thermal cracking effect when these leave the liquid phase that contains the catalyst. Typical light hydrocarbon reactions show pentanes decomposition begins

at 390 °C without dehydrogenation. Still, with increasing temperature, demethanization occurs along with deethanization and depropanation. At about 435 °C, butane usually decomposes into methane–propane, and ethane–ethylene. Propane has certain ethane formation, while the demethanization is approximately the same as the dehydrogenation [40]. The presence of carbon monoxide and carbon dioxides in gases may be due to the material’s origin and traces of organic and inorganic impurities over plastics and additives used in their manufacturing [41].

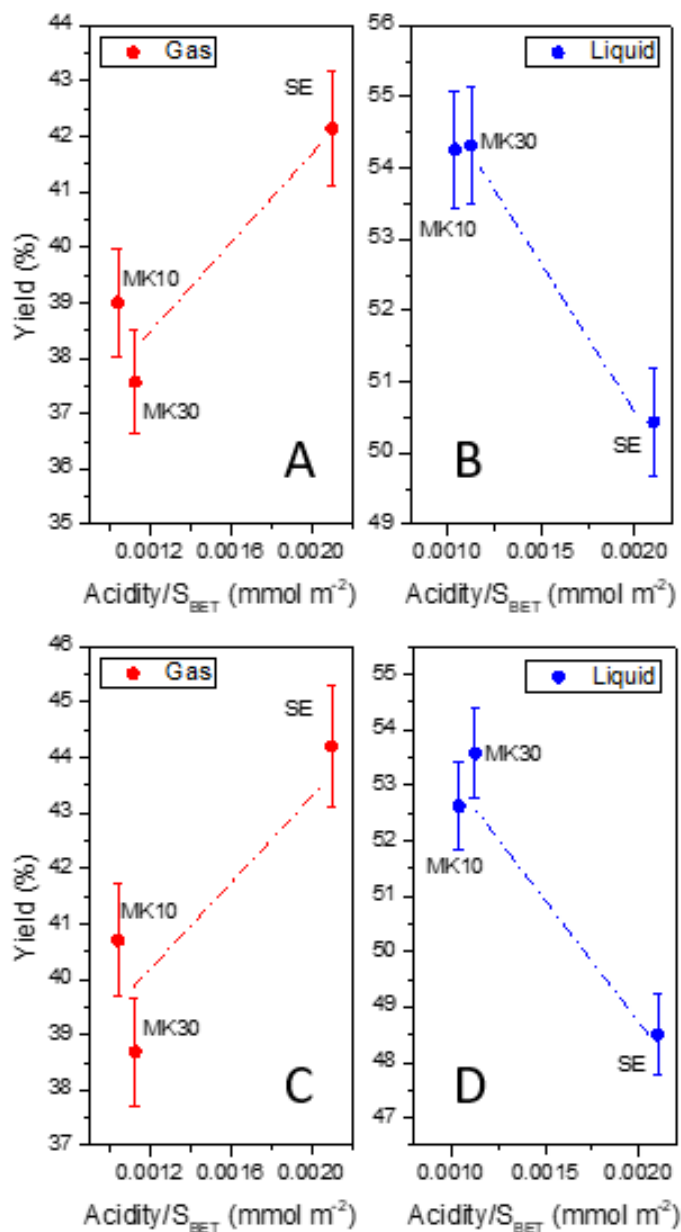


**Figure 5.3.** Acidity/S<sub>BET</sub> ratio as a function of the gas and liquid yield. (A) and (B) describe results obtained using 5 % of catalyst, and (C) and (D) the data using 10% of catalyst.



Table 5.3 shows the liquid products derived from pyrolysis expressed in wt. %. Concerning uncracked, there was a little nitrogenating from 0.1 to 0.3% promoted probably by catalytic and thermal cracking intermediates of reaction generated as by-products, along with deoxygenation reactions from 51 to 83% when the lowest amount of catalyst was used. The presence of catalysts and their relative augment was favorable for the hydrogenation of liquid fraction from 9 to 22%, calculated by carbon–hydrogen relation, which increases the heating value [42]. The proportions of elements registered vary over reasonably narrow limits like conventional petroleum (Carbon:  $83.4 \pm 0.5\%$ ; Hydrogen:  $10.4 \pm 0.2\%$ ; Nitrogen:  $0.4 \pm 0.2\%$  and Oxygen:  $1.0 \pm 0.2\%$ ) [43]; however, hydrogen content, from 41 to 56 % higher than petroleum, gives the obtained liquids a better heating value.

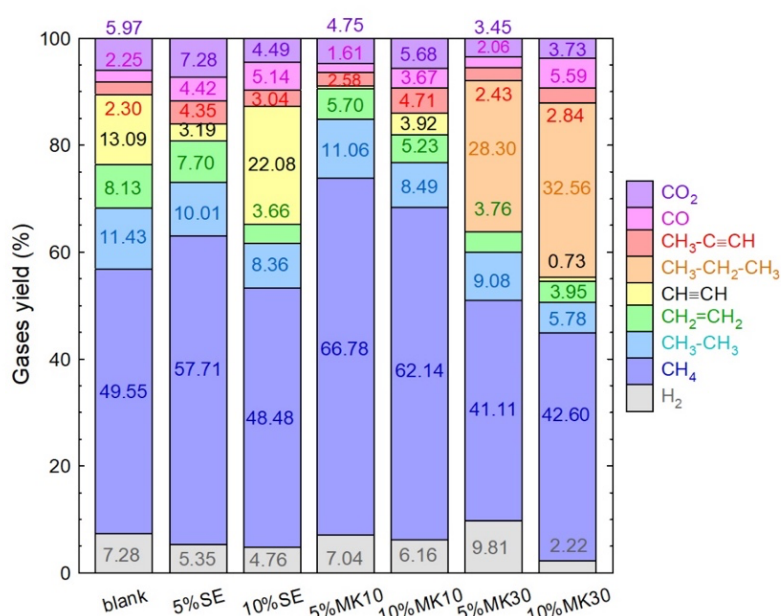


**Figure 5.4.** Gases composition under catalytic conditions and non-catalytic reference.

**Table 5.3.** Elemental composition of the liquid fraction obtained by noncatalytic and catalytic cracking.

Catalyst percentage in the waste plastic feed	Nitrogen (wt. %)	Carbon (wt. %)	Hydrogen (wt. %)	Oxygen (wt. %)
0%	0.0	84.1	13.4	2.5
5% SE	0.1	82.8	15.8	1.3
10% SE	0.2	82.0	15.9	1.9
5% MK10	0.3	84.0	15.3	0.4
10% MK10	0.3	79.6	16.2	3.9
5% MK30	0.2	84.3	14.7	0.8
10% MK30	0.1	79.8	15.4	4.7

A structural group analysis of obtained liquid samples was realized by Fourier Transform Infrared Spectroscopy (FTIR) to provide detailed information about the chemical constitution of these oils. The FTIR peaks frequency range showed similarity for noncatalytic and catalytic cracked liquids with some differences in the absorbance values; according to Beer's Law, the variations in the absorbance intensity are proportional to the concentration [44]. The main peaks, shown in Fig. 5.5, are between  $3080$  and  $3020\text{ cm}^{-1}$  (C-H medium stretch) for alkenes;  $2960$ – $2850\text{ cm}^{-1}$  (CH strong stretch) for alkanes;  $1760$ – $1670\text{ cm}^{-1}$  (C=O strong stretch) for aldehydes, ketones, carboxylic acids, and esters;  $1680$ – $1640\text{ cm}^{-1}$  (C=C medium and weak stretch) for alkenes;  $1650$ – $1580$  (N-H weak stretch) for amines;  $1600$ – $1500\text{ cm}^{-1}$  (C=C weak stretch) for aromatics rings;  $1470$ – $1350\text{ cm}^{-1}$  (variable scissoring and bending) for alkanes;  $1340$ – $1020\text{ cm}^{-1}$  (medium stretch) for amines;  $1260$ – $1000\text{ cm}^{-1}$  (strong stretch) for alcohols, ethers, carboxylic acids, and esters;  $1000$ – $675\text{ cm}^{-1}$  (C-H strong bend) for alkenes;  $870$ – $675\text{ cm}^{-1}$  (C-H strong bend) for phenyl ring substitution; and  $700$ – $610\text{ cm}^{-1}$  (C-H broad stretch) for alkynes [43]. Certain compounds could be attributed to the origin of plastic waste, its additives, and organic and inorganic impurities [45]. Although the drag nitrogen could form nitrogenated bonds, according to structure, these would influence pyrolytic oil instability as in the fuels obtained [46], in addition to the deposition of ammonium chlorine salts if exist traces of chlorine [47] by thermal cracking of PVC fragments. At the same time, oxygenated bonds would give particular acidity by naphthenic acid formation (linear, cyclic, and aromatic carboxylic groups) [48].

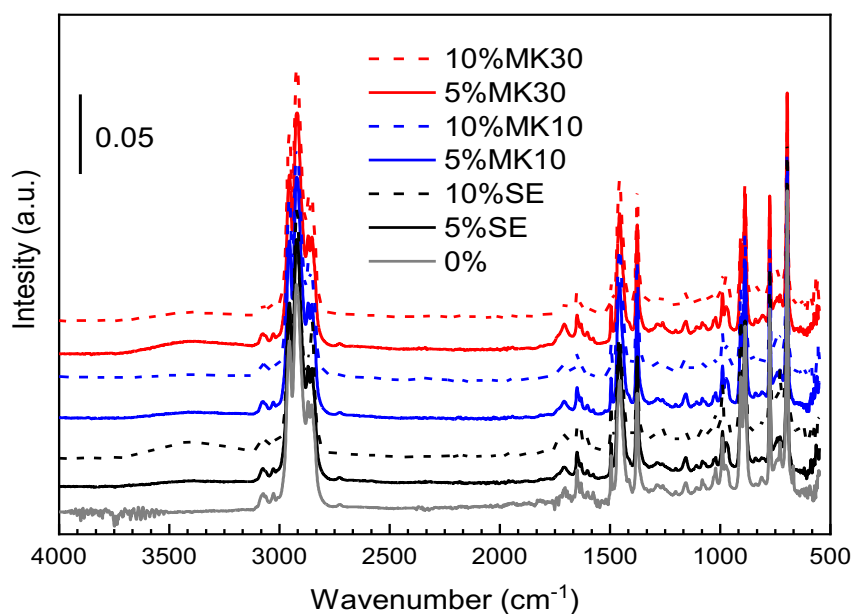


**Figure 5.5.** Chemical constitution of the liquid fraction obtained by noncatalytic and catalytic cracking.

### 5.3.3. Simulated distillation and product yield

The simulated distillation curves of liquid products derived from thermal and catalytic cracking of the mixture of plastics are shown in Fig. 5.6. Results indicate that the volatilization temperature increased for liquid products from catalytic cracking because of changes in the distribution of products provocative by the rising gas yield of up to 20 % due to the thermal cracking of light compounds of the liquid fraction, which reduced from 4 to 11 %, and the presence of a more significant amount of high boiling cuts, that increased from 5 to 42 %. The displacement of the distillation curves to the left shows a naphtha reduction of up to 36 %, kerosene rising by 32 %, distillate fuel oil by 33 %, and light and heavy vacuum gas oils by 21 and 41 %, respectively, concerning the thermal cracking.

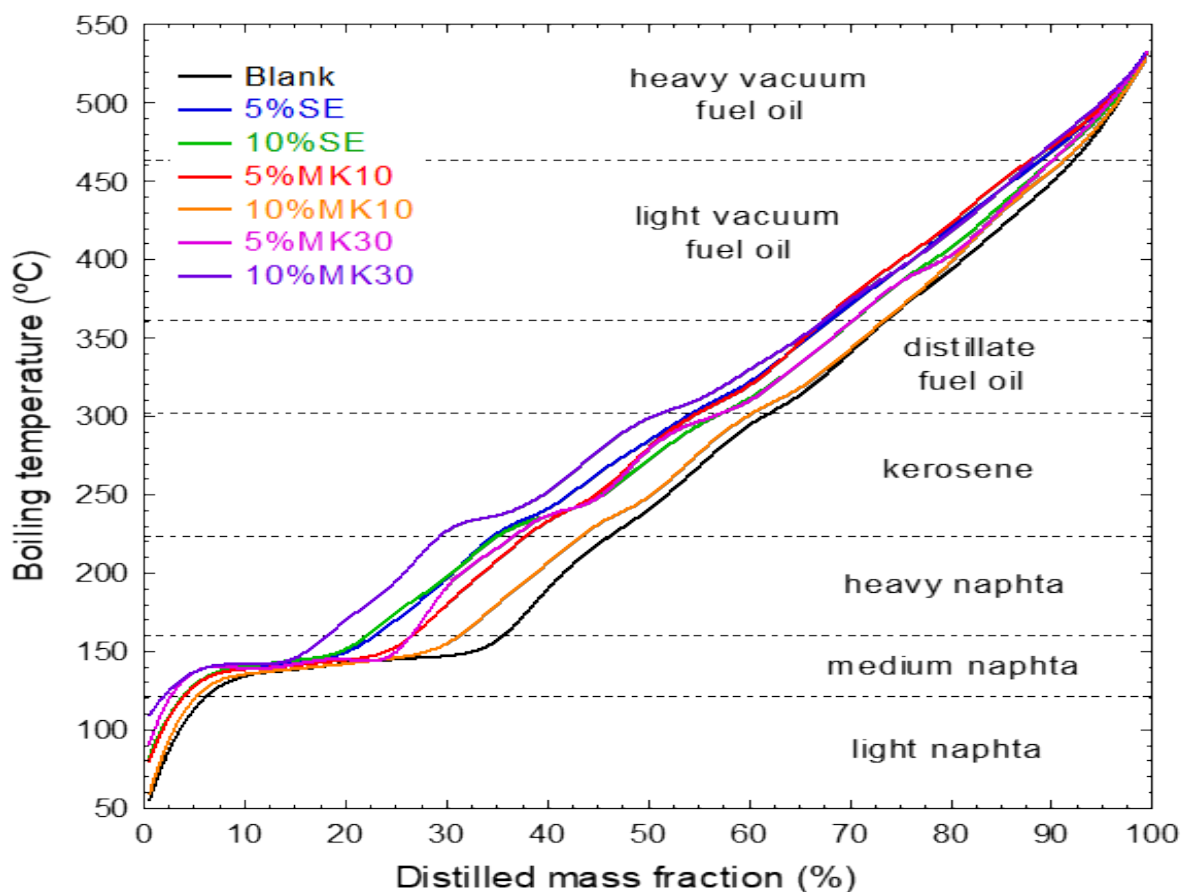


**Figure 5.6.** Boiling temperatures as a function of the distilled mass fraction (Simulated Distillation) of the liquid fraction obtained by noncatalytic and catalytic cracking.

The distribution of the products is reported in Table 5.4. When more SE is added, kerosine increases by cracking distillate and vacuum gas oils. Light naphtha (coming from heavy naphtha

cracking) absence could be due to this being broken into gases by the micropores' presence, which, regarding thermal cracking, augment from 15 to 20% in SE. The absence of micropores in MK10 reduces the cracking of heavy naphtha by about 8% compared to SE, and the little light naphtha formed is broken into gases. When MK10 increases, Light Vacuum Gas Oil (LVGO) and HVGO diminish to rise in light and heavy naphtha; light naphtha comes from medium naphtha, and a certain proportion is broken into gas. Unlike MK10, MK30 allows obtaining the highest amount of distillate Fuel Oil than other catalytic materials by breaking LVGO and HVGO, and more kerosine than MK10 and 5% SE, but with lesser heavy naphtha cut and cracking of the light naphtha present into gases. Adding more MK30, high boiling point cuts grow at the expense of light ones, and the little amount of light naphtha is transformed into gases.

**Table 5.4.** Products distribution.

Catalyst percentage in the waste plastic feed	Light Naphtha (wt. %)	Medium Naphtha (wt. %)	Heavy Naphtha (wt. %)	kerosine (wt. %)	Distillate Fuel Oil (wt. %)	Light Vacuum Gas Oil (wt. %)	Heavy Vacuum Gas Oil (wt. %)
0%	2.2	3.8	33.9	16.6	13.9	19.4	10.2
5% SE	-	3.8	25.5	18.9	16.3	22.2	13.3
10% SE	-	3.7	25.3	22.0	15.9	20.8	12.3
5% MK10	-	3.9	28.1	17.4	15.1	21.1	14.4
10% MK10	1.8	2.7	32.6	17.7	15.2	18.8	11.2
5% MK30	-	3.4	26.5	19.8	17.0	22.0	11.3
10% MK30	-	2.4	21.8	20.6	18.5	23.4	13.3

### 5.3.4. Chemical composition of the products

#### 5.3.4.1. Gasoline

For analogy with hydrocarbon present in petroleum, the analysis of light, medium, and heavy naphtha were made together as gasoline. Fig. 5.7 shows the ASTM D86 distillation curve for gasoline (A), its classification into paraffins, naphthenes, and aromatics (B), along with the categorization of hydrocarbon types in more detail (C). Some differences were observed in hydrocarbon group content according to the catalytic material used. The yield of paraffins, naphthenes, and aromatics varied when their amount increased, raising naphtha and paraffins by aromatics reduction; except on 10% MK10, where paraffins also reduced. At lower SE, the highest amount of alkylbenzenes formation was observed. For this reason, ASTM D86 distillations have higher boiling points than the gasoline obtained without a catalyst.

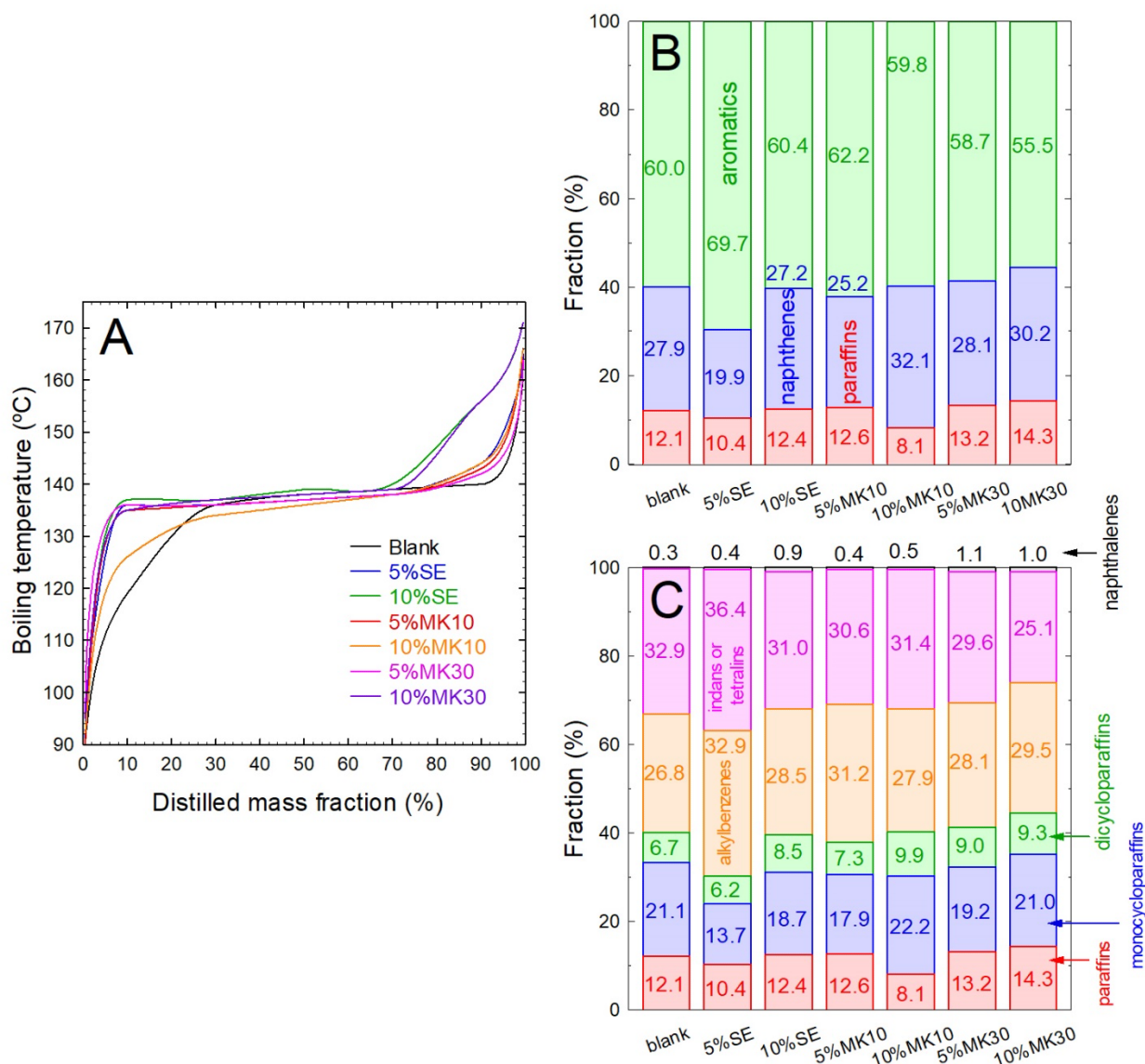


**Figure 5.7.** ASTM D86 distillation curve (A) Hydrocarbon group (B) and the hydrocarbon types (C) distributions from gasoline cut of the liquid fraction obtained by noncatalytic and catalytic cracking.

Saturated, the most chemically stable species, are present in gasoline from 20 to 80% (typically between 30 and 60 %) along with aromatic content to about 27 to 35 % to meet the emissions reduction requirements of the maximum permitted benzene (1%); aromatics have higher autoignition temperatures and increase octane and energy content [23,49]. The obtained gasoline does not comply with the low-temperature evaporation range according to 228 European Standard [49], and aromatic and paraffins are over specification; hence, they could be considered like base naphtha and form part of the gasoline pool for blending with low-octane number naphtha [50–52].

### 5.3.4.2. Kerosine

Making the analogy with petroleum fuels, this fraction, after appropriate cleanup (sweetening treatment), is marketed as a jet fuel [51] and, for this reason, is analyzed as Jet Fuel. The ASTM D86 distillation curve for Jet Fuel (A), its categorization into paraffins, naphthenes, and aromatics (B), as well as into the types of hydrocarbon present (C), are shown in Fig. 5.8. Comparing jet fuel obtained in non-catalytic cracking of thermal cracking, the catalytic materials increase the aromaticity reducing paraffins and naphthenes of the product, which is reflected in the distillation curves.

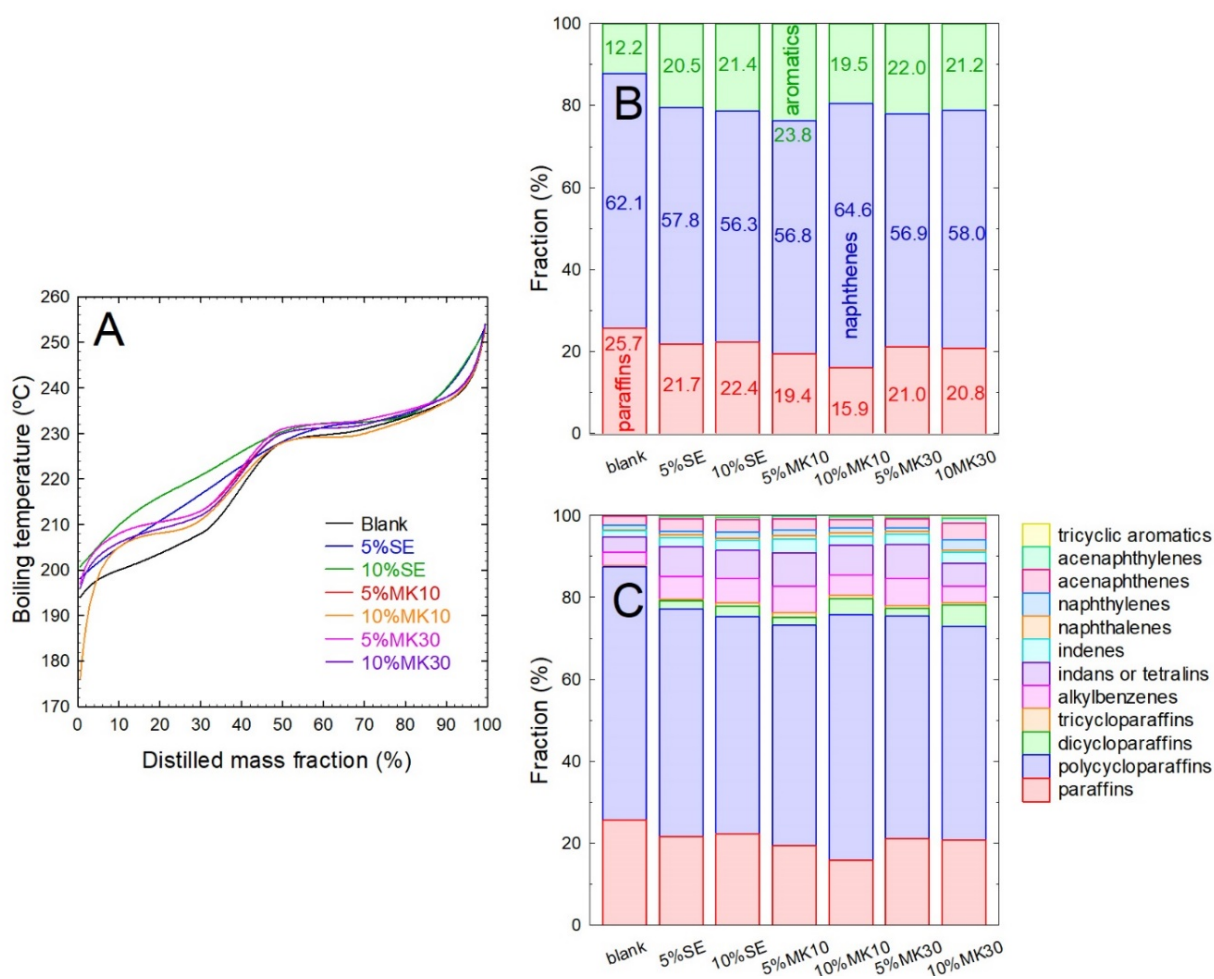


**Figure 5.8.** ASTM D86 distillation curve (A) Hydrocarbon group (B) and the hydrocarbon types (C) distributions from kerosine cut as Jet Fuel of the liquid fraction obtained by noncatalytic and catalytic cracking.

Straight-chain paraffins are the most critical molecules of the hydrocarbons normally in jet fuel since an amount of 8–10% forms a wax crystal matrix at low temperatures; in addition, microorganisms prefer to metabolize in these (C12 and higher ranges); nevertheless, provide the cleanest burning while aromatics do not. Double-ring aromatics or naphthalenes have poor combustion, so the total amount of aromatics is about 25% with  $\leq 3$  %vol of naphthalenes [40,23,52]. The volatility temperature at 10% distillation of the kerosine produced is over the range required [23], except that obtained by 10% MK10, and could be corrected by modifying the end distillation point of gasoline. Nevertheless, although aromatics and naphthalenes are below the specification requirement for Jet Fuel, even if the distillation requirement is met, paraffins will still be above the limit; they cannot be used as this fuel. At the boundaries of the boiling points considered in this study, since the saturated hydrocarbon derivatives of kerosine are desirable, they could be used as starting material for the production of petrochemical intermediates and the direct output of petrochemical products [53].

#### 5.3.4.3. Diesel

By analogy with fossil fuels, the distillate fuel oil was analyzed as a diesel product through to its ASTM D86 distillation curve (Fig. 5.9A) and its categorization into hydrocarbon groups (paraffins, naphthenes, and aromatics Fig. 5.9B) together with a detailed hydrocarbon type survey (Fig. 5.9C). Compared to the diesel product obtained by noncatalytic cracking or thermal cracking, aromatic hydrocarbon increased with a bit of paraffins by naphthenes reduction when the catalyst amount rose, except on 10% MK10, where naphthenes increased. As a result, little difference among ASTM D86 distillation curves is displayed.

Paraffins (aliphatic hydrocarbon, 64%) contribute majoritarian to fuel cetane number (decreases from n-paraffins to i-paraffins to n-olefins to i-olefins to naphthenes and aromatics); however, straight-chain paraffins supply a ignite readily under compression. In contrast, branched paraffins and aromatics react more slowly. Although aromatics have a negative impact on emissions and cetane index, they contribute to the lubrication properties, so the maximum allowed total aromatics is 10–35% (alkylbenzenes and 2-ring, 3-ring aromatics derivatives of 35% v/v, and less than 8 % m/m of polycyclic aromatics) [23,49,53]. Although the catalytic materials have an excellent performance in producing diesel due to the distillation requirements according to the 590 European Standard, their polyaromatic content would not allow them to be considered as such [49].

#### 5.3.4.4. Bottoms

As with the VGO of petroleum, light, and heavy gas oils were analyzed together as bottoms, a semi-finished product usually processed in the fluid catalytic cracking unit (FCCU) in a refining



process [53]. Fig. 5.10A shows this fraction classified into paraffins, naphthenes, and aromatics, while Fig. 5.10B shows detailed categorization by hydrocarbon types. No significant changes were observed concerning the obtained by noncatalytic cracking; nevertheless, the presence of the catalyst increased the paraffins from about 14 to 39% with a reduction from 4 to 32% of aromatics; naphthenes increased with MK10 materials (3 to 6%) and 10% of MK30. Compared to a typical fossil feedstock of an FCCU (23.9% paraffins, 37.8% cycloparaffins, 15% monoaromatics, 8.9% diaromatics, 7.9% of polyaromatics, 5% of others [54]), all fraction has low paraffinic, high cycloparaffins, and aromatics totals amounts, the last is an acid coke precursor [37] so that these fractions could be processed in FCC unit by blending with traditional feed.

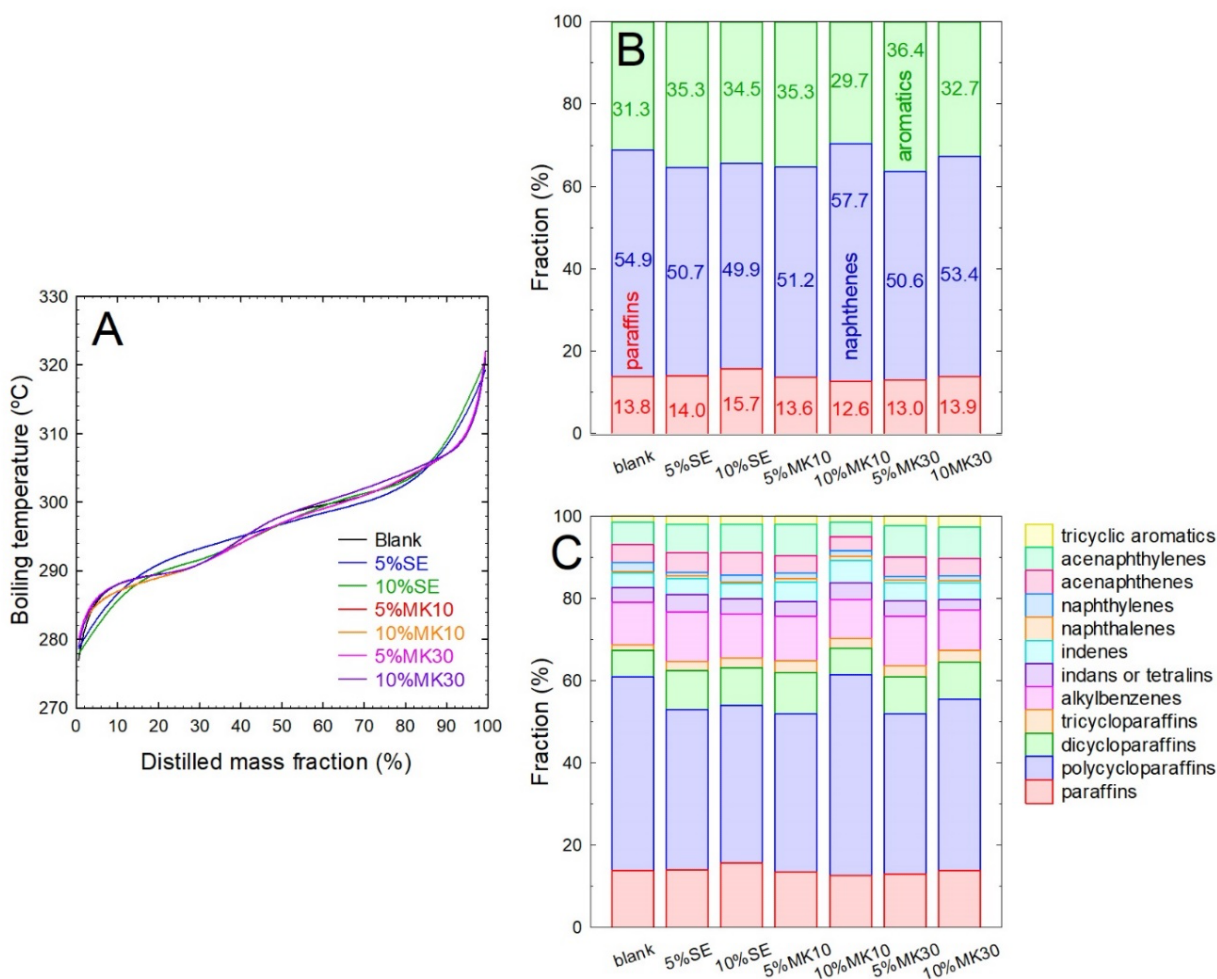


**Figure 5.9.** ASTM D86 distillation curve (A) Hydrocarbon group (B) and the hydrocarbon types (C) distributions from distillate fuel oil cut as a diesel of the liquid fraction obtained by noncatalytic and catalytic cracking.



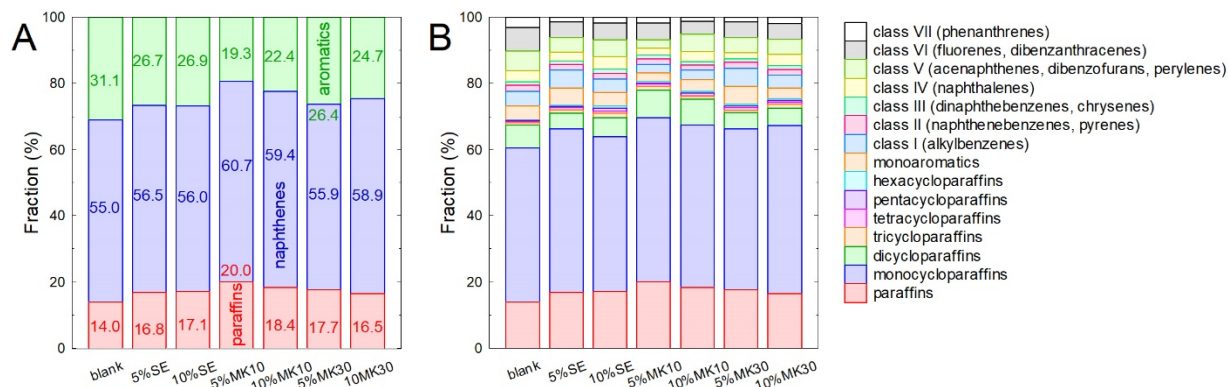


**Figure 5.10.** Hydrocarbon group (A) and the hydrocarbon types (B) distributions from gas oil cuts as bottoms of the liquid fraction obtained by noncatalytic and catalytic cracking.

## 5.4. Conclusions

A study of the potential of a catalytic pyrolysis process to valorize plastic wastes of the rejected fractions of Granada's mechanical biological treatment plant has been carried out. A complete analysis of the products focuses on identifying and classifying the fuel fractions, taking as references the fractions commonly obtained in oil refining processes (such as gasoline, kerosene, diesel, etc.).

Sepiolite and montmorillonites were used as catalysts. The commercial materials were subjected to a simple heat treatment to obtain samples with a well-defined porous structure and advantageous acidity properties for the catalytic step. Montmorillonites exhibited  $\text{NH}_3$ -TPD with a dominant peak associated with weak acid sites, while sepiolite displayed acid sites of greater strength and a broad band with a maximum located at  $315\text{ }^\circ\text{C}$ . The analysis of a combined morphologic/ acidity parameter provides a quantitative conclusion that confirms that higher liquid fraction can be optimized using Montmorillonites with high surface area and weak acid sites. The porous distribution also showed a clear influence on the yield products.

The results indicate that the volatilization temperature of the liquid products obtained from catalytic cracking increased due to changes in the product distribution, which were caused by a substantial rise in gas yield, up to 20 wt%. This increase in gas yield can be attributed to the thermal cracking of light compounds within the liquid fraction, leading to a reduction in their concentration from 4 to 11 wt%.

A remarkably higher amount of high boiling cuts was detected, which increased from 5 to 42 wt%. The leftward shift of the distillation curves indicates a decrease in naphtha by up to 36 wt%, while kerosene experienced a rise of 32 wt%.

Distillate fuel oil showed an increase of 33%, and both light and heavy vacuum gas oils exhibited a rise of 21% and 41%, respectively, compared to thermal cracking conditions.

A full screening of gasoline, kerosine, diesel, and bottoms, by analogy with hydrocarbon present in petroleum, was carried out by Simulated Distillations. At optimized operating conditions, the process could allow obtaining liquid.

This approach critically assesses the potential of a thermal-catalytic valorization scheme for real plastic waste in the current energy context, which is still dominated by fuels derived from the petroleum industry. The assessment is based on a strict analysis of the fractions using Simulated Distillation.

At optimized operating conditions, the process could allow obtaining liquid products which can be part of the gasoline pool for blending with low-octane number naphtha, a fraction with similar properties to the diesel fraction, a kerosene fraction to be used as starting material for the production of petrochemical or the commonly called button fraction products with properties similar to the vacuum gas oil of petroleum industry (light and heavy gas oils) which could be processed in FCC units.

The approach situates, with a critical perspective and based on a strict analysis of the fractions by Simulated Distillation, the potential of a thermal-catalytic valorization scheme of real plastic solid waste in the current energy context, which is still dominated by the fuels generated by the petroleum industry.

### Acknowledgments

This work has received funds from the project PID2019-108826RB- I00/SRA (State Research Agency)/10.13039/501100011033 and the project B-RNM-78-UGR20 (FEDER/Junta de Andalucía-Ministry of Economic Transformation, Industry, and Universities). Funding for open access charge: Universidad de Granada / CBUA.

### References

- [1] S. D. Anuar Sharuddin, F. Abnisa, W. M. A. Wan Daud, and M. K. Aroua, "A review on pyrolysis of plastic wastes," *Energy Convers. Manag.*, vol. 115, pp. 308–326, 2016, doi: 10.1016/j.enconman.2016.02.037.
- [2] M. S. Qureshi *et al.*, "Pyrolysis of plastic waste: Opportunities and challenges," *J. Anal. Appl. Pyrolysis*, vol. 152, no. February, 2020, doi: 10.1016/j.jaap.2020.104804.
- [3] S. H. Gebre, M. G. Sendeku, and M. Bahri, "Recent Trends in the Pyrolysis of Non-Degradable Waste Plastics," *ChemistryOpen*, vol. 10, no. 12, pp. 1202–1226, 2021, doi:

- 10.1002/open.202100184.
- [4] A. E. Schwarz, T. N. Ligthart, D. Godoi Bizarro, P. De Wild, B. Vreugdenhil, and T. van Harmelen, "Plastic recycling in a circular economy; determining environmental performance through an LCA matrix model approach," *Waste Manag.*, vol. 121, pp. 331–342, 2021, doi: 10.1016/j.wasman.2020.12.020.
- [5] S. Budsareechai, A. J. Hunt, and Y. Ngernyen, "Catalytic pyrolysis of plastic waste for the production of liquid fuels for engines," *RSC Adv.*, vol. 9, no. 10, pp. 5844–5857, 2019, doi: 10.1039/c8ra10058f.
- [6] L. Quesada, A. Pérez, V. Godoy, F. J. Peula, M. Calero, and G. Blázquez, "Optimization of the pyrolysis process of a plastic waste to obtain a liquid fuel using different mathematical models," *Energy Convers. Manag.*, vol. 188, no. March, pp. 19–26, 2019, doi: 10.1016/j.enconman.2019.03.054.
- [7] M. F. Paucar-Sánchez, M. Calero, G. Blázquez, R. R. Solís, M. J. Muñoz-Batista, and M. Á. Martín-Lara, "Thermal and catalytic pyrolysis of a real mixture of post-consumer plastic waste: An analysis of the gasoline-range product," *Process Saf. Environ. Prot.*, vol. 168, no. October, pp. 1201–1211, 2022, doi: 10.1016/j.psep.2022.11.009.
- [8] R. R. Solís, M. Á. Martín-Lara, A. Ligeró, J. Balbís, G. Blázquez, and M. Calero, "Revalorizing a Pyrolytic Char Residue from Post-Consumer Plastics into Activated Carbon for the Adsorption of Lead in Water," *Appl. Sci.*, vol. 12, no. 16, 2022, doi: 10.3390/app12168032.
- [9] D. A. Wijesekara, P. Sargent, C. J. Ennis, and D. Hughes, "Prospects of using chars derived from mixed post waste plastic pyrolysis in civil engineering applications," *J. Clean. Prod.*, vol. 317, no. December 2020, p. 128212, 2021, doi: 10.1016/j.jclepro.2021.128212.
- [10] M. M. Harussani, S. M. Sapuan, U. Rashid, A. Khalina, and R. A. Ilyas, "Pyrolysis of polypropylene plastic waste into carbonaceous char: Priority of plastic waste management amidst COVID-19 pandemic," *Sci. Total Environ.*, vol. 803, p. 149911, 2022, doi: 10.1016/j.scitotenv.2021.149911.
- [11] S. Parrilla-Lahoz *et al.*, "Materials challenges and opportunities to address growing micro/nanoplastics pollution: a review of thermochemical upcycling," *Mater. Today Sustain.*, vol. 20, p. 100200, 2022, doi: 10.1016/j.mtsust.2022.100200.
- [12] S. M. Al-Salem, A. Antelava, A. Constantinou, G. Manos, and A. Dutta, "A review on thermal and catalytic pyrolysis of plastic solid waste (PSW)," *J. Environ. Manage.*, vol. 197, no. 1408, pp. 177–198, 2017, doi: 10.1016/j.jenvman.2017.03.084.
- [13] R. Miandad, M. A. Barakat, A. S. Aburizaiza, M. Rehan, and A. S. Nizami, "Catalytic pyrolysis of plastic waste: A review," *Process Saf. Environ. Prot.*, vol. 102, pp. 822–838, 2016, doi: 10.1016/j.psep.2016.06.022.
- [14] Y. Peng *et al.*, "A review on catalytic pyrolysis of plastic wastes to high-value products," *Energy Convers. Manag.*, vol. 254, no. December 2021, p. 115243, 2022, doi: 10.1016/j.enconman.2022.115243.

- 
- [15] L. Dai *et al.*, "Pyrolysis technology for plastic waste recycling: A state-of-the-art review," *Prog. Energy Combust. Sci.*, vol. 93, no. June, p. 101021, 2022, doi: 10.1016/j.pecs.2022.101021.
- [16] K. Wang, P. A. Johnston, and R. C. Brown, "Comparison of in-situ and ex-situ catalytic pyrolysis in a micro-reactor system," *Bioresour. Technol.*, vol. 173, pp. 124–131, 2015, doi: 10.1016/j.biortech.2014.09.097.
- [17] American Society for Testing and Materials, "Surface Area of Catalysts and Catalyst Carriers," *ASTM Int.*, vol. 05, no. Reapproved, pp. 1–5, 2007.
- [18] American Society for Testing and Materials, "Standard Test Method for Determining Micropore Volume and Zeolite Area of a," *ASTM Int.*, vol. 05, no. Reapproved, pp. 1–6, 2001.
- [19] American Society for Testing and Materials, "Standard Practice for Calculation of Pore Size Distributions of Catalysts from," *ASTM Int.*, vol. 94, no. Reapproved 2006, pp. 1–6, 2012, doi: 10.1520/D4641-17.2.
- [20] American Society for Testing and Materials, "Standard Test Methods for Instrumental Determination of Carbon, Hydrogen, and Nitrogen in Petroleum Products and Lubricants," *Man. Hydrocarb. Anal. 6th Ed.*, pp. 852-852–5, 2008, doi: 10.1520/mnl10969m.
- [21] American Society for Testing and Materials, "Standard Test Method for Boiling Range Distribution of Petroleum Fractions by Gas Chromatography," *ASTM International*. p. 20, 2008.
- [22] R. G. Montemayor, *Distillation and Vapor Pressure Measurement in Petroleum Products*. West Conshohocken: ASTM International, 2008.
- [23] G. Totten, S. Westbrook, and R. Shah, *Fuels and Lubricants Handbook: Technology, Properties, Performance, and Testing*, ASTM. Glen Burnie: ASTM International, 2003.
- [24] American Petroleum Institute, "Technical Data Book American Petroleum Institute," *American Petroleum Institute*. 1999.
- [25] American Society for Testing and Materials, "Standard Test Method for Hydrocarbon Types in Low Olefinic Gasoline by Mass Spectrometry," *ASTM Int.*, vol. i, no. Reapproved 2016, pp. 1–7, 2013.
- [26] American Society for Testing and Materials, "Standard Test Method for Hydrocarbon Types Analysis of Gas-Oil Saturates Fractions by High Ionizing Voltage Mass Spectrometry," *ASTM Int.*, no. Reapproved 2016, pp. 1–8, 1991.
- [27] American Society for Testing and Materials, "Standard Test Method for Aromatic Types Analysis of Gas-Oil Aromatic Fractions by High Ionizing Voltage Mass Spectrometry," *ASTM Int.*, no. Reapproved 2016, pp. 1–15, 1991.
- [28] American Society for Testing and Materials, "Standard Test Method for Hydrocarbon Types in Middle Distillates by Mass," vol. i, no. Reapproved 2009, pp. 1–6, 2013, doi: 10.1520/D2789-05R16.2.

- [29] M. Thommes *et al.*, “Physisorption of gases, with special reference to the evaluation of surface area and pore size distribution (IUPAC Technical Report),” *Pure Appl. Chem.*, vol. 87, no. 9–10, pp. 1051–1069, 2015, doi: 10.1515/pac-2014-1117.
- [30] J. M. Campelo, A. Garcia, D. Luna, and J. M. Marinas, “Textural properties, surface chemistry and catalytic activity in cyclohexene skeletal isomerization of acid treated natural sepiolites,” *Mater. Chem. Phys.*, vol. 24, no. 1–2, pp. 51–70, 1989, doi: 10.1016/0254-0584(89)90045-X.
- [31] M. Suárez and E. García-Romero, “Variability of the surface properties of sepiolite,” *Appl. Clay Sci.*, vol. 67–68, pp. 72–82, 2012, doi: 10.1016/j.clay.2012.06.003.
- [32] F. W. Harun, E. A. Almadani, and S. M. Radzi, “Metal cation exchanged montmorillonite K10 (MMT K10): Surface properties and catalytic activity,” *J. Sci. Res. Dev.*, vol. 3, no. 3, pp. 90–96, 2016, [Online]. Available: [www.jsrad.org](http://www.jsrad.org).
- [33] B. S. Jang, K. H. Cho, K. H. Kim, and D. W. Park, “Degradation of polystyrene using montmorillonite clay catalysts,” *React. Kinet. Catal. Lett.*, vol. 86, no. 1, pp. 75–82, 2005, doi: 10.1007/s11144-005-0297-z.
- [34] E. Karimi *et al.*, “Red mud as a catalyst for the upgrading of hemp-seed pyrolysis bio-oil,” *Energy and Fuels*, vol. 24, no. 12, pp. 6586–6600, 2010, doi: 10.1021/ef101154d.
- [35] M. Chen *et al.*, “Hydrogen production by ethanol steam reforming over M-Ni/sepiolite (M = La, Mg or Ca) catalysts,” *Int. J. Hydrogen Energy*, vol. 46, no. 42, pp. 21796–21811, 2021, doi: 10.1016/j.ijhydene.2021.04.012.
- [36] J. Zhang *et al.*, “Catalytic Cracking of n-Decane over Monometallic and Bimetallic Pt-Ni/MoO<sub>3</sub>/La-Al<sub>2</sub>O<sub>3</sub> Catalysts: Correlations of Surface Properties and Catalytic Behaviors,” *Ind. Eng. Chem. Res.*, vol. 58, no. 5, pp. 1823–1833, 2019, doi: 10.1021/acs.iecr.8b04712.
- [37] J. T. Richardson, *Principles of Catalyst Development*, Second Pri. New York: Springer Science+Business Media, LLC, 1992.
- [38] C. H. Zhou *et al.*, “Roles of texture and acidity of acid-activated sepiolite catalysts in gas-phase catalytic dehydration of glycerol to acrolein,” *Mol. Catal.*, vol. 434, pp. 219–231, 2017, doi: 10.1016/j.mcat.2016.12.022.
- [39] J. Pérez Pariente, V. Fornés, A. Corma, and A. Mifsud, “The surface acidity and hydrothermal stability of sepiolite derivatives,” *Appl. Clay Sci.*, vol. 3, no. 4, pp. 299–306, 1988, doi: 10.1016/0169-1317(88)90021-X.
- [40] P. (IFP) Wuithier, *Le Pétrole REFFINAGE ET GÈNIE CHIMIQUE, Tome 1*, 2nd ed. Paris: Technip, 1972.
- [41] L. Quesada, M. Calero, M. Á. Martín-Lara, A. Pérez, M. F. Paucar-Sánchez, and G. Blázquez, “Characterization of the Different Oils Obtained through the Catalytic In Situ Pyrolysis of Polyethylene Film from Municipal Solid Waste,” *Appl. Sci.*, vol. 12, no. 8, 2022, doi: 10.3390/app12084043.

- [42] M. R. Riazi, *Characterization and Properties of Petroleum Fractions*, 1st ed., vol. 1, no. 1. Philadelphia: ASTM, 2005.
- [43] J. G. Speight, *The Chemistry and Technology of Petroleum*, Fourth. Boca Raton: CRC Press, 2006.
- [44] B. C. Smith, *Infrared Spectral Interpretation: a systematic approach*, vol. 3, no. April. Boca Raton: CRC Press, 1999.
- [45] M. Kusenberg *et al.*, "A comprehensive experimental investigation of plastic waste pyrolysis oil quality and its dependence on the plastic waste composition," *Fuel Process. Technol.*, vol. 227, no. November 2021, p. 107090, 2022, doi: 10.1016/j.fuproc.2021.107090.
- [46] J. W. Bauserman, G. W. Mushrush, and D. R. Hardy, "Organic nitrogen compounds and fuel instability in middle distillate fuels," *Ind. Eng. Chem. Res.*, vol. 47, no. 9, pp. 2867–2875, 2008, doi: 10.1021/ie071321n.
- [47] P. Schempp, S. Köhler, M. Menzebach, K. Preuss, and M. Tröger, "Corrosion in the crude distillation unit overhead line: Contributors and solutions," *EUROCORR 2017 - Annu. Congr. Eur. Fed. Corros. 20th Int. Corros. Congr. Process Saf. Congr. 2017*, no. September, 2017.
- [48] C. G. Cárdenas, B., "Analysis of the acid number of crude oils with different API gravity and their typical fractions," National Polytechnic Institute of Mexico, 2015.
- [49] B. O. del E. (BOE), *Real Decreto 1088/2010 por el que se modifica el Real Decreto 61/2006, de 31 de enero, en lo relativo a las especificaciones técnicas de gasolinas, gasóleos, utilización de biocarburantes y contenido de azufre de los combustibles para uso marítimo*. Madrid: Agencia Estatal Boletín Oficial del Estado, 2010.
- [50] M. R. Rahimpour, M. Jafari, and D. Iranshahi, "Progress in catalytic naphtha reforming process: A review," *Appl. Energy*, vol. 109, pp. 79–93, 2013, doi: 10.1016/j.apenergy.2013.03.080.
- [51] R. A. Meyers, *Handbook of Petroleum Refining Processes*, Second. Third, 2004.
- [52] J.-P. (IFP) Wauquier, *El Refino Del Petróleo*. Madrid: Díaz de Santos - ISE, 2004.
- [53] J. G. Speight, *Handbook of Petrochemical Processes*. Boca Raton: CRC Press, 2019.
- [54] S. H. Ng, "Conversion of Polyethylene Blended with VGO to Transportation Fuels by Catalytic Cracking," *Energy and Fuels*, vol. 9, no. 2, pp. 216–224, 1995, doi: 10.1021/ef00050a003.

## 5.S. Supplementary materials

### Collection and starting analysis of the raw material.

The evaluation of the composition and characteristics of the non-recyclable containing in the municipal solid waste (fraction non-recovery selectively) was performed. A total of 100 kg of dirty non-recyclable plastics from municipal solid waste was collected from EcoCentral Granada. Identification and quantification of plastics existing in this fraction were conducted following the following general scheme.

- Collection of waste provided by EcoCentral de Granada (about 500-600 kg).
- Random selection of 100 kg of plastic waste according to the random sampling method based on American Society of Testing and Materials (ASTM) standard.
- Sorting plastic by category (including visual inspection, density measurements, Differential Scanning Calorimetry (DSC) and Fourier Transform Infrared Spectroscopy (FTIR).

**Table 5S1.** Classification of Products.

	Product	Cut Temperatures, °C
Gasoline	Light Naphtha	C <sub>5</sub> – 79
	Medium Naphtha	79 – 121
	Heavy Naphtha	121 – 191
Middle Distillates	Kerosine	191 – 277
	Distillate Fuel Oil	277 – 343
Gas Oil	Light Vacuum Gas Oil (LVGO)	343 – 455
	Heavy Vacuum Gas Oil (HVGO)	455 – C <sub>+</sub>

**Table 5S2.** Crude section cuts.

Stream	Carbon Number	Approximate Boiling Range, °C
Naphtha	C <sub>6</sub> – C <sub>10</sub>	85 – 190
Kerosine or Kerosine Jet	C <sub>9</sub> – C <sub>15</sub>	160 – 275
Diesel	C <sub>13</sub> – C <sub>18</sub>	250 – 340
Bottoms	C <sub>16</sub> – C <sub>+</sub>	> 315

**Table 5S3.** Correlations and equations to calculate the true boiling temperature at any percent distilled from the predicted 50% true boiling point temperature, API procedure 3A3.2 [8].

$$\text{ASTM (50)} = 0.77601 \cdot \text{SD (50)}^{1.0395}$$

Where:

ASTM (50) = ASTM D86 temperature at 50% *volume* percent distilled, degrees Fahrenheit.

SD (50) = simulated distillation temperature at 50 *weight* percent distilled, degrees Fahrenheit.

$$\text{ASTM (0)} = \text{ASTM (50)} - U_4 - U_5 - U_6$$

$$\text{ASTM (10)} = \text{ASTM (50)} - U_4 - U_5$$

$$\text{ASTM (30)} = \text{ASTM (50)} - U_4$$

$$\text{ASTM (70)} = \text{ASTM (50)} + U_3$$

$$\text{ASTM (90)} = \text{ASTM (50)} + U_3 + U_2$$

$$\text{ASTM (100)} = \text{ASTM (50)} + U_3 + U_2 + U_1$$

**Table 5S4.** Constants and Restrictions to the determination of the differences between adjacent cut points, API procedure 3A3.2 [8].

$$U_i = E \cdot (T_i)^F$$

Where:

$U_i$  = ASTM D86 distillation temperature difference between two cut points, degrees Fahrenheit.

$T_i$  = SD temperature difference between two cut points, degrees Fahrenheit.

$E, F$  = constants varying for cut point range, described as follows.

$i$	Cut Point Range	$E$	$F$	Approximate Maximum Allowable $T_i$ , (°F)
1	100% – 90%	2.6029	0.65962	100
2	90% – 70%	0.30785	1.2341	100
3	70% – 50%	0.14862	1.4287	100
4	50% – 30%	0.07978	1.5386	100
5	30% – 10%	0.06069	1.5176	150
6	10% – 0%	0.30470	1.1259	150



**Table 5S5.** Properties of the catalytic raw materials.

<b>Catalyst</b>	<b>S<sub>BET</sub> (m<sup>2</sup>·g<sup>-1</sup>)</b>	<b>S<sub>MP</sub> (m<sup>2</sup>·g<sup>-1</sup>)</b>	<b>S<sub>EXT</sub> (m<sup>2</sup>·g<sup>-1</sup>)</b>	<b>V<sub>T</sub> (cm<sup>3</sup>·g<sup>-1</sup>)</b>	<b>V<sub>MP</sub> (cm<sup>3</sup>·g<sup>-1</sup>)</b>	<b>Average Pore Size (Å)</b>
Raw Sepiolite	285	142	143	0.555	0.074	78
Raw Montmorillonite K10	246	-	246	0.365	-	59
Raw Montmorillonite K30	264	-	264	0.400	-	61



## Chapter 6

# Impact of metal impregnation of commercial zeolites on the pyrolysis of a real mixture of post-consumer plastic waste

Marco F. Paucar-Sánchez, Mónica Calero, Gabriel Blázquez, Rafael R. Solís, Mario J. Muñoz-Batista and M. Ángeles Martín-Lara

*Department of Chemical Engineering University of Granada, 18071 Granada, Spain*

Applied Science-Basel, ISSN: N/A, eISSN: 2073-4344. Published by MDPI.

*Volume:* 14

*Number:* 168

*Country:* Switzerland

DOI: <https://doi.org/10.3390/catal14030168>

- *Category:* Chemistry, Physical. *Journal Impact Factor, JIF (2022):* 3.9. *Category Ranking:* 71/161 (Q2).

*Article history:*

Received 17 January 2024

Revised 16 February 2024

Accepted 20 February 2024

Published 24 February 2024



## Abstract

This work reports the study of the catalytic pyrolysis of rejected plastic fractions collected from municipal solid waste whose mechanical recovery is not plausible due to technical or poor conservation issues. The chemical recycling through catalytic pyrolysis was carried out over commercial zeolites formulas, i.e., HY and HZSM-5, in which Ni or Co metals were deposited at two different loadings (1 and 5%, wt.). The presence of these transition metals on the zeolitic supports impacted the total production of compounds existing in the liquid oil. The samples were characterized in terms of structural, chemical, and morphologic properties, and the production of different fuel fractions (gasoline, light cycle oil, and heavy cycle oil) was correlated with a combined parameter defined as a ratio of Acidity/BET area.

**Keywords:** Catalytic pyrolysis; Chemicals; Metal incorporation; Plastics waste; Zeolites

## 6.1. Introduction

Plastics made from hydrocarbons have been the most manufactured material due to the shift from durable to single-use plastics since the 1950s [1]. Recent estimations have shown that only one-third of the collected plastic waste (10.2 Mt) is recycled. Still, around 6.9 Mt (23%) are sent to landfills [2], which generates another future problem like the plausible leaching of hazardous chemicals that could reach the soil and the water, along with microplastics generated in those that do not have adequate protection [3–5]. To solve this, a series of actions to reduce waste have been proposed, among which are expanding and improving separate collections, favoring the reuse and recycling of plastics in opposition to landfilling or incineration [6]. Although many classification processes have been optimized, the accumulation of large amounts of mixed dirty plastics is still high, and their separation, primarily via mechanical procedures, is not economically feasible [7].

Chemical recycling is a viable alternative for plastic waste processing because it allows for the handling of a more comprehensive range of plastic waste, including those that are difficult to recycle mechanically [8,9]. Among all the types of chemical recycling methods, pyrolysis (thermal cracking) is the preferred method for many industries. However, thermal cracking is an uncontrolled breakdown pathway in plastic waste process treatment to obtain an adequate feedstock to produce chemicals [10], but the presence of catalytic materials solves certain limitations concerning temperature dependence by including specific catalytic characteristics such as surface area, pore size distribution, and acidity [11]. Up to this point, several studies have researched the thermal degradation of different plastic waste over catalytic materials; some of them aimed at the production of aromatic hydrocarbons using commercial zeolites like HY and

HZSM-5 [12–18], and others intended to compare the effect of contact mode on product distribution either operating under in situ or ex situ schemes [10,19,20], others focused on the production of hydrogen-rich syngas and carbon nanomaterials [13,21].

The generation of improved fuels and high-value chemicals in the liquid product from the pyrolysis of biomass and plastic waste can be improved using metallic catalysts. In the pyrolysis of different types of waste, including plastic waste, metals have been integrated into a diverse variety of catalytic support materials, mainly including activated carbons and zeolites [22–24]. For instance, non-noble metals such as Fe, Co, Zn, and Ni have been deposited onto the zeolite HZSM-5 to upgrade the liquid or oil product obtained from the co-pyrolysis of wheat straw and polystyrene [20]. The presence of metals was reported to increase selectivity towards monoaromatic hydrocarbons when the metals were added, e.g., when the PVC-containing waste-derived vapor was processed [25], as well as considerably reducing coke production in the hydrocracking of residues [26], over Co\_HZSM-5; or producing ethylene by ethane dehydrogenation in CO<sub>2</sub> presence [27]. Cobalt (Co) and nickel (Ni) have also been used to modify the zeolite ZSM-5 and applied to the in situ pyrolysis of biomass [28], as over alumina to convert furfural to ethanol at high pressure in a hydrogen environment [29]. The incorporation of Co or Ni limited the zeolite's reactivity toward water production [23]. Finally, another example of in situ catalytic pyrolysis is upgrading pyrolysis oil from biomass using a modified HZSM-5 with P, Zn, and Ti. The addition of Zn to the zeolite aided in the formation of polyaromatic hydrocarbons, while Ti triggered the formation of monoaromatic and aliphatic hydrocarbons [30].

Since catalytic pyrolysis over real mixtures of post-consumer plastic waste destined for landfills has not been studied enough, this work aims to be one of the first approaches to the catalytic pyrolysis of mixed non-recyclable post-consumer plastic waste collected from municipal solid waste. Two commercial zeolites, HZSM and HY, were modified with two transition metals (Ni and Co). The presence of the metals was analyzed in terms of the effect produced by the product yields and, specifically, the composition of the liquid product.

## 6.2. Results and discussion

### 6.2.1. Characterization of the catalytic materials

Figure 6.1 illustrates the diffractograms of the thermally treated HY and HZSM-5 zeolites before and after the incorporation of Ni and Co oxides onto their surfaces. HY reference shows representative peaks at  $2\theta$  equal to  $6.39^\circ$ ,  $23.71^\circ$  and  $15.76^\circ$  [31], which are also detected in both Co- and Ni-modified samples. On the other hand, the HZSM-5-samples (references and metal-containing structures) exhibit the typical diffraction peaks of ZSM-5 zeolite at  $2\theta$  equal to  $7.9^\circ$ ,  $8.8^\circ$ ,  $23.1^\circ$  and  $23.8^\circ$  [32]. Incorporating 5% of Ni or Co did not alter the diffraction pattern, which

can be associated with the maintenance of the zeolitic structure after the incorporation of the metallic components. In the case of Ni addition, tiny peaks regarding the NiO refraction [33] were registered. Moreover, if the crystal size of the zeolites modified with Ni is analyzed, see values in Table 6.1, no change in the crystal size of the zeolites was achieved. Both evidence suggest Ni's presence as bulk NiO deposited on the zeolite's structure. However, a very different behavior was registered for the modification with Co. No contributions associated with the presence of oxidized Co species were detected. Considering the synthetic protocol used to prepare the metal-containing samples, it is expected that a significant number of Co-related species are forming  $\text{Co}_2\text{O}_3$ . However, despite the relatively low concentration of the minor metal oxide counterpart and its possible introduction in the porous structure of the support (HY and HZSM5) could be the main reason for the missing  $\text{Co}_2\text{O}_3$  XRD contributions, the possibility that Co-entities may have been exchanged in certain positions of the zeolitic structure is not discarded [34,35]. Further, the crystal size was raised in the case of Co addition, see Table 6.1, supporting the plausible metal incorporation in the zeolitic lattice as reported in the literature [36].

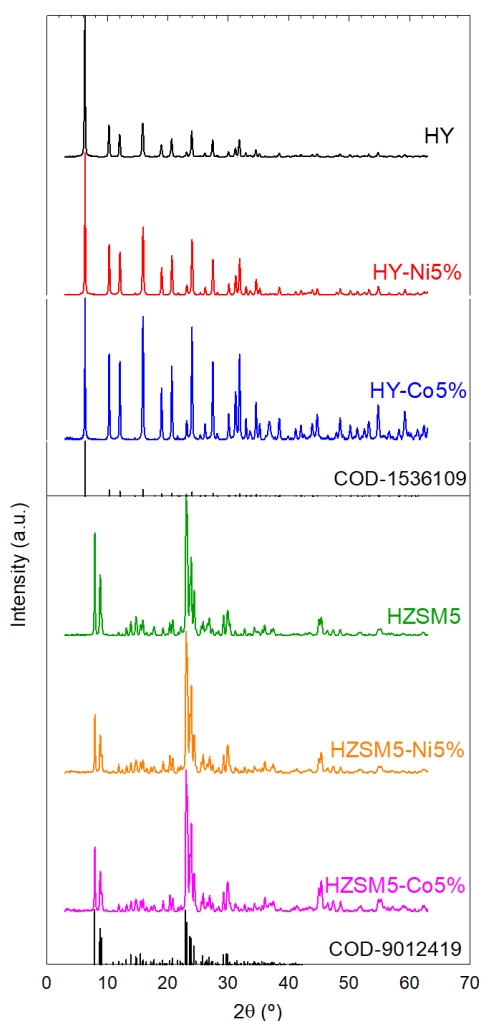


**Figure 6.1.** XRD patterns of the bare and metal-impregnated zeolites

A complete analysis of the chemical environment of the developed structures has been carried out using means of X-ray photoelectron spectroscopy. Figure 6.2A–G shows the Ni2p, Co2p, Si2p, Al2p, and O1s regions of both pure zeolites support (HY and HZSM5) and Co- and Ni-containing catalysts, respectively. Figure 6.2A shows typical spectra of well-studied NiO materials, with the Ni2p<sub>3/2</sub> and Ni2p<sub>1/2</sub> contributions (~854 eV and ~872 eV) and its satellites (862 eV and 879 eV) [37,38]. Although the electronic structure is complex (similar situation for Co-oxide) and a strict fit must include a multitude of contributions (i.e., form 3d<sup>8</sup> multiplet structure), a minimum of four contributions for each 2p (3/2 and 1/2) should be used to reproduce the experimental spectrum (Figure 6.2F). Although the structure is analyzed in terms of simplified modeling, the analysis of Figure 6.2F allows the identification of the existence of NiO with a reference peak at ~854 eV (ascribed to local screening from lattice oxygen). The Co2p data of the catalytic samples describes spectra with profiles that have been previously associated with the presence of Co<sub>3</sub>O<sub>4</sub> (Figure 6.2B). Although the variation in the position of the main contributions for the CoO and Co<sub>2</sub>O<sub>3</sub> species is small, which makes it difficult to make a strict characterization of the structure, the existence of the regions associated with satellites (e.g., ~788 eV) with relatively lower intensity (as detected in the materials studied) is commonly related to the dominant existence of the Co<sub>2</sub>O<sub>3</sub> structure [39,40], which is in addition favored by the synthesis conditions. On the other hand, although the O1s region is clearly dominated by the majority aluminium–silicate structure (~532.4 eV), in the samples with the highest concentration of metal oxides (5%Ni-samples and 5%Co-samples), a pronounced shoulder at lower binding energies (~530 eV) is detected, which are related with metal-O bonds [39]. The regions presented in Figure 6.2D,E, Si2p, and Al2p identify the zeolitic supports used [41].

Table 6.1 shows the characterization of the bare and metal-impregnated zeolites analyzed using N<sub>2</sub> adsorption–desorption isotherms. Figure 6.2 depicts the isotherms obtained and the mesopore size distribution. Regarding the IUPAC classification of physisorption isotherms, the prepared materials could be classified as type IV with capillary condensation hysteresis loops of type H4 [42]. The micropore ratio, understood as micropore volume concerning the total volume ( $V_{MP}/V_T$ ), was very similar in both zeolites before metal incorporation. Although incorporating metallic particles decreased the surface area, the  $V_{MP}/V_T$  was kept without significant alteration, ranging in values within 61–63%. Adding 5% of metal to HZSM-5 supposes an exception as a certain decrease in the microporosity was observed, i.e.,  $V_{MP}/V_T \sim 57\%$ . Further, certain differences in pore distribution were observed concerning the base materials, as depicted in Figure 6.3B,D, probably due to a dealumination effect promoted by the thermal treatment after the impregnation step [43].



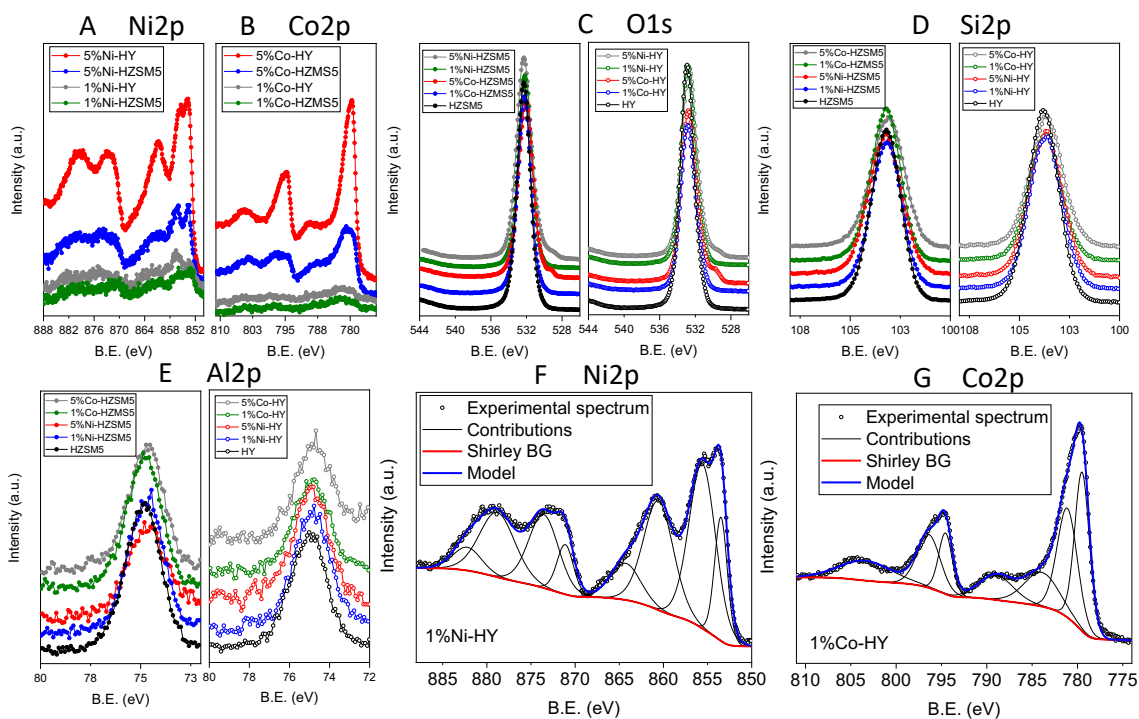


**Figure 6.2.** XPS spectra of references and metal-containing catalytic samples. (A) Ni2p region, (B) Co2p region, (C) O1s, (D) Si2p, (E) Al2p, (F) curve-resolved XPS Ni2p region and (G) Co2p regions for 5%-metal and HY zeolite support.

**Table 6.1.** Textural characteristics of the native and metal-impregnated zeolite catalysts.

Catalyst	L (nm)	$S_{\text{BET}}$ (m <sup>2</sup> /g)	$S_{\text{MP}}$ (m <sup>2</sup> /g)	$V_{\text{T}}$ (cm <sup>3</sup> /g)	$V_{\text{MP}}$ (cm <sup>3</sup> /g)	$V_{\text{MP}}/V_{\text{T}}$ (%)	$D_{\text{ave}}$ (Å)	Total acidity (μmol/g)
HY	51.91	1384	1274	0.705	0.432	61.3	50.5	576
1%Co-HY	-	1044	961	0.521	0.326	62.6	55.5	709
5%Co-HY	59.38	959	884	0.476	0.300	63.0	54.9	728
1%Ni-HY	-	1022	943	0.511	0.320	62.6	56.6	768
5%Ni-HY	51.91	974	893	0.494	0.304	61.5	54.0	836
HZSM5	47.03	488	440	0.241	0.149	61.8	31.4	1045
1%Co-HZSM5	-	472	423	0.230	0.143	62.2	40.2	1300
5%Co-HZSM5	52.90	432	388	0.230	0.131	56.9	41.0	1302
1%Ni-HZSM5	-	469	422	0.230	0.142	61.7	32.7	1383
5%Ni-HZSM5	47.02	413	368	0.215	0.124	57.7	36.4	1509

L: crystal size obtained from the highest XRD peak with Scherrer equation;  $S_{\text{BET}}$ : total specific surface area by BET method;  $S_{\text{MP}}$ : micropore surface area by t-plot method;  $V_{\text{T}}$ : total pore volume from N<sub>2</sub> uptake at p/p~0.99;  $V_{\text{MP}}$ : volume of micropores from t-plot method;  $D_{\text{ave}}$  average mesopore width by BJH method

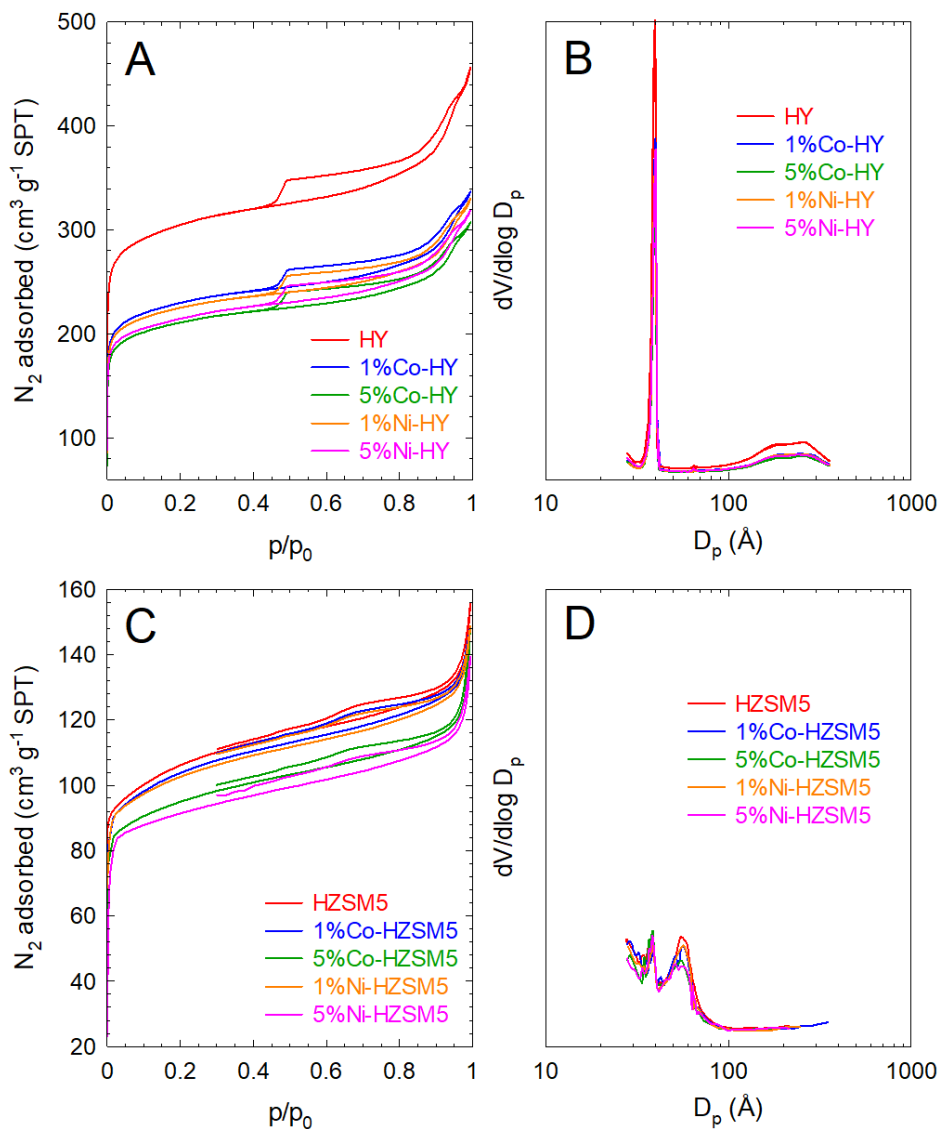


**Figure 6.3.** N<sub>2</sub> adsorption-desorption isotherms of impregnated HY (A) and HZSM5 (C) catalysts and the pore width distribution of metal-impregnated zeolites HY (B) and HZSM5 (D).

Figure 6.4 provides the NH<sub>3</sub>-TPD of the prepared material that was carried out to assess the total acidity and acid strength distribution of the bare and metal-impregnated zeolites. The metallic surface area and dispersion for those impregnated with metals are also shown. Compared to the native zeolites, the impregnation of the commercial zeolites had a low effect on the porosity properties of the materials. However, the incorporation of the metals implied some important modifications in the strength distribution of the acidity by adding a third peak. According to their TPD profiles, peaks among 434–481 °C and 535–600 °C would be considered strong acid centers accounting also for metal/zeolite interaction, while the lowest-temperature peaks (around 183–222 °C and 336–377 °C) can be labeled as weak and medium acidic sites [44,45].

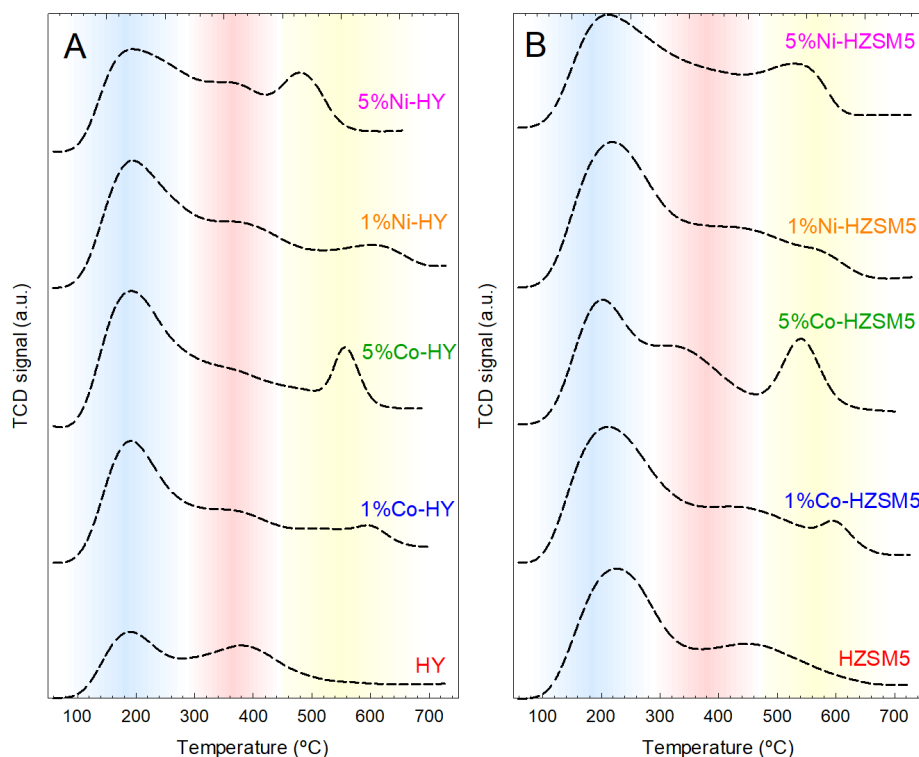


**Figure 6.4.** Thermal Programmed Desorption (TPD) of metal impregnated onto zeolites HY (A) and HZSM5 (B)

## 6.2.2. Catalytic performance of the metal-impregnated zeolites

### 6.2.2.1. Effect on product yields and the functional groups of the liquid product

As can be seen in Table 6.2, the HY and HZSM5 provide a gas, liquid, and char fraction (%wt.) of  $58.1 \pm 2.2$ ,  $35.0 \pm 2.2$  and  $6.9 \pm 0.6$ , and  $58.3 \pm 2.7$ ,  $34.3 \pm 2.7$  and  $7.5 \pm 0.6$ , respectively. Compared to the native zeolites, the metal-impregnated zeolites showed a small decrease in gas production ( $\sim 50\%$ wt.) and increased liquid yield (42%wt.). This observation was especially evident for tests with metal-impregnated zeolite HY materials, which presented an average enhancement factor for the liquid fraction of 1.22. On the other hand, the gas fraction for metal-modified HY materials was 1.1. These factors were less pronounced for the samples that contain the HZSM5 support as the majority component, in which values of 1.1 (enhancement factor for the liquid fraction) and 1.05 (reduction factor for the gas fraction) were obtained. The char fraction showed negligible differences for zeolite references (HY and HZSM5) and metal-modified materials, with values ranging between 6.6 and 7.2 5%wt. The final Coke/Catalyst ratio, expressed also in %wt., was usually below 6.5% and 3% for HY- and HZSM5-related samples. Other researchers, such as Razzaq et al. (2019), previously informed us of their investigation of using metal-impregnated HZSM-5 in the co-pyrolysis of polystyrene and wheat straw [46]. Regarding the carbon

deposition, expressed as the mass of coke relative to the total mass of the recovered catalyst after pyrolysis, no valuable influence was monitored. In most of the experiments, an increase was detected; in other cases, a small reduction was observed. Certain reactions between compounds of pyrolytic vapors, such as dehydrogenation or polymerization, can cause the deposition of coke, which causes the deactivation of catalysts [47,48].

**Table 6.2.** Product distribution expressed as %wt. and carbon deposition (coke development) on the catalytic pyrolysis of a real mixture of post-consumer plastic waste.

Catalyst	Coke/Catalyst (%wt.)	Gas (%wt.)	Liquid (%wt.)	Char (%wt.)
HY	4.4±0.4	58.1±1.8	35.0±2.2	6.9±0.6
1%Co-HY	6.2±0.6	50.9±2.6	41.0±2.6	6.6±0.5
5%Co-HY	4.1±0.5	50.2±2.5	43.1±2.5	6.6±0.6
1%Ni-HY	4.2±0.4	51.9±2.0	41.3±2.0	6.8±0.5
5%Ni-HY	4.1±0.4	49.6±2.4	43.2±2.4	7.2±0.7
HZSM5	1.3±0.3	58.3±2.7	34.3±2.0	7.5±0.6
1%Co-HZSM5	2.0±0.4	53.6±2.0	39.3±2.0	7.2±0.7
5%Co-HZSM5	2.0±0.4	57.1±2.6	38.5±2.6	6.9±0.5
1%Ni-HZSM5	2.2±0.5	57.2±1.8	38.3±1.8	6.7±0.5
5%Ni-HZSM5	1.5±0.2	53.2±2.6	39.8±2.6	7.0±0.7

By obtaining high liquid product yields in pyrolysis, a reduction in the dependency on fossil fuels can be achieved since the process can provide an alternative source of energy by converting plastic waste into valuable fuels obtained from pyrolysis oil, which can be used as a substitute for conventional fossil fuels. On the other hand, low liquid product yields may result in a less economically viable solution.

Other authors like Akubo et al. [49] or Razzaq et al. [46] reported similar results in their investigations about the catalytic pyrolysis of different types of plastics over metal-impregnated zeolite catalysts. For example, Akubo et al. [49] investigated the catalytic cracking of the vapors produced by the high-density polyethylene (HDPE) pyrolysis over Y zeolite impregnated with Ni at 600 °C for 30 min in a two-stage reactor. The authors only reported small differences in oil and gas yields compared to the native Y zeolite. However, these researchers obtained a significant increase in carbon deposition on the metal-Y-zeolite catalyst. Additionally, Razzaq et al. [46] indicated increased liquid product yield when wheat straw and polystyrene (PS) were co-pyrolyzed in a fixed bed reactor using metal-impregnated HZSM5 zeolite.

Regarding the functional group analysis of the liquid products, Figure 6.5 shows the results of FTIR spectra of all liquid products. It is expected that the liquid fraction will be a heterogeneous mixture with a multitude of components, which makes its identification relatively complicated. In fact, the spectra obtained using FTIR showed no appreciable differences between samples. In general, it is possible to identify functional groups at  $2850$  and  $3000\text{ cm}^{-1}$  which corresponds to C-H stretch of diverse saturated and unsaturated aliphatic and aromatic compounds; contribution around at  $1650\text{ cm}^{-1}$ , C=C stretch of alkenes; at  $1495\text{ cm}^{-1}$ , C=C stretch in the ring of aromatic compounds; at  $1375\text{ cm}^{-1}$ , C-H asymmetric of alkanes; at  $1075$ ,  $1067$  and  $1056\text{ cm}^{-1}$ . C-O bond stretch associated with the existence of carboxylic groups or esters and C-H in-plane of aromatics; at  $885$  and  $775\text{ cm}^{-1}$ ,  $\text{CH}_2$  out-of-plane of alkenes and C-H out-of-plane of alkenes; and at  $695\text{ cm}^{-1}$ , C-H out-of-plane of aromatics were detected as well [50]. Differences between samples are discussed in terms of fuel fractions of interest (e.g., gasoline, LCO, etc.), where various component compounds are grouped using simulated distillation as described below. This chromatographic approach allows for effective identification with better applicability, considering that it identifies fuel fractions that dominate the current energy sector.

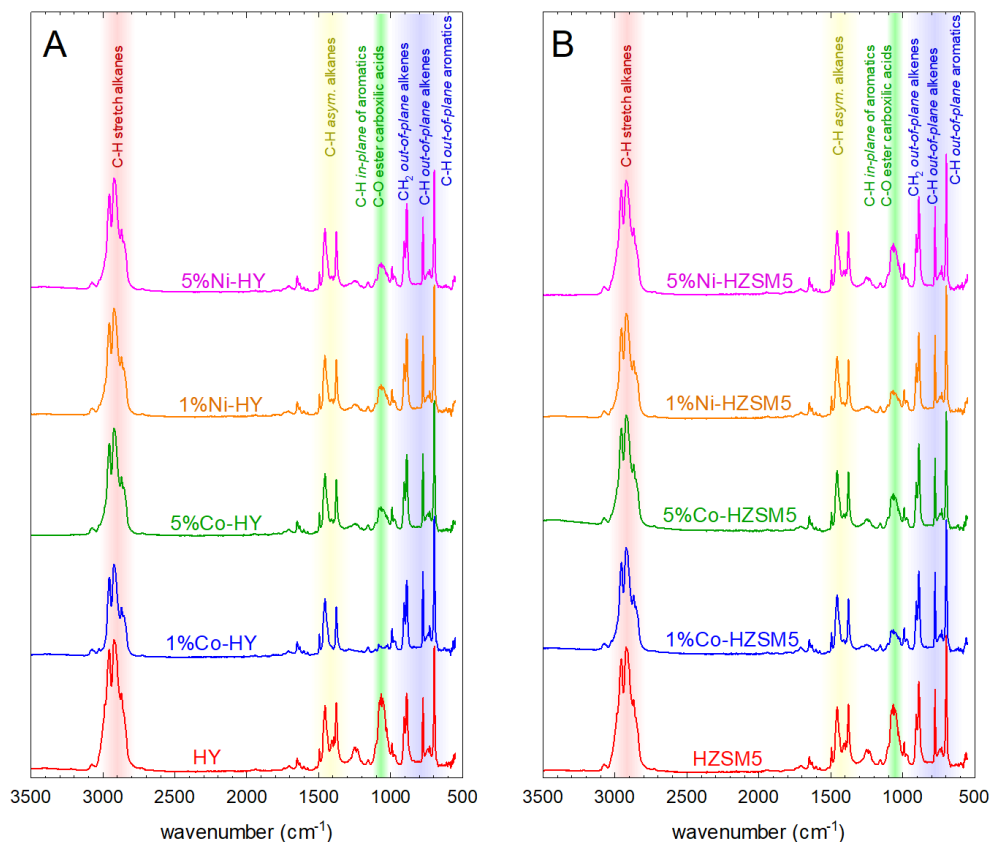


**Figure 6.5.** FTIR spectra of the liquid products obtained from catalytic pyrolysis of the mixture of post-consumer plastic waste using metal-impregnated HY (A) and HZSM5 (B) catalysts.

### 6.2.2.2. Effect on simulated distillation boiling points of the liquid product

The simulated distillation curves of the liquid product obtained from the thermal and catalytic pyrolysis of the mixture of post-consumer plastic waste are shown in Figure 6.6.

Although the differences between the curves are minimal, the detailed examination of Figure 6.6A suggests that impregnation with metals of HY zeolite generally reduced the boiling temperatures of the components of the liquid product compared to the catalytic pyrolysis over native zeolite. Conversely, no significant changes are observed in the boiling point distributions of liquids derived from native HZSM5 and metal-impregnated HZSM5 materials (Figure 6.6B).

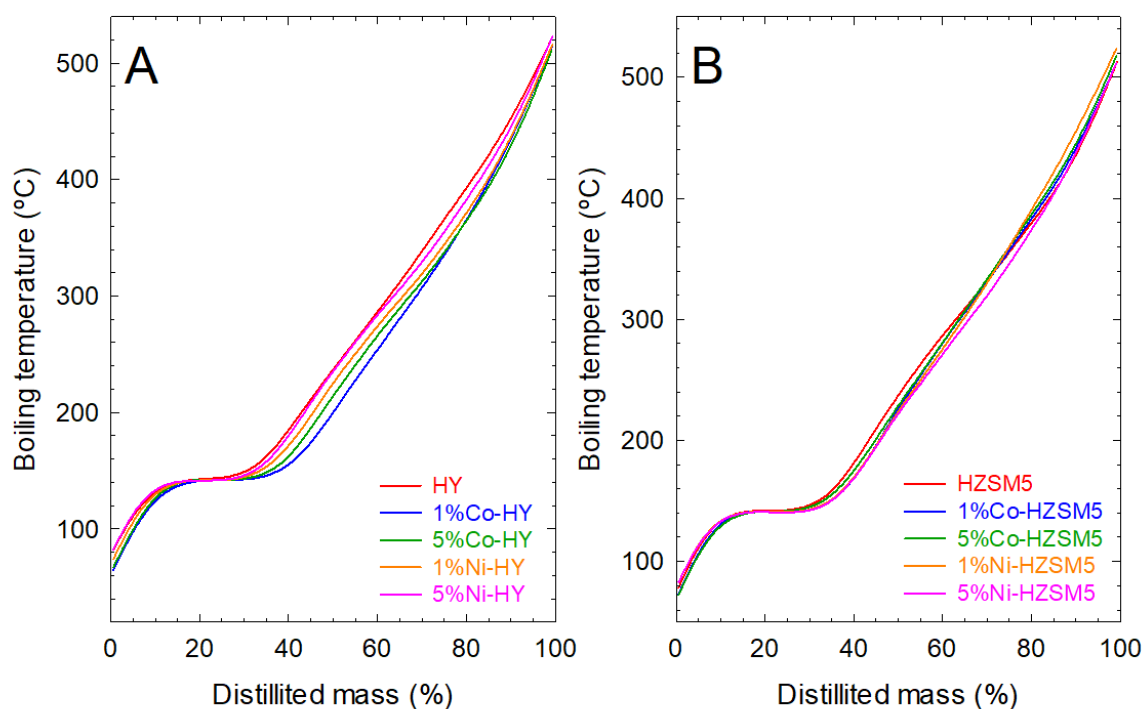


**Figure 6.6.** Simulation distillation curves of the liquid fraction obtained from the catalytic pyrolysis of a mixture of plastic waste with metal-impregnated onto zeolites HY (A) and HZSM5 (B).

Tables 6.3 and 6.4 report the weight percentage of common fractions in pyrolysis oil obtained from catalytic pyrolysis over native and metal-impregnated zeolites. The predominant product of all liquids was the gasoline-range product, with total mass percentages between 44.28% and 50.29%. Additionally, most of the gasoline was mid-naphtha, with percentage values ranging from 30.75% to 36.36%. In our previous work [51], the oil liquid from the thermal pyrolysis (without any catalytic material) of the same mixture of plastic waste had a distribution of 47.7% gasoline, 22.1% LCO, and 30.2% HCO. In general, it is a more liquid product richer in heavy compounds, at least in HCO-range products.

The presence of cobalt in the HY catalyst seems to slightly increase the amount of light and mid-naphtha. On the contrary, impregnation with cobalt decreases the yield of products in the HCO range. The presence of Ni in the HY catalysts has a similar, but even less measurable, effect. In the case of the HZSM5 catalyst, the presence of metals has practically no effect on the percentage of the fractions. The results of the simulation distillation curves obtained with the zeolite impregnated with metals are very similar to those found with the catalyst without metal, and variations can be attributed to the accuracy of determining such values.

However, although the composition of the liquid fraction obtained from the catalytic pyrolysis of the mixture of plastic waste did not show remarkable differences in the function of the zeolite used (native or metal-impregnated), the total production of liquid compounds changed due to the differences in liquid product yields obtained.

**Table 6.3.** Weight percentage of common fractions in pyrolysis oil obtained from catalytic pyrolysis over native and metal-impregnated HY zeolite.

Products	Fraction	HY	1%Co-HY	5%Co-HY	1%Ni-HY	5%Ni-HY
Gasoline	Light Naphtha	1.7±0.4	3.4±0.2	3.1±0.3	2.5±0.2	1.7±0.4
	Mid Naphtha	30.8±2.5	36.4±2.0	34.5±2.3	33.1±2.5	32.3±2.0
	Heavy Naphtha	11.8±0.9	10.6±1.0	10.6±0.8	11.1±1.1	11.2±1.0
	<b>Total</b>	44.3±2.5	50.3±2.0	48.3±2.3	46.7±2.5	45.2±2.0
LCO	Light Gas Oil	9.8±0.7	9.6±0.6	9.8±0.5	9.9±0.9	9.8±0.8
	Mid Gas Oil	9.2±0.4	9.2±0.7	9.9±0.5	9.9±0.7	9.6±0.7
	Heavy Gas Oil	10.3±0.8	9.5±0.6	11.2±1.1	11.3±1.4	11.2±0.9
	<b>Total</b>	29.3±0.8	28.2±0.7	30.9±1.1	31.1±1.4	30.6±0.9
HCO	Light Vacuum Gas Oil	12.0±0.9	9.3±0.5	10.1±0.8	10.8±0.8	11.9±1.0
	Mid Vacuum Gas Oil	7.2±0.5	5.7±0.6	5.2±0.3	5.5±0.5	6.1±0.5
	Heavy Vacuum Gas Oil	7.2±0.3	6.5±0.4	5.6±0.4	5.9±0.5	6.2±0.3
	<b>Total</b>	26.4±0.9	21.5±0.6	20.8±0.8	22.2±0.8	24.2±1.0

Table 6.5 reports the yields of the different types of products obtained from the catalytic pyrolysis over the different catalytic materials studied in this work, evaluated as g by kg of plastic waste. The major yield was observed for the gasoline-range product in oils from catalytic pyrolysis over metal-impregnated zeolites, with values ranging between 179.4 and 208.3 g by kg of plastic waste. Lower gasoline production, 155.1 and 153.2 g by kg of plastic, was observed in liquid oil from the catalytic pyrolysis over native zeolite HY and HZSM-5, respectively. If the results of Table 6.5 are compared to those of thermal pyrolysis (240.4 g by kg of plastic for gasoline, 111.4 g by kg of plastic for LCO-range product, and 152.2 g by kg of plastic for HCO-range product), a lower production of gasoline and HCO products was observed [51].

**Table 6.4.** Weight percentage of common fractions in pyrolysis oil obtained from catalytic pyrolysis over native and metal-impregnated HZSM5 zeolite.

Products	Fraction	HZSM5	1%Co-HZSM5	5%Co-HZSM5	1%Ni-HZSM5	5%Ni-HZSM5
Gasoline	Light Naphtha	2.0±0.4	2.5±0.3	2.9±0.3	1.7±0.2	1.7±0.3
	Mid Naphtha	31.9±2.3	34.0±2.7	34.7±2.6	34.8±2.4	34.9±2.2
	Heavy Naphtha	10.8±0.9	10.0±1.0	10.6±1.1	10.6±0.8	10.6±0.7
	<b>Total</b>	44.7±2.3	46.5±2.7	48.2±2.6	47.1±2.4	47.2±2.2
LCO	Light Gas Oil	9.5±0.7	9.0±0.7	9.0±0.9	9.3±0.7	9.6±0.9
	Mid Gas Oil	9.6±0.8	8.9±0.6	9.0±0.8	8.7±0.6	9.5±0.7
	Heavy Gas Oil	12.2±1.1	10.8±0.9	10.3±0.8	9.4±0.9	10.8±0.8
	<b>Total</b>	31.3±1.1	28.7±0.9	28.3±0.9	27.4±0.9	29.9±0.9
HCO	Light Vacuum Gas Oil	12.8±1.2	12.2±1.1	11.7±0.9	10.9±1.1	10.9±0.6
	Mid Vacuum Gas Oil	5.6±0.4	6.4±0.5	5.8±0.6	7.1±0.4	5.8±0.6
	Heavy Vacuum Gas Oil	5.6±0.3	6.2±0.4	6.0±0.5	7.5±0.8	6.1±0.7
	<b>Total</b>	24.0±1.2	24.8±1.1	23.5±0.9	25.5±1.1	22.9±0.7

**Table 6.5.** Gasoline, LCO, and HCO product yields (data in g by kg of plastics waste) obtained from catalytic pyrolysis over native and metal-impregnated zeolites.

Catalyst	Gasoline	LCO	HCO
HY	155.1±8.8	102.7±5.3	92.5±4.8
1%Co-HY	203.4±13.0	120.0±7.6	86.9±5.5
5%Co-HY	208.2±12.0	133.3±7.7	89.8±5.2
1%Ni-HY	192.8±10.0	128.6±6.2	91.6±4.4
5%Ni-HY	202.5±11.0	132.1±7.3	97.8±5.4
HZSM5	153.2±8.9	107.2±6.3	82.3±4.8
1%Co-HZSM5	182.7±11.0	112.9±5.7	97.3±5.0
5%Co-HZSM5	185.4±13.0	109.0±7.4	90.6±6.1
1%Ni-HZSM5	180.0±9.2	111.5±5.2	92.0±4.3
5%Ni-HZSM5	188.0±12.0	119.3±7.8	91.0±6.0

**Figure 6.7** shows the relationship between gasoline, LCO, and HCO products yields (data in g by kg of plastics waste) and absolute acidity ( $\text{Acidity}/S_{\text{BET}}$ ,  $\mu\text{mol NH}_3/\text{m}^2$ ) obtained from catalytic pyrolysis over native and metal-impregnated zeolites.

According to the obtained data, there is no clear relation between  $S_{\text{BET}}$  and the obtained fraction (data not analyzed). However, the acidity properties seem to be relevant to producing liquid fractions, which can be grouped as fractions with LCO and/or gasoline properties. Further, such correlation is expressed as acidity normalized by the superficial area, providing the data presented in Figure 6.7, which considers that the interaction occurs on the active catalytic surface by interaction with the metal-support active sites. The observable ( $\text{acidity}/S_{\text{BET}}$ ) ratio allows for



the analysis of both morphologic and acidity (two of the main properties of aluminum-silicate materials) as a combined factor and its influence on the catalytic response of the catalyst. With this approach, it is possible to identify the influence of the acidity normalized by the surface area (observable acidity/ $S_{\text{BET}}$ ), which is related to the availability of active sites for selective production of interest fractions like gasoline. Concerning the acidity/ $S_{\text{BET}}$  ratio, the rise of metal concentration increased for HY and HZSM-5 zeolites; HY with Ni augmented from 80% up to 106% and with Co from 63% to 82% while HZSM5 with Ni rushed from 38% to 71% and 27% up to 41% with Co. An increase in gasoline production was observed when metal was introduced into the zeolites. The higher the amount of metal in the zeolite, the higher the absolute acidity and the higher the gasoline production. This result is less pronounced in the production of the LCO fraction, which increases to a lesser extent with the introduction of the metal and the increase in absolute acidity for the HY catalyst. In contrast, for the HZSM-5 catalyst, there is practically no variation. Additionally, the data in Figure 6.7 suggests that no influence of impregnation with cobalt or nickel was detected in the production of HCO. In any case, and although understanding the behavior of catalysts under reaction conditions during the production of a specific fraction is complex, the data presented in Figure 6.7 suggest that the improvement in the lightest fractions (mainly gasoline) is associated with the increase in the value of the combined parameter here defined as Acidity/ $S_{\text{BET}}$ .

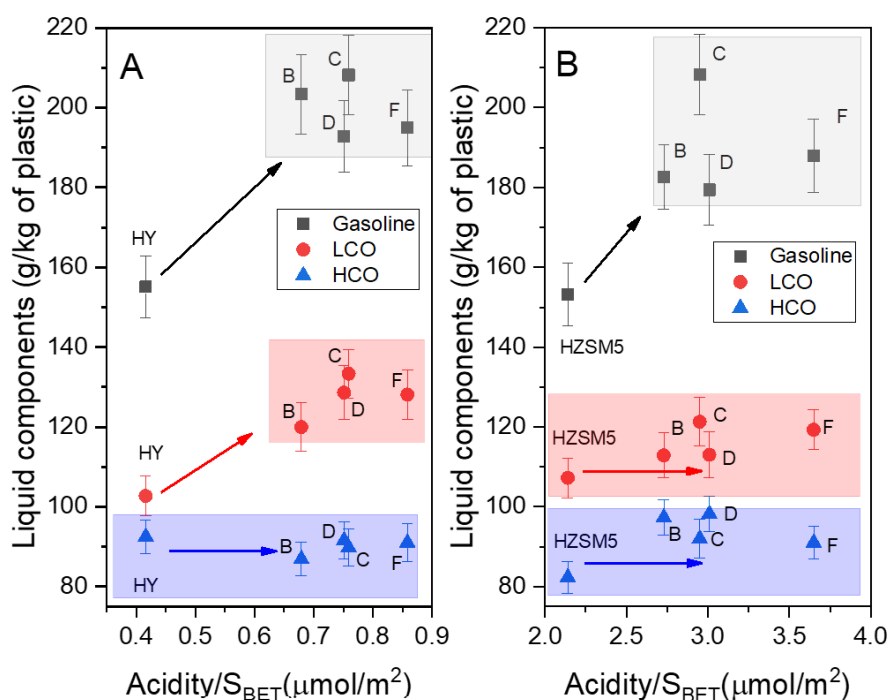


**Figure 6.7.** Relationship between gasoline, LCO, and HCO products yields (data in g by kg of plastics waste) and  $\text{Acidity}/S_{\text{BET}}$  ( $\mu\text{mol}/\text{m}^2$ ) obtained from catalytic pyrolysis over native and metal-impregnated zeolites. B: 1%Co-HY or 1Co-HZSM5, C: 1%Ni-HY or 1%Ni-HZSM5, D: 5%Co-HY or 5%Co-HZSM5 and F: 5%Ni-HY or 5%Ni-HZSM5.

The composition of the gasoline-like fractions of liquid products is summarized in Table 6.6. The gasoline fraction contained paraffins, naphthenics, and aromatic hydrocarbons. There were no considerable differences in the composition of the gasoline fraction obtained over several metal-impregnated zeolites. Only a slight increase in naphthenic content and a slight decrease in aromatics were noticed when metal-impregnated HZSM-5 zeolites were used as catalysts. Therefore, incorporating metal (cobalt or nickel) generated insignificant changes in the performance of commercial HY and HZSM-5 zeolites concerning gasoline liquid composition. Other authors studying the pyrolysis of plastics and biomass over different catalysts found similar results regarding the addition of promoter cobalt and nickel as promoter metals onto zeolite catalysts [49,52,53]. However, other researchers reported that loading a certain amount of metal onto the zeolites and activated carbons gave more aromatics content than metal-free catalysts [11,20,22,28].

**Table 6.6.** Composition of the gasoline product obtained from catalytic pyrolysis over native and metal-impregnated zeolites.

Catalyst	Paraffins, %	Naphthenics, %			Alkylbenzenes	Aromatics, %		
		Monocycloparaffins	Dicycloparaffins	Total		Indan or tetralins	Naphthalenes	Total
HY	19.2±1.2	19.9±1.2	29.1±2.4	49.3±2.4	22.1±1.6	7.8±1.4	1.6±0.5	31.5±1.6
1%Co-HY	18.1±2.0	19.7±1.7	30.0±1.9	49.7±1.9	22.3±2.2	8.1±1.0	1.8±1.0	32.2±2.2
5%Co-HY	19.8±1.9	18.8±1.4	25.8±1.9	44.6±1.9	24.0±2.0	10.2±0.8	1.4±0.4	35.6±2.0
1%Ni-HY	19.2±1.2	20.1±0.9	30.0±2.1	50.1±2.1	20.7±1.5	8.2±1.2	1.8±0.6	30.7±1.5
5%Ni-HY	19.4±2.4	20.5±2.0	27.5±1.4	48.0±2.0	23.2±1.6	8.01±0.6	1.4±0.5	32.6±1.6
HZSM5	19.4±2.1	20.4±2.2	25.3±2.3	45.6±2.3	26.3±1.0	8.2±1.1	0.5±0.2	35.0±1.1
1%Co-HZSM5	20.5±1.5	19.8±3.1	27.0±1.9	46.8±3.1	22.5±3.4	8.8±0.6	1.3±0.5	32.7±3.4
5%Co-HZSM5	20.3±2.5	21.1±1.8	30.0±3.4	51.2±3.4	20.3±1.9	7.2±0.7	1.1±0.4	28.6±1.9
1%Ni-HZSM5	19.2±3.0	20.9±2.9	29.6±4.4	50.5±4.4	20.9±2.3	7.8±0.8	1.7±0.6	30.3±2.3
5%Ni-HZSM5	18.7±1.9	20.8±1.0	29.1±1.6	49.9±1.6	22.1±3.1	8.1±1.2	1.3±0.3	31.4±3.1

## 6.3. Materials and methods

### 6.3.1. Raw material

The mixture of plastic waste used in this study came from the rejected plastic fraction obtained from the solid urban waste treatment plant in Granada (Spain). The average composition of the plastic mixture was as follows: 56.10% of polypropylene (PP), 10.05% of expanded polystyrene (EPS), 8.55% of high impact polystyrene (HIPS), 12.65% of polypropylene film (PP film), and 12.65% of films of different polymer materials (non-PP film). Detailed information about the raw material and its characterization can be found in our previous work [51].

### 6.3.2. Preparation and characterization of the catalysts

The commercial zeolites used in this work were HZSM-5 ammonium zeolite ( $\text{SiO}_2/\text{Al}_2\text{O}_3$  molar ratio, 30) and hydrogen Y-zeolite ( $\text{SiO}_2/\text{Al}_2\text{O}_3$  molar ratio, 5.2) provided using Alfa Aesar ©, Massachusetts, United States.

For mechanical properties stabilization, the generation of the active phase, and the definition of a pore distribution size [54], the purchased zeolites were first calcined for 3.5 h at 550 °C using a tubular furnace of Nabertherm (L 3/11/B180 Model, Nabertherm, Lilienthal, Alemania) under an air atmosphere. Then, the zeolites were impregnated using the incipient wetness method, which involves adding a liquid solution to the solid sample until the first signs of wetting are observed. We used aqueous solutions of  $\text{Ni}(\text{NO}_3)_2$  and  $\text{Co}(\text{NO}_3)_2 \cdot 6\text{H}_2\text{O}$  salts to get a loading of 1% and 5% (wt.), typical concentration values of the minor components (metallic-related species) in the final catalyst. This method was chosen to achieve uniform distribution of the active component. Finally, to promote the formation of crystalline metal oxides, after the impregnation step, the catalytic materials were dried for 24 h at 80 °C and activated by calcination for 3.5 h at 550 °C under an air atmosphere [54].

The crystalline structure of the metal-impregnated zeolites was assessed using X-ray diffraction (XRD) technique in a Bruker D8 Discover device (Bruker, Massachusetts, Estados Unidos) equipped with a Pilatus3R 100K-A detector working with radiation of  $\text{Cu K}\alpha$  ( $\lambda = 1.5406 \text{ \AA}$ ). The diffractograms were recorded in  $2\theta$  within 3 and 80° (0.02° per step, 30 s per step). The software QualX2.0® was used to process the diffractograms, and the estimation of the peak properties for the quantification of the crystal size was realized using the Scherrer equation [55]. The Crystal Open Database (COD) was used for the crystal phase identification of the zeolites.

X-ray Photoelectron Spectroscopy (XPS) was applied for the study of the surface of the materials in a Kratos AXIS UltraDLD device (Kratos Analytical, Manchester, United Kingdom) working with an X-ray source from Al K $\alpha$ . CASAXPS (version 2.3.15) software was used for the analysis. The spectra were referenced to the C1s peak (284.6 eV).

The textural properties were analyzed using N<sub>2</sub> physisorption. The N<sub>2</sub> adsorption–desorption isotherms at –196 °C were conducted in an ASAP<sup>®</sup> 2429 instrument from Micromeritics<sup>®</sup> (Micromeritics Instrument Corporation, Georgia, United States). Samples were previously outgassed at 150 °C under vacuum overnight. The total surface area ( $S_{\text{BET}}$ ) was determined using the standardized Brunauer-Emmett-Teller (BET) method. The total pore volume ( $V_{\text{T}}$ ) was calculated from the N<sub>2</sub> adsorption uptake at  $p/p_0 \sim 0.99$ . The t-plot method was used to quantify the contribution of micropores on the surface ( $S_{\text{MP}}$ ) and volume ( $V_{\text{MP}}$ ). The Barrett, Joyner, and Halenda (BJH) method was applied to obtain the pore width ( $D_{\text{p}}$ ) distribution and the average  $4V/A$  value ( $D_{\text{ave}}$ ) of mesopores.

The surface acidity was analyzed using chemisorption by ammonia Temperature Programmed Desorption (TPD) in an AutoChem II 2920 analyzer from Micromeritics<sup>®</sup>, equipped with Thermal Conductivity Detector (TCD). Before chemisorption, the samples were pretreated at 450 °C under He atmosphere for 1 h and cooled to room temperature. The NH<sub>3</sub>-TPD analysis was carried out using 50 mL min<sup>-1</sup> of 10% of NH<sub>3</sub> in He mixture from room temperature up to 800 °C with a rate of 30 °C min<sup>-1</sup>.

### 6.3.3. Pyrolysis reactor and pyrolysis conditions

The pyrolysis experiments were carried out on a tubular horizontal reactor made of stainless steel 316 (internal diameter: 4 cm and length: 43.25 cm) inserted in a Nabertherm R 50/250/12 model furnace. A flowmeter and a chiller were integrated to regulate the nitrogen flow and condense the final vapors. Figure 6.8 provides a scheme of the experimental setup.

About 20 g of sample was placed in a closed tubular vessel (internal diameter: 27.25 mm and length: 30.6 cm) made of stainless steel and approximately 1 g of catalytic material into a basket at the radiant zone end of the reactor, then heated to up to 500 °C at a rate of 10 °C/min, optimum conditions for maximizing the liquid yield, according to previous work [56]. Finally, the temperature was maintained for 60 min with a constant flow of 0.8 L/min N<sub>2</sub>. After that, the furnace was cooled to room temperature under a permanent N<sub>2</sub> purge of 0.2 L/min. The condensate product was collected in a glass vessel submerged in a cooling bath at –7 °C. The tubular vessel, basket, and condenser were weighed before and after each pyrolysis experiment.

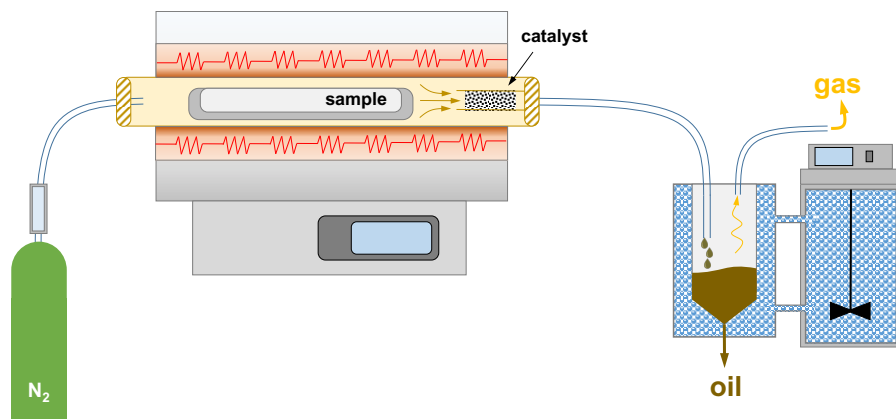


**Figure 6.8.** Graphical representation of the experimental equipment used for the catalytic pyrolysis tests.

The solid, liquid, and gas product yields were calculated according to the following equations:

$$\eta_l = \frac{m_l}{m_m} \cdot 100 \quad (6.1)$$

$$\eta_s = \frac{m_s}{m_m} \cdot 100 \quad (6.2)$$

$$\eta_g = 100 - (\eta_l + \eta_s) \quad (6.3)$$

where the weights are represented by  $m_m$ ,  $m_l$ , and  $m_s$  correspond to the mass of the total plastic sample, liquid, and solid products, respectively, and the yields of liquid, solid, and gas are indicated by  $\eta_l$ ,  $\eta_s$  and  $\eta_g$ , respectively. All experiments were carried out in triplicate, and a relative standard deviation was provided.

The determination of deposited carbon onto the catalysts, namely coke, was carried out from the recovered catalyst after the pyrolysis tests. A two-stage thermal decomposition was programmed over 20 mg of spent catalyst in a PerkinElmer TGA thermobalance (model STA6000). The first stage (stripping) was carried out under an N<sub>2</sub> atmosphere with a constant flow of 20 mL/min, raising the temperature from 30 °C to 500 °C under a heating rate of 15 °C /min. The end temperature was maintained for 30 min, and then, in the second stage, the gas changed from N<sub>2</sub> to O<sub>2</sub>, promoting fast combustion from 500 to up 550 °C. The loss weight enabled the determination of the volatile fraction (first stage) while the non-volatile fraction, named carbon deposition or coke (second stage), was calculated as follows:

$$\eta_c = \frac{w_i - w_f}{w_f} \cdot 100 \quad (6.4)$$

the carbon deposition yield is represented by  $\eta_c$ , while the sample weights at the start and end of the combustion stage are depicted by  $w_i$  and  $w_f$ .

### 6.3.4. Liquid product analysis

The nature of the oils was qualitatively analyzed using Fourier Transform InfraRed spectroscopy (FTIR) by identifying functional groups. A Perkin Elmer Spectrum 65 FTIR device was used to record the spectra between the frequency range of 4000 and 400  $\text{cm}^{-1}$  under a resolution of 1  $\text{cm}^{-1}$ .

The identification of the gasoline chemical composition present in the oil samples was performed using gas chromatography coupled with Mass Spectrometry (GC-MS/MS) according to the ASTM D2789 method summing of characteristic mass fragments [57]. The separation of the analytes was performed in an 8860 Agilent GC system (Agilent Technologies, California, United States) equipped with a Phenomenex column of a nonpolar phase, i.e., ZB-5 ms (30 m long, 0.25 mm internal diameter, and 0.25  $\mu\text{m}$  of fill thickness), and the mass of the ionized analytes was determined in a triple-quadrupole mass spectrometer detector (5977 model from Agilent, with ionization energy by the electronic impact of 70 eV and a scan speed of  $\leq 20,000$  Da/s. The oven was programmed with the same injection temperature (240  $^{\circ}\text{C}$ ). The starting temperatures were 40  $^{\circ}\text{C}$  for 5 min, while the ending temperatures reached 240  $^{\circ}\text{C}$  by 6 min at 15  $^{\circ}\text{C}/\text{min}$  heating rates. The oil samples were diluted in 1 mL of chloroform and injected in split mode (5:1) with a constant flow of 1 mL/min of He.

A mixture of hydrocarbons encompassing the boiling range specified by the ATSM D 2887 [58] was used as a reference to identify gasoline's retention times and the boiling temperature. Referential hydrocarbons were also confirmed using the NIST 08 mass spectrum library database from the National Institute of Standards and Technology (NIST).

The boiling points of each compound in the sample were calculated based on the retention times and boiling points of the standards according to the following linear interpolation:

$$BP_x = \left( \frac{BP_2 - BP_1}{RT_2 - RT_1} \right) \cdot (RT_x - RT_1) + BP_1 \quad (6.5)$$

where the boiling points and retention times of the standards are represented by  $BP_1$ ,  $BP_2$  and  $RT_1$ ,  $RT_2$ , while the retention times and boiling points of the sample compounds are represented by  $RT_x$  and  $BP_x$ .

The simulated distillation (SD) at high temperature by gas chromatography (GC) was used to characterize the boiling temperature distribution of the oils, setting the contribution of the light, medium, and heavy fractions. Determination of the distribution of the boiling range of the compounds identified in the chromatograms was performed according to the ASTM D2887

standard [58] using a PerkinElmer Clarus 590 Gas Chromatograph with a dimethylpolysiloxane ELITE 2887 capillary column of 10 m length and 0.53 of inner diameter and 2.65  $\mu\text{m}$  of film. Viscous samples were diluted with carbon disulfide.

The distribution of products was quantified in weight percent according to their boiling points. Compounds with boiling points between 35  $^{\circ}\text{C}$  and 205  $^{\circ}\text{C}$  were classified as gasoline-range products. Those with values ranging from 205  $^{\circ}\text{C}$  to 370  $^{\circ}\text{C}$  were labeled light cycle oil (LCO). Finally, those whose boiling temperature was over 370  $^{\circ}\text{C}$  were accounted for the heavy cycle oil (HCO) fraction. Table 7 summarizes the main products, the common fractions, and their nominal boiling points.

**Table 6.7.** Common fractions in pyrolysis oil and their nominal boiling points.

Products	Fraction	Boiling Point ( $^{\circ}\text{C}$ )
Gasoline	Light Naphtha	36-90
	Mid Naphtha	90-160
	Heavy Naphtha	160-205
LCO	Light Gas Oil	205-260
	Mid Gas Oil	260-315
	Heavy Gas Oil	315-370
HCO	Light Vacuum Gas Oil	370-430
	Mid Vacuum Gas Oil	430-480
	Heavy Vacuum Gas Oil	480-565

## 6.4. Conclusions

The contribution describes the development of new composite materials with potential applications as catalysts during the pyrolysis of real non-recyclable mixtures of post-consumer plastic waste. Two zeolitic materials, HY and HZSM-5, were modified, and a simple method was employed to deposit Ni and Co on their surfaces to improve the catalytic response toward obtaining fuel fractions of interest.

The catalytic materials, both references (HY and HZSM-5) and materials containing the precursor metals (Ni and Co modified samples) were characterized in terms of their structural, morphological, and chemical properties. The results show limited structural modifications according to XRD spectra results, where the most relevant results are associated with a lack of

Co oxides, which could indicate that the Co minor phase may have been exchanged in certain positions of the zeolitic structure. More important were the detected modifications of acidity properties. A new third peak was recorded (compared to zeolites not modified with metals) in all samples containing the metallic-related element, which generated a clear increase in the total acidity of the sample. In addition, the modification of morphological properties by including metallic components on the surface of the active zeolitic supports was detected. The BET area and pore volume reduction detected can be associated with the accumulation of metallic components blocking certain pore channels of the zeolite.

In terms of activity, differences in the product amount of char, gas, and liquid are not relevant between samples modified with metals and the active supports HY and HZSM; however, a noticeable relationship has been detected between the quantity produced of a certain liquid fuel fraction (grouped as gasoline, light cycle oil, and heavy cycle oil) and a parameter defined in this work as  $\text{Acidity}/S_{\text{BET}}$ , expressed in  $\mu\text{mol NH}_3$  per  $\text{m}^2$  of catalytic surface. In all cases, it was detected that the increase in the amount of gasoline fraction that can be extracted from the plastic waste is associated with this parameter, which relates to the morphological and chemical properties of the samples. Furthermore, considering the experimental error, it can also be concluded that for the HY-based materials, this combined parameter is also relevant to producing the light cycle oil fraction.

In an energy context still dominated by traditional fractions (gasoline, kerosene, etc.) obtained from oil refining processes, this work presents a relevant waste recovery alternative since it provides advances in producing fuels from plastic waste that could be used directly or with small treatments.

The analysis has demonstrated the potential value-added fuels that can be derived from the liquid oil product. However, it is crucial to investigate the environmental and economic feasibility of using pyrolysis oils as a renewable energy source on a larger scale and explore the potential of integrating pyrolysis technologies with existing industries. Additionally, a deep investigation of the potential of pyrolysis byproducts, such as char, in adsorption applications or carbon sequestration initiatives is needed. Therefore, further research and development in this field are of utmost importance to fully exploit the potential of the liquid oil product and minimize its environmental impacts.

**Author Contributions:** Conceptualization, M.C., G.B., M.J.M.-B., and M.Á.M.-L.; methodology, G.B., M.F.P.-S., and M.C.; validation, M.F.P.-S., G.B., and R.R.S.; formal analysis, M.F.P.-S. and G.B.; investigation, M.F.P.-S., M.C., G.B., R.R.S., M.J.M.-B., and M.Á.M.-L.; resources, M.C. and M.Á.M.-L.; data curation, R.R.S., M.J.M.-B., and M.Á.M.-L.; writing—original draft preparation,



M.F.P.-S., M.Á.M.-L., and R.R.S.; writing—review and editing, M.J.M.-B. and M.Á.M.-L.; supervision, M.J.M.-B., M.Á.M.-L., M.C., and G.B.; project administration, M.Á.M.-L. and M.C.; funding acquisition, M.C. and M.Á.M.-L. All authors have read and agreed to the published version of the manuscript.

**Funding:** This research was funded by project PID2019-108826RB-I00/SRA (State Research Agency)/10.13039/501100011033.

**Data Availability Statement:** The data presented in this study are available

**Acknowledgments:** The authors acknowledge the support provided by the external services of the University of Granada (“Centro de Instrumentación Científica”, CIC) for the support with the characterization of the catalysts.

**Conflicts of Interest:** The authors declare no conflicts of interest.

## References

1. United Nation Environment Programme. *Single-Use Plastics: A Roadmap for Sustainability*; Canno, T. Ed.; United Nations Environment Programme: Nairobi, Kenya, 2018.
2. Plastics Europe. Plastics Europe Association of Plastics Manufacturers Plastics—The Facts 2021 An analysis of European Plastics Production, Demand and Waste Data. In *Plastics-Facts 2021*; Plastics Europe: Bruxelles, Belgium, 2021; p. 34. Available online: <https://plasticseurope.org/knowledge-hub/plastics-the-facts-2021/> (accessed on 1 January 2024).
3. Wan, Y.; Chen, X.; Liu, Q.; Hu, H.; Wu, C.; Xue, Q. Informal landfill contributes to the pollution of microplastics in the surrounding environment. *Environ. Pollut.* **2022**, *293*, 118586. <https://doi.org/10.1016/j.envpol.2021.118586>.
4. Su, Y.; Zhang, Z.; Wu, D.; Zhan, L.; Shi, H.; Xie, B. Occurrence of microplastics in landfill systems and their fate with landfill age. *Water Res.* **2019**, *164*, 114968. <https://doi.org/10.1016/j.watres.2019.114968>.
5. Sun, J.; Zhu, Z.-R.; Li, W.-H.; Yan, X.; Wang, L.-K.; Zhang, L.; Jin, J.; Dai, X.; Ni, B.-J. Revisiting Microplastics in Landfill Leachate: Unnoticed Tiny Microplastics and Their Fate in Treatment Works. *Water Res.* **2020**, *190*, 116784. <https://doi.org/10.1016/j.watres.2020.116784>.
6. European Commission. European Strategy for Plastics in a Circular Economy. EUR-Lex. 2018. Available online: <https://eur-lex.europa.eu/legal-content/EN/ALL/?uri=CELEX%3A52018DC0028> (accessed on 23 November 2022).
7. 7-Scheirs, J.; Kaminsky, W. *Feedstock Recycling and Pyrolysis of Waste Plastics: Converting Waste Plastics into Diesel and Other Fuels*; John Wiley & Sons, Ltd. West Sussex, UK, 2006.
8. Kusenbergh, M.; Eschenbacher, A.; Delva, L.; De Meester, S.; Delikonstantis, E.; Stefanidis, G.D.; Ragaert, K.; Van Geem, K.M. Towards high-quality petrochemical feedstocks from

- mixed plastic packaging waste via advanced recycling: The past, present and future. *Fuel Process. Technol.* **2022**, *238*, 107474. <https://doi.org/10.1016/j.fuproc.2022.107474>.
9. Huysveld, S.; Ragaert, K.; Demets, R.; Nhu, T.; Civancik-Uslu, D.; Kusenbergh, M.; Van Geem, K.; De Meester, S.; Dewulf, J. Technical and market substitutability of recycled materials: Calculating the environmental benefits of mechanical and chemical recycling of plastic packaging waste. *Waste Manag.* **2022**, *152*, 69–79. <https://doi.org/10.1016/j.wasman.2022.08.006>.
  10. Harscoet, E.; Chouvenec, S.; Faugeras, A.-C.; Ammenti-Deloitte, F. *Chemical and Physico-Chemical Recycling of Plastic Waste*; Final Report; Record: Villeurbanne, France, 2022. Available online: [www.record-net.org](http://www.record-net.org) (accessed on 1 January 2024).
  11. Peng, Y.; Wang, Y.; Ke, L.; Dai, L.; Wu, Q.; Cobb, K.; Zeng, Y.; Zou, R.; Liu, Y.; Ruan, R. A review on catalytic pyrolysis of plastic wastes to high-value products. *Energy Convers. Manag.* **2022**, *254*, 115243. <https://doi.org/10.1016/j.enconman.2022.115243>.
  12. Verma, A.; Sharma, S.; Pramanik, H. Pyrolysis of waste expanded polystyrene and reduction of styrene via in-situ multiphase pyrolysis of product oil for the production of fuel range hydrocarbons. *Waste Manag.* **2021**, *120*, 330–339. <https://doi.org/10.1016/j.wasman.2020.11.035>.
  13. Wang, J.; Jiang, J.; Wang, X.; Wang, R.; Wang, K.; Pang, S.; Zhong, Z.; Sun, Y.; Ruan, R.; Ragauskas, A.J. Converting polycarbonate and polystyrene plastic wastes into aromatic hydrocarbons via catalytic fast co-pyrolysis. *J. Hazard. Mater.* **2020**, *386*, 121970. <https://doi.org/10.1016/j.jhazmat.2019.121970>.
  14. Xue, Y.; Johnston, P.; Bai, X. Effect of catalyst contact mode and gas atmosphere during catalytic pyrolysis of waste plastics. *Energy Convers. Manag.* **2017**, *142*, 441–451. <https://doi.org/10.1016/j.enconman.2017.03.071>.
  15. Onwudili, J.A.; Muhammad, C.; Williams, P.T. Influence of catalyst bed temperature and properties of zeolite catalysts on pyrolysis-catalysis of a simulated mixed plastics sample for the production of upgraded fuels and chemicals. *J. Energy Inst.* **2019**, *92*, 1337–1347. <https://doi.org/10.1016/j.joei.2018.10.001>.
  16. López, A.; de Marco, I.; Caballero, B.; Laresgoiti, M.; Adrados, A.; Torres, A. Pyrolysis of municipal plastic wastes II: Influence of raw material composition under catalytic conditions. *Waste Manag.* **2011**, *31*, 1973–1983. <https://doi.org/10.1016/j.wasman.2011.05.021>.
  17. Valizadeh, B.; Valizadeh, S.; Kim, H.; Choi, Y.J.; Seo, M.W.; Yoo, K.S.; Lin, K.-Y.A.; Hussain, M.; Park, Y.-K. Production of light olefins and monocyclic aromatic hydrocarbons from the pyrolysis of waste plastic straws over high-silica zeolite-based catalysts. *Environ. Res.* **2023**, *245*, 118076. <https://doi.org/10.1016/j.envres.2023.118076>.
  18. Yousef, S.; Eimontas, J.; Striūgas, N.; Abdelnaby, M.A. Synthesis of value-added aromatic chemicals from catalytic pyrolysis of waste wind turbine blades and their kinetic analysis

- using artificial neural network. *J. Anal. Appl. Pyrolysis* **2024**, *177*, 106330. <https://doi.org/10.1016/j.jaap.2023.106330>.
19. Muneer, B.; Zeeshan, M.; Qaisar, S.; Razzaq, M.; Iftikhar, H. Influence of in-situ and ex-situ HZSM-5 catalyst on co-pyrolysis of corn stalk and polystyrene with a focus on liquid yield and quality. *J. Clean. Prod.* **2019**, *237*, 117762. <https://doi.org/10.1016/j.jclepro.2019.117762>.
  20. Kartik, S.; Balsora, H.K.; Sharma, M.; Saptorio, A.; Jain, R.K.; Joshi, J.B.; Sharma, A. Valorization of plastic wastes for production of fuels and value-added chemicals through pyrolysis—A review. *Therm. Sci. Eng. Prog.* **2022**, *32*, 101316. <https://doi.org/10.1016/j.tsep.2022.101316>.
  21. Zhang, X.; Jiang, Y.; Kong, G.; Liu, Q.; Zhang, G.; Wang, K.; Cao, T.; Cheng, Q.; Zhang, Z.; Ji, G.; et al. CO<sub>2</sub>-mediated catalytic upcycling of plastic waste for H<sub>2</sub>-rich syngas and carbon nanomaterials. *J. Hazard. Mater.* **2023**, *460*, 132500. <https://doi.org/10.1016/j.jhazmat.2023.132500>.
  22. Uemichi, Y.; Makino, Y.; Kanazuka, T. Degradation of polyethylene to aromatic hydrocarbons over metal-supported activated carbon catalysts. *J. Anal. Appl. Pyrolysis* **1989**, *14*, 331–344. [https://doi.org/10.1016/0165-2370\(89\)80008-7](https://doi.org/10.1016/0165-2370(89)80008-7).
  23. Nishino, J.; Itoh, M.; Fujiyoshi, H.; Uemichi, Y. Catalytic degradation of plastic waste into petrochemicals using Ga-ZSM-5. *Fuel* **2008**, *87*, 3681–3686. <https://doi.org/10.1016/j.fuel.2008.06.022>.
  24. Pinto, F.; Costa, P.; Gulyurtlu, I.; Cabrita, I. Pyrolysis of plastic wastes: 2. Effect of catalyst on product yield. *J. Anal. Appl. Pyrolysis* **1999**, *51*, 57–71. [https://doi.org/10.1016/s0165-2370\(99\)00008-x](https://doi.org/10.1016/s0165-2370(99)00008-x).
  25. Kang, J.; Kim, J.Y.; Sung, S.; Lee, Y.; Gu, S.; Choi, J.-W.; Yoo, C.-J.; Suh, D.J.; Choi, J.; Ha, J.-M. Chemical upcycling of PVC-containing plastic wastes by thermal degradation and catalysis in a chlorine-rich environment. *Environ. Pollut.* **2024**, *342*, 123074. <https://doi.org/10.1016/j.envpol.2023.123074>.
  26. Upare, D.P.; Park, S.; Kim, M.; Kim, J.; Lee, D.; Lee, J.; Chang, H.; Choi, W.; Choi, S.; Jeon, Y.-P.; et al. Cobalt promoted Mo/beta zeolite for selective hydrocracking of tetralin and pyrolysis fuel oil into monocyclic aromatic hydrocarbons. *J. Ind. Eng. Chem.* **2016**, *35*, 99–107. <https://doi.org/10.1016/j.jiec.2015.12.020>.
  27. Guo, H.; He, H.; Miao, C.; Hua, W.; Yue, Y.; Gao, Z. Ethane conversion in the presence of CO<sub>2</sub> over Co-based ZSM-5 zeolite: Co species controlling the reaction pathway. *Mol. Catal.* **2022**, *519*, 112155. <https://doi.org/10.1016/j.mcat.2022.112155>.
  28. Ewuzie, R.N.; Genza, J.R.; Abdullah, A.Z. Catalytic hydrogenolysis of lignin in isopropanol as hydrogen donor over nickel-cobalt supported on zeolite to produce aromatic and phenolic monomers. *Appl. Catal. A Gen.* **2023**, *667*, 119443. <https://doi.org/10.1016/j.apcata.2023.119443>.

29. Kurniawan, R.G.; Karanwal, N.; Park, J.; Verma, D.; Kwak, S.K.; Kim, S.K.; Kim, J. Direct conversion of furfural to 1,5-pentanediol over a nickel–cobalt oxide–alumina trimetallic catalyst. *Appl. Catal. B Environ.* **2023**, *320*, 121971. <https://doi.org/10.1016/j.apcatb.2022.121971>.
30. Cai, Y.; Fan, Y.; Li, X.; Chen, L.; Wang, J. Preparation of refined bio-oil by catalytic transformation of vapors derived from vacuum pyrolysis of rape straw over modified HZSM-5. *Energy* **2016**, *102*, 95–105. <https://doi.org/10.1016/j.energy.2016.02.051>.
31. Pedrosa, A.M.G.; Souza, M.J.; Melo, D.M.; Araujo, A.S. Cobalt and nickel supported on HY zeolite: Synthesis, characterization and catalytic properties. *Mater. Res. Bull.* **2006**, *41*, 1105–1111. <https://doi.org/10.1016/j.materresbull.2005.11.010>.
32. Lai, S.; Meng, D.; Zhan, W.; Guo, Y.; Guo, Y.; Zhang, Z.; Lu, G. The promotional role of Ce in Cu/ZSM-5 and in situ surface reaction for selective catalytic reduction of NO<sub>x</sub> with NH<sub>3</sub>. *RSC Adv.* **2015**, *5*, 90235–90244. <https://doi.org/10.1039/c5ra12505g>.
33. Cairns, R.W.; Ott, E. X-Ray Studies of the System Nickel-Oxygen-Water. *J. Am. Chem. Soc.* **1933**, *55*, 527–533.
34. Chupin, C.; Vanveen, A.; Konduru, M.; Després, J.; Mirodatos, C. Identity and location of active species for NO reduction by CH<sub>4</sub> over Co-ZSM-5. *J. Catal.* **2006**, *241*, 103–114. <https://doi.org/10.1016/j.jcat.2006.04.025>.
35. Seo, S.M.; Lim, W.T.; Seff, K. Single-crystal structures of fully and partially dehydrated zeolite Y (FAU, Si/Al = 1.56) largely Co<sup>2+</sup> exchanged at pH 5.1. *Microporous Mesoporous Mater.* **2013**, *170*, 67–74. <https://doi.org/10.1016/j.micromeso.2012.11.019>.
36. Núñez, F.; Chen, L.; Wang, J.A.; Flores, S.O.; Salmones, J.; Arellano, U.; Noreña, L.E.; Tzompantzi, F. Bifunctional Co<sub>3</sub>O<sub>4</sub>/ZSM-5 Mesoporous Catalysts for Biodiesel Production via Esterification of Unsaturated Omega-9 Oleic Acid. *Catalysts* **2022**, *12*, 900. <https://doi.org/10.3390/catal12080900>.
37. Biesinger, M.C.; Lau, L.W.M.; Gerson, A.R.; Smart, R.S.C. The role of the Auger parameter in XPS studies of nickel metal, halides and oxides. *Phys. Chem. Chem. Phys.* **2012**, *14*, 2434–2442. <https://doi.org/10.1039/c2cp22419d>.
38. Peck, M.A.; Langell, M.A. Comparison of Nanoscaled and Bulk NiO Structural and Environmental Characteristics by XRD, XAFS, and XPS. *Chem. Mater.* **2012**, *24*, 4483–4490. <https://doi.org/10.1021/cm300739y>.
39. Biesinger, M.C.; Payne, B.P.; Grosvenor, A.P.; Lau, L.W.M.; Gerson, A.R.; Smart, R.S.C. Resolving surface chemical states in XPS analysis of first row transition metals, oxides and hydroxides: Cr, Mn, Fe, Co and Ni. *Appl. Surf. Sci.* **2011**, *257*, 2717–2730. <https://doi.org/10.1016/j.apsusc.2010.10.051>.
40. Valero-Romero, M.J.; Sartipi, S.; Sun, X.; Rodríguez-Mirasol, J.; Cordero, T.; Kapteijn, F.; Gascon, J. Carbon/H-ZSM-5 composites as supports for bi-functional Fischer–Tropsch

- synthesis catalysts. *Catal. Sci. Technol.* **2016**, *6*, 2633–2646. <https://doi.org/10.1039/c5cy01942g>.
41. Vovchok, D.; Tata, J.; Orozco, I.; Zhang, F.; Palomino, R.M.; Xu, W.; Harper, L.; Khatib, S.J.; Rodriguez, J.A.; Senanayake, S.D. Location and chemical speciation of Cu in ZSM-5 during the water-gas shift reaction. *Catal. Today* **2019**, *323*, 216–224. <https://doi.org/10.1016/j.cattod.2018.07.049>.
  42. Thommes, M.; Kaneko, K.; Neimark, A.V.; Olivier, J.P.; Rodriguez-Reinoso, F.; Rouquerol, J.; Sing, K.S.W. Physisorption of gases, with special reference to the evaluation of surface area and pore size distribution (IUPAC Technical Report). *Pure Appl. Chem.* **2015**, *87*, 1051–1069. <https://doi.org/10.1515/pac-2014-1117>.
  43. Scherzer, J. Correlation between Catalyst Formulation and Catalytic Properties. In *Fluid Catalytic Cracking: Science and Technology*; Magee, J.S., Mitchell, M.M., Eds.; Elsevier: Amsterdam, The Netherlands, 1992; Volume 76, pp. 145–182.
  44. Reschetilowski, W.; Unger, B.; Wendlandt, K.-P. Study of the ammonia–zeolite interaction in modified ZSM-5 by temperature-programmed desorption of ammonia. *J. Chem. Soc. Faraday Trans. 1 Phys. Chem. Condens. Phases* **1989**, *85*, 2941–2944. <https://doi.org/10.1039/f19898502941>.
  45. Karge, H.G.; Dondur, V. Investigation of the distribution of acidity in zeolites by temperature-programmed desorption of probe molecules. 2. Dealuminated Y-Type Zeolites. *J. Phys. Chem.* **1991**, *95*, 282–288. <https://doi.org/10.1021/j100365a047>.
  46. Razzaq, M.; Zeeshan, M.; Qaisar, S.; Iftikhar, H.; Muneer, B. Investigating use of metal-modified HZSM-5 catalyst to upgrade liquid yield in co-pyrolysis of wheat straw and polystyrene. *Fuel* **2019**, *257*, 116119. <https://doi.org/10.1016/j.fuel.2019.116119>.
  47. Veses, A.; Puértolas, B.; Callén, M.; García, T. Catalytic upgrading of biomass derived pyrolysis vapors over metal-loaded ZSM-5 zeolites: Effect of different metal cations on the bio-oil final properties. *Microporous Mesoporous Mater.* **2015**, *209*, 189–196. <https://doi.org/10.1016/j.micromeso.2015.01.012>.
  48. Li, X.; Zhang, H.; Li, J.; Su, L.; Zuo, J.; Komarneni, S.; Wang, Y. Improving the aromatic production in catalytic fast pyrolysis of cellulose by co-feeding low-density polyethylene. *Appl. Catal. A Gen.* **2013**, *455*, 114–121. <https://doi.org/10.1016/j.apcata.2013.01.038>.
  49. Akubo, K.; Nahil, M.A.; Williams, P.T. Aromatic fuel oils produced from the pyrolysis-catalysis of polyethylene plastic with metal-impregnated zeolite catalysts. *J. Energy Inst.* **2019**, *92*, 195–202. <https://doi.org/10.1016/j.joei.2017.10.009>.
  50. Calero, M.; Solís, R.R.; Muñoz-Batista, M.J.; Pérez, A.; Blázquez, G.; Martín-Lara, M. Oil and gas production from the pyrolytic transformation of recycled plastic waste: An integral study by polymer families. *Chem. Eng. Sci.* **2023**, *271*, 118569. <https://doi.org/10.1016/j.ces.2023.118569>.

51. M. F. Paucar-Sánchez, M. Calero, G. Blázquez, R. R. Solís, M. J. Muñoz-Batista, and M. Á. Martín-Lara, "Thermal and catalytic pyrolysis of a real mixture of post-consumer plastic waste: An analysis of the gasoline-range product," *Process Saf. Environ. Prot.*, vol. 168, no. October, pp. 1201–1211, 2022, <https://doi.org/10.1016/j.psep.2022.11.009>.
52. Miskolczi, N.; Bartha, L.; Deák, G. Thermal degradation of polyethylene and polystyrene from the packaging industry over different catalysts into fuel-like feed stocks. *Polym. Degrad. Stab.* **2006**, *91*, 517–526. <https://doi.org/10.1016/j.polymdegradstab.2005.01.056>.
53. Iliopoulou, E.; Stefanidis, S.; Kalogiannis, K.; Delimitis, A.; Lappas, A.; Triantafyllidis, K. Catalytic upgrading of biomass pyrolysis vapors using transition metal-modified ZSM-5 zeolite. *Appl. Catal. B Environ.* **2012**, *127*, 281–290. <https://doi.org/10.1016/j.apcatb.2012.08.030>.
54. Richardson, J.T. *Principles of Catalyst Development*, 2nd ed.; Springer Science: New York, NY, USA, 1992.
55. Altomare, A.; Corriero, N.; Cuocci, C.; Falcicchio, A.; Moliterni, A.; Rizzi, R. QUALX2.0: A qualitative phase analysis software using the freely available database POW\_COD. *J. Appl. Crystallogr.* **2015**, *48*, 598–603. <https://doi.org/10.1107/S1600576715002319>.
56. M. F. Paucar-Sánchez, M. Calero, G. Blázquez, M. J. Muñoz-Batista, and M. A. Martín-Lara, "Characterization of liquid fraction obtained from pyrolysis of post-consumer mixed plastic waste: A comparing between measured and calculated parameters," *Process Saf. Environ. Prot.*, vol. 159, pp. 1053–1063, 2022, <https://doi.org/10.1016/j.psep.2022.01.081>.
57. *ASTM D2789-95*; Standard Test Method for Hydrocarbon Types in Low Olefinic Gasoline by Mass Spectrometry. American Society for Testing and Materials, ASTM International: West Conshohocken, PA, USA, 2016; pp. 1–7.
58. *MNL10902M*; Standard Test Method for Boiling Range Distribution of Petroleum Fractions by Gas Chromatography. ASTM International: West Conshohocken, PA, USA, 2008; pp. 444–454. <https://doi.org/10.1520/mnl10902m>.

**Disclaimer/Publisher's Note:** The statements, opinions and data contained in all publications are solely those of the individual author(s) and contributor(s) and not of MDPI and/or the editor(s). MDPI and/or the editor(s) disclaim responsibility for any injury to people or property resulting from any ideas, methods, instructions or products referred to in the content.

## **IV CONCLUSIONS**





## Chapter 7

### Conclusions

This doctoral thesis has proposed a thermal-catalytic alternative to treat the plastics mixed unrecovered from solid municipal waste to generate liquid fractions with a higher proportion of naphtha content, the main raw material to produce primary petrochemicals, under a fixed set of experimental conditions, and equivalent standard analysis methods to the refining industry; without being involved the physical separation or distillation of the samples to determine the chemical composition of their cuts. To do so, optimal thermal cracking conditions and physical and chemical properties behavior evaluation were obtained as the starting point. This was followed by a comparative assessment of plastic mix constituents in the liquid conversion and the reactivity of thermally cracked vapors over basic materials, undoped and metal-doped commercial zeolites, and liquid phase reactivity with less active materials such as clays. The main general conclusions drawn are:

- The operating conditions and the system configuration are decisive in obtaining better yields of the liquid fraction along with an appropriate distribution for catalytic cracking. The effects are reflected in pyrolytic oil properties by chemical changes due to hydrogenation reactions, with the hydrogen detached from the over-cracking light compounds and dehydrogenating of heavy ones.
- Predictive mathematical correlations, like those used in hydrocarbon refining, must be adequate for characterizing pyrolytic oils of different compositions. However, when experimental data are unavailable, the proposed equations could be suitable for calculating the specific gravity and refractive index parameter of pyrolytic oils obtained from the plastic waste mixture of the same investigated composition.
- The composition of post-consumer plastic waste and the types present in the rejected fraction directly impact the liquid fraction's yield and chemical composition. Olefin-based plastics reduce the presence of the heavy aromatics that would cause the dehydrogenation of styrene-based components, allowing a chemical composition near heavy straight-run naphtha.
- Acid commercial materials reduce liquid yields and increase aromatics. However, they condense gases and augment liquid fractions when metal-doped due to metal-zeolite interaction; HZSM-5 and only Ni at low concentration reduce the aromatics compared to base zeolites.

- Although basic materials reduce liquid yields less than zeolites, they promote aromatic formation at approximately the same level of HZS-5 and allow naphtha cut conservation by reducing heavy fractions, compared to the amount obtained in thermal cracking.
- In-situ catalytic cracking with clays showed little difference in liquid yield proportion to the thermal cracking but with lower naphtha amounts compared to those obtained by acid materials, along with few changes in the chemical composition. The increase in material amounts modified the result, reducing liquid yield and naphtha production in sepiolite and montmorillonite K30, while the K10 increased, slightly modifying the chemical composition.

## Conclusiones

Esta tesis doctoral ha propuesto una alternativa termo-catalítica en el tratamiento de los plásticos mezcla no recuperados de los desechos sólidos municipales para general fracciones líquidas con una alta proporción de nafta, principal materia prima para producir productos petroquímicos primarios, bajo condiciones experimentales fijas y métodos de análisis estándar equivalentes a los de la industria de la refinación; sin que implique separación física o destilación de las muestras para determinar la composición química de sus cortes. Par hacerlo, partimos de las condiciones óptimas de craqueo térmico y la evaluación del comportamiento de las propiedades físicas y químicas. Seguido de una evaluación comparativa de los componentes de la mezcla de plásticos en la conversión de líquido y la reactividad de los vapores craqueados térmicamente sobre materiales básicos, zeolitas comerciales impregnadas con mentales y sin impregnar, así como la reactividad en fase líquida con materiales menos activos como las arcillas. Las principales conclusiones generales son:

- Las condiciones de operación y la configuración del sistema son determinantes para obtener mejores rendimientos de la fracción líquida junto con una adecuada distribución para el craqueo catalítico. Los efectos se reflejan en las propiedades del aceite pirolítico mediante cambios químicos debido a reacciones de hidrogenación, con el hidrógeno desprendido por el sobre craqueo y deshidrogenación de compuestos ligeros y pesados.
- Las correlaciones matemáticas que se emplean en la refinación de hidrocarburos deben ser adecuadas para caracterizar aceites pirolíticos de diferentes composiciones. Sin embargo, cuando no se dispone de datos experimentales, las ecuaciones propuestas podrían ser adecuadas para calcular la gravedad específica y el parámetro del índice de refracción de aceites pirolíticos obtenidos a partir de la mezcla de residuos plásticos con la misma composición investigada.
- La composición de los residuos plásticos posconsumo y los tipos presentes en la fracción rechazada impactan directamente en el rendimiento y la composición química de la fracción líquida. Los plásticos con base olefínica reducen los compuestos aromáticos pesados que provocarían la deshidrogenación de los componentes a base de estireno, lo que permite una composición química cercana a la nafta pesada de primera destilación.
- Aunque los materiales básicos reducen menos los rendimientos líquidos que las zeolitas, promueven la formación de aromáticos aproximadamente al mismo nivel de la zeolita HZSM-5 y permite la conservación de la nafta, en comparación con la cantidad obtenida en el craqueo térmico, al reducir las fracciones pesadas.

- Los materiales comerciales ácidos reducen los rendimientos líquidos y aumentan los aromáticos. No obstante, condensan gases y aumentan las fracciones líquidas cuando están impregnados con metales debido a la interacción metal-zeolita; la zeolita HZSM-5 y el Ni a baja concentración reducen los aromáticos en comparación con las zeolitas base.
- El craqueo catalítico in situ con arcillas mostró poca diferencia en la proporción de rendimiento líquido respecto al craqueo térmico, pero con menores cantidades de nafta en comparación con las obtenidas con materiales ácidos, junto con pocos cambios en la composición química. El incremento de las cantidades modificó el resultado reduciendo el rendimiento líquido y la producción de nafta en la sepiolita y montmorillonita K30, mientras que la K10 aumentó, modificando levemente la composición química.

## **V FUTURE WORK**



## Chapter 8

### Future works

The development of adequate predictive mathematical correlations for characterizing pyrolytic oils of different compositions becomes imperious when experimental data are unavailable, above all when small samples are driven. In addition, the validation of methods that allow obtaining all the information of small samples without previous physical separation or distillation should be done.

The optimum operation conditions that allow a high liquid yield from thermal cracking with minor naphtha content should be investigated, as well as the obtention of catalytic materials that have a bimodal distribution of pores and low acidity under appropriate thermal or hydrothermal procedures, with or without chemical treatment, for provocation framework changes and increase their selectivity towards the naphtha generation. Then, an adequate metal for naphtha reforming should be investigated to be added to it.

The economic barriers and financial constraints hindering this technology's widespread adoption, environmental concerns, and the evaluation of emissions associated with using pyrolysis by-products as valuable sources could be solved by the proposed pathway and the development of appropriate assay procedures. Particular interest should be placed in validating the methods shown in the suggested methodology to extract the greatest possible information from the analysis of small samples.





## Trabajos Futuros

El desarrollo de correlaciones matemáticas predictivas adecuadas para caracterizar aceites pirolíticos de diferentes composiciones se vuelve imperioso cuando no se dispone de datos experimentales, sobre todo cuando se manejan muestras pequeñas. Además, se deben validar métodos que permitan obtener toda la información de muestras pequeñas sin previa separación física o destilación.

Se debe investigar las condiciones de operación que permita un alto rendimiento líquido a partir del craqueo térmico con menor contenido de nafta, así como la obtención de materiales catalíticos que tengan una distribución bimodal de poros y baja acidez mediante procedimientos térmicos o hidrotermales apropiados, con o sin tratamiento químico, para provocar cambios en la estructura y aumentar su selectividad a la generación de nafta. Luego de aquello, evaluar la incorporación de un metal adecuado para el reformado catalítico.

Las barreras económicas y las limitaciones financieras que obstaculizan la adopción generalizada de esta tecnología, como de las preocupaciones ambientales y la evaluación de las emisiones asociadas con el uso de subproductos de la pirólisis como fuentes valiosas, podrían resolverse mediante la ruta propuesta y el desarrollo de procedimientos de ensayos apropiados. Se debe poner especial interés en validar los métodos mostrados en la metodología sugerida para extraer la mayor información posible del análisis de muestras pequeñas.



## **VI ANNEX**



# Characterization of the different oils obtained through the catalytic in-situ pyrolysis of polyethylene film from municipal solid waste

Lucía Quesada, Mónica Calero, María Ángeles Martín-Lara, Antonio Pérez, Marco F. Paucar-Sánchez and Gabriel Blázquez

*Department of Chemical Engineering University of Granada, 18071 Granada, Spain*

Applied Science-Basel, ISSN: N/A, eISSN: 2076-3417. Published by MDPI.

Volume: 12

Number: 4043

Country: Switzerland

DOI: <https://doi.org/10.3390/app12084043>

- *Category: Chemistry, Multidisciplinary. Journal Impact Factor, JIF (2022): 2.7. Category Ranking: 100/178 (Q3).*
- *Category: Engineering, Multidisciplinary. Journal Impact Factor, JIF (2022): 2.7. Category Ranking: 42/90 (Q2).*
- *Category: Materials Science, Multidisciplinary. Journal Impact Factor, JIF (2022): 2.7. Category Ranking: 207/342 (Q3).*
- *Category: Physics, Applied. Journal Impact Factor, JIF (2022): 2.7. Category Ranking: 77/159 (Q2).*

*Article history:*

Received 15 February 2022

Accepted 14 April 2022

Published 16 April 2022



## Abstract

Nowadays, the thermal and catalytic decomposition of plastic wastes by pyrolysis is one of the best alternatives to convert these wastes into quality fuel oils, thus replenishing part of the petroleum resources. Thus, in this work, the catalytic pyrolysis of polyethylene film waste from the remaining organic fraction has been studied on different catalysts under dynamic operating conditions in a batch reactor. To see the possible differences in the use of the catalyst, these catalysts have been characterized through isotherms of adsorption-desorption with N<sub>2</sub> and with X-rays powder diffraction for structural characterization. The results obtained have been compared with the pyrolysis of the same material without catalyst. Special attention has been paid to the similarities and differences with thermal pyrolysis. The characterization of the liquid fraction including physical and chemical properties has been carried out. The liquid yield varies from 37 to 43%; it has good calorific values of 46-48 MJ/kg, an average density of 0.82 g/cm<sup>3</sup>, a fairly low viscosity when compared to the product without catalyst. Other properties like American Petroleum Institute (API) gravity or pH were also determined and were found they are similar to those of conventional fuels. Regarding composition, oils mainly are composed of paraffins, naphthenes and aromatic hydrocarbons. The general distribution of carbons is C7 to C31. Finally, a detailed analysis of the composition of liquid products shows they present heavy naphtha, kerosene, and diesel fractions in different proportions in the function of the catalyst used.

**Keywords:** polyethylene, plastic pyrolysis, catalysis, zeolites, characterization, waste recycling

## 1. Introduction

Today humans are dependent on plastic materials because of their uses and their advantages. So, 368 Mt of plastic are produced worldwide in 2019 and 58 Mt in Europe, this leads to a large production of plastic waste. In 2018, 29.1 Mt of post-consumer plastic waste was collected in Europe and about 25% of plastic waste ends up in landfills (in Spain this value increased to 39%) [1]. Spain has two collection systems, the selective collection of municipal waste in homogeneous fractions which are normally recycled in their great majority and, the collection of non-segregated waste (fraction of municipal waste not collected selectively) that includes a great amount of organic fraction mixed with other types of municipal waste. This second flow of municipal waste has more disadvantages to recycling due to the high heterogeneity and variety of materials it contains. Unfortunately, the non-selective collection system is the most popular among Spanish citizens with 86% of municipal waste collected in this system, for provinces such as Granada [2]. This organic-rest fraction is composed of 12.6% of plastics [3] that could be recovered and used through a recycling or valorization process. Between techniques of

valorization, the conversion of plastics into valuable hydrocarbon fuels has attracted attention [4]. There are numerous techniques for recycling plastic waste, mainly mechanical recycling and chemical recycling. Ragaert et al. [5] make a comprehensive compilation about the ways to recycle different plastic waste and found that chemical recycling, and in particular pyrolysis, is a promising complementary model to support a circular economy for all plastics since it is specially focused on the plastic waste that cannot be mechanically recycled for technical or economic reasons as mixed polymers (including multilayers, multi-materials, very dirty plastics, etc.). In addition, Papari et al. [6] carried out a review on the potential of pyrolysis for the recovery of plastic waste. In their work, they discuss the different types of pyrolysis, operating conditions, use of catalysts, etc., and their effect on the characteristics of the pyrolysis products obtained. Al-Salem et al. [7] studied the most influential factors in the pyrolysis process, the products that can be obtained as well as the differences when using catalysts. Sharuddin et al. [8] carry out a review of the plastic waste pyrolysis process analyzing the parameters that most influence the characteristics of the final products such as temperature, residence time, pressure, catalyst or type of reactor.

Also, in a recent study, Li et al. [9] made an extensive review on the current state of the conversion of plastic waste to fuels. The authors include a review of traditional technologies such as thermal pyrolysis and new technologies including catalytic pyrolysis, hydrothermal liquefaction, and advanced oxidation processes such as photocatalytic oxidation, Fenton oxidation, and electrocatalytic oxidation. The authors indicate that it is possible to achieve an efficient conversion to fuel of plastic waste through the use of catalysts, although problems such as the deactivation of the catalyst and its cost must be taken into account. In this sense, the authors include as a line of research in the future, a greater study on the use of catalysts, emphasizing the development of catalysts that have good adaptability, high activity and recyclability. Therefore, pyrolysis can be considered as an interesting recycling technology for municipal mixed plastic waste such as mixed polyethylene (PE) (high density-HDPE and low density-LDPE) or polyolefin mixtures (PE, polypropylene (PP) and polystyrene (PS)) that are currently not mechanically recycled but incinerated and/or dumped to landfill. Thermal or non-catalytic pyrolysis involves heating municipal mixed plastic waste at moderate temperatures in an inert atmosphere to produce three main products: gas, liquid (oils), and solid (char). One of the particularities of the thermal pyrolysis process is the flexibility to achieve the product of interest by changing the operating parameters mainly temperature, residence time and heating rate [4]. Unlike mechanical recycling, thermal pyrolysis can handle highly contaminated waste and it is also economically viable [5]. There have been numerous studies on the thermal pyrolysis of particular types of plastic waste. For example, authors such as Ahmad et al. [10], Onwudili et al. [11] and Quesada et al. [12] carried out thermal pyrolysis tests to convert PE plastic waste into



valuable oils. The main disadvantage of this process is that the oil obtained has high wax content with too much energy consumed.

One possibility for improving the performance of pyrolysis is the use of a specific catalyst (catalytic pyrolysis). The catalyst allows using less stringent reaction conditions, lowering the temperature and residence time of the overall process and as such affecting the total operating cost. In addition, the use of the catalyst allows the product spectra to be directed towards fuel, valuable chemicals, depending on the process conditions, being more selective [5,13]. In short, the catalyst plays an important role in the consumption of energy and composition and properties of pyrolysis products [4, 12]. A wide variety of catalysts have been assayed in the pyrolysis of plastic waste, placed in the pyrolysis reactor (in situ), or an independent catalytic bed (ex-situ) [14-16]. Most of the used catalysts are structures of aluminum-silicate minerals with high surface area and high acid strength like HY, HUSY, HBeta and HZSM-5 zeolites. There are numerous works such as Lopez et al. [14], where the catalytic pyrolysis of plastic waste was carried out in situ in the reactor. One of the disadvantages of this process is that the presence of contaminants like additives (plasticizers, stabilizers, antioxidants, etc.) and other materials (organic matter, papers, etc.) can have a direct effect on the acid centers of the catalyst, reducing its catalytic activity or favoring the formation of coke [17].

The problems related to the global waste generation and management and plastic waste release, in particular, are increasing in recent years. Therefore, there is a growing need to search for integrated solutions to respond to this problem. Achieving a model based on zero-waste includes different actions such as sustainable design, reduction, reuse and recycling of waste or product responsibility [18]. In this sense, this work aims to give added value to PE film waste through catalytic pyrolysis, helping to achieve the objectives of reducing the amount of waste and avoiding environmental problems. For this, the characterization of different oils obtained through the catalytic in-situ pyrolysis of PE film from the non-selectively collected fraction from municipal solid waste in a fixed-bed batch type pyrolysis reactor with different commercial catalysts has been carried out. Also, characterization of catalyst was carried out using different techniques, including X-ray powder diffraction (XRD) and N<sub>2</sub> adsorption isotherms

## **2. Materials and Methods**

### **2.1. Materials**

PE used in this study comes from the residual fraction of municipal solid waste and has been supplied by the municipal solid waste treatment plant Ecocentral, located in the province of Granada (Spain). The characterization of this material can be found in our previous published paper [12], where the material was characterized both physically and chemically. To optimize the

volume of this plastic waste, in the present work, the material has been transformed into pellet. In the study by Soto et al. [19], the process of obtaining the PE in the municipal solid waste treatment plant was described, as well as its transformation into recycled PE pellets performed in an industrial plastic recycling plant located in Germany. The size of the pellets obtained was approximately 4 mm.

To carry out the catalytic pyrolysis tests, the catalysts indicated in Table 1 were used. Information about Brønsted and Lewis acidity was obtained from literature [20-24]. Before the experiment, the catalysts were calcinated in a muffle furnace at 773 K for 5 h to stabilize it and then placed in a desiccator before use. The catalysts were characterized according to the methodology indicated in the following subsection.

**Table 1.** Information of used commercial catalysts.

<b>Zeolite</b>	<b>Molecular formula</b>	<b>Nominal cation form</b>	<b>Si/Al molar ratio</b>	<b>Brønsted acidity (<math>\mu\text{mol/g}</math>)</b>	<b>Lewis acidity (<math>\mu\text{mol/g}</math>)</b>	<b>Total acidity (<math>\mu\text{mol/g}</math>)</b>	<b>Commercial name Zeolyst</b>
Zeolite HY	-	Hydrogen	2.6	272	104	995	CBV 600
Zeolite HUSY	$\text{H}_{11.3}\text{Al}_{11.3}\text{Si}_{181}\text{O}_{384}$	Hydrogen	15	160	318		CBV 720
Zeolite Ammonium Beta (HBEA)	$(\text{NH}_4)_{3.33}\text{Al}_{3.33}\text{Si}_{61}\text{O}_{128}$	Ammonium	12.5	448	208	1030	CP 814E

## 2.2. Characterization of the catalysts

### 2.2.1. Textural parameters

A Micromeritics ASAP 2010 instrument was used for determining the textural parameters from  $\text{N}_2$  adsorption isotherms at 77 K. Before adsorption, the zeolite samples were degassed at 363 K for 1 h and then at 623 K for 3 h under vacuum. The microporous volume and the external surface area were calculated using the t-plot method, the total pore volume was estimated from the adsorbed volume of nitrogen for a relative pressure  $P/P^0$  of 0.95, mesopore volume was estimated by the difference between total pore volume and microporous volume. Finally, Brunauer-Emmett-Teller (BET) specific surface area was calculated using the BET theory.

### 2.2.2. XRD

The structural characterization of the parent and modified samples was made from XRD patterns that were obtained in a Bruker AXSAdvancedD8 diffractometer, using  $\text{Cu K}\alpha$  radiation (1.5406 Å)

and operating at 40 kV and 40 mA. Diffractograms were obtained by continuous scanning from 5 to 80° (2θ), with a step size of 0.05° 2θ and 0.05 s acquisition for each step.

### 2.3. Catalytic pyrolysis tests

PE in the shape of pellets was pyrolyzed in a Nabertherm model R50/250/12 horizontal furnace reactor. About 20 g of pellets together with 10% by weight of the different types of catalysts were well-mixed to obtain a well-mixed mixture and fed into the pyrolysis reactor. The operating temperature was 773 °K, with a heating rate of 20 K/min and a residence time of 120 min, in an inert atmosphere with a constant nitrogen flow of 100 mL/min. The exhaust gas condensation system consists of a glass bottle immersed in an ice bath installed at the exit of the reactor. In this bottle, the liquid fraction is collected and quantified. Nitrogen was maintained by a continuous flow through the reactor during all operation time, while the PE was introduced at the beginning of the operation and was taken out when the operation time was finished.

### 2.4. Physical characterization of the pyrolytic oils

The pH value of oil was determined using a digital pH meter. Density was determined by following the Archimedes' Principle using an Ohaus density determination kit at room temperature.

The American Petroleum Institute (API) gravity was determined according to ASTM D-1298 (Eqs. (1) and (2)).

$$API\ gravity = \left( \frac{141.5}{\rho_{pyrolysis\ oil}} \right) - 131.5 \quad (1)$$

$$\rho_{pyrolysis} = \frac{\rho_{oil}}{\rho_{water}} \quad (2)$$

Where  $\rho_{pyrolysis}$  oil is determined at 288.6 K.

According to API gravity, the oils are classified as [25]:

Light oil: API gravity > 31.1°

Medium oil: API gravity between 22.3° and 31.1°

Heavy oil: API gravity < 22.3°

Extra-heavy oil: API gravity < 10°

## 2.5. Chemical characterization of the pyrolytic oils

### 2.5.1. Elemental analysis and calorific value

Elemental analysis of oil sample was done by combustion analysis using an Elemental Fison's Instruments EA 1108 CHNS. High heating value (HHV) was determined according to Dulong equation (Eq. (3)) [26].

$$HHV = 8080 \cdot C + 34460 \cdot \left[ H - \frac{O}{8} \right] + 2250 \cdot S \quad (3)$$

Where, C, H, O and S are the mass fractions of carbon, hydrogen, oxygen and sulphur. The results of this equation are provided in kcal/kg. However, in this work they were converted to MJ/kg.

### 2.5.2. Thermogravimetry analysis (TGA)

The TGA tests are performed on a Perkin-Elmer TGA-DSC thermobalance, model STA 6000. The conditions used for the TGA test were: temperature from 298 to 873 K, heating rate of 10 K/min, nitrogen flow of 20 mL/min and an approximately sample mass of 20 mg. TGA test was used to determine the volatilization characteristics of the oil.

### 2.5.3. Fourier-transform infrared spectroscopy (FTIR) analysis

To determine the FTIR spectrum of the oil samples, a Perkin-Elmer Spectrum 65 spectrophotometer was used. The spectrum was recorded at a wavenumber between 4000 and 400  $\text{cm}^{-1}$  with a resolution of 2  $\text{cm}^{-1}$ . This method is considered appropriate for the qualitative identification of organic and inorganic compounds.

### 2.5.4. Gas chromatography–mass spectrometry (GC-MS)

The analyses were performed using an Agilent high-resolution GC, model 7890A, coupled to a Waters triple-quadrupole mass spectrometer, model micro GC. The operating conditions were: injector and transfer line temperature, 523 K with the injector operating in split mode; carrier gas (helium) flow of 1 mL/min; nonpolar phase ZB-5MS capillary column, Phenomenex (USA), (30 m  $\times$  0.25 mm, ID  $\times$  0.25  $\mu\text{m}$  film); the oven was programmed to hold at 313 K during 4 min, heat to 553 K with at a heating rate of 6 K/min and held at this temperature for 6 min. The operation conditions of Mass Selective Detector were: interface temperature, 523 K, full scan, 30-650 Da and electron ionization energy, 70 eV. The identification of compounds was based on the National Institute of Standards and Technology; NIST MS Search 2.0 software integrated to MassLynx V4.1 with mass spectrum library NIST 08 [12]. The referential retention times of normal paraffins were identified from a calibration mixture to determine the boiling points of pyrolytic

oils compounds and, by linear interpolation, construct the simulated distillation curves according to the Test Method ASTM D2887 [27]. In short, chromatography gives us a qualitative and quantitative idea of the compounds present in these liquid fractions.

### 3. Results and discussions

#### 3.1. Characterization of the catalysts

Figure S1 shows the N<sub>2</sub> adsorption-desorption isotherms and Table 2 presents the textural properties for the three used zeolites. According to IUPAC classification the three studied zeolites can be classified as type IV isotherms and mesoporous channels are presented in these materials [28].

HUSY CBV 720 zeolite showed the higher BET surface area, micropore volume and micropore area with values of 762 m<sup>2</sup>/g, 0.24 cm<sup>3</sup>/g and 589 m<sup>2</sup>/g, respectively. However, the higher mesopore and total volumes were obtained for HY CBV 600 zeolite with values of 0.94 and 1.11 cm<sup>3</sup>/g, respectively., Ammonium Beta zeolite had a higher external surface (218 m<sup>2</sup>/g) compared to HY and HUSY zeolites (CBV 600 with 78 m<sup>2</sup>/g or CBV 720 with 173 m<sup>2</sup>/g).

**Table 2.** Pore volumes and surfaces of parent zeolites by N<sub>2</sub> adsorption-desorption

Catalyst	HY	HUSY	HBEA
	CBV 600	CBV 720	CP 814E
Micropore volume (cm <sup>3</sup> /g)	0.19	0.24	0.13
Mesopore volume (cm <sup>3</sup> /g)	0.94	0.22	0.42
Total volume (cm <sup>3</sup> /g)	1.13	0.46	0.56
Micropore area (m <sup>2</sup> /g)	474	589	324
External surface area (m <sup>2</sup> /g)	78	174	218
BET surface area (m <sup>2</sup> /g)	553	762	542

Wei et al. [29] reported the characterization results of the same commercial HY catalysts obtaining similar results to those of this work. Elordi et al. [30] studied an HBeta zeolite-based catalyst (commercial name CP811E-75), and its characterization is very different from ours obtaining a micropore volume of 0.041 cm<sup>3</sup>/g and a mesopore volume of 0.27 cm<sup>3</sup>/g however, it is important to remark that these authors studied a different commercial beta zeolite than that of this work.

Kenvin et al. [31] also worked with commercial HUSY CBV 720 zeolite, determining similar textural properties. For example, these authors reported a micropore volume of 0.36 cm<sup>3</sup>/g and a mesopore volume of 0.23 cm<sup>3</sup>/g. Finally, Simon-Masseron et al. [32] characterized the

Ammonium Beta zeolite, obtaining a microporous volume of 0.19-0.26 cm<sup>3</sup>/g and a surface area of 178 m<sup>2</sup>/g.

In addition XRD patterns for the three used zeolites are shown in Figure S2. HY and HUSY zeolites were purely crystalline with the typical diffraction pattern of FAU (faujasite) framework (Structural information on all the Zeolite can be consulted at <http://www.iza-structure.org/databases/>). Ammonium Beta CP 814E EA zeolite is purely crystalline with the typical diffraction pattern of the BEA framework [32,33].

### 3.2. Physical characterization of pyrolytic oil

In a previous work of Quesada et al. [34], a study was carried out on the liquid yields using these catalysts, obtaining a liquid yield of 37% for HY, 39% for HUSY and 43% for HBEA.

The pH and viscosity of oil samples were determined in previous work [35]. The pH of all the samples was 6. The oil obtained with the HY catalyst had a viscosity of 137 cSt, the oil obtained with the HUSY zeolite 209 cSt and the oil obtained with the Ammonium Beta zeolite 89 cSt at 313 K [33]. Other physical properties measured for the different oils are shown in Table 3.

**Table 3.** Physical characterization of the pyrolytic oil samples using different zeolites

Catalyst	Without catalyst	HY	HUSY	Ammonium Beta
		CBV 600	CBV 720	CP 814E
C (wt%)	83.2	83.8	84.5	83.4
H (wt%)	14.0	13.5	13.8	12.8
N (wt%)	0.28	0.44	0.18	0.22
O (wt%)	2.61	2.24	1.55	3.58
H/C (molar ratio)	2.01	1.93	1.96	1.84
O/C (molar ratio)	0.024	0.020	0.014	0.032
Density (g/cm <sup>3</sup> )	0.823	0.816	0.825	0.817
API gravity	40.2	41.8	39.8	41.6
Viscosity (cSt*)	1352	137	209	89
HHV (MJ/kg)	47.6	47.2	48.0	45.8
pH*	5.9	6.0	6.0	6.0

\* Data from [12, 34,35]

The values for carbon and hydrogen contents differ only slightly between samples. Particularly, the oils obtained with the different catalysts had carbon content between 83.4 and 84.5%, similar to that obtained without a catalyst (83.2%) and an almost hydrocarbon-carbon ratio. Similar elemental analysis was observed by Lopez-Urionabarrenechea et al. [36] for oils obtained from

the pyrolysis of a mixture of PE, PP, PS, poly(ethylene terephthalate) (PET) and poly(vinyl chloride) (PVC) at 713 K for 30 min using a zeolite as a catalyst or Singh et al. [37] in oils derived for HDPE using a pyrolysis-catalytic cracking process with copper carbonate catalyst. The density of the four samples was 0.816 to 0.825 g/cm<sup>3</sup>, their API gravities within 40-42°, and the calorific values varied between 45.8 and 48.0 MJ/kg. The values of the HHV show an interesting result since they are among those of gasoline (46.1-48.2 MJ/kg and kerosene/diesel (44.0-46.9 MJ/kg). The liquid product obtained by the HBEA catalyst is closer to the diesel range, whilst the density of all of them was within the range of kerosene (0.774-0.840 g/cm<sup>3</sup>).

As was indicated in the materials and methods section, the API gravity is used to classify the pyrolytic oils as light, medium, heavy or extra-heavy. According to values reported in Table 3, the pyrolytic oils are categorized as light oil.

Regarding viscosity, the high values show the need for a viscosity reduction process. For example, a viscosity range between 1 and 100 cSt at 293 °K is the most common range for commercial fuels and could be adequate for pyrolysis oils to facilitate its recovery, transportation and final use. The addition of Ammonium Beta CP 814E catalyst promoted the decrease of viscosity, however, yet it was still a very high value, due to the characteristics and proportion of the catalyst used.

### 3.3. Chemical characterization of pyrolytic oil

#### 3.3.1. TGA analysis

Figure 1 shows the TGA curves of the oils obtained without catalyst (data from Quesada et al., [12]) and with three different studied catalysts. Similar behavior was shown independently of the catalyst used during the pyrolysis. The pyrolytic oil samples presented a large mass loss between approximately 370 °K to 670 °K, which corresponds to the volatilization of compounds. Similar results were found by Lee et al. [38]. These authors showed the weight changes in function of temperature of pyrolysis oil obtained from pyrolysis of plastic wastes. Also, a comparison of TG curves of oils from catalytic pyrolysis with that obtained without catalyst shows that the catalytic pyrolysis reduced the volatilization temperature due to presence of lighter compounds. Approximately equal mass loss is shown up to about 470 °K (Naphtha cutoff) in catalyzed oils. Up to 550 K (kerosene cutoff) oils catalyzed by HY and HBEA have similar behavior. Although all catalyzed oils have about the same amount of diesel cut (13.29 to 13.71%), the lower mass loss of HUSY compared to the others may be associated with the interaction between the kerosene and diesel cuts due to its low content (HUSY: 12.29%, HBEA: 15.98% and HY: 17.9%). From here, the behavior is markedly different, dominated by the heavy fraction, where it is evident that the highest amount of bottoms is in the oil obtained by HUSY (HUSY: 65.12%, HBEA: 41.12% and HY:

50.97%). These results show that the liquid fraction obtained by HBEA zeolite, the zeolite with the largest external surface ( $218 \text{ m}^2/\text{g}$ ), has the highest amount of volatile compounds (58.88%) followed by HY zeolite ( $174 \text{ m}^2/\text{g}$ ), liquid fractions with the highest API degrees; simulated distillation allows graphically showing that these liquid fractions have the highest proportion of light constituents.

Figure 2 shows simulated distillation curves of the pyrolytic oils obtained by thermal and catalytic cracking. These curves show that the liquid fraction obtained by HBEA catalyst produce lightest compounds followed by the HY and HUSY catalysts because of the external surface area (HBEA:  $218 \text{ m}^2/\text{g}$ , HY:  $174 \text{ m}^2/\text{g}$  and HUSY:  $78 \text{ m}^2/\text{g}$ ), the latter, although it is catalyzed oil, has more heavy compounds (65.12 % of bottoms) than the oil obtained without catalyst (59.02% of bottoms) and therefore has the lowest API gravity.

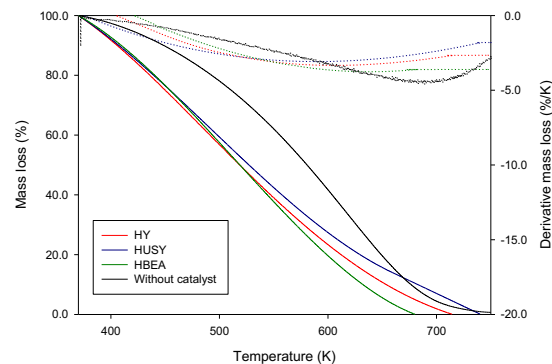


**Figure 1.** Thermogravimetric curves of the pyrolytic oil samples obtained by thermal (without catalyst) and catalytic cracking (HY, HUSY and HBEA).

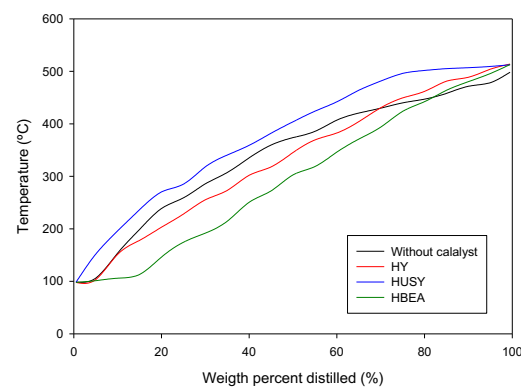


**Figure 2.** Simulated distillation curves of the pyrolytic oil samples obtained by thermal (without catalyst) and catalytic cracking (HY, HUSY and HBEA).



### 3.3.2 FTIR analysis of the pyrolytic oil

Figure 3 shows the FTIR spectra of the pyrolytic oil samples obtained from the pyrolysis of PE waste without the use of a catalyst [12] and with the use of the three studied catalysts. The peaks observed in the FTIR of oil without catalyst were practically equal to the peaks obtained with commercial catalysts, but absorbance values without catalyst were higher. These variations in the intensity of the absorbance may be related to changes in the concentration of the compounds involved and the path length through the sample. In addition, some technical aspects such as the pressure of the material on the ATR crystal could also have an influence. The main peaks found were  $2917\text{ cm}^{-1}$  and  $2850\text{ cm}^{-1}$  (C-H medium stretch) of alkanes;  $1714\text{ cm}^{-1}$  (C=O strong stretch) of aldehydes, ketones, carboxylic acids and esters;  $1642\text{ cm}^{-1}$  (C=C medium and weak stretch) of alkenes;  $1465\text{ cm}^{-1}$  (C-H variable scissoring and bending) of alkanes;  $1150\text{ cm}^{-1}$  (C-O strong stretch) of alcohols, ethers, carboxylic acids and esters;  $970\text{ cm}^{-1}$ ,  $890\text{ cm}^{-1}$  and  $720\text{ cm}^{-1}$  (C-H strong bend) of alkenes [39].

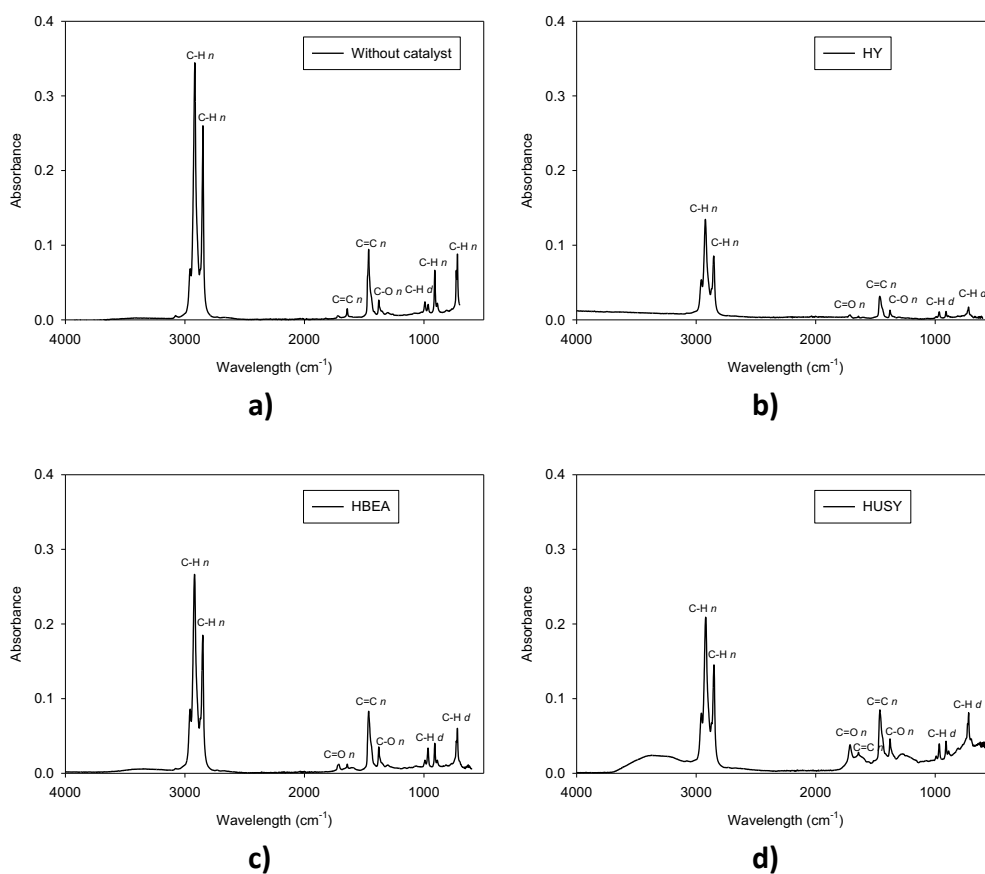


**Figure 3.** FTIR spectra of the pyrolytic oil samples from thermal and in-situ catalytic pyrolysis

In addition, the presence of certain compounds may be due to the origin of the plastic waste used, in this case plastics that have already been processed and that contain additives that have been added in the manufacturing process as well as traces of organic and inorganic impurities [40]. In this way, since hydrocarbons acidity is mainly due to the presence of naphthenic acids (aliphatic, cyclic and aromatic carboxylic groups), the C=O and C-O bonds would be related to the slightly acid pH of liquid fractions, which increase around 1,69 % when the catalysts are used.

Colantonio et al. [41] studied the pyrolysis of different polymer wastes with HUSY and HZSM5 catalysts and obtained peaks similar to those determined in this work.

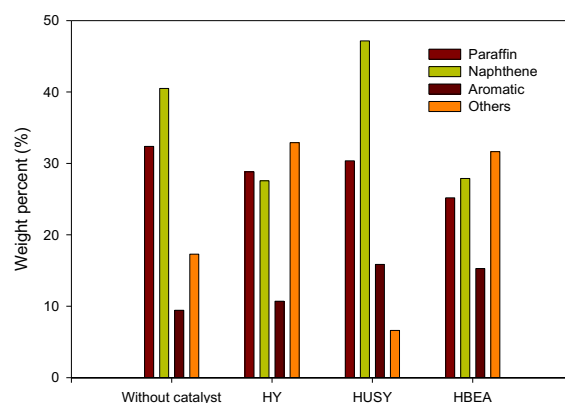


**Figure 4.** Hydrocarbon type distribution of the pyrolytic oil samples using different zeolites and without catalyst.

Similar results were obtained by Bagri and Williams [43], who studied the catalytic pyrolysis of PE waste with zeolites HY and ZSM-5 or Ding et al. [44] who found that the thermal degradation of PE yielded compounds ranging in carbon number from  $C_1$  to  $C_{27}$  and higher, while the catalytic cracking of PE gave products with lower carbon numbers (from  $C_1$  to  $C_{17}$ ). Manos et al. [45] studied the catalytic degradation of HDPE on different zeolites obtaining a range of hydrocarbons from  $C_3$ - $C_{15}$ . These authors studied the zeolite HY with a Si/Al molar ratio of 2.5, zeolite  $\beta$  (HBEA) with a Si/Al molar ratio of 25 that are similar to those used in this work, although they also worked with other catalysts such as ZSM-5 and modernite. HY zeolites and HBEA zeolite produced a higher amount of alkanes, with less amount of alkenes and aromatics and very small amounts of cycloalkanes and cycloalkenes, while modernite and ZSM-5 gave a higher amount of olefins. Most of the alkanes were isoparaffins, having a high octane number, which produces a high-quality fuel. Attique et al. [46] studied the catalytic pyrolysis of virgin LDPE with kaolin as catalyst. The authors obtained a distribution of  $C_9$ - $C_{25}$  hydrocarbons, mainly alkanes and alkenes. Colantonio et al. [41] studied the thermal and catalytic pyrolysis of a mixture of plastic waste (PE, PP and

PET). The authors found that the use of zeolites produces a decrease in the heavy oil fraction and wax formation. Also, HUSY had the best results in terms of the total monoaromatic yield and HZSM5 promoted the production of gases.

Figure 5 shows the liquid products yield of the pyrolytic oil samples from thermal and in-situ catalytic pyrolysis. The retention times of the representative carbon compounds of each oil show that there are valuable cuts in the range of heavy naphtha ( $C_6-C_{10}$ ), kerosene ( $C_9-C_{15}$ ) and diesel ( $C_{13}-C_{18}$ ) [27], their proportion increased according to the bimodal distribution of pore area of the catalyst used [47]. HBEA produces the largest amount of transportation fuels due to its smallest microporous surface area along with largest mesoporous surface area, the former reduce gases formation from the light fraction and the latter increase the cracking of heavy fractions. In addition, the HHV values in the range of 46.9 to 47.0 MJ/kg were obtained using the components of each oil sample shown in Fig. 3. These results confirm those determined from the elemental analysis of the oil samples (Table 3).

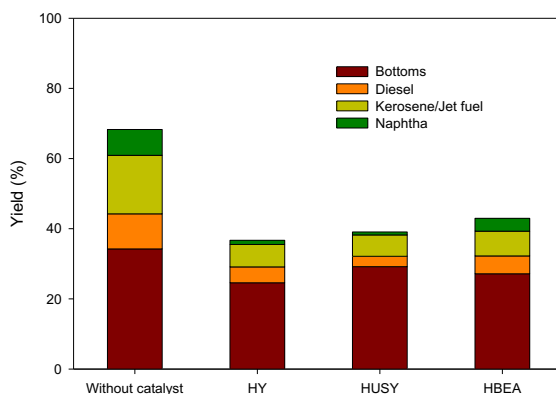


**Figure 5.** Liquid products yield of the pyrolytic oil samples from thermal and in-situ catalytic pyrolysis

The catalytic conversion and products yield of the liquid fraction from pyrolytic oil obtained by thermal pyrolysis shown in Figure 6 reflect that the three catalysts are gases selective, but provide important amounts of useful or valuable liquid cuts (jet fuel and diesel) that have to be added for the activity consideration when liquid fuels are the target. In this way, HY zeolite is the most active followed by HBEA and HUSY zeolites.

Two types of acid sites are present in studied zeolites; Brønsted acid sites and Lewis acid sites. In general, an increase in Si/Al molar ratio typically decreases the acidity of this type of material [48,49]. Figure 7 shows the catalytic conversion as a function of the Brønsted/Lewis acid site

ratio. These results show that the HUSY catalyst (the zeolite with highest Si/Al molar ratio and lowest Brønsted/Lewis acid site ratio) had lower activity compared to those HY and HBeta catalysts. Thus, the fraction of light products in pyrolytic oil from catalytic pyrolysis with HUSY catalyst was relatively low. In summary, it can be appreciated that conversion decreases when the Brønsted/Lewis acid site ratio also decreases, while the non-cracked bottoms yield increases. Generally, bottoms fraction is composed of a large amount of paraffins and heavy compounds.

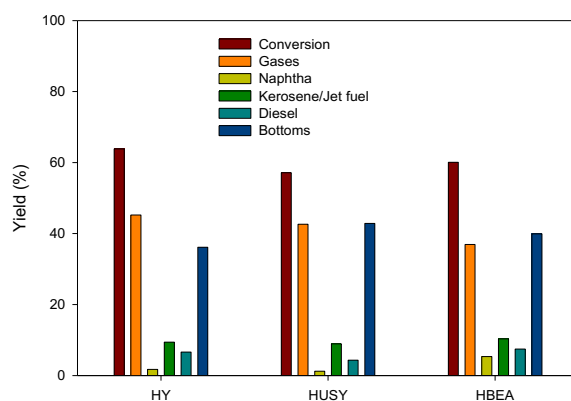


**Figure 6.** Products yield of catalytic conversion of the liquid fraction obtained by thermal pyrolysis

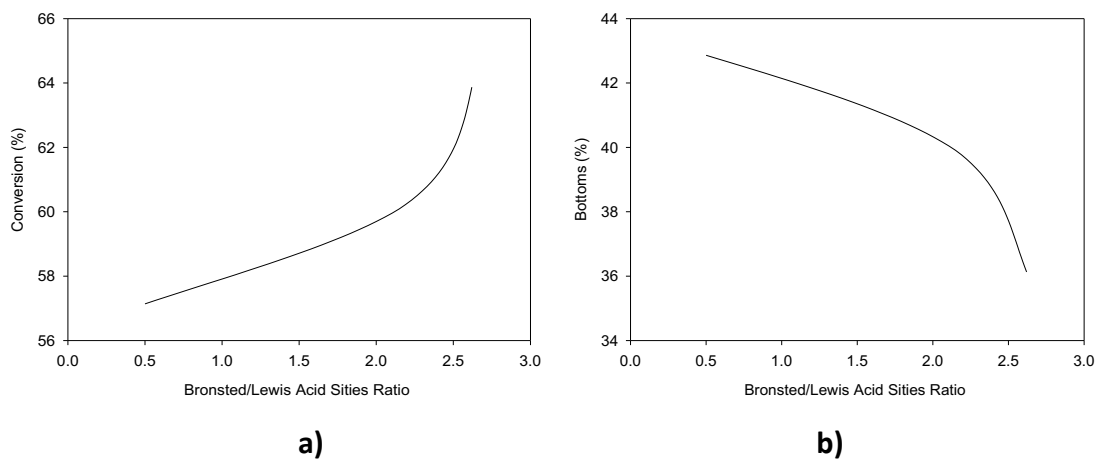


**Figure 7.** The effect of the Brønsted/Lewis acid site ratio in: (a) catalytic conversion of the liquid fraction obtained by thermal pyrolysis; (b) bottoms percentage of the liquid fraction obtained by thermal pyrolysis

Olivera et al. [50] studied the catalytic pyrolysis of LDPE and found differences in the catalytic activity of the materials used mainly due to differences in their acid properties. Sarker et al. [51], while studying the co-pyrolysis of poplar wood sawdust and HDPE with acid-modified ZSM-5 as a

catalyst, found that acid treatment affects the catalytic activity of ZSM-5 by changing the amount of acid sites.

On the other hand, since mesopores in the zeolites seem to present a selective catalytic behavior [48], a study of the conventional conversion, which consider gases and naphtha, and the liquid yield in the function of mesopores area was also performed. Figure 8 shows that the decrease in the conversion and yield of the liquid fraction as the mesopores area increases. In this sense, the zeolite with lowest mesopore area (HY zeolite,  $78 \text{ m}^2/\text{g}$ ) presented the highest in the conversion (68%) and amount of liquid fraction (37%). Conversely, the pyrolysis performed with HBEA zeolite, the zeolite with the highest mesopore area ( $218 \text{ m}^2/\text{g}$ ), showed the biggest conversion (71%) and liquid content (43%).

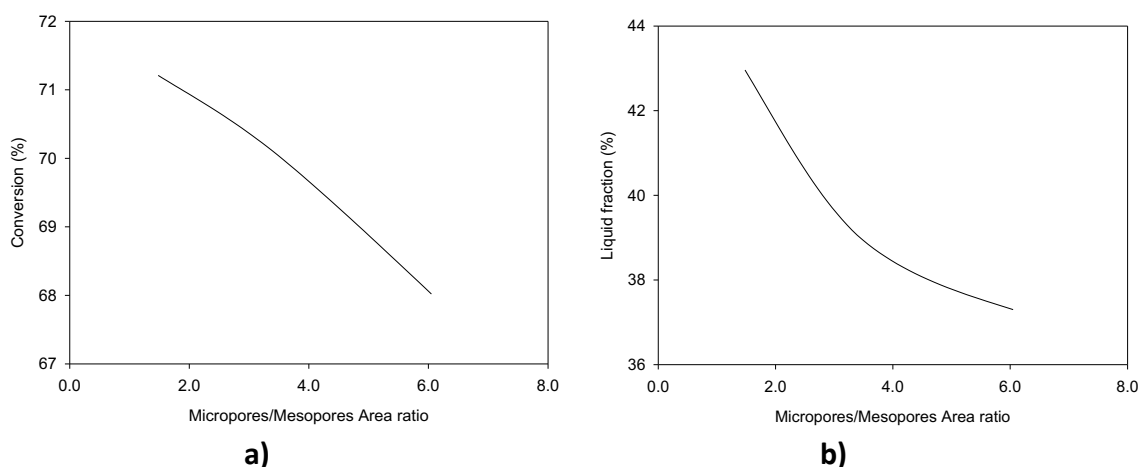


**Figure 8.** The effect of micropores and mesopores area ratio in: (a) catalytic conversion of the oil obtained by thermal pyrolysis; (b) liquid fraction percentage of the oil obtained by thermal pyrolysis.

## 4. Conclusions

Catalytic pyrolysis experiments of PE from the non-selectively collected fraction from municipal solid waste were investigated in this work.

Thermal pyrolysis of PE residue produces greater quantities of liquids than gases, while catalytic pyrolysis with HY, HUSY and HBEA catalysts produces a greater quantity of gases. This fact demonstrates the role of catalysts in the degradation of plastic materials, facilitating the cracking process. In such a way that with the use of Y and  $\beta$  catalysts, we could reduce the temperature and reaction time compared to the thermal pyrolysis process, since the use of this typology of catalysts favors the breaking of the C-C bonds of the polymeric chains, obtaining higher yields of

the gaseous fractions especially with HY and HUSY catalysts. This result may be associated with the acidic properties of HY and HUSY zeolites that promote polymer degradation significantly.

The characteristics of the liquid oil resulting from catalytic pyrolysis reveal those values of density, API gravity, ash content and calorific value similar to those of fuels from fossil fuels. It is noteworthy how the use of HY, HUSY and HBeta catalysts greatly reduces the viscosity of the liquid product when compared to the wax obtained in thermal pyrolysis; in this area, the HBEA zeolite stands out as the one that reduces the viscosity of the liquid product the most. The thermal degradation is similar in the three catalysts used. All TG curves show a great weight loss between 370 to 670 K, this weight loss occurs at a higher rate than in the product obtained in the thermal pyrolysis.

Thermal pyrolysis of the PE residue results in a liquid product composed mainly of olefins and n-paraffins. However, catalytic pyrolysis caused a decrease in the concentration of paraffinic compounds and increased the content of, in some cases, aromatic and naphthene compounds. Also, the range of carbon number of compounds was changed to C<sub>7</sub>-C<sub>32</sub>.

Although there are numerous catalysts available for the pyrolysis process the suitability of these depends on numerous variables, operating conditions, reactor typology and most importantly the nature of the feed, which is very unfavorable in our work, since the residue used comes from the fraction not selectively collected so it is quite heterogeneous both in the dirt that accompanies it and in the difference in proportion that can be found of LDPE and HDPE in the sample chosen in each experiment. All the catalysts used in this work produce a quality liquid product, with similar properties among them; the most relevant differences being the viscosity and calorific value.

**Supplementary Materials:** The following supporting information can be downloaded at: [www.mdpi.com/xxx/s1](http://www.mdpi.com/xxx/s1), Figure S1: N<sub>2</sub> adsorption-desorption isotherms at 77 K of: (a) HY CBV 600 zeolite; (b) HUSY CBV 720 zeolite; (c) Ammonium Beta CP 814E zeolite.; Figure S2. Ray-X pattern of: (a) HY CBV 600 and HUSY CBV 720 zeolite; (b) HBEA CP 814E; Figure S3 GC-MS chromatogram and simulated distillation curve of the pyrolytic oil samples from non-catalytic and in-situ pyrolysis: a) without catalyst; b) HY; c) HUSY; d) HBEA; Table S1 Summary of the hydrocarbon types results of GC-MS chromatogram of pyrolytic oil samples from non-catalytic and in-situ pyrolysis according designations ASTM D2425, D2786, D2789 and ASTM D3239.

**Author Contributions:** Contextualization and methodology, M. Calero and M.A. Martín-Lara; Formal analysis: L. Quesada; Investigation: L. Quesada and M.F. Paucar; Writing-original draft preparation: G. Blázquez, A. Pérez; Validation and Supervision: all authors; Funding acquisition: M. Calero and M.A. Martín-Lara.

**Funding:** This work has received funds from the project PID2019-108826RB-I00/SRA (State Research Agency)/10.13039/501100011033.

**Conflicts of Interest:** The authors declare no conflict of interest.

## References

1. PlasticsEurope. An Analysis of European Plastics Production, Demand and Waste Data. Plastics - the Facts 2020 PlasticsEurope; 2020. Available online: <https://plasticseurope.org/knowledge-hub/plastics-the-facts-2020/> (accessed on 14 February 2022).
2. Provincial Council of Granada. Municipal Waste Treatment Service. Municipal waste collection in the province of Granada (Spain); 2015. Available online: [https://www.resurgranada.es/datos\\_recogidas\\_RM.php](https://www.resurgranada.es/datos_recogidas_RM.php) (accessed on 14 February 2022).
3. Calero, M.; Martin-Lara, M.A.; Godoy, V.; Quesada, L.; Martinez, D.; Peula, F.; Soto, J.M. Characterization of plastic materials present in municipal solid waste: preliminary study for their mechanical recycling. *Detritus* **2018**, *4*, 104–112.
4. Rajendran, K.M.; Chintala, V.; Sharma, A.; Pal, S.; Pandey, J.K.; Ghodke, P. Review of catalyst materials in achieving the liquid hydrocarbon fuels from municipal mixed plastic waste (MMPW). *Mater. Today Commun.* **2020**, *24*, 100982.
5. Ragaert, K.; Delva, L.; Van Geem, K. Mechanical and chemical recycling of solid plastic waste. *Waste Manage.* **2017**, *69*, 24–58.
6. Papari, S.; Bamdad, H.; Berruti, F. Pyrolytic conversion of plastic waste to value-added products and fuels: a review. *Materials* **2021**, *14*, 2586.
7. Al-Salem, S.M.; Antelava, A.; Constantinou, A.; Manos, G.; Dutta, A. A review on thermal and catalytic pyrolysis of plastic solid waste (PSW). *J. Environ. Manage.* **2017**, *197*, 177–98.
8. Sharuddin, S.D.A.; Abnisa, F.; Daud, W.M.A.W.; Aroua, M.K. A review on pyrolysis of plastic wastes. *J. Energy Convers. Manage.* **2016**, *115*, 308–26.
9. Li, N.; Lium H.X.; Cheng, Z.N.; Yan, B.B.; Chen, G.Y.; Wang, S.B.; Conversion of plastic waste into fuels: a critical review. *J. Hazard. Mater.* **2022**, *424*, 127460.
10. Ahmad, I.; Khan, M.I.; Khan, H.; Ishaq, M.; Tariq, R.; Gul, K.; Ahmad, W. Pyrolysis study of polypropylene and polyethylene into premium oil products. *Int. J. Green Energ.* **2015**, *12*, 663–71.
11. Onwudili, J.A.; Insura, N.; Williams, P.T. Composition of products from the pyrolysis of polyethylene and polystyrene in a closed batch reactor: effects of temperature and residence time. *J. Anal. Appl. Pyrol.* **2009**, *86*, 293–303.
12. Quesada, L.; Calero, M.; Martin-Lara, M.A.; Pérez, A.; Blázquez, G. Characterization of fuel produced by pyrolysis of plastic film obtained of municipal solid waste. *Energy* **2019**, *186*, 115874.

13. Miandad, R.; Barakat, M.A.; Aburizaiza, A.S.; Rehanb, M.; Nizami, A.S. Catalytic pyrolysis of plastic waste: A review. *Procees Saf. Environ. Prot.* 2016, 102, 822-38.
14. Lopez, G.; Artetxe, M.; Amutio, M.; Bilbao, J.; Olazar, M. Thermochemical routes for the valorization of waste polyolefinic plastics to produce fuels and chemicals. A review. *Renew. Sust. Energ. Rev.* **2017**, 73, 346–68.
15. Benedetti, M.; Cafiero, L.; Angelis, D.D.; Dell’Era, A.; Pasquali, M.; Stendardo, S.; Tuffi, R.; Cipriotti, S.V. Pyrolysis of WEEE plastics using catalysts produced from fly ash of coal gasification. *Front. Environ. Sci. Eng.* 2017, 11, 11.
16. Kremer, I.; Tomic, T.; Katancic, Z.; Erceg, M.; Papuga, S.; Vukovic, J.P.; Schneider, D.R. Catalytic pyrolysis of mechanically non-recyclable waste plastics mixture: Kinetics and pyrolysis in laboratory-scale reactor. *J. Environ. Manage.* 2021, 296,113145.
17. Aguado, J.; Serrano, D.P.; Miguel, G.S.; Escola, J.M.; Rodriguez, J.M. Catalytic activity of zeolitic and mesostructured catalysts in the cracking of pure and waste polyolefins. *J. Anal. Appl. Pyrol.* **2007**, 78, 153–61.
18. Awan, U.; Kraslawski, A.; Huiskonen, J. Progress from blue to the green world: multilevel governance for pollution prevention planning and sustainability. In *Handbook of environmental materials management*; Hussain C.M., Eds.; Springer, Cham, Switzerland, 2020; pp. 1–22.
19. Soto, J.M.; Blázquez, G.; Calero, M.; Quesada, L.; Godoy, V.; Martin-Lara, M.A. A real case study of mechanical recycling as an alternative for managing of polyethylene plastic film presented in mixed municipal solid waste. *J. Clean. Prod.* **2018**, 203, 777–87.
20. Lakiss, L.; Gilson, J.-P.; Valtchev, V.; Mintova, S.; Vicente, A.; Vimont, A.; Bedard, R.; Abdo, S.; Bricker, J. Zeolites in a good shape: Catalyst forming by extrusion modifies their performances, *Microporous Mesoporous Mater.* 2020, 299, 110114.
21. Nichterwitz, M.; Grätz, S.; Nickel, W.; Borchardt, L. Solvent-free hierarchization of zeolites by carbochlorination. *J. Mater. Chem. A* 2017, 5, 221-229.
22. Batalha, N.; Comparot, J.-D.; Le Valant, A.; Pinard, L. In situ FTIR spectroscopy to unravel the bifunctional nature of aromatics hydrogenation synergy on zeolite/metal catalysts. *Catalysis Sci. Technol.* 2022, 12, 1117-1129.
23. Awan, I.Z.; Beltrami, G.; Bonincontro, D.; Gimello, O.; Cacciaguerra, T.; Tanchoux, N.; Martucci, A.; Albonetti, S.; Cavani, F.; Di Renzo, F. Copper-nickel mixed oxide catalysts from layered double hydroxides for the hydrogen-transfer valorisation of lignin in organosolv pulping. *Appl. Catal. A: Gen.* 2021, 609, 117929.
24. Zhang, R.; Xu, S.; Raja, D.; Khusni, N.B.; Liu, J.; Zhang, J.; Abdulridha, S.; Xiang, H.; Guan, Y.; Jiao, Y.; Fan, X. On the effect of mesoporosity of FAU Y zeolites in the liquid-phase catalysis. *Microporous Mesoporous Mater.* 2019, 278, 297-306.
25. Gaurh, P.; Pramanik, H. Production and characterization of pyrolysis oil using waste polyethylene in a semi batch reactor. *Indian J. Chem. Techn.* **2018**, 25, 336–44.



26. Kathiravale, S.; Yunus, M.N.M.; Sopian, K.; Samsuddin, A.H.; Rahman, R.A. Modeling the heating value of municipal solid waste. *Fuel* **2003**, *82*, 1119-25.
27. Totten, G.; Westbrook, S.; Shah, R. *Fuels and lubricants handbook: technology, properties, performance, and testing*. 2nd ed. American Society for Testing & Materials: Seattle, United States, 2019. <https://www.astm.org/mnl37-2nd-eb.html>.
28. Thommes, M.; Kaneko, K.; Neimark, A.V.; Olivier, J.P.; Rodriguez-Reinoso, F.; Rouquerol, J.; Sing, K.S.W. Physisorption of gases, with special reference to the evaluation of surface area and pore size distribution (IUPAC Technical Report). *Pure Appl. Chem.* **2015**, *87*, 1051–69.
29. Wei, B.Y.; Jin, L.J.; Wang, D.C.; Shi, H.; Hu, H.Q. Catalytic upgrading of lignite pyrolysis volatiles over modified HY zeolites. *Fuel* **2020**, *259*, 116234.
30. Elordi, G.; Olazar, M.; Lopez, G.; Amutio, M.; Artetxe, M.; Aguado, R.; Bilbao, J. Catalytic pyrolysis of HDPE in continuous mode over zeolite catalysts in a conical spouted bed reactor. *J. Anal. Appl. Pyrol.* **2009**, *85*, 345–51.
31. Kenvin, J.; Mitchell, S.; Sterling, M.; Warringham, R.; Keller, T.C.; Crivelli, P.; Jagiello, J.; Pérez-Ramírez, J. Quantifying the complex pore architecture of hierarchical faujasite zeolites and the impact on diffusion. *Adv. Funct. Mater.* **2016**, *26*, 5621–30.
32. Simon-Masseron, A.; Marques, J.P.; Lopes, J.M.; Ribeiro, F.R.; Gener, I.; Guisnet, M. Influence of the Si/Al ratio and crystal size on the acidity and activity of HBEA zeolites. *Appl. Catal. A-Gen.* **2007**, *316*, 75–82.
33. Baerlocher, Ch.; McCusker, L.B.; Olson, D.H. *Atlas of Zeolite Framework Types*, 6th ed; Elsevier: Amsterdam, the Netherlands, 2007.
34. Quesada, L.; Calero, M.; Martin-Lara, M.A.; Luzón, G.; Blázquez, G. Performance of different catalysts for the in situ cracking of the oil-waxes obtained by the pyrolysis of polyethylene film waste. *Sustainability-Basel* **2020**, *12*, 5482.
35. Quesada, L.; Calero, M.; Martin-Lara, M.A.; Pérez, A.; Blázquez, G. Production of an alternative fuel by pyrolysis of plastic wastes mixtures. *Energ. Fuel* **2020**, *34*, 1781–90.
36. Lopez-Uribebarrenechea, A.; de Marco, I.; Caballero, B.M.; Laresgoiti, M.F.; Adrados, A. Catalytic stepwise pyrolysis of packaging plastic waste. *J. Anal. Appl. Pyrol.* **2012**, *96*, 54–62.
37. Singh, M.V.; Kumar, S.; Sarker, M. Waste HD-PE plastic, deformation into liquid hydrocarbon fuel using pyrolysis-catalytic cracking with a  $\text{CuCO}_3$  catalyst. *Sustain. Energ. Fuels* **2018**, *2*, 1057–68.
38. Lee, D.; Nam, H.; Wang, S.; Kin, H.; Kim, J.H.; Won, Y.; Hwang, B.W.; Kim, Y.D.; Nam, H.; Lee, K.-H.; Ryu, H.-J. Characteristics of fractionated drop-in liquid fuel of plastic wastes from a commercial pyrolysis plant. *Waste Manage.* **2021**, *126*, 411-422.
39. Panda, A.K.; Singh, R.K. Experimental optimization of process for the thermo-catalytic degradation of waste polypropylene to liquid fuel. *Adv. Energ. Eng.* **2013**, *1*, 74–84.

40. Kusenberg, M.; Zayaud, Azd.; Roosen, M.; Dao Thi, H.; Abbas-Abadi, M.S.; Eschenbacher, A.; Kresovic, U.; De Meester, S. A comprehensive experimental investigation of plastic waste pyrolysis oil quality and its dependence on the plastic waste composition. *Fuel Proces. Technol.* **2022**, 227, 107090
41. Colantonio, S.; Cafiero, L.; De Angelis, D.; Ippolito, N.M.; Tuffi, R.; Cipriotti, S.V. Thermal and catalytic pyrolysis of a synthetic mixture representative of packaging plastics residue. *Front. Chem. Sci. Eng.* **2020**, 14, 288–303.
42. Kasar, P.; Sharma, D.K.; Ahmaruzzaman, M. Thermal and catalytic decomposition of waste plastics and its co-processing with petroleum residue through pyrolysis process. *J. Clean. Prod.* **2020**, 265, 121639.
43. Bagri, R.; Williams, P.T. Catalytic pyrolysis of polyethylene. *J. Anal. Appl. Pyrol.* **2002**, 63, 29–41.
44. Ding, W.B.; Liang, J.; Anderson, L.L. Thermal and catalytic degradation of high density polyethylene and commingled post-consumer plastic waste. *Fuel Process. Technol.* **1997**, 51, 47–62.
45. Manos, G.; Garforth, A.; Dwyer, J. Catalytic degradation of high-density polyethylene over different zeolitic structures. *Ind. Eng. Chem. Res.* **2000**, 39, 1198–202.
46. Attique, S.; Batool, M.; Jalees, M.I.; Shehzad, K.; Farooq, U.; Khan, Z.; Ashraf, F.; Shah, A.T. Highly efficient catalytic degradation of low-density polyethylene using a novel tungstophosphoric acid/kaolin clay composite catalyst. *Turk. J. Chem.* **2018**, 42, 684–93.
47. Mitchell, M.M., Hoffman, J.F., Moore, H.F. Residual feed cracking catalysts. In *Studies in surface science and catalysis. Fluid Catalytic Cracking: Science and Technology*; Magee, J.S., Mitchell, M.M., Eds.; Elsevier: Amsterdam, The Netherlands, 1993. p. 293–338.
48. Paucar-Sanchez, M.F. Study of the activity of the circulating catalyst in the fluidized catalytic cracking unit (FCC) of the Esmeraldas State Refinery (REE). M.S. Degree Final Dissertation, University of San Francisco, Quito USFQ, 2011 [in Spanish].
49. Li, J.H.; Wang, Y.N.; Jia, W.Z.; Xi, Z.W.; Chen, H.H.; Zhu, Z.R.; Hu, Z.G.. Effect of external surface of HZSM-5 zeolite on product distribution in the conversion of methanol to hydrocarbons. *J. Energ. Chem.* **2014**, 23, 771–80.
50. Olivera, M.; Musso, M.; De Leon, A.; Volonterio, E.; Amaya, A.; Tancredi, N.; Bussi, J. Catalytic assessment of solid materials for the pyrolytic conversion of low-density polyethylene into fuels. *Heliyon* **2020**, 6, e05080.
51. Sarker, M.; Liu, R.H.; Rahman, M.M.; Li, C.; Chai, M.Y.; Nishu, N.; He, Y.F. Impact of acid-modified ZSM-5 on hydrocarbon yield of catalytic co-pyrolysis of poplar wood sawdust and high-density polyethylene by Py-GC/MS analysis. *J. Energ. Inst.* **2020**, 93, 2435–43.

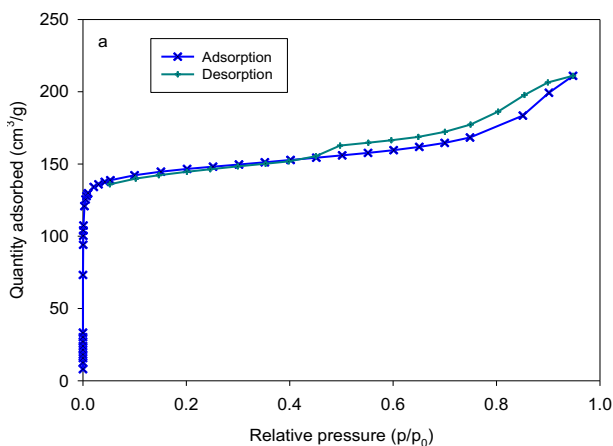
## S. Supplementary materials

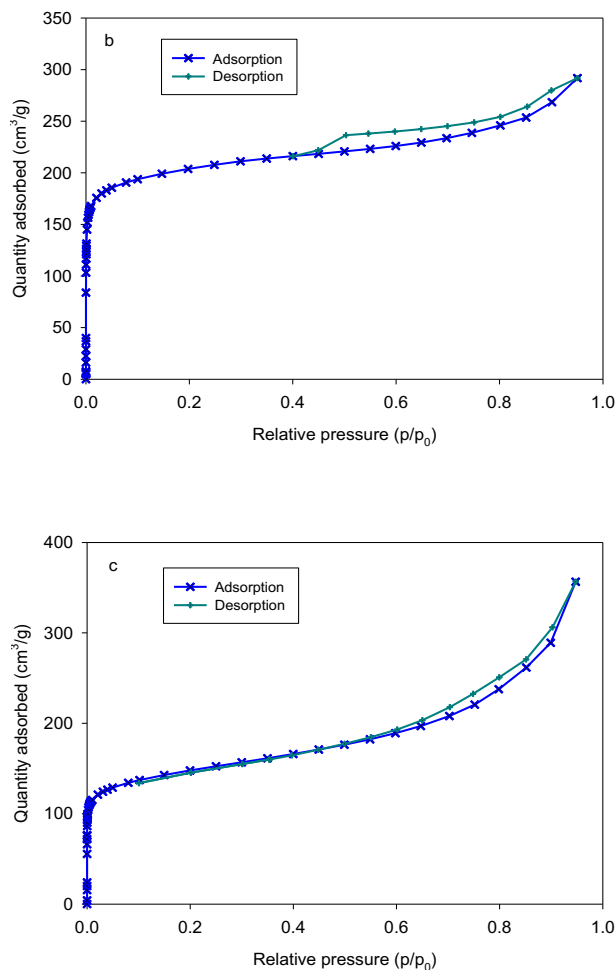
### Characterization of the different oils obtained through the catalytic in-situ pyrolysis of polyethylene film from municipal solid waste

Lucía Quesada, Mónica Calero, M<sup>a</sup> Ángeles Martín-Lara, Antonio Pérez, Marco F. Paucar-Sánchez, Gabriel Blázquez

#### 3.1. Characterization of the catalysts

Figure 1 shows the N<sub>2</sub> adsorption-desorption isotherms for the three used zeolites. According to IUPAC classification, microporous materials having small external surfaces lead to Type I isotherms; nonporous or macroporous adsorbents yield Type II isotherms; Type III and Type V isotherms represent cases in which there is no identifiable multilayer formation, meaning that there are relatively weak adsorbent–adsorbate interactions; Type IV isotherms are given by mesoporous materials (with pores of 2–50 nm); and Type VI isotherms represent layer-by-layer adsorption on a highly uniform nonporous surface. According to Fig. 1, the N<sub>2</sub> isotherms of the three studied zeolites can be classified as type IV isotherms with a well-defined plateau at medium relative pressures and an increase at high relative pressures. Since type IV isotherms are given by the three zeolites, mesoporous channels are presented in these materials [28]. For HY and HUSY zeolites the initial stage of the isotherms sharply rises and then, the isotherm is concave to the P/P<sub>0</sub> axis and the amount adsorbed is lower. The more pronounced uptake at low P/P<sub>0</sub> is associated with the filling of micropores. However, for Ammonium Beta zeolite, the pronounced uptake at low P/P<sub>0</sub> is also observed but, at high P/P<sub>0</sub>, with increasing the P/P<sub>0</sub>, the zeolite shows a higher adsorption amount (Fig. 1c). The differences in the shapes of hysteresis loops indicated also differences in the pore structure and adsorption mechanisms. For example, the value of P/P<sub>0</sub> in which the hysteresis loop starts shows some differences among HY, HUSY and Beta zeolite. In addition, hysteresis loops more similar to type H4 loops can be observed for HY and HUSY zeolites and hysteresis loop of type H3 for Beta zeolite. H4 loops are often found with aggregated crystals of zeolites, some mesoporous zeolites, and micro-mesoporous carbons and loops of type H3 are more frequently given by non-rigid aggregates of plate-like particles.

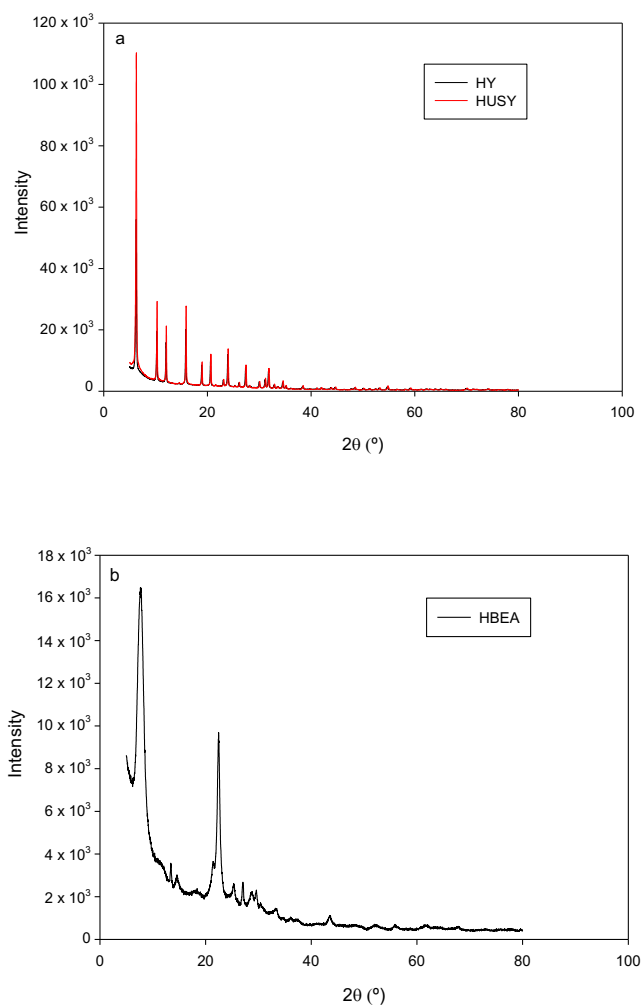




**Figure S1.** N<sub>2</sub> adsorption-desorption isotherms at 77 K of: (a) HY CBV 600 zeolite; (b) HUSY CBV 720 zeolite; (c) Ammonium Beta CP 814E zeolite.

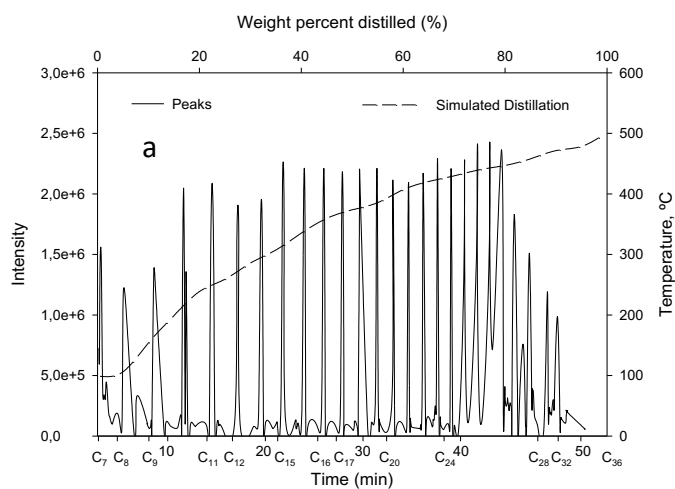
XRD patterns of HY and HUSY samples are shown in Fig. 2a. Both zeolites were purely crystalline with the typical diffraction pattern of FAU (faujasite) framework (Structural information on all the Zeolite can be consulted at <http://www.iza-structure.org/databases/>). These are characterized by peaks at 6, 10, 12, 15 and 18° 2 $\theta$ . The FAU structures, sodalities cages are put in the same way as the carbon atoms in diamond and are joined to one another via double 6-rings. This results in what is known as supercages of 1.4 nm at the intersection of the channels and a three-dimensional channel with an equivalent minimum pore size of 0.74 nm [33].

Figure 2b shows the XRD pattern of Ammonium Beta CP 814E EA zeolite. It was purely crystalline with the typical diffraction pattern of the BEA framework. This is characterized by two main peaks at around 7.6 and 22.4° 2 $\theta$ . This zeolite is made up of two cross-linked polymorphs (A and B) stacked almost randomly, generating straight 3D channels with an equivalent minimum pore size of 0.66 × 0.67 nm [33]. This structure gives rise to a significant number of terminal silanol groups. The large diffraction peaks are the result of stacking failures generated by the presence of the two isomorphs [32].



**Figure S2.** Ray-X pattern of: (a) HY CBV 600 and HUSY CBV 720 zeolite; (b) HBEA CP 814E

### 3.3.3. GC-MS



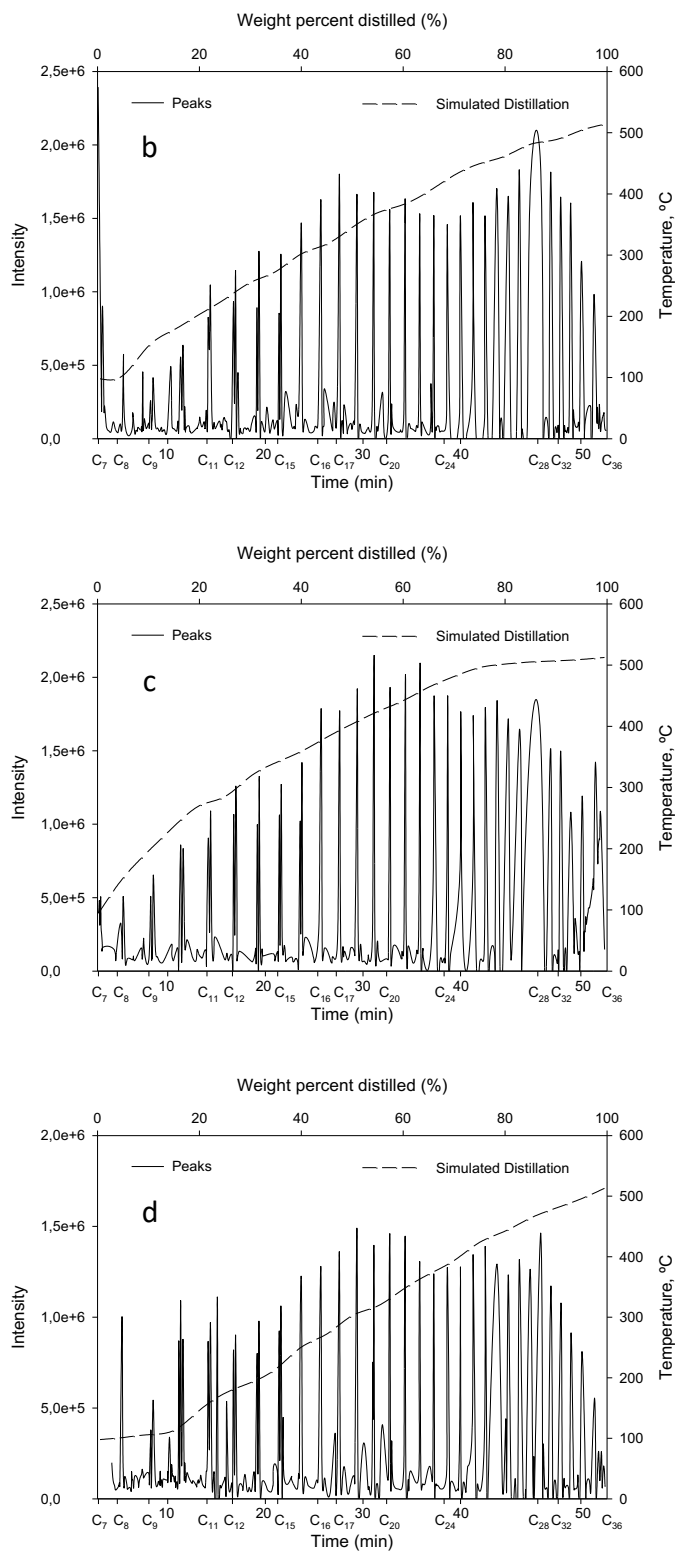


**Figure S3** GC-MS chromatogram and simulated distillation curve of the pyrolytic oil samples from non-catalytic and in-situ pyrolysis: (a) without catalyst; (b) HY; (c) HUSY; (d) HBEA

**Table S1** Summary of the hydrocarbon types of pyrolytic oil samples from non-catalytic and in-situ pyrolysis according designations ASTM D2425, D2786, D2789 and ASTM D3239

Hydrocarbons	Hydrocarbon Type	Without catalyst, %Wt	HY, %Wt	HUSY, %Wt	HBEA, %Wt
Paraffins	Paraffins	32.38	28.82	30.36	25.18
Naphtha	Monocycloparaffins	25.66	17.45	19.04	16.79
	Dicycloparaffins	10.80	7.89	13.08	8.11
	Tricycloparaffins	1.11	0.82	12.79	1.15
	Tetracycloparaffins	0.44	0.23	0.40	0.28
	Pentacycloparaffins	1.39	0.69	0.92	0.91
	Hexacycloparaffins	1.09	0.49	0.93	0.67
Aromatics	Monoaromatic	0.36	0.32	0.05	0.33
	Alkyl benzenes	1.65	2.76	2.88	2.14
	Indans or tetralins, or both	0.52	1.42	3.29	2.67
	Indenes or $C_nH_{2n-10}$ , or both	1.12	1.02	1.70	2.43
	Naphthalene	0.68	0.79	0.86	2.29
	Naphthalenes	2.24	0.95	1.05	1.10
	Acenaphthenes or $C_nH_{2n-14}$ , or both	1.03	1.02	1.35	1.07
	Acenaphthylenes or $C_nH_{2n-16}$ , or both	1.59	1.64	2.42	2.42
Tricyclic aromatics	0.25	0.79	2.27	0.82	
Others	Olefins and others	17.69	32.90	6.61	31.65

## References

- Thommes, M.; Kaneko, K.; Neimark, A.V.; Olivier, J.P.; Rodriguez-Reinoso, F.; Rouquerol, J.; Sing, K.S.W. Physisorption of gases, with special reference to the evaluation of surface area and pore size distribution (IUPAC Technical Report). *Pure Appl. Chem.* **2015**, *87*, 1051–69.
- Simon-Masseron, A.; Marques, J.P.; Lopes, J.M.; Ribeiro, F.R.; Gener, I.; Guisnet, M. Influence of the Si/Al ratio and crystal size on the acidity and activity of HBEA zeolites. *Appl. Catal. A-Gen.* **2007**, *316*, 75–82.
- Baerlocher, Ch.; McCusker, L.B.; Olson, D.H. *Atlas of Zeolite Framework Types*, 6th ed; Elsevier: Amsterdam, the Netherlands, 2007.

